DYNAMIC THERMAL MODELLING USING CFD

A thesis submitted for the degree of Doctor of Engineering

by
Shini Somarathne

Department of Mechanical Engineering,
Brunel University

ACKNOWLEDMENTS

ABSTRACT

Buildings expend vast quantities of energy, which has a detrimental impact on the environment. Buildings systems are often oversized to cope with possible extreme environmental conditions. Building simulation provides an opportunity to improve building thermal design, but the available tools are typically used in combination in order to overcome their individual deficiencies. Two such tools, often used in tandem are computational fluid dynamics (CFD) and dynamic thermal modelling (DTM). DTM provides a coarse analysis, by considering external and internal thermal conditions over a building (including its fabric) over time. CFD is usually used to provide steady state analysis. Boundary conditions typically in the form of surface temperatures are manually input from DTM into CFD. CFD can model buildings dynamically, but is not commonly used, since solving for hugely different time constants of solid and air pose significant limitations, due to data generated and time consumed. A technique is developed in this study to tackle these limitations.

There are two main strands to the research. DTM techniques had to be incorporated into CFD, starting from first principles of modelling heat transfer through solid materials. These were developed into employing the use of functions such as the 'freeze flow' function (FFF) and the 'boundary freeze' function (BFF) in combination with a time-varying grid schedule to model solids and air simultaneously. The FFF pauses the solution of all governing equations of fluid flow, except temperature. The BFF can be applied to solid boundaries to lock their temperatures whilst all other equations are solved. After extensive research the established DTM-CFD Procedure eventually used the FFF and BFF with transient periods and steady state updates, respectively.

The second strand of research involved the application of the DTM-CFD Procedure to a typical office space over a period of 24-hours. Through inter-model comparisons with a fully transient simulation, the DTM-CFD Procedure proved to be capable of providing dynamic thermal simulations 16.4% more efficiently than a typical CFD code and more accurately than a typical DTM code. Additional research is recommended for the further improvement of the DTM-CFD Procedure.

CONTENTS

Appendix D – Application of DTM-CFD Tool

Appendix E - Publications

Somarathne, S., Seymour, M., Kolokotroni, M., (2003), Efficient Dynamic Thermal Modelling using CFD, Healthy Buildings Conference, Singapore

Somarathne, S., Seymour, M., Kolokotroni, M., (2002), Transient Solution Methods for Dynamic Thermal Modelling within CFD, International Journal of Ventilation Vol. 1, No. 2, pp141-156.

Somarathne, S., Seymour, M., Kolokotroni, M., (2002), A Single Tool To Assess The Heat And Airflows Within An Enclosure: Preliminary Test, ROOMVENT 2002 Eight International Conference, Air Distribution in Rooms, Copenhagen, Denmark 8-11 September, CD-ROM.

Somarathne, S., Seymour, M., Kolokotroni, M., (2001), A Single Tool To Assess the Thermal And Environmental Performance Of Office Buildings, Proc. Clima2000 Conference, Napoli, Italy, 15-18 September, CD-ROM.

LIST OF FIGURES

4.6	Last 2 days (out of 5 days in total) solved using DTSP#2 – Temperatures within enclosure	85
4.7	Comparison of temperatures recorded using 3 different DTSPs over 6 hours of transient solutions	86
5.1	% Errors of Transient 'Frozen Flow' Periods for Material C1W1	98
5.2	% Error of Time Steps for Material C3W1 for an External Ambient Change of 3.75°C	101
5.3	% Error of Transient 'Frozen Flow' Period for Material C3W1, using the Original Sinusoidal Ambient	103
5.4	% Error of Transient 'Frozen Flow' Period for Material C3W1, using a Double Amplitude Sinusoid	104
5.5	Sinusoidal Ambient Profile (15°C Amplitude and 5 hour Period)	106
5.6	% Error of Transient Frozen Flow for a High Frequency External Ambient Sinusoid tested on Material C3W1 (STEADY STATE VALUES)	107
5.7	% Error of Transient Frozen Flow for a High Frequency External Ambient Sinusoid tested on Material C3W1 (TRANSIENT VALUES)	108
5.8	Rate of Change of Sinusoidal Ambient Profile (15°C Amplitude and 5 hour Period)	110
5.9	6-minute transient period showing the Relationship between dT Air (w) (ss) and RE (cumulative) [Note: the number labels represent the time step numbers]	113
5.10	12-minute transient period showing the Relationship between dT Air (w) (ss) and RE (cumulative). [Note: the number labels represent the time step numbers]	114
5.11	6-minute transient period showing the Relationship between dT Solids (trans) and RE (cumulative)	115
5.12	Error profiles generated by a linearly increasing ambient of 0.125°C/min	121

A1	One-dimensional Heat Transfer by Conduction	A4
A2	Fig A2: Geometry of Conduction Test	A5
A3	Geometry of Convection Test Case, as constructed within FLOVENT	A8
A4	Geometry of Radiation test as constructed within FLOVENT	A12
A5	Cuboid including the configuration of the 3-Dimensional Grid	A21
A6	Graph to show Temperature (°C) over Time (s) as recorded at the single Monitor Point located within the Solution Domain	A22
B1	Geometry of Test B1	B4
B2	Temperatures recorded at the 2 MPs using Brickwork (outer leaf) as the wall slab	B8
B3	Phase Lag through the wall as recorded at each monitoring point within the wall	B9
B4	Geometry of Test B3	B12
B5	Graph of Temperatures recorded at a Monitoring Point located within the airspace	B13
B6	Z-Plane Visualisation of the Temperature Results	B14
B7	Geometry of Test B4	B16
B8	Steady state temperature profile of Test B3	B23
B9	Steady state velocity profile of Test B3	B23
C1	Test Geometry used to assess the performance of the 'Freeze Flow' Function	C2
C2	Temperature profiles of the Temperature data collection points within the Enclosure	C3
C3	% Errors of Transient 'Frozen Flow' Periods for Material C1W1	C5
C4	% Error of Transient 'Frozen Flow' Periods for Material C1W2	C6
C5	% Error of Temperatures of the Fully Transient Cases and Various Transient Periods for Material C1W3	C7
C6	% Error of Transient 'Frozen Flow' Periods for Material C2W1	C8

C7	% Error of Transient 'Frozen Flow' Periods for Material C2W2	C9
C8	% Error of Transient 'Frozen Flow' Periods for Material C2W3	C11
C9	% Error of Transient 'Frozen Flow' Periods for Material C3W1	C12
C10	% Error of Transient 'Frozen Flow' Periods for Material C3W2	C13
C11	% Error of Temperatures of the Fully Transient Cases and Various Transient Periods for Material C3W3	C14
C12	Flow Chart indicating the influences upon error incurred by using the DTM-CFD tool	C16
C13	Cross-section of an Enclosure	C17
C14	Comparison between Simulation Results Collected for the Existing and Revised DTM-CFD Procedure using 12 min transient periods of Frozen Flow	C23
D1	Solar Visualisation of Solar Radiation penetrating through the transparent glass window	D4

LIST OF TABLES

EXECUTIVE SUMMARY

I. BACKGROUND INFORMATION

The Engineering Doctorate Programme (EngD) is a four-year research degree, awarded for industrially relevant research, based in industry and supported by a programme of professional development courses. The EngD Programme is sponsored by the Engineering and Physical Science Research Council (EPSRC) and was set up in response to industry needs for more industrially orientated research. The industrial perspective of the work included in this thesis was instigated by Flomerics Ltd. who also provided additional funding to the EPSRC sponsorship, as required by the EngD Programme.

At present, there exist ten EngD centres based in UK Universities. The work included in this thesis was carried out within a centre managed jointly by Brunel and Surrey Universities. All research projects undertaken at the Brunel/Surrey EngD centre follow the theme of "Environmental Technology" and aims to 'provide graduates with the necessary skills to balance environmental risks with all of the traditional variables of cost, quality, shareholder value and legislative compliance'. The Brunel/Surrey programme aims to balance a number of competing interests. The research engineer must reconcile both academic and industrial requirements of the research while considering the environmental issues inherent in the project undertaken. Figure i sums up the three elements of an EngD research project.
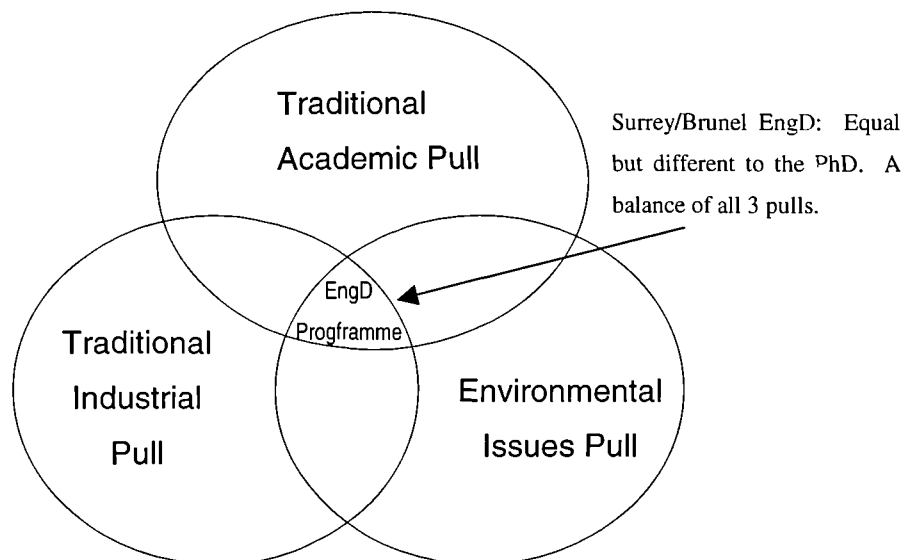
Figure i: The three elements of an EngD research project (EngD Course Handbook, 2003)

The EngD programme includes complementary courses that must be completed by the EngD Candidates. These courses have the following aims:

- To present a view of the relationship between engineering and the environment including sociological aspects.
- To provide professional development in key business skills and competencies.
- To close any gaps in the knowledge required in undertaking the research project.

The programme of courses is comprised of compulsory and elective modules and the completion of a relevant assignment is usually required after each course. The modules taken and successfully completed during this research are outlined in Table i, below.

Table i: Modules completed by the Research Engineer

Year 1	Induction course: Communication & Leadership I Clean Technology and Sustainability Project Management Life Cycle approaches Hands on Audit Risk Perception and Management
Year 2	Sociology I: Research methods Research Methodology Leadership II Environmental Law
Year 3	Sociology II: Environmentalism Risk Management
Year 4	Talking to the media Financial Management Scientific Paper Writing Elective Course (Diploma in Public Relations)

The EngD Candidates are also given the opportunity to present their research either orally or through poster presentations, at the annual EngD Conference. The conferences are attended by all EngD Candidates, supervisors and invited delegates. Papers written for the conference by the Research Engineer are included in published proceedings.

From the research conducted in this thesis, the following papers were written and published for the EngD conferences:

1. Somarathne S, Seymoure M and Kolokotroni M, (2000). *A Single Tool To Assess The Thermal And Environmental Performance Of A Typical Office Building*, Proc. Engineering Doctorate in Environmental Technology Annual Conference 1999, Brunel University and the University of Surrey, 12-13 September, pp190-199.

2. Somarathne S, Seymoure M and Kolokotroni M, (2002). *A Single Tool To Assess The Heat And Airflows Within An Enclosure: Preliminary Tests.* Proc. Engineering Doctorate in Environmental Technology Annual Conference 2002, Brunel University and the University of Surrey, 12-14 January, pp305-314.

3. Somarathne S, Seymoure M and Kolokotroni M, (2003). *An Efficient Dynamic Thermal Modelling Tool using CFD.* Proc. Engineering Doctorate in Environmental Technology Annual Conference 2002, Brunel University and the University of Surrey, 25-26 June, pp113-125.

Writing the EngD conference papers was extremely beneficial in reaching specific milestones in the research. The themes of the papers helped to maintain the direction of the project and confirm the overall validity of the work produced. Orally presenting at the EngD conferences contributed to clarifying an understanding of the research. Exposure to queries concerning the research from members of the conference audience was extremely invaluable in gauging its legitimacy from a wider academic perspective.

In addition to attending courses, submitting assignments and presenting the results of the research to the EngD Conferences, EngD candidates are also expected to complete a progress report every six months. The aim of these progress reports is to inform the EngD Programme Management Committee and supervisors of the progress made towards the completion of research projects at given stages during the programme.

This section gives a brief introduction to the EngD Programme in order to describe the overall framework of the research work included in this thesis. The following sections of the executive summary describe in more detail the research carried out. This includes a description of the research work including objectives, research methods and main results (Section II). A statement of the original facets of this research work follows together with a list of papers published in scientific refereed journals and conferences (Section III). The following Section IV describes the link between the research carried out in this thesis and a commercial project, in order to highlight the industrial and environmental relevance of the EngD research project undertaken over the four years.

II. INTRODUCTION TO THE RESEARCH TOPIC AND OBJECTIVES

The particular techniques researched in this thesis are novel to the field of commercial building services design. Similar attempts have been made by other researchers, but none have succeeded in establishing a dynamic thermal modelling procedure using computational fluid dynamics (CFD) alone. The main objectives of the research documented in this thesis are to provide the building services industry with an efficient and useful tool. In summary, two main objectives of the research have been to:

Research objectives

1. Develop an efficient dynamic thermal modelling (DTM) procedure within CFD, largely for the commercial use within building services design;

2. To apply an efficient DTM-CFD Procedure to a realistic case study of a building.

III. RESEARCH METHODS AND MAIN RESULTS

This section summarises the research methods and main research results from the research project carried out as part of this EngD Programme and are presented in detail in the following chapters of this research thesis.

After having gained experience in building services design (due to academic and industrial experience gained prior to undertaking the EngD), it was evident that using two building simulation tools in tandem in order to overcome each other's deficiencies as individual tools was an inefficient procedure. The building services industry has required an efficient dynamic thermal modelling (DTM) tool that is able to provide the accuracy and detail of CFD simulation.

Such a tool would provide the opportunity to improve the efficiency of building services design and hence reduce the impact on the environment through decreasing the demand for energy. The requirement for this more accurate, efficient, useful and environmental tool was especially apparent when contributing to the PII Project (a research project aimed at designing/demonstrating a more efficient building envelope and consequent energy efficient design), see Section V.

The need for a DTM-CFD tool has stimulated the necessity for research programs over a few decades. A literature survey was conducted in order to discover the nature of the various methodologies used by other researchers in the past. The survey revealed that a variety of techniques were attempted. The rate of progress of most of the research was mostly dependent on the rate of improvement in hardware capability. The literature survey also indicated that the proposed development of the DTM-CFD Procedure conducted in this research, had never been attempted before.

The proposed methodology of the research documented in this thesis involved developing an existing CFD tool to include functionalities of typical dynamic thermal models. In industry, three options were currently available to design engineers to obtain building simulations. The first method had been to use CFD to

model steady state simulations. In order to safely design and size building systems, CFD would be used to simulate 'worst-case' scenarios, such as the hottest day in summer and the coldest day in winter. The grid of the CFD model would be confined to the volume of air enclosed by boundaries. Boundary conditions would be supplied by a DTM, which would usually be in the form of surface temperatures. A DTM would simulate the time-dependant internal and external thermal conditions over an enclosure (including boundaries).

A second commonly used and less involved method would be to use CFD alone, without employing a DTM. To obtain boundary conditions, steady state heat transfer coefficient calculations involving the solids of the model would be performed in the CFD code. Ventilation rates (pressure/temperature driven) would be imposed and not calculated. This method ignored the thermal lag of the material, with a tendency to produce extreme results. Although the advantage of this method was that the extreme results were likely to be conservative from an engineering perspective, as a consequence, designs influenced by this method of building simulation were also likely to be wasteful of energy resources once the building was operational.

A third method was to include building fabric within the CFD calculation. Similarly to the second method, this method would also not require additional DTM simulation. This method was restricted to very simple enclosures, because to calculate for the different time constants over solids and air simultaneously was highly computationally expensive. Hence, the usefulness of this method was extremely limited.

Transient modelling within CFD is computationally demanding but is a necessary function for dynamically modelling buildings within CFD, especially when trying to capture the thermal changes resulting from external ambient conditions. As observed from the three methods of building simulation, commonly used within industry, all could not provide realistic analysis of the thermal heat transfer and airflow patterns within a building, over time. The focus of the research documented in this thesis was to develop transient modelling to function more efficiently than has

been currently available within CFD, and to a higher degree of accuracy than is available in DTM.

Once an efficient DTM Procedure was developed within CFD, it was tested, reviewed and revised. This process of development led to the establishment of a robust DTM-CFD Procedure. This procedure was then subjected to a series of further testing to determine what aspects of the procedure were vunerable to inaccuracies, and how these could be overcome.

Following the complete development of the CFD-DTM Procedure, the success of the methodology was put to the test by applying it to a realistic design case. The success of the solution was based on how well the DTM-CFD results compared with a fully transient solution (i.e. inter-model comparison).

The main results of the research were that the developed DTM-CFD Procedure did reduce the overall computational time required to produce a dynamic thermal simulation. The reduction in the computational time, however, took approximately 20% less time than solving a fully transient solution. The research did prove the developed DTM-CFD Procedure to be an effective and accurate method in solving a dynamic thermal CFD case. Measures were outlined for the further development of the tool, which could perhaps further increase the efficiency of the procedure.

IV. ORIGINAL CONTRIBUTION TO THE BODY OF KNOWLEDGE AND PUBLICATIONS

The particular facets of the work that are original are listed below:

- Dynamic modelling within CFD is relatively new;

An attempt has been made in the past to dynamically model time-dependant internal conditions within CFD, Tang (1998). No attempts have been made to incorporate fabric response to external ambient conditions within CFD, due to the problems arising from the differences in time constants of solids and air.

- The procedure of freezing and unfreezing flow has never been attempted before.

The 'freeze flow' function is not a new function within the CFD code. Its application for overcoming the problem of incompatible time constants of solids and air, however, is novel.

List of publications

The research carried out during this EngD programme has been published, both in peer reviewed journals and presented at academic international conferences.

Peer Reviewed Journal Papers

International Journal of Ventilation Vol. 1 (2002), Transient Solution Methods for Dynamic Thermal Modelling within CFD, Vol 1.

Peer Reviewed Conference Papers

1. Healthy Buildings (2003) Efficient Dynamic Thermal Modelling using CFD, Singapore

2. RoomVent (2002), A Single Tool To Assess The Heat And Airflows Within An Enclosure: Preliminary Test, Denmark Copenhagen.

3. Clima 2000 (2000), A Single Tool To Assess the Thermal And Environmental Performance Of Office Buildings, Naples, Italy.

V. INVOLVEMENT IN COMMERCIAL PROJECTS

Before research (documented in this thesis) into dynamic thermal modelling began, a contribution was made to a research project led by Oscar Faber, Building Services Consultants (now Faber Maunsell) on the PII (Partners in Innovation) Project. The title of the PII Project was HVAC Strategies For Well-Insulated Airtight Buildings and was conducted in order to explore the potential for high performance building envelopes to simplify the design and operation of HVAC (heating, ventilation and cooling) systems. The PII Project resulted in a CIBSE publication, CIBSE (2002). Contributors to the PII Project were:

Oscar Faber Group Ltd. (Now Faber Maunsell)

Building Research Establishment Ltd.

BSRIA Ltd.

Building Science Ltd.

CIBSE

Department of Trade and Industry

Flomerics Ltd.

IPPEC Systems Ltd.

Klima-Therm (Distribution) Ltd.

Pilkington plc

Trox (UK) Ltd.

SAS International Ltd.

The EngD candidate contributed to the PII Project by supplying CFD analysis of a single zoned office. Boundary conditions for the CFD model were manually applied to the CFD model in the form of surface temperatures, which were provided by a DTM analysis conducted by Oscar Faber Building Services Consultants.

Contribution to the PII Project confirmed the necessity for the research conducted in this thesis, since the results of the project suggested that there were significant commercial benefits to be had from high performance building envelopes. By taking advantage of the effects of thermal capacities of building materials upon the air they

enclosed, comfort conditions and space utilisation could be improved and operating and management costs of a building could be reduced. These conclusions were drawn from the implementation of a combination of steady state CFD modelling, dynamic thermal modelling and experimental work. The efficiency of the research conducted in the PII Project could have been greatly improved with the use of an integrated dynamic thermal CFD tool.

The influence of the PII Project has been most prominent both in the initial requirement of the research into the development of an efficient and effective DTM-CFD tool, and at the end. The DTM-CFD Procedure developed in the research documented in this thesis was then applied to a case study based on that originally modeled in the PII Project, with the objective of exposing the developed tool to a typical industrial application.

CHAPTER 1

INTRODUCTION TO BUILDING MODELLING TECHNIQUES

CHAPTER 1 - Introduction to Building Modelling Techniques

1.1.1 Introduction

Buildings expended 44% of the total energy consumed within the UK in 2001 (see Figure 1.1). 14% of this energy was consumed by service sector buildings of which 55% was for space heating, 3% for cooling ventilation and 15% for lighting (DTI 2002). A significant proportion of that energy is wasted due to inefficient design. Building services systems are often designed to heat, ventilate, air-condition and illuminate in accordance with several factors such as occupancy rates, building envelope design and external environmental conditions. The interaction of these factors are usually very complex, especially with sophisticated building envelope designs; hence building services designers and architects increasingly rely on the simulations of computational tools to predict how well their building systems will perform under different environmental scenarios.
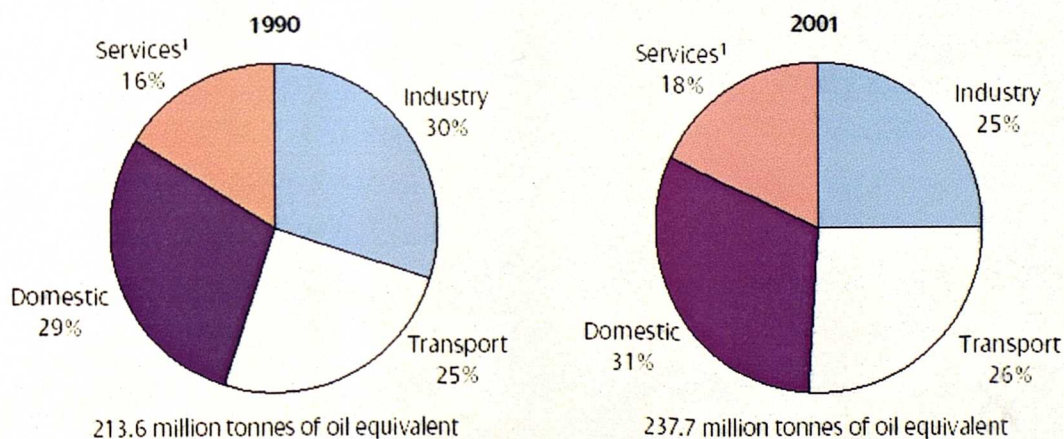
Figure 1.1:   Final Energy Consumption by end use, 1990 and 2001 (DTI 2002)

Current simulation tools are limited by hardware capacity, since high computational analysis is required to represent accurate and detailed airflow patterns and thermal conditions within buildings over a substantial period of time. A less time and computationally intensive option (which is commonly used within industry today) is to solve time independent simulations that are constructed to represent single worst-

case scenarios; such as an extremely cold winter's day; or a very hot summer's day. If building systems can perform under these extreme conditions, then they are assumed to function throughout the year.

Simulating the conditions in buildings for extreme conditions using simulation tools usually results in over-designed buildings. An excessive amount of energy is wasted as a result of manufacturing over-sized plant rooms, which are likely to be running at a reduced efficiency, creating an unnecessary detrimental impact on the environment. The costs involved in running a business, particularly human resources costs often exceed energy costs and therefore reducing environmental impact is not a priority for engineers, architects, employers and building managers. Hence a simulation tool should allow environmental considerations to be easily factored into building design.

Hence, what is required within industry is a single computational simulation tool that takes into account all internal and external environmental factors of a building, such as indoor air quality (IAQ), thermal comfort and energy consumption. Currently such varied aspects of a building are simulated using separate computational tools. Much research has been carried out to integrate these simulation tools, but there is still room for further development.

Computational simulations of building environmental performance (from a thermal comfort, ventilation effectiveness and energy consumption point of view) in industry today are commonly performed using two software tools in tandem, a dynamic thermal model (DTM) and computational fluid dynamics (CFD). Both tools are used to compensate for each other's deficiencies as individual building simulation tools to provide an overall indication of the environmental performance of a building. A DTM provides a holistic, but relatively simplistic evaluation of an entire building over a length of time, accounting for internal and external conditions, including the building envelope, weather patterns, ventilation patterns and occupancy rates.

A DTM can provide boundary conditions, usually in the form of surface temperatures, which are then manually transferred to a CFD model. A CFD model will then be used to accurately model the internal conditions of a building under

3

worst-case conditions in steady state (i.e. for one particular snap-shot in time). The CFD model will provide a highly detailed (subject to grid configuration) simulation of the thermal conditions within the building.

The current procedure of using two simulation tools in tandem does not easily permit the simulation of a building over a period of time. To obtain such results would require high computational power to be able to simulate the heat transfer between different mediums of a building such as building material and air, both of which have significantly different rates of thermal response.

To allow the design of more environmentally efficient building systems, by encompassing most aspects of a building, such as building fabric and HVAC systems, an integrated commercial tool must be developed that incorporates the functionalities of DTM and CFD, (Donn (2001)). This tool could provide building services engineers and architects (through specialist modellers) with an opportunity to effectively simulate the fabric response, air movement and heat transfer simultaneously for selected zones of a building (or even an entire building) over a length of time. The integrated tool should provide accuracy comparable to existing CFD codes to alleviate the detrimental effect excessive energy consumption has on the environment.

1.2   Modelling Techniques for Buildings

1.2.1   Theory and Description of Numerical Models

Much research has already been undertaken to achieve a more integrated and accurate design tool that can model the thermal response of buildings dynamically. A comprehensive review of previous research is reported in Chapter 2. However, in order to fully appreciate how and why certain previous techniques have been attempted, and not yet become commercially successful, requires background knowledge of DTM and CFD. In this section the numerical models of each tool are described. A review of the feasibility of combining the two tools is presented by examining the similarities and differences between them.

Dynamic Thermal Modelling (DTM)

DTM can be used to simulate the thermal conditions within a building (which could be multi-zonal) by considering the thermal exchanges internally and externally to the building. The thermal exchanges that occur are usually driven by time-varying weather conditions and fluctuating internal thermal loads. Internal and external thermal conditions interact simultaneously by three thermal mechanisms, conduction, convection and radiation. Conduction will predominantly occur between the layers of fabric used within the building envelope; while convection will occur between solid building fabric and internal/external air. Radiation occurs between internal solid surfaces and from external surfaces of a building to external ambient conditions.

To simulate over various building mediums by accounting for their differing rates of thermal response, the different components of a DTM (i.e. individual layers of building fabrics and zones) are usually represented by nodes. Thermal exchanges between the nodes are calculated using the conservation of mass and energy via a finite difference method. (See Equations 1.2 and 1.4).

The network of nodes of each building component assumes thermal uniformity within the various components, i.e. a zone of a building could contain one node and hence one averaged air temperature for this zone will be calculated at this nodal point. Generally, most DTM codes do not consider the detailed airflow patterns within a zone or over a layer of building fabric and hence do not provide a detailed thermal analysis of thermal exchanges within the components themselves.

Some DTM codes have enhanced thermal models where additional codes have been incorporated into the software to account for detail when necessary. For example, the dynamic thermal modelling of tall buildings could be implemented in DTM software, which also contains additional code that can account for stratification effects (for example IES-Facet) based on the solution of additional conservation equations.

DTM has been developed extensively (Hong, 2000), particularly towards integrating various other building services software tools to achieve a more holistic thermal analysis of buildings. Generally, however, one of the fundamental differences between DTM and CFD is that the Conservation of Momentum (Eqn 1.3) is not considered in a DTM code and ventilation rates are assumed or derived from empirical models.

Computational Fluid Dynamics (CFD)

Computational Fluid Dynamics focuses on simulating much more detailed flow, usually for a particular zone of a building. The grid used over the zone is usually much denser than that used by a DTM. A finite-volume numerical model is employed within most CFD codes, which considers the temperature, pressure, velocity and turbulence characteristics of each finite volume. In addition to all the equations that are also used in DTM, momentum equations and equations associated with turbulence modelling are further included to the set of governing equations in CFD. Again, the equations are based on the principles of conservation of:

- Fluid mass (continuity)

- Fluid Momentum in the Cartesian grid, x, y, and z directions – u, v, and w
- Thermal energy – T

All equations used in the computational model of CFD can be expressed in a common form:

$$\frac{\partial}{\partial t}(\rho\varphi) + div(\rho\vec{V}\varphi - \Gamma_\varphi \ grad\varphi) = S\varphi \qquad (1.1)$$

transient +convection-diffusion = source

where:

$\vec{V}$ =velocity (ms^{-1})

ρ =density (Kgm^{-3})

φ dependent variable

Γ_φ= exchange coefficient (laminar plus turbulent)

S_φ = source or sink term

Equation 1.1 can be broken down into individual equations, as follows:

Continuity:

$$\frac{\partial\rho}{\partial t} + \frac{\partial}{\partial x}(\rho u) + \frac{\partial}{\partial y}(\rho v) + \frac{\partial}{\partial z}(\rho w) = 0 \qquad (1.2)$$

ρ = density (Kg/m^3)

u, v, w = Velocity vectors in the x, y and z directions (respectively) (m/s)

t = time (s)

x = Momentum (y and z similar):

$$\frac{\partial}{\partial t}(\rho u)+\frac{\partial}{\partial x}(\rho uu)+\frac{\partial}{\partial y}(\rho vu)+\frac{\partial}{\partial z}(\rho wu)-\frac{\partial}{\partial x}\left(\mu_{\mathit{eff}}\frac{\partial u}{\partial x}\right)-\frac{\partial}{\partial y}\left(\mu_{\mathit{eff}}\frac{\partial u}{\partial y}\right)-\frac{\partial}{\partial z}\left(\mu_{\mathit{eff}}\frac{\partial u}{\partial z}\right)=-\frac{\partial P}{\partial x}$$

$$\mu_{\mathit{eff}}=\mu+\mu_{t}$$

(1.3)

ρ = density (kgm^{-3})

u, v, w = Velocity vectors in the x, y and z directions (respectively) (ms^{-1})

t = time (seconds)

P = Fluid Static Pressure (Pa)

μ_{eff} = Effective Viscosity (laminar plus turbulent) (Nsm^{-2})

μ = Turbulent Viscosity (Nsm^{-2})

μ_t = Laminar Dynamic Viscosity (Nsm^{-2})

Temperature:

$$\frac{\partial(\rho C_p T)}{\partial t}+\frac{\partial(\rho u C_p T)}{\partial x}+\frac{\partial(\rho v C_p T)}{\partial y}+\frac{\partial(\rho w C_p T)}{\partial z}-\frac{\partial}{\partial x}\left(\lambda_{\mathit{eff}}\frac{\partial T}{\partial x}\right)-\frac{\partial}{\partial y}\left(\lambda_{\mathit{eff}}\frac{\partial T}{\partial y}\right)-\frac{\partial}{\partial z}\left(\lambda_{\mathit{eff}}\frac{\partial T}{\partial z}\right)=\frac{\partial P}{\partial t}$$

$$\lambda_{\mathit{eff}}=\lambda+\lambda_{t}$$

(1.4)

ρ = density (kgm^{-3})

x, y and z directions (respectively) (m)

t = time (s)

P = Fluid Static Pressure (Pa)

C_P = Specific Heat Capacity (Jkg^{-1}K^{-1})

T = Temperature (K)

λ_{eff} = Effective Thermal Conductivity (Wm^{-1}K^{-1})

λ = Thermal Conductivity (Wm^{-1}K^{-1})

λ_t = Turbulent Conductivity (Wm^{-1}K^{-1})

These equations combined with the k-ε Turbulence model, complete the set of governing equations used in CFD.

Turbulence models:

In this research, a Revised k-ε turbulence model was chosen as being one of the most commonly used turbulence models for simulations within buildings. For the nature of the research conducted, the choice of turbulence model is not critically important. The important factor is that the choice of turbulence model is consistent throughout the research. This is because the development and testing of DTM within CFD is largely through intermodel comparisons of developed DTM solution procedures.

The Revised k-ε turbulence model is used instead of the Standard k-ε turbulence model. The Standard k-ε model calculates the turbulent viscosity for the fluid cells immediately adjacent to the cells on the internal surface of the solid surfaces as a function of two field variables, the kinetic energy of the turbulence (k) and its rate of dissipation (ε). These two field variables are determined by the solution of two additional differential equations, which these variables satisfy (Lauder, 1974). For the cells immediately adjacent to the wall, a skin friction factor is computed, (Hinze, 1975).

The Revised k-ε Turbulence model calculates an identical value of the turbulent viscosity for the bulk fluid, as does the k-ε Standard Model option, but it allows the value to vary according to the.log law of the wall for those cells close to solid surfaces. (Agonafer, 1996). The Revised k-ε model was developed for more accurately capturing flow along the solid boundaries of the CFD model, which tend to contain flow with low Reynolds' numbers (i.e. <5000).

The transport equations for k and ε are:

$$\frac{\partial \rho \overline{U}_i k}{\partial x_i} = \frac{\partial}{\partial x_i}\left(\left(\mu + \frac{\mu_T}{\sigma_k}\right)\frac{\partial k}{\partial x_i}\right) + P + G - \rho\varepsilon \qquad (1.5)$$

$$\frac{\partial \rho \overline{U}_i k}{\partial x_i} = \frac{\partial}{\partial x_i}\left(\left(\mu + \frac{\mu_T}{\sigma_k}\right)\frac{\partial \varepsilon}{\partial x_i}\right) + C_1 \frac{\varepsilon}{k}(P + C_3 + G) - C_2 \rho \frac{\varepsilon^2}{k}$$

(1.6)

where:

$\overline{U}$ = Mean Velocity (ms^{-1})

U_T = Eddy Viscosity (Nsm^{-2}), defined as:

$$U_T = C_\mu \rho \frac{k^2}{\varepsilon}$$

P = Shear Production, defined as:

$$P = \mu_{eff} \frac{\partial \overline{U}_i}{\partial x_j}\left(\frac{\partial \overline{U}_i}{\partial x_j} + \frac{\partial U_j}{\partial x_i}\right)$$

(1.7)

μ_{eff} = Effective Viscosity (laminar plus turbulent) (Nsm^{-2})

μ = Turbulent Viscosity (Nsm^{-2})

μ_t = Laminar Dynamic Viscosity (Nsm^{-2})

G = Production of turbulence kinetic energy due to buoyancy, defined as:

σ_k = Coefficient (see Table 1.1)

$$G = \frac{\mu_{eff}}{\sigma_T}\beta g_i \frac{\partial T}{\partial x_i}$$

(1.8)

β = Turbulent Prandtl Number for Temperature (K^{-1})

g = gravity (ms^{-2})

ρ = density (kgm^{-3})

Table 1.1 Constants used in k-ε Revised Turbulence model Equations:

C_μ	C_1	C_2	C_3	σ_k	σ_ε
0.09	1.44	1.92	1.00	1.00	1.22

(Values of Constants have been taken from the Flovent Reference Manual 1994)

1.3 Fundamental Differences between CFD and DTM

Both software packages function on fundamental similarities of the basic principles of heat transfer, and both require the specification of similar building details. Yet both tools are commonly used as independent software codes and their results are manually swapped between them; mainly in the form of surface temperatures used as boundary conditions from the DTM tool. The main differences between DTM and CFD have been summarised in Table 1.2.

Table 1.2: Fundamental Differences between DTM and CFD.

DTM	CFD
DTM is focused on the overall building system, including the building plant systems, inter-space airflow, intra-constructional heat flux, occupancy and control systems and external weather details.	CFD models are useful for modelling localised fluid flow regions within a building system. CFD is usually used to model zones with regions that cause problematic flow, such as supply and extract openings.
DTM provides relatively simplistic information of a multi-zone building over long periods of time.	CFD typically provides highly accurate simulation of a particular instant in time for a specific zone.
DTM is employed where air is considered to be more mixed.	CFD is used where air property gradients are judged to be crucial.
The rate of heat transfer is considered over long lengths of time. DTM takes into consideration, external and internal ambient variation, and the consequential thermal response of the building envelope.	CFD models are usually run in steady state, hence, it is assumed that the conditions in the model do not change. The solution provides a simulation for a representative snap-shot in time.
The behaviour of the fluid is prescribed in terms of macroscopic properties, such as average volumes (which could even be whole zones of a building), pressure, and temperature, and their space and time derivatives.	CFD takes a finite-volume approach, examining significantly smaller volumes of air, compared to that of a DTM code.

Internal surface convection cannot be properly computed.	CFD can effectively model surface convection by incorporating wall functions into the solution process.

The most significant hindrance to combining the two codes is the time constants under which they operate. The time constants required over building fabric are vastly different to the time constants over air and hence, have made the fusion of the two packages almost impossible. CFD contains a complete set of governing mathematical equations of heat transfer and the conservation of mass and momentum, and therefore has the capacity to undertake all of the functions of DTM, but the computational capacity required to simulate the slow response over building materials is excessive. The consequence is that CFD programs have not been developed to act as DTM codes and therefore do not contain such features as plant models or weather data.

CFD is commonly used only to provide steady state analysis, even when incorporated into DTM codes. In order for a CFD model to independently account for dynamic thermal changes, it would have to operate under transient conditions. The differences between the steady state and transient functions have been clarified below:

- Steady State Modelling

  A solution process that allows the thermal conditions and initial thermal settings within the domain to reach equilibrium. The results are not time dependant.

- Transient Modelling

  Transient modelling is time-dependant. A transient grid is superimposed over a chosen transient *period*, each transient time grid cell is referred to as a transient *time step*. Thermal conditions can then be predicted over the specified time period according to the thermal loads (which could be subject to change) that occur over time. Airflow and temperature solutions can be

saved and viewed from the simulations at any chosen time within a transient period.

Despite the fundamental incompatibilities between DTM and CFD, techniques have been researched and developed to combine the two tools. The following chapter describes the previous techniques used to develop DTM and CFD individually to enhance their performance as DTM tools and ways in which the two software codes have been merged together.

1.4 Chapter Summary

The similarities between the mathematical techniques of DTM and CFD and their requirements for the specification of similar building design characteristics, indicate that the two procedures could be effectively and usefully combined.

There are, however, fundamental differences between the two software approaches, which must be resolved before the two packages are coupled. Embedding DTM techniques into CFD will improve the accuracy of the CFD simulations, but solving for time constants required over different physical mediums will provide the biggest hurdle in achieving a combined tool. Nevertheless, CFD contains all the necessary functions and governing equations, in order to simulate heat transfer through the building fabric.

The following chapter examines the variety of methodologies of past research groups in coupling the two computational methods. Much research has been produced in this field, but has often been hindered by computational hardware capability.

Chapter 3 reports the development of a preliminary dynamic thermal modelling procedure in CFD from first principles. The performance of the procedure is improved through additional testing. The nature of the preliminary procedure called DTSP#1, is reviewed. As a result, Chapter 4 reports the development of a revised dynamic thermal modelling procedure, called DTSP#2. The performance of DTSP#1 and DTSP#2 are compared against each other and with a fully transient

CFD model. Chapter 4 concludes that the DTSP#2 is the better dynamic thermal modelling procedure and is used for further development, documented in Chapter 5. At this stage in the research, DTSP#2 is renamed the DTM-CFD Procedure.

Chapter 5 reports the tests conducted to refine the DTM-CFD Procedure. The tests focus on identifying the cause of residual errors generated by using the procedure. Rigorous investigations are conducted to establish the constraints within which the DTM-CFD Procedure functions. The tests reveal that the procedure is flawed under certain extreme modelling conditions.

After the tests of Chapter 5 establish the optimum conditions under which the DTM-CFD Procedure performs, the procedure is then applied to a realistic case study. Chapter 6 reports the implementation and results of applying the DTM-CFD Procedure to model a typical office over a 24-hour period. Overall the DTM-CFD Procedure was successful in providing a more efficient solution to dynamic modelling, but recommendations for future work have been suggested to improve the performance of the DTM-CFD Procedure in Chapter 7.

CHAPTER 2

PREVIOUS RESEARCH IN COMBINING

DTM AND CFD

CHAPTER 2 – Previous Research In Combining DTM and CFD

2.1 Improving the power of DTM

Various attempts have been made to combine the two packages together. The earliest record of awareness for the need for a more integrated code was in 1988, by Clarke and Irving (1988). Their aim at that time was to publicise the need for a more accurate and general-purpose building simulation tool, which linked and exchanged information provided by separate academic arenas, such as:

1. heat transfer and fluid flow from thermodynamics;
2. numerical methods from mathematics;
3. graphics from computer science;
4. knowledge engineering techniques from the artificial intelligence community.

A group of building simulation packages was collectively referred to as computer aided building design (CABD), although it went through a series of developments, starting off as a graphics package. It was viewed that the development of such a tool could have significant environmental implications and create an opportunity for substantial energy savings. Inefficient building thermal design was viewed as an unnecessary waste of energy resources, which could be overcome through better building design.

At that time, CABD was viewed as the most likely tool to be developed to provide a useful energy analysis of a building. The input required from the design engineer into CABD, describing geometrical and thermal information, was then further developed to incorporate numerical techniques, using the information it stored. As research continued, CABD was combined with additional building simulation software.

Due to hardware limitations, the proposal of Clarke and Irving (1988) of a powerful design tool, was more of an ideal vision, rather than a realistic goal, at that point in

time. Nevertheless, their work outlined a direction for its progress, and called for the development of various additional computational building simulation elements to enhance the overall performance of CABD. In 1988, Clarke (1989) wrote another paper highlighting various other building simulation codes, which were being developed simultaneously.

During the late 1980's, the integration of CFD techniques was receiving less attention compared with integrating a variety of other building simulation codes, such as lighting and solar calculations. Clarke (1989) outlined four key stages of the development and progression of a powerful building simulation design tool: Stage one involved starting from simple steady-state cases and stage four involved modelling time-varying fully integrated advanced numerical methods. Clarke (1989) was fully aware, that the progression towards such a tool would be slow and heavily influenced by computational capability.

The research conducted by Clarke (1989) utilised the EPS (Energy Performance Simulations) System, which was viewed as existing between the 2nd and 3rd stages of the development of the 'ideal' thermal design tool. The EPS system would have incorporated a variety of software modules (used in the simulation of various aspects of a building), where information is exchanged between them. Clarke (1989) also described the Energy Kernel System (EKS), a software/hardware environment, which allowed the construction of a program from pre-existing objects. A technique similar to that used by CABD.

Since the late 1980's, Hong et al. (1997) contributed in further developing a more useful thermal design tool. IISABRE (Intelligent Integrated System for the Analysis of the Building theRmal Environment) was created by the HVAC (Heating, Ventilation and Air-Conditioning) division of Tsinghua University, Beijing.

IISABRE (illustrated in Figure 2.1) contained CABD, the building thermal performance (BTP) code, IISPAM (IISPAM is a knowledge-based system for translating the STEP-based building database into ASCII-based data files required by BTP) and a STEP (Standard for the Exchange of Product Model Data, ISO 10303

(1992)) - based building database, which could be generated within CABD, to provide an open mechanism with which to share the building database with other simulation programs.

As time progressed, the nature of the development of a more powerful tool was becoming more refined. The focus of the research was on the improvement of codes for thermal analysis rather than a graphics based tool, by linking information from separate building simulation software codes, as illustrated in Figure 2.1.

Tianzhen Hong et al.
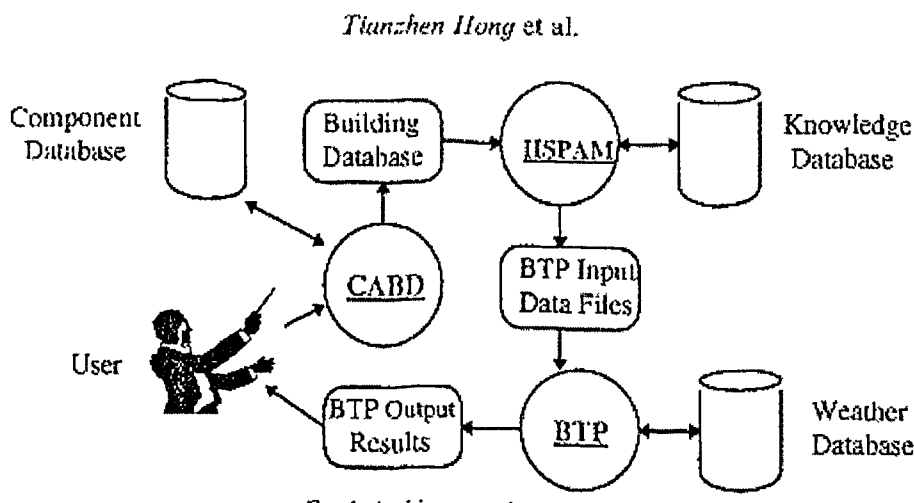
Fig. 2.1: Architecture of IISABRE (Hong (1997))

The overall potential for linking different modules together is rapidly increasing, especially with the speedy development of internet capacity, Lam et al. (2002). As building design becomes more sophisticated, the availability of building constructional details for the use of DTM codes can be made available and automated through the World Wide Web. Such facilities may become necessary since the amount of information required on the building geometry, construction materials, properties and context (such as weather) for example, is increasing.

However, whether linking building simulation details locally or across the web, there have been problems associated with the technique of combining various modules, predominantly, the incompatibility of various sources of information, which

complicate the further development of a single tool. In comparison, however, the advancement of individual components has not been hindered. BTP, developed by Hong *et al.* (1997) at Tsingua University since 1990, was considered to be a state-of-the-art simulation strategy, at that time.

Within their BTP package, the simulation process was grouped into three stages, a technique similar to a transfer-function technique introduced by ASHRAE (1975). In the first stage, the building thermal model was generated, i.e. the solution was solved on a macroscopic level including the effects of outdoor and indoor thermal changes, thermal radiation, and the effects of heating/cooling systems. The room thermal response vectors were generated for all heat disturbances.

The second stage of the solution process in BTP included the calculation of the sealed zone temperature caused by internal and external heat sources and sinks. This stage of the solution did not take into account the HVAC system of the building. The third and final stage of the solution calculated the rise of zone temperature caused by airflow. The temperatures obtained in this stage of the solution were compared with the temperatures obtained within the previous stage. The differences in temperature as a result of the heating or cooling of the HVAC system were taken into account. This solution procedure used was similar to most other BTP packages, at the time.

During the mid-1990's, BTP codes based on the 'network flow' model had been developed, such as TARP (Thermal Analysis Research Program). Most of these 'network-flow' models, at that time, were unable to model detailed airflow patterns within a zone. This was because the formulation of these models usually included only the steady state mass-balance equations per time step for a coarse network of nodes (superimposed over various components of a building zones, such as walls and air) and ignored the momentum equations for the flow elements between the nodes.

Similarly, most thermal models such as BLAST (Building Loads Analysis and System Thermodynamics), SERIRES (Solar Energy Research Institute Residential Energy Software), and TASC (Total Air-Conditioning system Simulation Code),

were based on the heat balance method. The heat balance method calculated heating and cooling loads for each time point by solving the transient heat balance equations for each thermal node simultaneously. The transient heat fluxes through the building materials used the response factor method or the finite difference method.

Tuomaala and Rahola (1995) used the BUS (v3.2), which modelled the dynamic behaviour of airflow and heat transfer in a simple zone, simultaneously. The code used was novel at this time, since it used an improved SIMPLE (Semi-Implicit Method for Pressure-Linked Equations) algorithm to solve the mass balance equations at every node and the momentum equations of each flow element simultaneously. The method also used a similar process of three iteration levels (also used by previous and subsequent researchers).

The first iteration process in BUS (v3.2) solved the SIMPLE algorithm, where the air node pressures (and airflow rates between the nodes) were solved, within a building zone. The second iterative process consisted of an algorithm called the Preconditioned Conjugate Gradient (PCG) algorithm, which solved for both linearised airflow and thermal analysis problems. Again, as the method described by Hong *et al.* (1997) also illustrates, the third iterative process was to compare the solutions of both the airflow and heat transfer simulations before being combined.

In the mid to late 1990's, the nature of the research seemed to have divided. Some research focused on developing powerful CABD, with a good thermal modelling capacity and an excellent graphical interface. Other research focused on developing a more sophisticated DTM code, which utilised effective numerical techniques to solve detailed heat transfer and airflow patterns simultaneously, since airflow directly affects thermal conditions and they often could not be considered seperately.

The latter represented the work carried out by Tuomaala and Rahola (1995), but as a result, BUS (v3.2) still had to resolve the problem of a weak graphical interface and include a storage facility for data (for component libraries and coefficients). The representations of the external conditions to the modelled zone, also contained inaccuracies, which had to be further improved.

The work conducted by Tuomaala and Rahola (1994), was important in directing research towards combining the effects of heat transfer and airflow paths simultaneously in dynamic thermal cases. However, significant further work was required to improve BUS (v3.2) and similar tools, especially in including the effects of thermal heat transfer through the building envelope and air contained within the building envelope.

A paper published by Boyer *et al.* (1996), documented this concept, by considering mono-dimensional heat conduction in the walls and well mixed air volumes of each thermal zone in a building. The program used, CODYRUN, was developed specifically for the research conducted by Boyer *et al.* (1996) to model both natural ventilation and moisture transfer in multi-zones of a building.

The problem identified by Boyer *et al.* (1996), was that in performing multiple stages of calculations, significant amounts of data had to be combined and then stored. Their research identified that the various stages of solutions had to be confined in size, in order to reduce the computational time. Nevertheless, the procedure of thermal modelling the air inside an entire building zone, including the building envelope, appeared to have good potential for further development.

In further work written by Boyer *et al.* (1998), the code had been developed to model thermal conditions inside the building and through the building envelope, for varying conditions over time. The software was again split into three separate modules, used to describe the building. The idea behind splitting the software into three modules, was to divide the building into 3 three types of entities called zones:

1. thermal zones of the building;
2. inter-ambiences (separations between zones, the outside being considered as a particular zone);
3. component (walls, windows, air-conditioning systems etc.).

The application of CODYRUN was more useful in simulating a building (mono-zonal or multi-zonal) to estimate energy consumption over any length of time ranging from one day to one year. The processes of combining the thermal and airflow analysis of all components of a building were necessary to aid those calculations. Emphasis was less focussed on providing a good thermal analysis of the internal conditions of the building for system design purposes.

Schibuola (1997) also supported the concept of developing DTM for energy consumption analysis, rather than a detailed airflow and heat transfer analysis tool. Schibuola (1997) stressed in his paper that a review of databases containing building materials and element property data, HVAC technical performances and meteorological data was necessary to simplify the pre-processing process of data inputting.

The published research described above, all examined various aspects of developing a more powerful BTP tool. Each of the researchers had independent objectives for their research. Some researchers wanted to develop a more applicable tool for determining specific quantities such as energy consumption, some wanted a more generalised tool to provide a more accurate thermal analysis of multi-zones, for example.

2.2 Combining CFD into DTM to improve accuracy

It was not until after the mid to late 1990's that DTM codes incorporating CFD came into existence, although some of the earliest publications of the concept of the combination of CFD and DTM were given by Chen and Jiang (1992) and Holmes *et al.* (1990). DTM and CFD were used in parallel to swap and compare information. By combining the techniques of DTM and CFD and also by incorporating pre- and post- processing techniques, it was felt that a powerful airflow and heat transfer analysis could be achieved over simulated time frames.

A technique, effective in modelling the heat transfer through the building envelope and the internal air simultaneously, was the conjugate heat transfer approach. This approach was experimented with by Moser *et al.* (1995), Kato *et al.* (1995) and Schild (1997). In this approach, the airflow calculation included the solid walls and part of the external airflow. The walls were then treated by the CFD program not as air but as a different type of medium with material properties of the wall structure.

Moser *et al.* (1995) used this approach, and concluded that three problems would have to be resolved, to improve the overall performance of coupling thermal solutions for airflow and transfer through solid materials simultaneously. These three problems were as follows:

1. defining the interfaces and linking the parameters;
2. formulating acceptable simplifications to make the numerical task manageable (reasonable computing times);
3. developing robust algorithms that converge quickly without complicated user interface.

Moser *et al.* (1995) claimed that the computational effort for the whole thermal problem of a zone was enormous due to the long physical time spans of several hours involved. Hence, as a result, their research was limited to a restricted number of simple cases but they did, however, conclude that this methodology was successful.

Although briefly suggested in their work, Moser *et al.* (1995) did not implement the use of a variety of time step lengths over the solid material and the internal air. However, Moser *et al.* (1995) did briefly suggest this technique as a possible solution to the problems of vast quantities of data generated. The non-use of this technique may have been due to the under-development of transient time-steps, at that time, although this is not entirely clear.

Despite using the 'conjugate heat transfer' method, Moser *et al.* (1995) continued to use a separate dynamic thermal calculation to provide initial boundary conditions for

the zone modelled. This seemed to be a common technique of research at this time, since appropriate initial boundary conditions for the model were required.

Even to this present day, the codes remained separated, despite attempts to embed DTM techniques into CFD, Bartak *et al.* (2002). The differences between the work of the various research groups, appeared to be how the information between the two codes were combined. Essentially, the following three research groups (described below) outlined by Zhang (1990), maintained DTM and CFD as separate codes, where the data generated by both codes was exchanged through the use of a third communal tool.

Research Group 1 – The Modified Air Temperature Gradient
Information from CFD is fed directly into a DTM code

The technique used by Negrao (1998) to combine DTM and CFD involved embedding CFD within the DTM package. Negrao (1998) used the code, EPS-r. Although this had been a common approach in the past, the technique he used was more successful this time, because the developments in hardware allowed the storage of larger quantities of data generated. Essentially, his approach was to identify initially problematic zones within the building model, and then apply CFD in these regions. This would ensure that the detail of flow (generated by CFD) in these areas, would provide enough information to simulate more accurately the complex behaviour of the air in these areas.

The two algorithms, (of DTM and CFD) and the subsequent sub-matrices, were essentially solved independently under transient conditions. Negrao (1998) stated that it was fundamental to the success of the technique that the two codes remained separate. The connection between the two solutions was made at the interface of the systems (zone internal surfaces and openings) where conservation principles were obeyed. These results were integrated and compared through a further iterative process.

Negrao (1998) pointed out that the comparison of momentum equation results of DTM and CFD solutions (through the further iterative process) generated convergence problems. Temperature equations, however, posed less of a problem; proving to provide a strong link between the two simulations. Negrao (1998) also used the technique of solving only the energy equations at the solid/air boundaries. These equations calculated energy balances for inter-constructional energy and air zone balances. Using this technique, the matrix coefficients for each time step were determined.

The research conducted by Negrao (1998) assumed that undetailed behaviour in one zone (which is prejudged by the software user) would not influence what happened within adjacent detailed zones (where the CFD was imposed). This assumption would have compromised on accuracy, although, the method used by Negrao (1998) increased accuracy of the thermal analysis of a zone, compared to using DTM alone.

The success of the method used by Negrao (1998) relied on the relative lack of detail of space and time of the CFD code and the increased detail of space and time required from the DTM code. Larger gradients obtained within a zone using CFD created convergence problems when comparing solutions within DTM. The methodology used in this research appeared to be effective for the particular case study presented. The simulated zones within the room had openings rather than closed doors and air could flow freely between them, therefore providing information on the thermal relationship between building zones. This methodology, however, still required substantial further development to be used as a general-purpose technique.

Research Group 2 – The Sequential Substitution Method
Solving both DTM and CFD in sequence and comparing the Results

Neilson and Tyggrason (1998) used a similar technique to Negrao (1998) in that CFD was used with DTM and the results were compared through an additional process of iteration. The emphasis of the research work conducted was to study the influence of the airflow between different zones in a building. The methodology

26

used was to compare the air exchange values obtained from DTM (tsbi3) and the CFD code, FLOVENT, as separate codes. The model produced was for a particular instant in time, hence changing boundary conditions, with time, and the consequential effects on the internal conditions with the CFD model were not addressed.

The theme of combining CFD into DTM has continued into the 21st Century, Bartak *et al.* (2002), because the methodology appears to provide one feasible solution towards detailed dynamic thermal modelling, although research has been required to improve the technique. Since, the zonal network and CFD are maintained as individual tools, where information is swapped between them, the extant problem of data-coupling remains. Continual research along this particular technique of the development of DTM, has seen an improvement towards increased accuracy by interdicting additional techniques such as a 'conflation controller', Beausoleil-Morrison (2000) and the 'gradient diffusion hypothesis (GGDH), Daly and Harlow (1970).

One of the main disadvantages of developing a DTM code by incorporating CFD is that CFD could only be used in a limited number of zones of a building. The user of this tool would have to compromise on where CFD would be placed within the solution domain, and naturally would choose zones with known problematic region of airflow. Nevertheless, researchers who have taken this route of approach still continue to develop a far more holistic tool, Clarke (2001).

Research Group 3 – The Construction Multi-Division Method

Both CFD and DTM are solved, both packages are similar in detail, i.e. the DTM is more detailed and the CFD model is less detailed.

Tang (1998) used Microflo in his research, which was a progression of the work produced on the development of CABD techniques in research conducted by Hong *et al.* (1997). Microflo also utilised the 'suite of software modules' concept by grouping them together. The core element of Microflo, however, was a CFD simulation engine, while the research involving CABD did not include much CFD

27

coding. Using a CFD engine as the core of a dynamic thermal model, was a relatively novel technique. Microflo was capable of modelling problems associated with transient three-dimensional turbulent airflow, with thermal buoyancy and concentration diffusion for either inside or outside of buildings.

This research marked a change in the direction of development of building simulation research. Rather than improving DTM, emphasis was finally placed on increasing the accuracy of building simulation packages by incorporating DTM simulation into CFD. Tang (1998) still maintained the various codes involved, as separate modules, linked via a communal database, as illustrated in Fig 2.2.
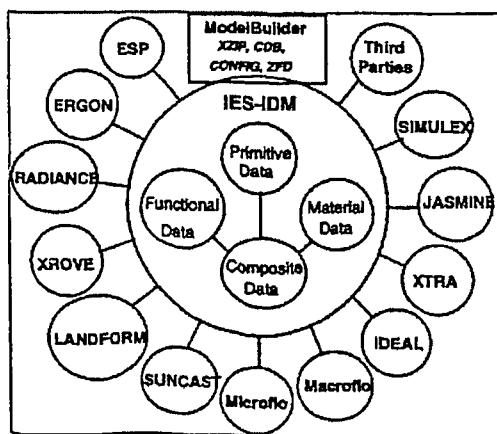
Fig. 2.2: Architecture of IES (Tang 1998)

One major advantage of Microflo, was the necessity to specify every characteristic of the building's construction. Each model then became a useful database of information of the building. For comprehensive thermal analysis, and the boundary conditions for the CFD model, ESP and Macroflo were used.

ESP took into consideration the effects of the building structural, thermal, occupancy, operations of the HVAC system and control against realistic climatic conditions of the entire building. Macroflo considered the flow on a more macroscopic level of the airflow-simulation system. It would take into account the effects of internal ventilation, wind pressure outside the building, buoyancy and

stack effect, infiltration from the opening of windows and doors and any cracks or gaps of the building and operations of the control system.

Both ESP and Macroflo ran simultaneously and provided adequate boundary conditions, which could be input, either manually or automatically into the CFD model. The boundary conditions could then be fed back into ESP and Macroflo, after being used in the CFD model, to be corrected and updated. This technique underlined the principle of the Modified Air Temperature Gradient Method.

The two novel techniques introduced by Tang (1998) at this time, was firstly, dynamically modelling within CFD using transient functions, and also the use of variable time stepping, to allow for faster steady-state solutions. Hence, Microflo could provide the use of time-dependant boundary conditions, which could have been defined either as continuous time functions or time discrete events. By doing this, Microflo was able to model the real time, instantaneous responses of the building, such as the disturbances caused by the activation of a ventilation fan or pressure on windows of a high rise building due to changes in wind direction.

The procedure proposed in the research described in this thesis, will involve the use of time-varying time stepping and transient functionalities, purely within CFD (discussed in detail in Chapter 4), hence discarding the use of other separate modules, particularly DTM (unlike Microflo, which still used a separate DTM and network airflow simulation packages).

2.3 Other improved DTM Techniques

Research claiming to be neither DTM-based nor CFD-based was conducted by Musy *et al.* (2002). The aim of the research was to provide more accurate heat transfer than the DTM approach, but provide adequate accuracy of temperature simulations and air flow distribution to be able to predict thermal comfort. The research used 'zonal modelling' techniques, whereby the inside of a room was divided into a small number of zones or cells. Mass and heat balance equations are applied to the cells

and the exchanges are calculated between them. In order to account for all aspects of a building, modules were developed as part of a library, where appropriate models were assembled to form zonal models of an entire building.

Using the equations on volumes rather than finite difference, the tool, however, required extensive development and still did not provide the detailed analysis provided by CFD, but did provide simulations, which may have been sufficient for a more general analysis of the building.

By reviewing all methods and techniques used to combine DTM and CFD, the research produced by Tang (1998), appeared to be very promising. This research did not indicate how accurately the proposed methodology provided airflow analysis, since his work only provided an introduction to the concept. Validation was required by comparing the results to empirical data. However, it was noted that the collective inaccuracies of the 'grouped modular' approach appeared to outweigh the inaccuracies caused by manually inputting data from separate software packages.

Transient modelling within CFD was also developed by Takeya *et al.* (1998) to model dynamic thermal conditions inside a building, containing thermostatically-controlled air-conditioners. Their research used TASC (Total Air-conditioning system Simulation Code), a 3-D transient CFD code, designed to solve coupled heat transfer between airflow and indoor materials, based on the Heat Balance Method (HBM) (Onishi *et al.* (1990), Kitagawa *et al.* (1996)).

The transient methodology of the HBM consists of:

(i)   transient heat balance at the wall surfaces and;

(ii)   transient heat conduction through the walls in one dimension.

The research produced by Takeya *et al.* (1998) did not examine the effect of simultaneous changes between external and internal dynamic conditions, both as outflow and inflow. In fact, their research raised the question of how to represent fluctuating external conditions. The model constructed in their research contained

constant external conditions of 7°C. The research conducted by Takeya *et al.* (1998) identified the problems arising with initial conditions, since none were specified in their model. As a result, the solution showed a significant initial overshoot in convergence, caused by the first effects of the ventilation system within the modelled zone.

Initial conditions provided by pre-solutions of the DTM were still required, hence, not overcoming the overall objective of avoiding the use of a separate dynamic thermal model. Nevertheless, the research reported within this paper, Takeya *et al.* (1998) was successful in solving a transient indoor airflow, and the effect of various ventilation system scenarios, under thermostatic control. The time steps (30 seconds) were significantly shorter than those used in the research conducted by Tang (1998), where time steps were 1 hour. Such short time steps were necessary in the research produced by Takeya *et al.* (1998), because the thermostatically-controlled ventilation system tended to create frequent changes in airflow.

Both the work conducted by Tang (1998) and Takeya *et al.* (1998), examined the heat transfer through the building fabric and air simultaneously, over a substantial period of time. This research marked a substantial progression towards an integrated thermal tool.

In summary, much work has been conducted on improving the performance of DTM by striving to achieve CFD levels of detail into DTM code. The initial emphasis on the development of DTM rather than CFD, may have been influenced by a combination of the need for an improved holistic thermal analysis tool and hardware limitations. A more holistic thermal design tool was perceived to be more useful at that time, compared to a detailed analysis of a specific zone.

With a continual improvement in hardware capacity, the direction of focus of subsequent research shifted by incorporating larger volumes of CFD into DTM. The latest research indicates a development of CFD alone, to undertake the techniques of DTM.

The research group, led by Takeya *et al.* (1998) has developed transient modelling using a 'conjugate heat transfer' method in CFD alone, to model a transient case; where internal loads are fluctuating. This research group has not yet identified how to model external fluctuating conditions. Other research groups developed transient functionalities and time-varying time steps, by exchanging information from separate DTM and CFD codes.

This latest research of Tang (1998) and Takeya *et al.* (1998) does explore the various techniques, which will be further developed in the research described in this thesis. No research group, however, has yet outlined a rigorous procedure to dynamically model the thermal conditions inside a building zone (including the thermal variations over the building fabric, as a result of the fluctuating weather patterns, with time), using CFD alone.

2.4 Grid Configuration, Wall Functions and Turbulence Models

Grid configurations, wall functions and turbulence models are all inter-related. For the past two decades to the present day, much research has and is being conducted to improve the above mentioned aspects of CFD modelling. Wall functions and turbulence models have been researched in order to reduce grid density at the boundaries of CFD models, in order to reduce the computational load required to capture boundary layers. For commercial applications, wall functions were viewed as being the best alternative to a fine grid analysis (Craft et al. 2002), where fine grid was expected less than $0.1mm^3$.

Wall-functions themselves contain omissions, even in their most elaborate forms for more academic applications. Logarithmic wall functions are used in most research and commercial CFD codes to describe the momentum and heat transfer from the internal surfaces of a room. The majority of these wall functions have been empirically derived from forced convection in pipes and flat plates, Yuan et al. (1992).

Numerous turbulence models exist, but the most commonly used turbulence model for the simulation of airflow and heat transfer within single zonal buildings in CFD is the Standard k-ε Turbulence model with the Log Law wall functions. A development of DTM by combining CFD patches conducted on a simple zone was conducted by Bartak et al. (2002). Their research used improved forms of the k-ε Turbulence model, which was based on the generalised gradient diffusion hypothesis. Their research was endorsed by comparisons with experimental data, where the improved k-ε Turbulence model was proved to show better agreement (to within the measurement uncertainty of ±0.5°C) than the standard k-ε Turbulence model. The improved turbulence model performed better than the standard model in terms of convergence, speed and the prediction of the temperature distribution within the simple zonal model.

The k-ε turbulence models in general, provide good predictions for airflow and heat transfer within simple single zone rooms. The turbulence model assumes that turbulent flows are fully developed. The k-ε Turbulence model may not perform so well for flows that are driven by natural convection along solid surfaces due to the numerical procedure of the Log-Law wall functions. Other alternatives to the k-ε Turbulence model are available, but none of them can be used as a replacement, since the alternatives do not perform well under general room conditions. Research into the development of DTM techniques incorporated CFD into the code, have recently been developed to include mechanisms which allow appropriate turbulence models and wall functions to be automatically selected from within the software, Beasoliel-Morrison (2002).

Henkes and Hoogendoom (1989) also tested various turbulence models for calculation of natural convection heat transfer from vertical plates. The models they examined can be grouped as: (i) a standard k-ε model; (ii) low Reynolds number k-ε models; and (iii) an algebraic stress model. They found that the Cebeci-Smith algebraic model calculates a low heat transfer coefficient whereas the Standard k-ε model gives a high value compared with experimental data. They therefore concluded that the accurate prediction of surface heat transfer requires the use of low

Reynolds number k-ε models. Hazim (1998) also confirmed that a low Reynolds number turbulence model was a better alternative, but also found that this model was also as computationally expensive as the other options. Hazim (1998) recommended using experimentally derived expressions for the internal surface heat transfer coefficients.

2.5 Chapter Summary

This chapter reviewed the various techniques developed during the last twenty years in combining DTM and CFD models. The emphasis of the research has evolved over time, largely due to the influence of computational capacity. Some techniques have been more successful than others, particularly those techniques that embedded CFD into DTM. No techniques, however, have been successful for further development as a single commercial design tool. Some aspects of past research bear some similarity to the proposed methods of the research documented in this thesis, whereby DTM methods were embedded into CFD. No past research, however, has developed a technique whereby efficiency of dynamic thermal modelling within CFD has been directly addressed and solved.

The following chapter develops a technique to solve for the transient heat transfer through both building fabric and air enclosed. The main objective of the development of a dynamic thermal CFD tool is to create a more efficient simulation package. The methodology devised in the next chapter utilises functions currently available within CFD to overcome excessive data generation as a result of solving for two very different mediums, i.e. over fabric and air, simultaneously.

CHAPTER 3

DEVELOPMENT OF A PRELIMINARY DYNAMIC THERMAL MODELLING PROCEDURE IN CFD

CHAPTER 3 - DEVELOPMENT OF PRELIMINARY DYNAMIC THERMAL MODELLING PROCEDURE IN CFD

3.1 Introduction

The nature of this research into combining dynamic thermal modelling techniques into CFD is different from previous research approaches. Rather than allowing DTM and CFD to exist as two separate packages and developing an efficient link between them, which has been a popular technique in the past, as described in Chapter 2; this research aims to develop a single CFD tool which can dynamically model buildings, without the use of an additional DTM tool. In order to discontinue the use of a separate DTM package, the essential techniques used by DTM, must be adopted by CFD. One of the most fundamental facility of DTM, is the ability to simulate the heat transfer through building fabric over long periods of time.

Preliminary tests have been conducted to confirm that heat transfer through building fabric can be conducted within the CFD code (Flovent) used throughout this research. The basic principles of heat transfer, i.e. conduction, convection and radiation through solids at steady state have been tested within the CFD code and compared with analytical techniques. The results of the tests are contained within Sections A1-4, Appendix A.

In addition to the tests conducted to confirm that heat can be transferred through materials, further tests have also been conducted to examine basic transient functions, within CFD. These are presented in Section A5, Appendix A. It is proposed that transient functions within CFD, can be used extensively to model buildings dynamically and can be used to tackle the problem of solving for the two different mediums of a building, i.e. of air and building envelope materials, over long periods of time.

CFD has always been able to model heat transfer through solid materials and air simultaneously in theory, by extending the physical computational grid over the entire solution domain (to include both the building envelope and the air it contains). This

procedure, however, is not easily implemented within any CFD code. One of the most significant limitations of doing so, especially when modelling transient solutions, is the amount of data, which could potentially be generated as a result.

To overcome the problem of large data generation and time consuming solving procedures, the 'freeze flow' technique could be used together with time-varying transient time stepping. The 'freeze flow' technique is a function available within FLOVENT, which allows the solution of all governing equations, except temperature to be paused, for a desired length of time.

Ideally, the 'freeze flow' function could be used to include the effects of significantly longer rates of heat transfer through the building fabric. Small incremental thermal changes in the building envelope fabric, will not significantly affect air conditions. Air responds virtually instantaneously to thermal changes compared to building fabric. It seems viable to allow a period of time for building envelopes to respond to changing thermal conditions, without simultaneously solving for the air over the same period. After a certain amount of time, the flow could be 'unfrozen', i.e. the full set of governing equations are switched back on and re-solved, allowing for the air inside the solution domain to be updated to any differences in thermal boundary conditions that may have occurred within the fabric.
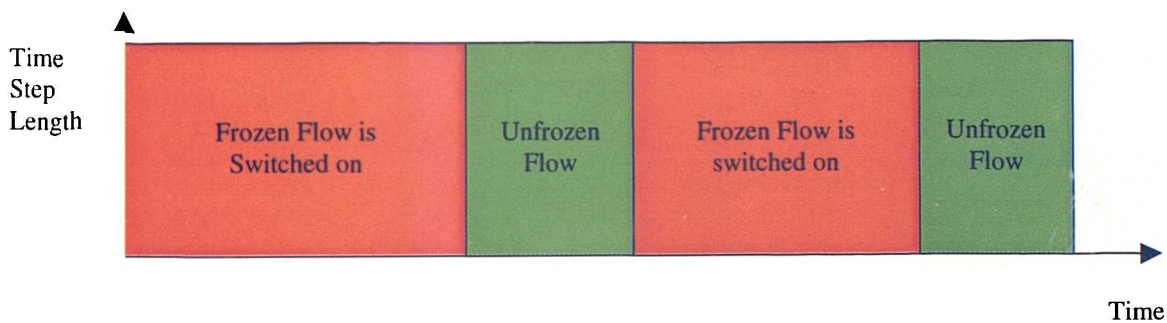
Figure 3.1: Time-Varying Transient Grid for Frozen and Unfrozen flow Periods

The lengths of time allocated for the periods of 'frozen' and 'unfrozen' flow, gives rise to a solution sequence of time-varying transient periods (Fig. 3.1). Large amounts of time are scheduled for the 'frozen flow' and shorter periods of time are allocated for the flow to be 'unfrozen' or updated to different thermal conditions that would have changed over the previous transient 'frozen' period. The time steps

lengths within a transient period of frozen/unfrozen flow are shown to be of equal size in Figure 3.1. Appropriate time step lengths and transient time periods, however, will be established through rigorous testing to be conducted at a later stage.

Before a DTM Procedure was implemented within CFD using time-varying transient time steps and 'frozen' flow techniques, a series of tests have been constructed. The tests aim to assess the feasibly and likely success of the proposed DTM Procedure to observe the effects of heat transfer through the building envelope fabric and their consequential effects on internal conditions within a simple enclosure.

The development of the tests begins by observing the performance of a series of cuboids used to mimic a fluctuating sinusoidal ambient condition through solid walls, since external ambient conditions cannot be directly modelled under transient conditions. These initial transient cases are gradually increased in complexity, to eventually simulate a basic enclosure containing air. Tests B1-B4 listed in Table 3.1 have been documented in more detail in Appendix B. The description of the methodology of Tests B1-B4 and the main findings of the tests are summarised in this chapter.

Table 3.1: *Summary of Tests Conducted*

(Note: Tests B1-B3 are located in Appendix B)

Test Name	Description
DYNAMIC THERMAL MODELLING THROUGH A SOLID INTERFACE	
B1	*Transient Modelling of Conduction through a Solid – 1st cuboid (representing an ambient condition) is given a transient sinusoidal profile. 5 Tests are conducted, each using wall materials with different thermal characteristics. Comparisons made between CFD results and analytical solutions, CIBSE (1986).*
DYNAMIC THERMAL MODELLING THROUGH A SOLID-AIR INTERFACE	
TRANSIENT MODELLING WITHIN AN ENCLOSURE – PRELIMINARY TEST	
B2	*The solution domain of Test B1 is extended to include a thin slice of air containing a fixed flow device. This is a forced transient convection test.*
B3	*Air space is extended, to resemble an enclosure. Temperatures and speeds of the air are collected at specific points within the room. The case is run as a natural convection steady state case.*

B4	*The enclosure of Test B3, is modelled as a transient case and the results of temperatures from the test will be used as reference data for the Test 3A.*
3A	Enclosure is modelled using a preliminary DTM technique in CFD.
3B	Sensitivity Analysis of the Time Step Length and Total Transient Unfrozen Flow Solution Period.

This chapter aims to describe the circumstances (whether positive or negative) in which the dynamic thermal modelling procedure can be developed taking into account resources currently available within the CFD code. Limitations towards the success of the DTM Procedure are identified and solutions are proposed to overcome these. Through the development of the tests, an overall assessment can be made as to whether the proposed dynamic thermal modelling procedure to be implemented within CFD is likely to provide an efficient solution to dynamic thermal modelling using a single tool.

3.2 Dynamic Thermal Modelling Through a Solid Interface

3.2.1 Introduction

The CFD code used in this study (Flovent) is predominantly used to simulate fluid flow. In order to model the dynamic thermal changes through a building envelope, heat transfer must also be calculated through solid fabrics. The 'Basic Physical Processes' tests (Section A1-A4, Appendix A), confirmed that conduction, convection and radiation can be accurately modelled through building fabric made from brickwork using CFD. Brickwork was chosen as being a commonly used material within buildings, with average thermal characteristics detailed below:

Thermal Conductivity = 0.84 W/ (mK)

Density = 1700 kg/m^3

Specific Heat Capacity = 800 J/(kgK)

The 'Basic Physical Processes' Tests, isolated each mode of heat transfer and tested their representation within FLOVENT, by comparison with analytical solutions. All of the tests conducted were run as steady state cases.

In developing the 'Basic Processes' (Appendix A) tests further to model heat transfer through solids under transient conditions, the first limitation posed by the software has been encountered. The CFD code does not allow a direct representation of ambient conditions within a transient solution procedure, although an ambient setting can be easily specified within a steady state solution. Initial tests were also conducted to establish an alternative to transient ambient representation. This research has been documented in Section A5 of Appendix A. The limitation was resolved by including a series of two cuboids. One cuboid was given a temperature profile to mimic time-varying thermal changes and the other cuboid was given a thermal resistance to mimic surface heat transfer coefficients as typically generated by external environments. Indirect and direct solar radiation effects have not been specifically addressed in the development of the DTM Procedure, but are considered in Chapter 6.

3.2.2: Simulating a Transient Ambient Condition using Cuboids

In order to observe the effects of a cuboidal representation of a transient ambient and their interaction with a variety of building materials during a transient solution process, Test B1 was developed, Appendix B. Test B1 models various materials that were exposed to sinusoidal ambient conditions within a transient scenario. The materials of Test B1 were derived by synthetically altering the thermal characteristics of the first material (Brickwork). A table of the materials used and their thermal characteristics is located in Appendix B, Table B3. The results of the CFD simulation were compared to analytical results outlined by CIBSE (1986).

Section A3-21 of CIBSE (1986) describes a procedure for manually calculating non-steady state thermal indexes. CIBSE (1986) approximates most external ambient conditions as varying sinusoidally and assumes that as external ambient conditions are transferred through the material they will be thermally lagged and deflected. The amount by which the external ambient sinusoidal profile is deflected and delayed as it passes through the material can be mathematically determined, by using a technique called the Admittance Procedure. The admittance procedure is relatively simple and requires the calculation of three additional factors to the U-value:

1. the admittance factor;

2. the surface factor;

3. the decrement factor.

Definitions of the three factors involved have been extracted from CIBSE (1986) of the Admittance Method, below:

> *'Admittance (Y-Value)*
>
> *The admittance is the rate of heat flow between the internal surface of the construction and the space temperature, for each degree of swing in space temperature about its mean value.'*

It can be considered as the cyclic U-value for heat flow between the space and the construction. For thin structures the admittance is equal to the U-value and there tends to be a limiting value for thicknesses greater than 100mm.'

> *'Surface Factor (F)*
>
> *The surface factor is the ratio of the variation of heat flow about its mean value readmitted to a space from the surface, to the variation of heat flow about its mean value absorbed in the surface. The surface factor decreases and its time lag increases with increasing thermal capacity and they are virtually constant with thickness.'*

> *'The Decrement Factor (f)*
>
> *This is the rate of heat flow through the structure to the internal space temperature for each degree of swing in external temperature about its mean value, to the steady state rate of heat flow or U-value. For thin structures of low thermal capacity the decrement factor is unity and decreases in value with increasing thickness and/or thermal capacity.'*

These factors are functions of the thickness, thermal conductivity, density and specific heat capacity of each of the materials used in a building construction. The factors are also normally expressed as an amplitude of the sine wave and time lag of the sine

wave. The typical values of the admittance/surface/decrement factors for commonly used building materials are listed in Table A3.16, CIBSE (1986).

The comparisons of the CFD simulations (using a series of cuboids acting as an external ambient) and the CIBSE Guide A analytic solutions were made. The comparisons indicated that the order of magnitude of the deflection and lag of the external ambient sinusoidal thermal profile were quite close to their equivalent analytical solutions as outlined by the Admittance Procedure in CIBSE (1986).

Tests B1 confirmed that sinusoidal temperature profile can be successfully attached to cuboids, to simulate the effects of time-varying ambient conditions. Fundamental differences between the CFD model and the Admittance Procedure CIBSE (1986) were responsible for the errors between the comparisons; i.e. one of the main causes of error was the absence of air adjacent on the internal surface of the material in the CFD model, so the effects of the internal surface heat transfer coefficient were ignored.

A following test, Test B2 further developed previous test cases, which had only modelled solids thus far, to examine the combined effect of CFD modelling through solid and air within a transient scenario. A thin slice of air was included within the CFD model of Test B2. Results were collected from within the air instead of within the last cell just inside of the internal surface of the solid. The comparisons of the deflection of the external ambient through the materials with the Admittance Procedure were good, since the internal surface heat transfer effects and additional thermal resistance between the air and the wall were included in the CFD model.

The thin slice of air adjacent to the inside surface of the wall was then extended to include a larger volume of air, in Test B3, Appendix B. The objective of Test B3 was to develop the test case into an enclosure construction. The CFD model of Test B3 contained one external wall (exposed to a fluctuating external ambient) and one internal partition, maintained at a fixed temperature. The internal partition acted as a heating source used to influence the nature of the flow and the external source acted as a source of cooling, this test was run as steady state. Geometrical grid was superimposed over the entire enclosure, including the solid boundaries.

The results of the steady state calculation of Test B3 illustrated that the heating and cooling walls were effectively creating a clockwise airflow pattern around the enclosure, as expected. The series of tests from B1-B3 marked a development towards the modelling of solids and air simultaneously. In the following section, Test B3 (Appendix B) has been further developed as a transient case exposed to a sinusoidal external ambient.

Hence, Test B4 models an enclosure, where the heat transfer through the solid boundaries and the air they enclosed are simulated under transient conditions. The enclosure was exposed to a weather pattern that varied sinusoidally over a period of 1 day, and had an amplitude of 20°C. The results of this test were used as reference data for the test which followed, Test 3A. Test 3A modelled the geometry of Test B4, but a more efficient DTM Procedure was introduced. The results of Test B4 and Test 3A are compared extensively in the following section.

3.3   Preliminary Dynamic Thermal Modelling Procedures in CFD

3.3.1   Introduction to Time-Varying Transient Solution Periods And 'Freeze Flow'.

A series of tests were conducted Tests B1-B3 (see Appendix B, Section B1-B3), which focused upon the development of transient modelling of solids and air simultaneously within the CFD code. The last test in the series, Test B4, provided the reference results of temperature and air velocities within the room, as a result of a cooling external wall (with a sinusoidal thermal profile), and a fixed temperature heated wall (located on a Y-Z plane at X=1m), see Section B4, Appendix B.

In Test B4 the entire set of governing equations, contained within CFD were solved for the thermal transfer through the air and building fabric, simultaneously under transient conditions. These equations were solved every 6 minutes (typical average solution time grid cell used in other typical DTM software) over 5 days. Data of temperatures and velocities of the fully transient test case was stored every 4th hour over the one-day period of simulation, to be used later for comparison with the results obtained from an efficient dynamic thermal modelling procedure within CFD Test 3A (section 3.4). The solution process used in Test B4 was computationally expensive.

The difference in time constants between solids and air is the main reason why dynamic thermal modelling cannot be efficiently implemented within CFD. All preliminary tests have indicated that a CFD code can successfully model both solids and air simultaneously but the process is computationally expensive and time consuming.

However, all equations of fluid flow are not necessary for solving over solids. Hence, to improve efficiency, not all equations need to be solved, since external boundary conditions are not likely to significantly change due to the effects of thermal fluctuations of the weather.   Compared to solids, air responds relatively instantaneously to changes in thermal conditions.

In this study, typical thermal responses of both solids and air have been exploited as a means of improving the efficiency of dynamic thermal modelling within CFD. For building zones that contain airflow that is purely driven by natural convection, the effects of boundary conditions are crucial to the nature of the airflow within the room. The changes in boundary conditions can be monitored and constantly accounted for by an iterative solving process of the temperature, hence solving predominantly for conduction. A representative airflow pattern could be used throughout the process of conduction calculations, and updated at regular intervals.

This potentially highly efficient procedure could be used within a CFD code, since FLOVENT contains a 'Freeze Flow' function, which allows all equations, except temperature to be temporarily paused, to increase the efficiency of a solution process, when the air flow patterns are not assumed to change very much. The temporary airflow patterns used are those that have been paused from a previously non-frozen calculation of air velocities.

In effect, the airflow patterns, whilst incremental thermal changes occur in the building fabric, are assumed to change only very slightly. It, therefore, seems viable to use the 'Freeze Flow' function in the DTM Procedure, whilst small thermal changes occur in the building fabric. So, for long lengths of time the 'Freeze Flow' function can be activated, and for shorter lengths of time, the airflow patterns are updated to the thermal changes in the building fabric, by malfunctioning the 'Freeze Flow' mechanism and allowing all the equations to solve. A case study was devised to test the feasibility of using the 'freeze flow' function during a transient simulation, with the main objective of achieving computational efficiency (Test 3A). The results of this case study were compared to the results of Test B4, which solved all equations at every time step.

3.4 'Freeze Flow' for Dynamic Thermal Modelling within CFD – Case Study

3.4.1 Test Description

In this test, Test 3A, the physical geometry of the model, including the grid construction remains identical to that of Test B4. The difference between this test and Test B4 is the construction of the transient grid schedule. Due to the time-varying transient periods and the use of the 'Freeze Flow' function, the solution must be manually interrupted and governing equations either switched off or on (i.e. flow either frozen or unfrozen), on the fifth day. The preceding four days pre-heat time, will be solved uninterrupted, with all equations fully functioning in both Tests B5 and 3A.

As a first approximation to the appropriate transient periods lengths for both fabric and air, a schedule of time-varying transient solution periods are constructed. Temperature only, (i.e. frozen flow) is solved over 3 hours and 54 mins. After this time, all other equations will then be unfrozen for 6 minutes, to update the airflow. The next solution period will then be activated, where the combination of 'frozen flow' for 3 hours and 54 minutes will be activated, then 6 minutes 'unfrozen flow' will follow. This cycle will continue until the end of the fifth day has been reached.

Table 3.1 shows an example of the schedule of time-varying-transient solution periods, with 'frozen' and 'unfrozen flow' used in this test, Test 3A. Later, additional research will be conducted to determine the more appropriate transient periods for building envelope materials of varying thermal mass (Chapter 5) and appropriate times for the airflow patterns to update, documented in Section 3.5.

Table 3.2:   *Transient Grid Structure of time varying solution periods for Test 3A Fifth Day*

Time Patches on Fifth Day	Start Time (s)	End Time (s)	Minimum No. Transient Time Step (1 Time Step = 6 mins)
Up to 4 Days	0	345600	960
4th Hours (Freeze Flow)	345600	359640	39
Air Flow Update 1	359640	360000	1
8th Hours (Freeze Flow)	360000	374040	39
Air Flow Update 2	374040	374400	1
12th Hour (Freeze Flow)	374400	388440	39
Air Flow Update 3	388440	388800	1
16th Hour (Freeze Flow)	388800	402840	39
Air Flow Update 4	402840	403200	1
20th Hour (Freeze Flow)	403200	417240	39
Air Flow Update 5	417240	417600	1
24th Hour (Freeze Flow)	417600	431640	39
Air Flow Update 6	431640	432000	1

Exactly the same points (located within the enclosure, see Table B5, Section B4, Appendix B) that recorded the temperature and velocities of the air within the geometry of Test B4, were used in Test 3A, to maintain consistency.

3.4.2 Results and Discussion

Data of temperature and airflow velocity were recorded at 15 points within the enclosure (see Table B5, Section B4, Appendix B). The 15 points were located within a 2-D network in the X-Y plane, with 3 points in the X-direction and 5 points in the Y-direction, to provide sufficient detail of the air flow conditions within the entire enclosure.

Figures 3.2 and 3.4 show a comparison of % errors between the results of temperature and velocities, respectively, collected in Test B4 and Test 3A on the 6 separate occasions on the fifth day. As a further extension to this test, the transient solution period was then extended for an additional day, for both Test B4 and Test 3A. Exactly the same procedure for solving the tests and collecting the results was adopted, as on the fifth day (% errors calculated by dividing the difference between the results of Test 3A and B4 by 15°C). An additional day of solving for both Test B5 and Test 3A was necessary because the results from the % error of temperatures appeared to be tending towards negative numbers. By solving for a sixth day, it was interesting to further examine whether the % error became more negative. This was not the case with the velocity % error results, suggesting that errors imposed by using the solution procedure were not cumulative. The extended transient schedules for both Test B4 and Test 3A, are tabulated in Table 3.4.
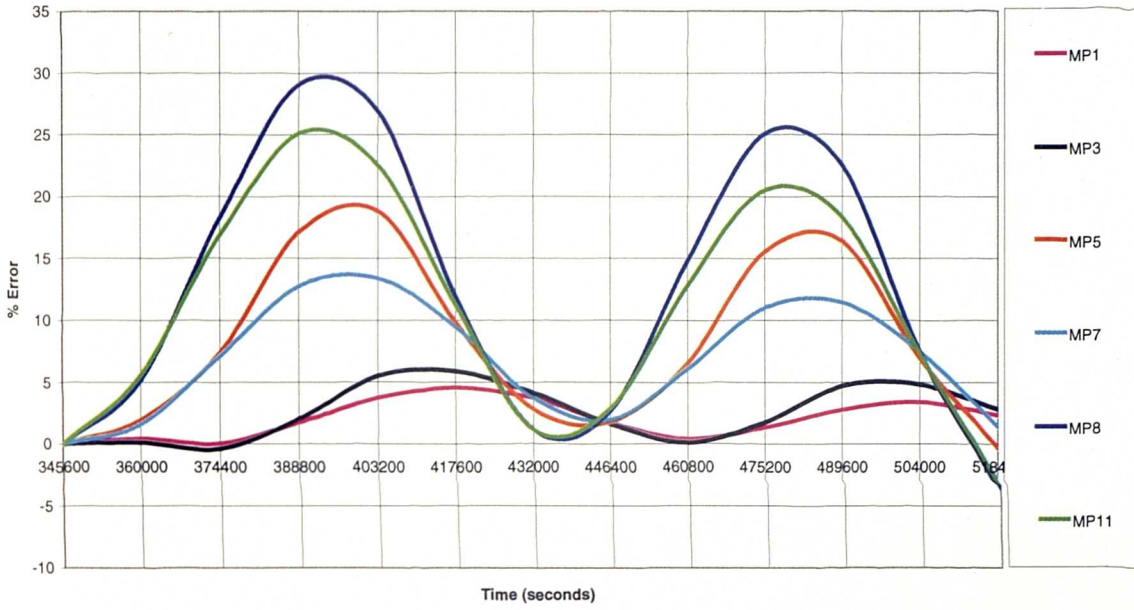
Fig. 3.2:   % Error Differences between the temperature results collected in Test B5 and Test 3A, as recorded at MP8.

Table 3.3: Continuation of the Transient Grid used in Test 3A – Sixth Day

Time Patches on Fifth Day	Start Time (s)	End Time (s)	Minimum No. Transient Grid Cells
Starting from airflow update 6 on at the end of 5th Day	431640	432000	1
4th Hour (Freeze Flow)	432000	446040	39
Air Flow Update 7	446040	446400	1
8th Hours (Freeze Flow)	446400	460440	39
Air Flow Update 8	460440	460800	1
12th Hour (Freeze Flow)	460800	474840	39
Air Flow Update 9	474840	475200	1
16th Hour (Freeze Flow)	475200	489240	39
Air Flow Update 10	489240	489600	1
20th Hour (Freeze Flow)	489600	503640	39
Air Flow Update 11	503640	504000	1
24th Hour (Freeze Flow)	504000	518040	39
Air Flow Update 12	518040	518400	1

The temperature errors range from 29% at midday, to approximately ±5% at the beginning and end of the fifth day (See Fig 3.2). The temperature % errors are more significant than the velocity errors, which range between ±12%, (see Fig. 3.4).

The errors are primarily caused by the method of 'freeze flow', but the % errors are not cumulative. Hence the larger % error values, occurring at midday, may also be

caused by the length of time allocated to update the airflow within the enclosure, which is only 6 minutes. During the 6 minutes of airflow update time, there is only 1 time grid cell, since the grid cells within the geometry are all 6 minutes long.

Since the external wall is constantly cooling by varying degrees, between -10°C and 10°C, and the internal wall is constantly heating at 30°C, very similar airflow patterns will occur inside the enclosure at each of the 4 hour time frames. Hence, updating the airflow patterns inside the enclosure within 6 minutes, appears to have generated smaller errors, compared to that of temperature, because less major adjustments need to be made to the airflow patterns at each update.

Airflow patterns are fundamental in transporting the heat around the room, and hence accurate airflow patterns are necessary to provide good temperature predictions around the enclosure. The changes in temperature and airflow patterns, as a result of the thermal heat transfer through the external wall are not appropriately transferred over the entire room. This is indicated by the temperatures and velocities recorded at points located in the centre of the room, i.e. at MP 5, 8 and 11 (See MP 5, 8, and 11 in Fig. 3.3). At these points the highest % errors for temperature are recorded.

13	14	15
10	11	12
7	8	9
4	5	6
1	2	3

Colour Key:

Significant errors achieved   Moderate Errors   Less significant Errors

Fig. 3.3:   Centrally located plane of data points within an X-Y Plane, showing Regions in the enclosure with the greatest errors.

High % errors in velocity are also obtained at the corners of the room, indicated at points 1, 3, 13 and 15. (See profiles of points MP 1, 3, 13 and 15, Fig 3.4). This indicates that the update time of the flow is inefficient in establishing the true airflow patterns, within highly turbulent regions, such as at the corners of the enclosure.

In the % error graphs of temperature (Fig. 3.2), all the profiles of the 15 MPs located within the room followed a similar trend. The % error graphs of velocity (Fig 3.4) seem to show less of a strong trend. Freezing the flow causes widespread inaccuracy in the airflow patterns, which in turn, affects the representation of the temperatures within the room.

The badly represented airflow patterns of the enclosure in Test 3A, may also be caused by the length of the time allocated for the flow to be 'frozen', i.e. for solving temperature equations only, over the entire solution domain. This time may be too long, and significant heat transfer at the walls, is not being appropriately represented at the boundaries of the enclosure, due to all equations of the flow, being paused during this time.

The enclosure walls, made from brickwork, have a thermal lag of 5/6 hours (according CIBSE (1986) and the tests conducted in Test B1, Section B1, Appendix B). From the profiles plotted in Figure 3.4, maximum errors appear to occur shortly after midday. Peak external ambient temperatures occur six hours into the transient simulation, but after 12 hours the effects of external ambient temperature increases have accumulated, whilst the external temperatures are starting to decrease at this time.

% Error Difference between Test 5 and Test 6
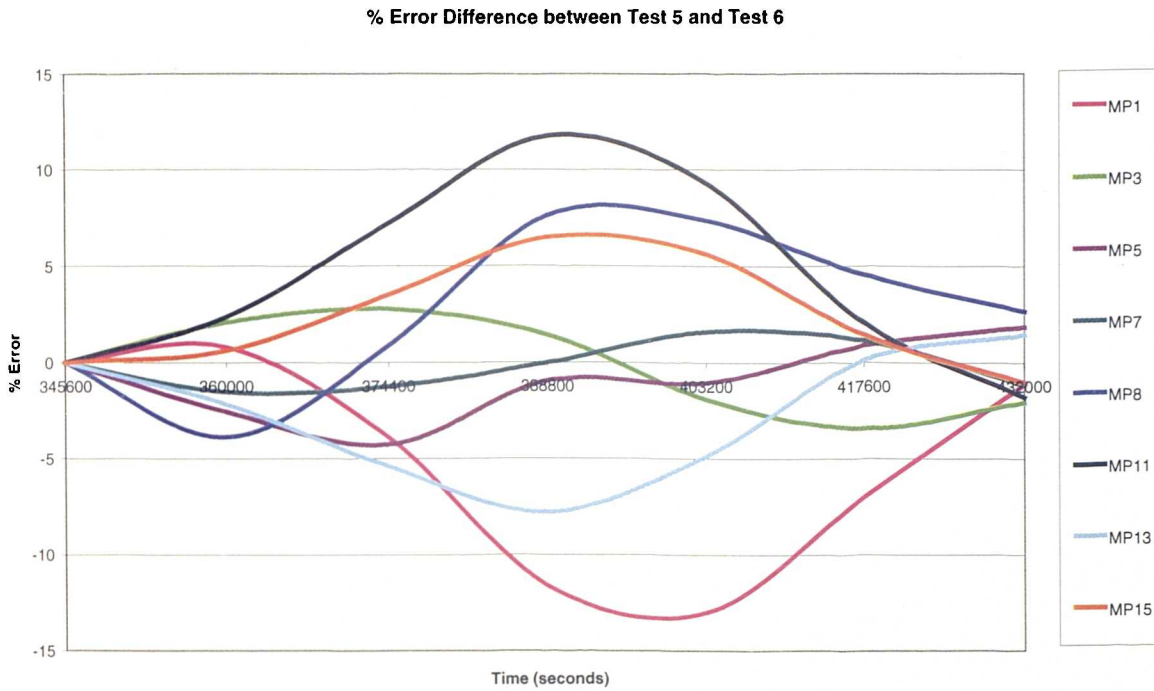
Fig.3.4:   % Error values between the results of velocities collected for Test B5 & Test 3A.

Further tests must be carried out in order to establish how appropriate this length of time is for updating the flow (these are presented in Chapter 4). As previously proposed, it may be necessary to have a function which detects large thermal changes in both the fabric and/or airflow, and hence adjusts transient grid time steps, in order to capture these significant thermal effects.

Overall, transient dynamic thermal modelling within CFD using 'freeze flow' shows very good potential for use as a single tool, with maximum errors in temperature of 30%. From this study, it is not clear exactly what causes the discrepancies between the results of Test B5 and Test 3A, since the errors are not cumulative. There is still much work required in establishing appropriate time steps and appropriate time step numbers, during the air flow update.

The possible sources of error have been identified as being:

1. Inappropriate time steps lengths during a transient unfrozen update period.

2. Inappropriate transient unfrozen periods.

3. Inappropriate transient frozen periods for the temperature calculations over the solids.

4. Inappropriate time step lengths over the transient frozen periods.

The first two sources of error will be examined in the following section, Section 3.5 and the sources 3 and 4 of error will be examined in Chapter 4.

3.5 Sensitivity Analysis of the Time Step Length and Total Transient Unfrozen Flow Solution Period

3.5.1 Test Description

An initial test of a preliminary procedure for dynamically modelling a building using CFD alone has been conducted (Test 3A). The procedure used a combination of transient (frozen flow)-transient (unfrozen flow) techniques, where longer periods of transient time are allocated for the frozen flow and shorter periods are allocated for unfrozen flow. This procedure involved solving for the thermal exchange over the solids, whilst the airflow pattern within the room continued to follow a representative airflow pattern, set when the flow was frozen. During the period of unfrozen flow, the airflow would be updated to the new airflow pattern, which would have occurred as a result of the thermal changes in the fabric during frozen flow.

This section of the research attempts to determine the necessary time step length required to accurately update the thermal conditions (as a result of the change of boundary conditions, during frozen flow) of the air contained inside the enclosure. The research also aims to determine the necessary total transient solution time of the period of unfrozen flow.

Therefore the objectives of this test (Test 3B) are:

1. To establish an appropriate transient time period to update the airflow (unfrozen flow)
2. To establish the optimum time step length required in each transient (unfrozen) time period.

For the tests conducted in Test 3A, 3 hours and 54 minutes were allocated for 'frozen' flow over the brickwork. Referring back to the results of Test B5 of temperature and velocities, it is evident that during the regular four-hour intervals (over the two days), the airflow in the centre of the room (MP8) had to be readjusted by temperature differentials of between ±1.2°C between frozen periods.

55

This order of magnitude of temperature change could be relatively low compared to other materials with much lighter thermal masses. For example, if the enclosure construction contained a greater content of glass, then perhaps the temperature re-adjustment, during the period of 'unfrozen' flow could be higher, due to the material's higher thermal conductivity.

By way of assessing the likely temperature adjustments, which could occur over a building fabric, typical external thermal profiles have been analysed. A representative weather data file, recorded in Kew, south London, in 1964 is referred to as one example of the weather to be expected in a typical year, CIBSE (1986). From the Kew weather data, the maximum temperature difference over an entire year is 40°C. On a monthly basis the highest and lowest temperature ranges over a selected day in each month are as follows:

Table 3.4: *Temperature Differences over a selected day in each month (each day is selected because a maximum temperature difference occurs during that month)*

Month	Min. Temp. difference	Max. Temp. Difference
January	1.1	9.3
February	1.4	7.2
March	2.1	20.1
April	2.8	12.3
May	1.7	15.7
June	2.1	12.6
July	2.5	9.4
August	4.7	12.5
September	1.2	11.3
October	1.6	12.2
November	1.7	8.5
December	0.8	13.8

From Table 3.4, it is evident that the expected temperature differential in the weather variation over a day is likely to be between 0 and 20°C, at most. This data indicates the possible variations of external ambient temperature and internal thermal fluctuations over a day. The extent of the change may influence how much time should be allocated for the update unfrozen flow period. The following tests have been constructed to determine appropriate time step lengths and time step periods during a transient unfrozen update period according to similar thermal step changes in temperature.

3.5.2 Geometry of Test Case 3B

The geometry of the CFD test case 3B, consists of a solution domain containing two plates situated in the YZ plane at X=0 and X=1.1m. The plates are 0.1m thick, but their thickness' have no thermal effect, since both plates have been given a fixed temperature and hence any thermal characteristics of the plates are over-ridden. The domain does not contain any walls, and all the surfaces of the CFD model domain enclosure are specified as being adiabatic. The geometry contains 9 monitoring points located within the central planes of the enclosure, on a 3 x 3 matrix formation.

The plate situated on the YZ plane at X=0m (referred to as the X-low plate) is designed to be able to switch from providing a cooling to providing a heating effect within the room in order to force a change in airflow patterns. The initial condition of the plate acts as a cooling source and is allowed to solve and converge to steady state. The plate is then reset to act as a heating source (but with the initial conditions of the converged cooling source case). This case will be resolved, but under transient conditions, where the temperatures are allowed to stabilise. This case is allowed to solve and converge, since the conditions are not to change during this transient simulation. The time taken for the transient solution to stabilise is observed and recorded.

The purpose of this succession of test cases is to force the airflow inside the solution domain to alternate directions. The plate at X=1.1m (referred to as the X-high plate)

is designed to constantly heat the room at 20°C. The geometry of the test case is illustrated in Fig 3.5.
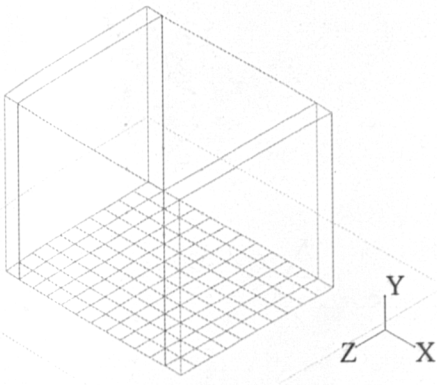
Fig 3.5: Geometry of the Test Case 3B

A summary of the procedure carried out in this test is as follows:

To investigate the effect of a temperature differential of 15°C (for example) between the initial temperatures (IT) and final temperature (FT) settings of the X-Low plate:

Step 1:   Run a steady state case where the X-Low plate is set to be 10°C.

Step 2:   Run a transient case where the X-Low plate uses the initial temperatures (IT) of 10°C. But in this test the X-Low plate is set at 25°C.

Step 3:   Run a steady state case where the X-Low plate is set at 25°C and compare the results with those of Step 2.

A range of temperature differentials between the heating and cooling settings of the 'switching' plate were tested to determine whether the magnitude of temperature step change affects the time step length and the overall total transient solution time.

The steady state cases were solved using a very detailed grid, each grid cell with dimensions of 0.01m x 0.01m x 0.01m. The transient geometry used a combination of 0.04m x 0.04m x 0.04m grid cells between 0.3m and 0.7m (in the each of the co-ordinate directions). A more detailed grid, each grid cell size being 0.01m x 0.01m x 0.01m was used at the boundaries of the enclosure between 0m-0.3m and 0.7m-1m in

all directions. The grid is symmetrical in all directions. Different grids between the steady state cases and transient cases were necessary, since the use of a highly detailed geometrical grid within the transient solution would have significantly increased CPU time. [Grid sensitivity tests have been conducted in the following chapter to observe the effects of grid density upon the DTM Procedure].

This transient solution period may depend on the transient time steps used within each transient period, so the following tests will also be conducted to examine the effects of transient time steps, see Table 3.5.

Table 3.5: The TRANSIENT CASES set of tests to be conducted

Test Description	Time Step Tests
Temperature Difference between the IT and FT of the plate located at X=0.1m is 15°C. IT of the steady state case - X-low plate is set to 12.5°C. The X-low plate is set to 27.5°C in the transient case.	3 secs (RC)
	6 secs
	60 secs
	120 secs
	360 secs
Temperature Difference between the IC and FC of the plate located at X=0.1m is 3°C. IT of the steady state case, where the X-low plate is set to 18.5°C. The X-low plate is set to 21.5°C in the transient case.	3 secs (RC)
	6 secs
	60 secs
	120 secs
	360 secs

The transient solution period (i.e. Step 2) was solved using a range of time step lengths. The most detailed being 3s (used as a reference case, (RC)). Other time steps tested in these tests are, 6s, 60s, 120s and 360s time steps, as shown in Table 3.5.

An acceptable level of accuracy is to allow the transient solutions of the temperatures and velocities of the transient cases to reach to within 0.5% of the final values of the steady state temperatures (calculated in Step 3). The % error calculation for Monitoring Point 5 (MP5) (which lies at the central point of the matrix of monitor points) is as follows:

$$\tau_{TMP5} - \tau_{TMP5} = \pm\, 0.5\%\; \tau_{SSMP5} \tag{3.1}$$

τ_{TMP5} = Temperature at MP5 at the end of a transient update

τ_{TMP5} = Temperature at MP5 during transient update solution

τ_{SSMP5} = Steady State Temperature at MP5

$\Delta\tau$ = Temperature difference between the plates in the final transient case = 7.5°C

3.5.3 Results and Discussion

The smaller the time step length, the less the total transient period required for the transient case to reach steady state. Over the range of time steps between 3s and 360s, the transient solution time varies between 36 minutes and 54 minutes, respectively, when reaching convergence for a temperature difference of 15°C. The time step length (s) and the time taken (s) for the transient solution to reach to within ± 0.5% of the equivalent steady state solution of temperature of this numerical study, was plotted and the linear relationship between them is described as being:

$$a = 3b + 2160 \tag{3.2}$$

where

a = Total Time Taken to reach convergence (s)

b = Time Step Length (s)

$$3\,(s) \le x \ge 60\,(s)$$
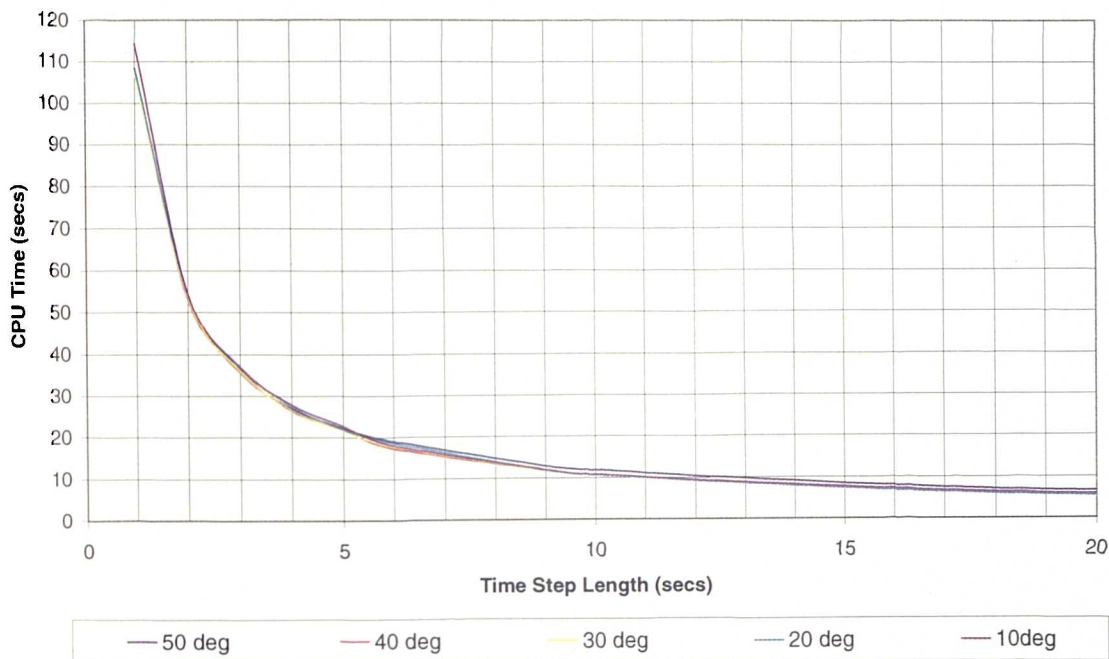
Figure 3.6:   CPU Time (secs) Vs Time Step Length (secs) for different temperature step changes

Using smaller time steps does significantly increase in CPU time required to solve the transient period (See Figure 3.6). All time step lengths provide accurate end results (provided that the total transient solution period is appropriate). The transient profiles do differ between different time step lengths during the course of total transient time, the smaller the time step length, the smaller the correction required at each time step. Building envelopes will continue to respond to the changes in external ambient conditions during the period of 'unfrozen' flow, when the air is updated, so the ideal scenario is to ensure that the period to updating is as short as possible, suggesting the use of larger time steps.

Further tests were conducted to examine the effect of reducing the temperature step change on the total transient time required for the solution to reach steady state. When the temperature difference between the initial conditions and final conditions of the walls located at X=0.1m and X = 1.32m is reduced to 3°C instead of 15°C. Using time steps lengths over the range of 3s – 360s required an overall transient solution time of 36 minutes – 60 minutes, respectively. This result was obtained by comparing the times at which the transient solution reached 0% error as opposed to an

error of 0.5% (of the previous tests) of the final steady state calculations, i.e. when the exact steady state final temperatures were reached in the transient cases for the various time steps. An alteration to the convergence criteria had to be made because most of the solutions during the transient period were within 0.5% of the fully transient case, even before the airflow was updated.

The CPU time taken for the convergence of the transient cases towards the correctly updated temperatures (as predicted by the steady state calculations) followed an inverted exponential curve, whereby the rate of change of adjustment of the temperatures is high for large temperature step changes (see Figure 3.6).

Thermal data, especially from weather data files are usually in the form of hourly recordings. 6 minute time steps are used on average in DTM simulations. Referring back to equation 3.2, 360s time steps would require a total transient period of 3240s, hence ensuring that convergence would be reached if a 1 hour period of unfrozen flow is used.

3.6 Conclusions

- The choice of time step length significantly affects the total CPU time for a given transient solution period. The CPU time does not depend on the thermal load of the CFD model. The smaller the time step the longer the CPU time, the larger the time steps the shorter the CPU time.

- The total time taken for the transient solution to reach steady state, for all time step lengths or a variety of temperature change that may occur within the airspace is approximately 3600 seconds. This total transient solution time may be reduced with the use of smaller time step lengths. A solution will not require longer than 3600 seconds to reach convergence, using any time step length and any initial temperature step change. One hour transient periods of unfrozen flow are convenient , since thermal data such as weather or occupancy rates are usually specified at hourly intervals.

3.7 Chapter Summary

In this chapter, a preliminary dynamic thermal modelling procedure, which uses a transient/frozen – transient/unfrozen methodology has been established through a series of stages, starting from first principles of heat transfer. The developed DTM Procedure has been tested and compared to a fully transient simulation (Test B5). Errors in the initial procedure were identified, the most significant being the length of time allocated for updating the airflow, i.e. the length of transient unfrozen flow time.

The error caused by time step length and transient time periods allocated to updating the airflow was directly tackled in Section 3.5, where tests were conducted to examine their effects for different temperature step changes. The results of the tests indicated that for increasingly detailed transient time grid, CPU time would also increase.

The transient time steps would not significantly influence accuracy. For a range of temperature step changes between 3-15°C, similar transient periods were necessary for all the MPs within the room to reach steady temperatures after a change had occurred. An optimum transient period to use for updating the airflow appeared to be 1 hour, with time steps of 8 minute or less.

In the following chapter, the dynamic thermal modelling procedure developed in this chapter is further reviewed. As a result, the procedure is amended and tested. The improvements to the dynamic thermal modelling methodology developed in the next chapter proves to further increase the efficiency of the overall tool.

65

CHAPTER 4

REVIEW OF THE DYNAMIC THERMAL MODELLING PROCEDURE WITHIN CFD

CHAPTER 4 – Review of a DTM Procedure Within CFD

4.1 Introduction

A preliminary dynamic thermal modelling procedure was developed and tested (Chapter 3), whereby two sets of transient solutions were run consecutively. The first transient solution solved temperature equations over a substantial period of time. Then a second transient simulation was solved over a relatively shorter period of time with all equations fully functioning. This double-transient procedure provided a satisfactory solution for the different time constants required over solid materials and air.

Tests were conducted to examine how long (in terms of transient time) the air within the enclosure would require to update to any thermal step changes. This time is equivalent to the time taken for temperatures within the room to reach steady state. If the air within the enclosure is to reach steady state, is there any use in running a transient solution at all? It is therefore proposed that rather than using a double transient solution procedure (with frozen and unfrozen flow), a transient/frozen – steady/unfrozen solution procedure should be used. The feasibility of this proposal is discussed in the following section.

4.2 Development of Boundary Freeze Function

In theory, using a steady state case to update the airflow appears to be a viable option, but there is at least one fundamental problem - the representation of the external ambient during transient and steady state cases. In the transient (frozen) – transient (unfrozen) case, the transient external ambient continues to take effect throughout. If the transient (frozen) part of the preliminary DTM Procedure was to be replaced by steady state calculations, then all parts of the CFD model would be solved to steady state, i.e. both solids and air would reach some form of thermal equilibrium.

If a steady state scenario were to replace the transient (unfrozen) part of the preliminary DTM Procedure, the temperatures within the boundary conditions would have to be fixed at the end of the preceding period of transient frozen flow period. To achieve this, an additional functionality is required within the flow, whereby the thermal conditions of the solid boundaries of the enclosure are locked, to ensure that the solids and air would both not reach an eventual thermal equilibrium.

A boundary freeze function (BFF) was developed within the CFD code to freeze the thermal conditions within the building fabric of the enclosure to prevent them from reaching steady state with the air they enclosed. The BFF could be attached to any solid in the same way that a material could be attached to any solid. This function contained thermal characteristics, which trapped the heat within the material during the steady state solution.

- Boundary Freeze Function

  This function permits the thermal conditions within a solid object / boundary to be temporarily fixed. This function is used when airflow conditions are updated in a steady state scenario following a transient period of frozen fluid flow.

The development of this function was tested, and proved to successfully fulfill the task of locking the thermal conditions within the solid material during a steady state solution. Details of the BFF tests are documented in Section C1, Appendix C.

4.3 Two Proposed Procedures for DTM within CFD

With the introduction of the steady state updating procedure, two possible methodologies evolved, and are both referred to as 'dynamic thermal simulations procedure' or DTSP. In this section, the two DTSPs were tested and compared with each other and a fully transient simulation (i.e. all equations were solved throughout a transient period), with the aim of selecting the optimum technique.

In order to limit the complexity of the CFD models used to develop a dynamic thermal modelling procedure within CFD, a single zone is modelled. This single zone is referred to as an enclosure. One external surface of the enclosure was exposed to an ambient which had sinusoidal thermal profile. This sinusoidal profile was selected to represent the effects of ambient thermal conditions over one day (or 86400s). The sinusoidal profile had a period of 1 day and the temperature, T (°C) which varied through 15°C (typical diurnal range) over time, t (s) by:

$$T = 7.5\sin 2\pi(t/86400) + 20°C \qquad (4.1)$$

DTSP#1 and DTSP#2, defined below, are two slightly different prototyped methodologies for dynamically modelling the airflow and heat transfer of the air inside an enclosure within CFD. The common objectives of both DTSP#1 and DTSP#2 are to reduce the average computational time of most other dynamic thermal modelling processes available within industry today, whilst providing accurate and detailed (comparable to CFD) simulation of heat transfer and airflow.

The periods of unfrozen flow were solved in a transient state in DTSP#1 and in a steady state case in DTSP#2. Both DTSP#1 and DTSP#2 techniques were applied to the modelled enclosure after a pre-conditioning time of 3 days. The pre-conditioning solution was solved under fully transient conditions (i.e. all equations were fully functioning). Short summaries of the methodologies of the two DTSPs, developed are as follows:

DTSP#1: Transient/Frozen-Transient/Unfrozen Solution

- 1st Transient period is 3 hours long and contains 360s time steps. During this period only the temperature equation is solved, i.e. the Fluid Freeze Flow Function is switched on.

- During the 2nd transient period, which lasts for 1 hour (as recommended from research documented in Section 3.5, Chapter 3) and contains 60-second time steps, the flow is unfrozen, i.e. all the equations are fully functional. During this unfrozen period, it is expected that the flow will be updated to the changes in boundary conditions which would have occurred during the 1st transient (frozen) period.

- The coupling of two transients (total sum of 4 hours) is repeated in succession over a total transient solution period of 2 days.

DTSP#1 is solved as one long transient case, which contains time varying transient solution periods. The case has to be manually stopped and re-started in order to specify the length of required transient period time, 3 hours for the frozen flow and 1 hour for the unfrozen flow updates; but essentially the case is run as a continuous CFD simulation.

Conversely, DTSP#2 can not be run as one continuous solution because steady state cases and transient cases can not be easily combined, due to their positions in time. Transient solutions are solved in real time, whereas steady state solutions do not theoretically exist in real time. Each solution (whether transient or steady state) must be solved as a separate case using initial conditions of the transient or steady state solution which preceded it. At the end of alternating between steady state and transient solutions, the results have to be pieced together to provide continuous simulation results over the entire transient simulation time.

DTSP#2: Transient/Frozen-Steady/Unfrozen Solution

- The methodology of obtaining the fully dynamic thermal solution begins with a transient solution, where the temperature equation is solved for 4 hours (14400 seconds) with the flow in a frozen state, i.e. the Fluid Freeze Flow Function is switched on. This transient solution period contains 360s time steps. At the end of 14400 seconds of transient solving, the solution is saved.

- This saved solution is then readjusted to being a steady state case, and the Fluid Freeze Flow Function is switched off and the boundary Freeze Function is switched on. By saving and re-saving, the initial conditions of this steady state solution are the final conditions of the previous transient solution. After the steady state solution has converged (and hence updated to changes in boundary conditions), the steady state case is saved.

- This steady state case is readjusted and resaved as a transient solution. The initial conditions of the steady state case, are the initial conditions of the next transient case.

- The coupling of transient and steady-state is repeated in succession over a total transient solution period of 2 days.

The simulation results of DTSP#1 and DTSP#2 are compared with a fully transient case, which is referred to as DTSP#0. DTSP#0 runs for 5 days using 360-second time steps, where all equations are fully functioning over the five days. The first three days of all three DTSPs solutions are identical, during these three days the enclosure is given sufficient time to become accustomed to the sinusoidally varying thermal ambient. For both the DTSP#1 and DTSP#2, the following 2-day simulation, using their individual DTSPs complete a total of 5 days simulation.

4.4 Testing the Proposed Dynamic Thermal Procedures

4.4.1 Description of Geometrical Model and Geometrical Grid

In order to test both dynamic thermal modelling procedures within CFD, a generic geometrical model has to be constructed that will be consistent throughout all of the tests of the DTSPs. The most important component of the CFD model construction, which will be common among all tests, is geometrical grid. Initial tests have been implemented to establish an optimum grid that does not require excessive computational time but also provides acceptable accuracy. The computational capacity required by the geometrical grid must be limited because the transient grid also requires high computational processing.

The generic CFD model (upon which the performance of the two DTSP's within CFD was tested) has been developed through a number of different stages, which are as follows:

1. *Determination of optimum geometrical grid to be embedded within the external wall. (STEADY STATE TESTS)*

2. *Determination of optimum geometrical grid to be embedded within the airspace of the enclosure. (STEADY STATE TESTS)*

3. *Comparisons of DTSPs with a fully transient case.*

In all tests, two walls form the boundaries of the enclosure used in the CFD code (Fig 4.1). The other bounding surfaces of the cubed enclosure are adiabatic (i.e. no heat transfer across them). The enclosure is sealed, i.e. unventilated in all cases. Unless stated otherwise, the internal dimensions of the enclosure used in all tests are 1m x 1m x 1m. The physical CFD model assumes that there is no dependence of the radiative exchange upon the frequency of the radiation, i.e. the "grey" approximation is used. The 'grey' approximation allows the absorptivity to equal the emissivity. All reflections of radiation from radiating objects are "diffuse", i.e. radiation is reflected in equal proportions in all directions with no dependence upon the angle of incident radiation.

The first wall acts as a divide between the enclosure and the external environment. It is located at X = 0.1m and is 0.22m thick. The wall is made from brickwork, with the following thermal characteristics:

Thermal Conductivity = 0.84 W/ (mK)

Density = 1700 kg/m^3

Specific Heat Capacity = 800 J/(kgK)
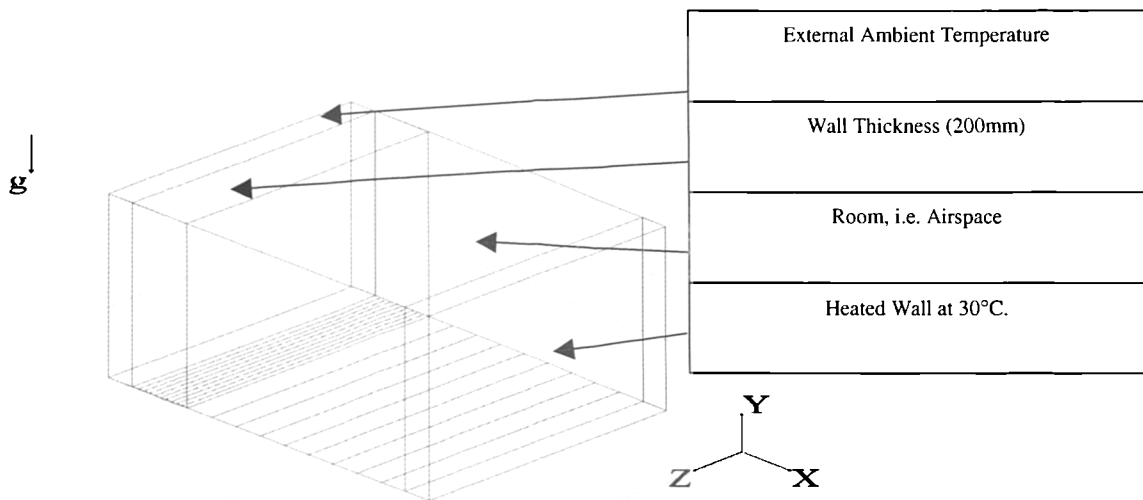
Figure 4.1:   Illustration of the geometry of the enclosure (including grid construction)

In steady state an external ambient setting will be applied as a cuboid (see Appendix A), in preparation for the transient tests which will follow. The external ambient cuboids are given a fixed temperature setting. Fixed temperature settings override any other material and thermal characteristics, and hence no materials are attached to the external ambient cuboid. The internal partition, located at X = 1.32m, also has a fixed temperature setting of 20°C.

The CFD code used in this research uses a finite volume scheme and a solution is considered to have converged if the parameters of flow reach 0.5% of their residual error. Since the flow patterns within all tests are generated by natural convection only, the solution process for velocity uses an estimated free convection velocity of 0.005m/s.

4.4.2 Determination of optimum geometrical grid to be embedded within the external wall

Applying geometrical grid to the CFD model through the use of a discretisation method means that a continuous variation of thermal patterns within the CFD model is represented by a series of discrete values at each grid cell. As the number of grid cells used increases, then the accuracy of the representation will improve. At some point the number of grid cells will be sufficient to achieve the desired level of accuracy. Therefore, a suitable grid embedded within the wall and the airspace inside the enclosure must be determined, in order to accurately capture the internal thermal conditions as a result of changing boundary conditions. The requirement of the accuracy provided by geometrical grid must also take into consideration the computational demands of the transient grid.

Four sets of tests were carried out to determine the optimum geometrical grid to be embedded within the external walls. The walls in every test were made of brickwork. 2 sets of tests used an enclosure with the dimensions of 1m x 1m x 1m. In these tests, 2 wall thickness were tested within each set of tests, 0.22m and 0.5m, to examine the effects of wall thickness on internal thermal conditions.

Additionally the last two tests were designed to examine the effects of a more realistic room geometry of 6m x 6m x 2.4m. Two wall thickness' (0.22m and 0.5m) were also tested. The internal and external specifications of the room are identical to the enclosure of size 1m x 1m x 1m, but the effects of scale on geometrical grid can be observed from these tests.

The external wall was maintained at 5°C in every test. The internal partition was maintained at a temperature of 20°C in every test. Throughout all the tests, the dimensions of each individual grid cell within the airspace inside the enclosure was constant at 0.1m x 0.1m x 0.1m. Table 4.1 summarises the tests carried out.

Table 4.1:   *Test Schedule for the determination of optimum geometrical grid to be embedded within the external wall*

Test Case (TC)	No. of Grid Cells in Wall
Test 4.4.2.1 – 1m^3 geometry with 0.22m thick walls	220 Reference Case (RC)
	40
	22
	11
	10
	5
	2
Test 4.4.2.2 – 1m^3 geometry with 0.5m thick walls	40 (RC)
	30
	25
	15
	10
	4
	3
	2
Test 4.4.2.3 - 6m x 6m x 2.4x geometry with 0.22m thick walls	44 (RC)
	22
Test 4.4.2.4 - 6m x 6m x 2.4x geometry with 0.5m thick walls	22
	11
	10
	5

Nine monitoring points (MP) were equally spaced in 3 x 3 matrix located in the YX plane at Z=0.3m and 3m for the 1m^3 and 6m x 6m x 2.4m sized enclosures, respectively.   These points record temperatures and velocities within the enclosure. MP1 was located in the top left-hand corner (i.e. closest to the external wall) of the enclosure and MP9 was located at the bottom right-hand corner of the enclosure. After each test, the results of the surface temperatures were also obtained.

Results of all tests were compared to a chosen reference case (RC). The reference case (RC) was chosen to be the case that provided the most accurate results (limited by hardware capability), i.e. the test containing the greatest number of grid cells within the wall. Table 4.2 presents the results.

Table 4.2:   % Errors of Surface Temperature, Temperature and Velocities (at all MPs collectively)

Test Case	% Error of Internal Surface Temperature on External Wall ST (°C) *[1]	% Error of Temperature, T (°C) within the Enclosure*[2]	% Errors of Velocity, V (m/s) within the Enclosure*[3]
Test 4.4.2.1 - 1m³ geometry with 0.22m thick walls	Between 0.3% and –0.9%	± 0.1%	± 1.5%
Test 4.4.2.2 - 1m³ geometry with 0.5m thick walls	Between 1% and - 0.4%	± 0.04%	± 0.5%
Test 4.4.2.3 - 6m x 6m x 2.4x geometry with 0.22m thick walls	±1.5%	± 0.01%	±2%
Test 4.4.2.4 - 6m x 6m x 2.4x geometry with 0.5m thick walls	Between 0 and 2.5%	Between –0.005% and 0.02%	±2%

The results of Table 4.2 were determined using the following calculations:

*[1] % Error Internal ST on External wall, ST (°C) =

ST[Test Case] – ST[RC] / (Mean Range of ST[RC])

(4.2)

[2] **% Error T =**

T[Test Case] – T[RC] / (Temp of Wall located at 0.1m [RC]– Temp of Wall located at 1.32m [RC])

$$(4.3)$$

[3] **% Error V =** V[Test Case] – V[RC] / (Max[RC] – Min[RC])

$$(4.4)$$

where:

ST = Surface Temperature (°C)

T = Temperature recorded at MP5 (°C)

V = Velocity recorded at MP5 (m/s)

The % error calculations are obtained by comparing the results of the test cases with the range of results of the reference cases [RC]. The % error results of surface temperatures, temperatures and velocities within the room indicate how accurate the results are compared to the most accurate results, which can possibly be obtained, given the limitations of hardware capability.

When comparing all results of the tests, it was clear that heat transfer was a linear thermal process through the building; the number of grid cells within the wall thickness had no effect upon the airflow within the room, when the external conditions were at steady state. The overall % errors of surface temperature for the tests containing 1m3 enclosure were less than ±0.5% and were not significantly improved by using 40 grid cells compared to a maximum of 220 grid cells.

Comparisons of the results of surface temperatures of Test 4.4.2.1 and Test 4.4.2.2 with the results of Test 4.4.2.3 and Test 4.4.2.4, indicate that there is no direct correlation between the inner dimensions of a 'room' and the number of grid cells to be placed within the building fabric. The smaller the inner dimensions of the room, the more prominent the airflow patterns in the room, and hence the smaller the overall % errors of temperature and velocity within the room. As few as 5 grid cells embedded within the wall thickness provided accurate results of the temperature

(less than ±0.2%) and velocities (less than ±1%) inside the enclosure. All other tests (using larger numbers of grid cells within the wall) achieved results of a similar magnitude.

4.4.3. Determination of optimum geometrical grid to be embedded within the airspace of the enclosure

Dynamically modelling within CFD is computationally expensive due to the large quantity of transient grid required to simulate the heat transfer and airflow patterns over a substantial period of time. Hence in order to limit the computational labour required, a suitable physical grid had to be selected over the airspace of the enclosure.

The use of a highly detailed geometrical grid provided very accurate solutions at a high computational cost. The objective of the tests presented in this section, however, is to determine the construction of a suitable geometrical grid over the air contained within the test enclosure, which will provide reliable results, whilst restraining the requirement of intensive computational solving, for the following tests presented in section 4.5.

Walls are not required for this test and hence the enclosure is bounded by thin cuboids (each 0.1m thick) that do not contain grid cells, but have fixed temperatures (i.e. material characteristics are not applicable). The boundaries located at X = 0m and X = 1.2m have fixed temperatures of 5°C and 20°C, respectively. The enclosure used in this test has dimensions of 1m x 1m x 1m. The test cases were solved to steady state, using the most suitable turbulence model for the application, which is the Revised k-ε Turbulence Model, (which accounts for low Reynolds Numbers at the wall) see Section 2.4, Chapter 2. Table 4.3 summarises the tests carried out.

Table 4.3:   *Test Schedule for the determination of optimum geometrical grid to be embedded within the airspace of the enclosure*

Test No.	No. of Grid Cells within the Enclosure in one co-ordinate direction
4.4.3.1	100 (i.e. each cell is 0.01m wide)
4.4.3.2	50 (0.02m)
4.4.3.3	25 (0.04m)
4.4.3.4	10 (0.1m)
4.4.3.5	5 (0.2m)
4.4.3.6	2 (0.5m)

Nine monitoring points were equally spaced in a 3 x 3 matrix located in the YZ plane at Z=0.3m. The monitoring points recorded the temperatures and velocities for each test. In these tests the Reference Case (RC) (Test No. 4.4.3.1, See Table 4.3) = 0.01m x 0.01m x 0.01m, placed uniformly within the space, the results provided by the reference case were assumed to be the most accurate that can be obtained with the computational hardware resources used.

The errors of the temperatures recorded at the MPs were calculated using the following formulae:

$$T[Test\ Case] - T[RC] / (Temp\ of\ Hot\ Wall\ (20°C) - Temp\ of\ Cold\ Wall\ (5°C))$$

$$(4.5)$$

The errors of the velocities recorded at the MPs were calculated using the following formulae:

$$V[Test\ Case] - V[RC] / 0.054\ m/s \qquad\qquad (4.6)$$

where 0.054 m/s = minimum representative velocity within the enclosure, calculated from 0.5% of the total momentum of the air within the enclosure.

Temperatures recorded in the space had maximum errors of ±7% (See Figure 4.2). The errors were concentrated along the top of the geometry and along the bottom of the geometry, and were largely due to natural convection currents. The largest errors were located in the top left hand corner and the bottom right hand corner of the enclosure where the air, although low in velocity, was within a region which is quite unstable (See Figure 4.3).
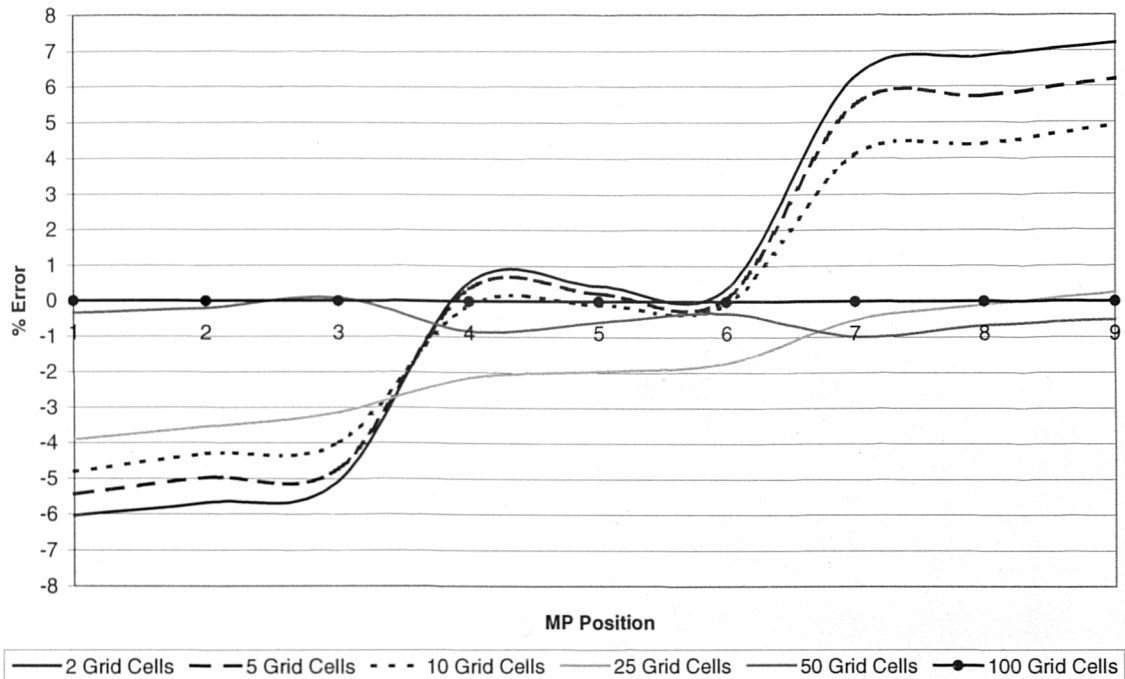
Figure 4.2:   % Error of Temperature within 1m^3 Enclosure using various Grid Cell Numbers (in the space)

The boundaries of the space contain high velocity gradients. The areas that do not contain high velocity gradients, i.e. within the centre of the room, recorded almost zero velocities. Hence the temperatures were easily predicted, regardless of the densities of the grid in this region. This region had very low % errors of temperature, no greater than 2%.

Velocities recorded within the space of all the test cases had maximum errors of between −1% and 4%. The largest errors were at the edges of the geometry, where regions of high velocity gradient were located. The velocity errors were mainly symmetrical within the room. The lowest recorded error was in the centre of the room, where the flow was almost zero.
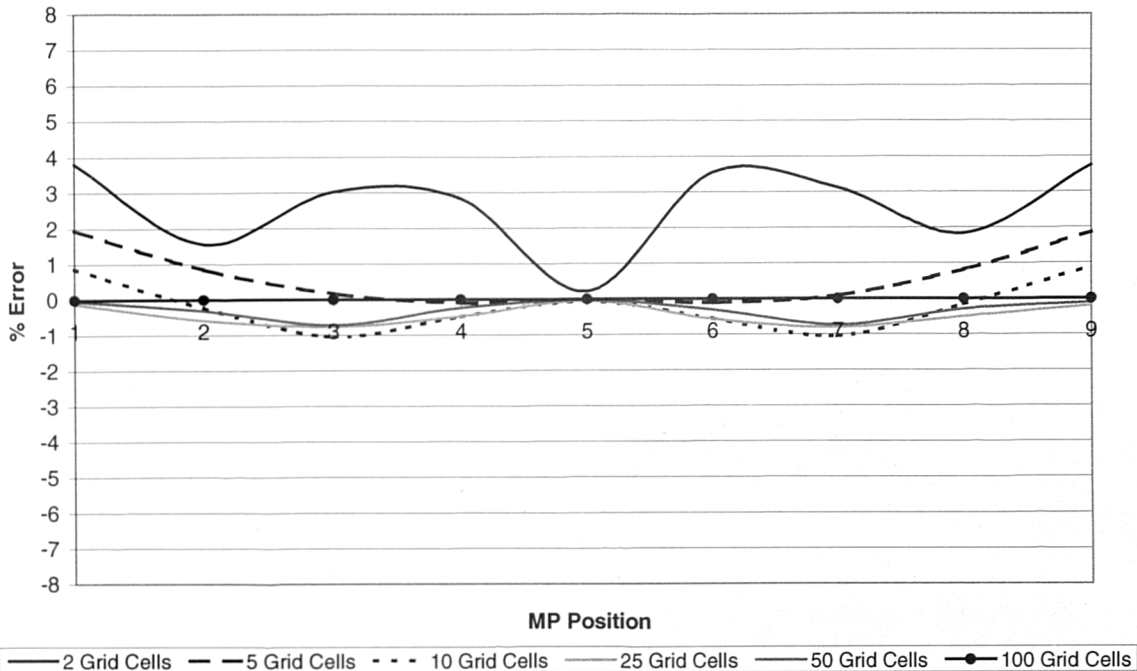
Figure 4.3:   % Error of Velocities within 1m³ Enclosure using various Grid Cell Numbers

The grid configurations that had the lowest error were between 25 and 50 cells in each co-ordinate direction. Maximum errors of temperature were 4% using 25 cells, while the 50 cells had a % error in temperature of between 0-1%. The % errors of velocity were between 0-1% for 25 and 50 grid cell cases.

To limit the time required in obtaining a complete transient simulation, a suitable geometrical grid had to be selected. 25 grid cells provided similar magnitudes of error of velocity as using 50 grid cells. Errors in temperature were higher using 25 grid cells, compared to using 50 grid cells. Maximum errors that occurred within the space were not be more than 4% and were limited to the high and low levels of the enclosure. By selecting to use a uniform grid configuration within the test enclosure

of Parts 4.5 of 25 x 25 x 25 grid cells, the error of temperature and velocity will be consistent.

For an enclosure of size $1m^3$, used in this study, a lack of detailed grid at the boundaries was not a significant cause of error. This contradicts well-documented studies that state that detailed grid should be used at the boundaries of a CFD model. The reason why this is not the case within the enclosure used in this study is due to the significantly low velocities at the wall. The flow at the boundaries are almost laminar, and hence detailed grid is not required at the walls. Turbulent flow does exist within the enclosure and will be accounted for by the Revised k-ε Turbulence model.

The same grid established in sections 4.4.2 and 4.4.3 will be used in every test conducted in section 4.5. It is understood from the outset that the use of a coarser grid will impose errors in the solutions, but these errors will be consistent in the tests of section 4.5, if the same grid is used consistently. The purpose of the transient tests documented in section 4.5, is to compare the performance of the two proposed solutions to dynamically modelling within CFD, so the actual quantitative solutions of the enclosure are of secondary concern. The primary objective of the tests of section 4.5 is to quantify the errors caused by the two proposed methods of dynamically modelling. Hence any errors incurred by using coarse geometrical grid will be identical and consistent in each transient test.

4.5 Comparison of DTSP#1 and DTSP#2 with a fully transient case

4.5.1 Introduction

A suitable geometrical grid over the airspace contained within the fabric of the enclosure and within the enclosure itself were established (documented in Sections 4.3 and 4.4, respectively) and the transient time steps over a period of unfrozen flow were also determined for the use in DTSP#1 (documented in Chapter 3, Section 3.5). Both the geometrical and transient grids have been chosen as providing good accuracy within the limits of computational capabilities available for this research. Using the results of the grid sensitivity tests, CFD models can be constructed to test the performance of the two proposed DTSPs.

A fully transient case of the enclosure exposed to an external sinusoidal temperature profile was run for 3 days. During these 3 days the enclosure was pre-conditioned to the periodic thermal conditions of the external sinusoid (described by Equation 4.1). The last two days of the solution were obtained by applying different DTSPs.

4.5.2 Test Geometry

The same dimensions (1m x 1m x 1m) of the enclosure were used in all tests, documented in this section. The uniform grid cell size within the enclosure is 0.04m x 0.04m x 0.04m, as determined from tests documented in Section 4.4. 10 grid cells in the x-direction are embedded within the external wall (brickwork) of the enclosure, which has a thickness of 0.22m. The wall is located at X = 0.1m. An internal partition is located at X = 1.32m and has a fixed temperature setting of 20°C. Located at X = 0m is another cuboid which is given a fixed temperature sinusoidal profile, which varies between 12.5°C and 27.5°C over a period of 24 hours; this temperature profile has been chosen to represent external ambient conditions. Nine monitor points were contained within the enclosure to record temperature and velocities within the room. They were placed equally on a 3 x 3 matrix in the XY plane at Z = 0.3m.

4.5.3 Results and Discussion

The results of these tests are presented below. To recap, DTSP#1 solves 3 hours of transient frozen flow and 1 hour of transient unfrozen flow, while DTSP#2 solves 4 hours of frozen transient flow followed by a steady state calculation.
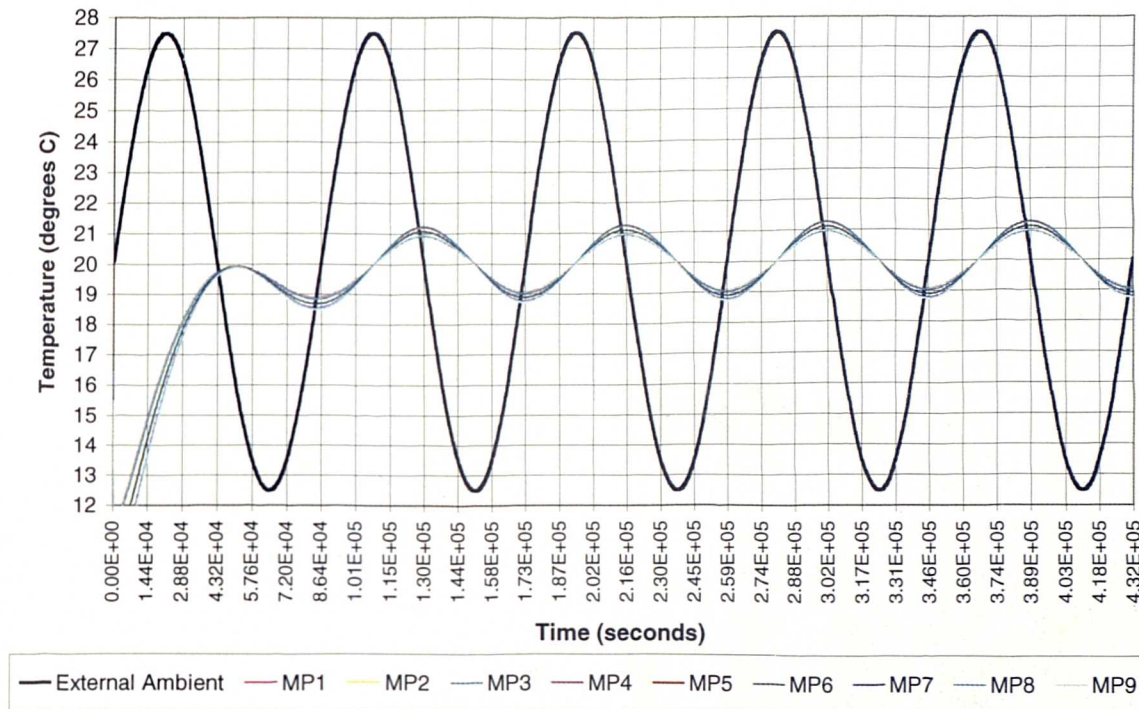
Figure 4.4:   Fully Transient Solution over 5 days (DTSP#0) - Temperature recorded within enclosure

Due to the nature of Fig.4.4, the solution process used by the fully transient dynamic thermal model, (DTSP#0), will differ from the temperature and velocity profiles of DTSP#1 and DTSP#2 (compare Figures 4.5 and 4.6). A comparison of the temperature profiles of each code between 259200s (end of the third hour) and 345600s (end of the fourth hour) indicate that the correct temperatures are reached after each session of updating the flow, despite different methodologies in reaching those temperatures. Every fourth hour, all temperatures reach the same value regardless of the methodology by which the case was solved. DTSP#2 is a less smooth curve compared to DTSP#1 (see Figure 4.6).

In both cases, when the temperatures are increasing the codes under-predict the conditions within the room because the frozen airflow patterns are not adequately conducting heat away from the wall. For the same reasons, when the temperatures within the room begin to decline, the codes over-predict the conditions within the room.

A detailed discussion of the results is presented below. DTSP#0 temperature results are shown in Figure 4.4, DTSP#1 in Figure 4.5 and DTSP#2 in Figure 4.6. The temperature results for the final day of all three codes are shown in Figure 4.7.
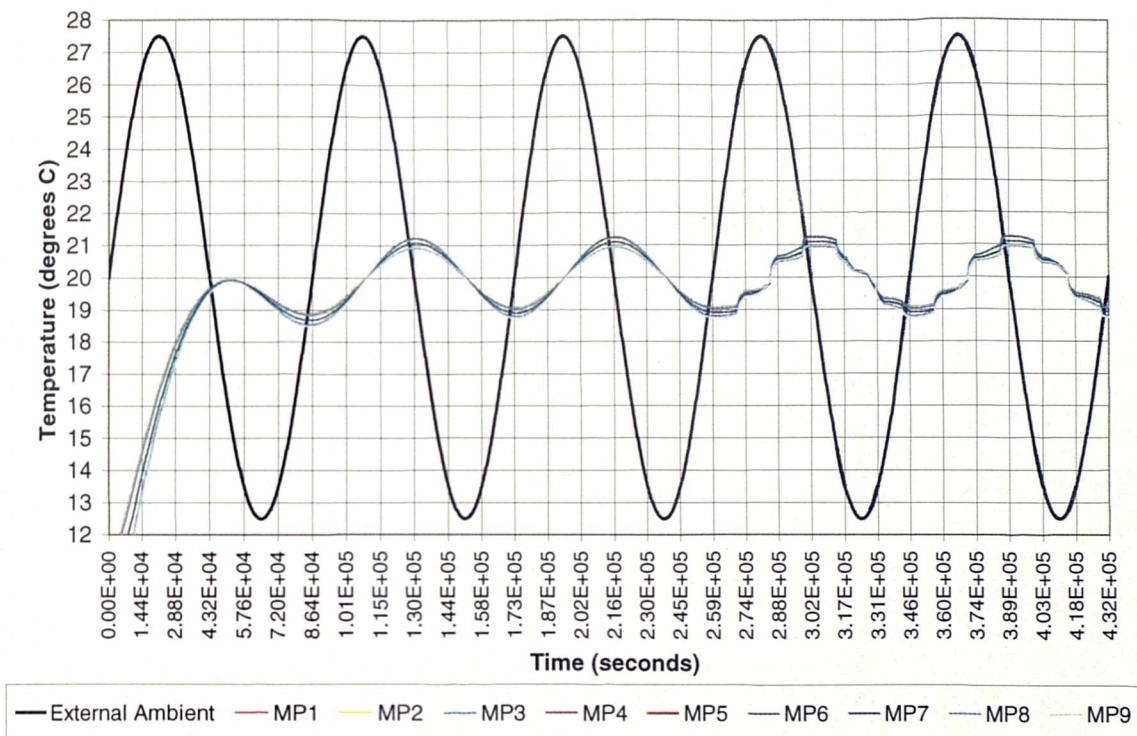
Figure 4.5:   Last 2 days (out of 5 days in total) solved using DTSP#1 – Temperatures within enclosure

The results from DTSP#1 show that during the periods of frozen flow, (where the velocities remain constant) the temperatures increase at a slower rate than the rate of change of external temperature. This is because the key mechanisms of heat transfer, i.e. the flow patterns have been paused. See Figure 4.5 and then Figure 4.7 for details during the fourth day.

When the flow is unfrozen, the first three minutes indicate zero change in velocities. During this period, the temperatures increase is insignificant (approximately

0.01°C). The following 27 minutes contain highly unstable velocities, and a steep increase in temperatures. By the start of the following half an hour of unfrozen flow, the velocities have reached stable magnitudes again and the temperatures are increasing at a slower rate.

An average temperature increase over the entire period of unfrozen flow is 0.45°C; across all MPs within the enclosure. Once the flows are unfrozen, latent energy is expended in adjusting the temperatures as a result of unfrozen flows. A total of 30 minutes is required for the velocities to adjust to the different boundary conditions (which would have occurred over the previous transient period of frozen flow) and the changing boundary conditions which will be occurring during this period of unfrozen flow (which will be relatively smaller). The final 30 minutes of this period is solving temperatures and velocities, which are responding to completely unrestricted conditions, i.e. no frozen flows. The solution during the final 30 minutes is effectively solving as a fully dynamic thermal case.
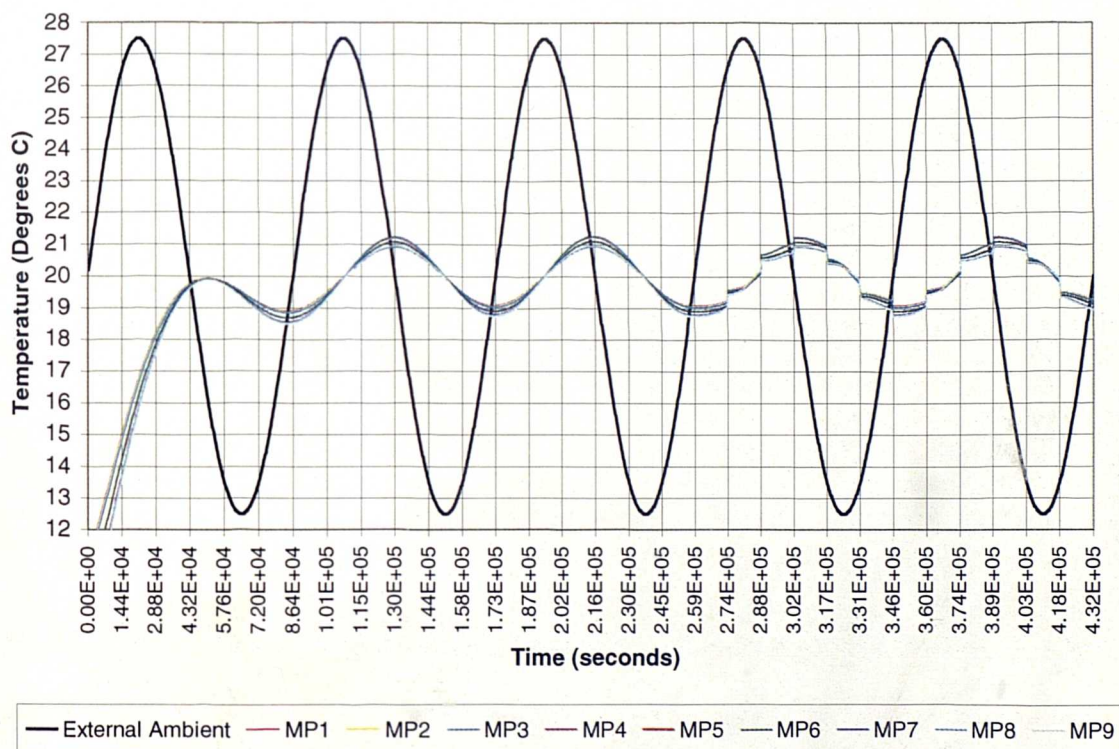
Figure 4.6:   Last 2 days (out of 5 days in total) solved using DTSP#2 – Temperatures within enclosure

During the 2nd period of frozen flow using, the external temperatures increase during the first 90 minutes (by 1°C) and then start to decrease by 0.2°C, for the final 90 minutes (all linear approximations). See Figure 4.6 for external temperature variations using DTSP#1. The temperature profiles of the MPs within the room do not decrease, but continue to increase over the entire period of frozen flow, by 0.3°C. During the first 15 minutes, the velocities are not quite frozen. After 15 minutes, the velocities are frozen and do not change throughout the rest of the period.

The 2nd and 3rd periods of frozen and unfrozen flow appear to be showing a response to the section of the ambient external sinusoidal that has the lowest rate of change of temperature (or even decrease in temperature), which occurred 6/7 hours prior to this time. This indicates that the building fabric material has a phase lag of 6/7 hours, which agrees with analytical calculations for a material with these thermal characteristics and thickness (Tests B1/B2/B3, Appendix B).
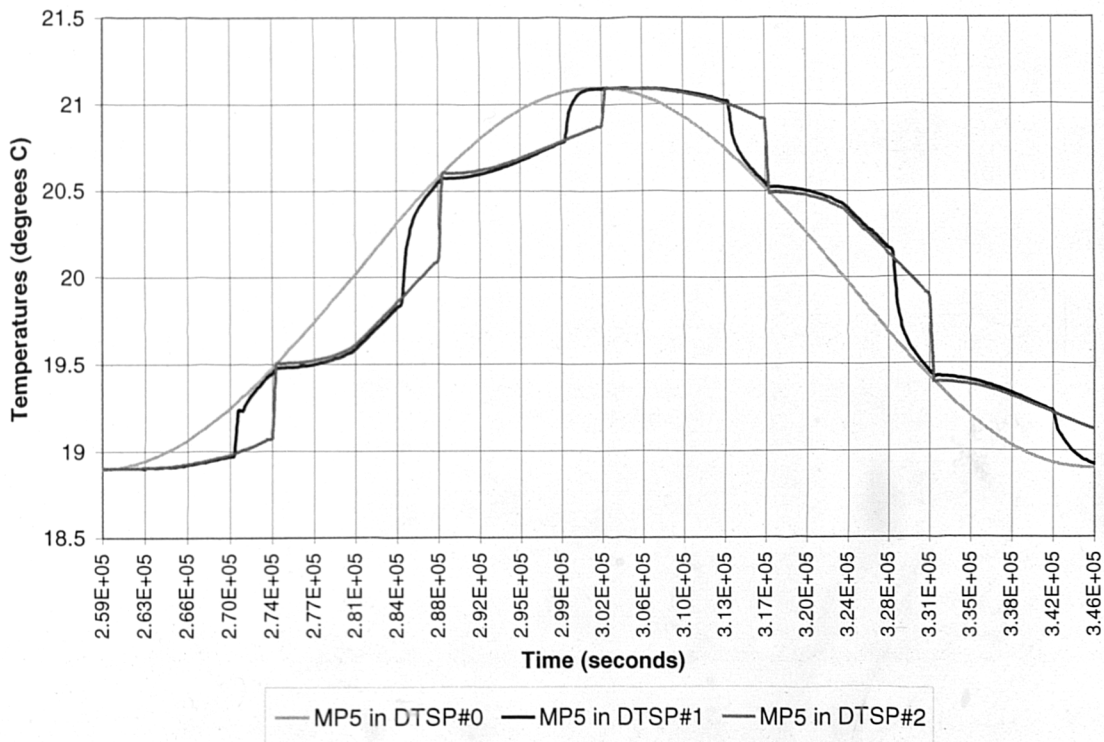
Figure 4.7:   Comparison of temperatures recorded using 3 different DTSPs over 6 hours of transient solutions

For the DTSP#2 test, during the first three hours of transient frozen flow, the temperature and velocity profiles follow the exact same pattern as those observed using DTSP#1. During the entire period of frozen flow, the temperatures within the room increase by 0.15°C. See Figure 4.6 and then Figure 4.7, for details during the fourth day.

In the first 12 minutes of the 2nd period of frozen transient flow, the temperatures catch up to the effects of the steady state, which would have been solved beforehand. As a result, the temperatures increase by a further 0.4°C in the first 12 minutes. The temperatures recorded at the end of a transient period of unfrozen flow in DTSP#1, will be reached in the early stages of the following transient period of unfrozen flow (which follows a steady state update) of DTSP#2. Hence, DTSP#2 at the end of the 4 hours of frozen flow is always behind in the temperature solution process by approximately 2% (compared to a fully transient case), that does not depend on the frequency of updating the solution.

As expected, the overall temperature profiles recorded by each code are very different. During the fourth hour, the external ambients continue to change throughout the transient period of unfrozen flow used in DTSP#1. During the unfrozen transient solution period of DTSP#1, the airflow patterns would have adjusted to changes in external ambient conditions. In a solution provided by a DTSP#2, the flow patterns in the room would have been frozen for the entire 4 hours. So, the airflow patterns at the start of the 4 hours would have been used to represent the airflow patterns that would have occurred over the entire 4 hours. This would have incurred errors between the two solution processes.

A comparison of the temperatures obtained by DTSP#0 with DTSP#1 and DTSP#2 at set times indicate that the errors were <0.1% and <2.5%, respectively. As an example of the magnitudes of the temperatures obtained, at the end of the fourth hour (before a steady state update) the temperature recorded at MP5, using the DTSP#2 solution was 20.91°C, compare this to the same value in DTSP#1 of 20.52°C and 20.52°C in DTSP#0.

During the first 12 minutes of the following transient period of frozen flow, the flow catches up to the adjustment made by the previous steady state calculations. The temperature reached at MP5 is approximately 20.6°C, as reached at the end of the 4th hour using DTSP#1. The availability of correct results from both the DTSP#1 and DTSP#2 are dissimilar. DTSP#1 provides correct results towards the end of a transient update (unfrozen flow period). The most accurate results provided by DTSP#2 can be obtained after a steady state update, during the first few time steps into the following period of transient unfrozen flow. Both DTSPs were quicker than solving a fully transient case, but DTSP#2 was by far the most efficient method.

4.6 Conclusions

Two procedures named DTSP#1 and DTSP#2 were tested against each other and against the results of a fully transient solution. DTSP#1 used a combination of two sets of transient periods and DTSP#2 used a combination of transient and steady state periods. Both procedures adopted DTM techniques into CFD by using freezing and unfreezing flow functions, to efficiently simulate the heat transfer through both the solids materials of the building envelope and the air enclosed.

The main objective of the tests carried out in Section 4.4 was to establish a suitable CFD model to be used to dynamically model an enclosure. Optimum geometrical grid through the wall thickness, optimum grid over the airspace of the enclosure, and optimum transient time steps to be used during a transient period of unfrozen airflow updating (documented in Section 3.5, Chapter 3) were established before the tests presented in Section 4.4 were run.

For an enclosure of size $1m^3$ containing an external wall thickness of 0.22m, the optimum number of grid cells is 10. The optimum grid cell size to be used within the airspace of the enclosure used in the test cases is 0.04m x 0.04m x 0.04m (for a uniform grid). Optimum grid was also considered to be constructed so as to provide good accuracy, whilst not significantly overloading computational time during transient solutions, where transient grid also had to be accounted for.

The simulations of a fully transient case were compared with the results of DTSP#1 and DTSP#2 and the results indicated that:

- DTSP#2 is the preferred method of solving dynamic thermal cases within CFD. The methodology provides an accurate analysis of the conditions inside an enclosure (dimensions, 1m x 1m x 1m). DTSP#2 is a far more computationally efficient method of dynamically thermally modelling since it took 90% less time (Total of 115.87 minutes) to run a total dynamic one-day simulation than a fully transient case. DTSP#0 took 1177.21 minutes of CPU time to solve for 1 day dynamic thermal simulation;

- DTSP#1 also provides a solution to solving dynamic thermal problems within CFD, but the methodology is not as efficient and can be computationally expensive because the solution requires a coupled transient procedure. DTSP#1 took 753minutes to solve for one day, 36% less time than running a fully transient case;

- Both methodologies provide equally accurate simulations (compared with a fully transient solution) at the end of each solution combination (i.e. either transient-transient or transient-steady); although the temperature and velocity profiles along the solution process vary.

4.7 Chapter Summary

In this chapter, the preliminary procedure for dynamic modelling, introduced in Chapter 3 was reviewed. The nature of transient unfrozen airflow updating was similar to simulating a steady state case. The question arose from the research of Chapter 3, as to why a steady state unfrozen flow update period could not be used instead.

Initial problems of successfully updating of the airflow under steady state conditions were solved by developing an additional function necessary for dynamically modelling within CFD – the Boundary Freeze Function. The methodologies of two DTSPs were clearly outlined, stating the order of use of necessary functions available within the CFD code. The DTSPs were tested against a fully transient case and each other.

To test the procedures fairly, a geometrical model of a simple enclosure was established in 3 fundamental stages. Given that dynamic thermal modelling is computationally demanding, the stages were vital in establishing an optimum grid that was not excessively computationally expensive, but did provide good accuracy. Once the geometrical CFD model was established, the performance of DTSP#1 (transient-transient) and DTSP#2 (transient-steady) were compared against a fully transient solution and DTSP#2 was selected as being the most efficient procedure for dynamically modelling more realistic buildings.

In the chapter to follow, DTSP#2 will be used in further intermodel comparisons and testing to establish appropriate transient periods and time steps of frozen flow for a comprehensive range of fabrics. The relationship between the rate of heat transfer through a particular material will directly influence the length of the transient frozen period and will influence the frequency of airflow steady state updates. From this point onwards, DTSP#1 will be abandoned and DTSP#2 will now be referred to as the established DTM-CFD procedure, since the techniques used in DTSP#2 will be further developed and refined in the next chapter.

CHAPTER 5

REFINEMENT OF DTM-CFD PROCEDURE

CHAPTER 5 – Refinement of DTM-CFD Procedure

5.1 Introduction

After having compared the performance of DTSP#1 and DTSP#2 with a fully transient procedure, the results indicate that both DTSP#1 and DTSP#2 provide highly accurate simulations. Solving DTSP#1, however, is far more time consuming, since two transient cases must be solved in succession. At this point in the research, the development of DTSP#1 will be suspended. DTSP#2 will be used and further developed as the new technique for dynamically modelling within CFD. DTSP#2 will now be referred to as the DTM-CFD Procedure.

In preliminary tests using the DTM-CFD Procedure, the transient period for frozen flow was set to 1 hour. During this hour the airflow enclosed within the building was temporarily paused to the thermal conditions set in the preceding steady state airflow update. The most useful information from the dynamic thermal modelling procedure is assumed to be found after each steady state update. At this point both the airflow and heat transfer within the room and boundary conditions of the fabric are most concurrent. Research conducted using the DTM-CFD Procedure (referred to as DTSP#2), reported in Chapter 4, indicate that the accuracy of the solutions provided at the end of each steady state airflow update is likely to depend on the following factors:

1. the length of the transient frozen flow period;
2. the length of the time steps lengths within the frozen flow period;
3. the amount of thermal change between steady state updates.

When dynamically modelling the thermal environment of buildings that are exposed to fluctuating external ambient conditions, the three factors listed above are influenced by the thermal characteristics of materials used in building envelopes. The amount of thermal change across the boundaries of the building depends on the

rate of thermal transfer through the material, which is predominantly controlled by material characteristics.

In order to observe the relationship between the accuracy of simulation provided by the DTM-CFD Procedure and material thermal characteristics, nine representative materials have been contrived. The thermal characteristics of these nine materials were chosen so as to span a wide spectrum of thermal values observed from common materials used in building construction. The nine materials selected for the following tests have been chosen categorised by two main thermal characteristics, which are;

1. the thermal conductivity of the material;
i.e. the measure of the ability of a substance to conduct heat.

2. the specific heat capacity of the material.
i.e. the quantity of heat required to raise temperature of a body one degree, taking as the unit of measure the quantity required to raise the same weight of water from zero to one degree.

The thermal conductance of the material depends upon the thickness of the material because the thermal resistance of a material depends upon its thickness. In order to restrict the number of parameters examined in each test, the thickness of all nine materials was kept constant at 0.22m (commonly used thickness of building material). The specific heat capacity of the materials also relates to the density of the material and is a measure of a materials thermal mass/weight, hence the following combination of material characteristics were tested:

Conductivity (W/mK):

C1 = 0.03   (typically Polyurethane Board)

C2 = 0.84   (typically Brickwork)

C3 = 1.5   (typically less than Concrete Heavy Block)

Thermal Mass (J/m^{3}K) (Density x Specific Heat Capacity):

W1 = 10 x 1400 = 14000   (typically Urea Formaldehyde, UF Foam)

W2 = 1700 x 800 = 1360000   (typically Brickwork)

W3 = 2300 x 1000 = 2300000   (typically Concrete Block, heavyweight)

Table 5.1:   *Matrix of Thermal Characteristics, containing the names of all nine materials to be tested.*

	C1	C2	C3
W1	W1C1 C1 = 0.03 W1 = 14000	W1C2 C2 = 0.84 W1 = 14000	W1C3 C3 = 1.5 W1 = 14000
W2	W2C1 C1 = 0.03 W2 = 1360000	W2C2 (Brickwork) C2 = 0.84 W2 = 1360000	W2C3 C3 = 1.5 W2 = 1360000
W3	W3C1 C1 = 0.03 W3 = 2300000	W3C2 C2 = 0.84 W3 = 2300000	W3C3 C3 = 1.5 W3 = 2300000

From Table 5.1 above, nine batches of tests were derived and carried out. Within each batch of tests, the effects of the following were tested:

1. length of the transient frozen flow period (Section 5.2);

2. length of the time steps lengths within the frozen flow period (Section 5.3);

3. the amount of temperature change within the boundaries between steady state updates; will be tested (Section 5.4).

5.2   Establishing Lengths of Transient Frozen Flow Periods

5.2.1   Test Specification

For each of the nine materials, a range of transient frozen flow periods were tested to examine the relationship with the accuracy obtained at the end of each steady state update. The transient time periods tested ranged from 6 minutes to 8 hours depending on the individual responses of each of the nine materials. It was expected that materials with a greater thermal weight may require longer transient frozen periods due to responding very slowly to external thermal variations.

The thermal conditions fluctuate on the external surface of the material, since ambient conditions vary sinsoidally over a period of one day, with an amplitude of 15°C (see Equation 4.1, Chapter 4). Hence the heat transfer coefficients on the internal surface of the wall also change. The longer the length of a period of transient frozen flow, the greater the probability of a larger thermal change across the boundaries of the enclosure.

Large thermal differences between frozen flow periods could create inaccuracies when updating at steady state, since the frozen airflow patterns are likely to misrepresent the true nature of the thermal conditions inside the space during a period of frozen flow. If an airflow pattern becomes exceedingly non-representative, a steady state update may occur too late.

The aim of this test was to find one appropriate length of the transient frozen flow period to be used in the DTM-CFD Procedure, which is common to all nine materials. One transient frozen flow period could then be used on any of the nine materials (or even a combination), since they are likely to be modelled in real design simulations, as a combination of materials in a multi-layered building envelope.

5.2.2 Geometrical Configuration of Test Enclosure

The physical geometry of the test case remains the same as the tests carried out in Chapter 4 (see Section 4.5). In these tests, additional Monitoring Points (MP) were placed immediately adjacent to the internal surface of the wall, where data could be collected. The results obtained of temperature at these points provided an indication of the modelling of heat transfer coefficients at the internal surface of the wall. The heat transfer coefficients at the boundaries of an enclosure strongly influence the internal airflow patterns over the boundaries. This effect has consequences on the air movement within the space. At the end of a solution of steady state unfrozen flow, the heat transfer coefficients at the boundaries contribute to setting airflow patterns within the room for the following transient period of frozen flow.

All 9 materials were subjected to a 1-hour transient frozen flow period test, and depending on the rate of response to the thermal conditions, transient time periods were either increased or decreased in subsequent tests. As recommended from Equations 3.2 reported in Chapter 3, time steps were kept constant at 360s for all tests, since 1-hour of transient frozen flow was used as a base case test for all 9 materials. All of the materials were also solved under fully transient conditions (all equations fully functioning), to provide reference values to which the results provided by the DTM-CFD Procedure were compared.

5.2.2 Results and Discussion

Due to the excessive number of tests and vast quantities of data generated, a full description of the tests, results and discussions are included in Appendix C, Section C2. This section summarises the main findings observed from the tests. The flow within the centre of the enclosure is almost stagnant and therefore, difficult to obtain comparisons. Therefore, the errors in using various transient periods have been measured by discussing the results provided by the DTM-CFD Procedure with the results of a fully transient case of the temperature at a central location on the Y-Z plane adjacent to the internal surface of the external wall. The flow within the enclosure is dominated by natural convection and hence is most prominent at the

boundaries. Hence, errors caused by using the DTM-CFD procedure are likely to be the most prominent in this region. The differences between the fully transient and DTM-CFD Procedure results are represented as a percentage of the maximum temperature range of the sinusoidal external ambient (i.e. 15°C).

Generally, the errors incurred by using the procedure are so low that cumulative error effects do not appear to have a significant effect. The errors are low for materials with the lightest thermal weight. The errors reduce further still with increased thermal weight. Errors appear to be more affected by the conductivity of the material rather than the thermal weight of the material. The largest errors recorded after a steady state update were 0.3% (~0.06°C) and occurred with conductivities of 1.5 W/mK (thermal characteristic C3), see Table 5.1.

Materials with a high thermal weight respond very well to the DTM-CFD procedure, even if they have high thermal conductivity. This is because the fluctuations of the external sinusoidal ambient gets trapped within resistance of the material. When the steady state update is performed, the temperatures within the boundaries, which are virtually steady anyway (due to the high thermal resistance of the material) do not have to be significantly adjusted. Airflow patterns consequently change very little during each update.

The less thermally conductive materials respond very slowly to the thermal fluctuations and hence longer periods of frozen transient flow may be used in the DTM-CFD Procedure. Unfortunately, no direct correlation between the material's thermal characteristics and the error associated after a steady state update can be detected. An engineering judgement should be made as to how long the flow should be frozen. The chosen length of frozen flow should take into consideration:

1. the frequency at which results need to be collected;
2. the internal and external thermal driving forces to the room;
3. the rate at which external thermal changes conduct through the material Thermal lag).

The internal and external thermal driving forces such as ventilation systems and weather, respectively, are the thermal forces that will cause the internal airflow patterns to change. Significant changes in internal and external thermal conditions must be monitored by the engineer. Ideally an automated process to detect thermal changes within a CFD simulated zone could be developed in the future, which would automatically start a steady state update to capture significant differences in airflow patterns. This idea has been tested later and contained within the following Chapter 6.

Research has already been conducted in examining a relationship between building thermal mass and real-time dynamic thermal modelling (Chen (2001)). The emphasis of the research was based on the link between the operations of building mechanical systems and the thermal mass stored within building materials, whereby significant energy savings could be made by reducing energy costs by replacing mechanical heating and cooling with the thermal energy stored within building fabric. Although the emphasis of the research conducted by Chen (2001) was different to the requirements of this research, similar trigger mechanisms could be designed in order to detect thermal change within building fabrics, which could stimulate a steady state update, especially for thermal changes that could significantly affect airflow patterns within an enclosure.

As time progresses, the frozen airflow patterns at the start of a transient period will become increasingly obsolete, especially if external thermal conditions are highly variable. Hence, the errors along a transient period of frozen flow do tend to increase with time. Errors are significantly reduced when a steady state update is performed, but are not completely eliminated since the constant delay in updating after a period of frozen flow will always be responsible for a certain amount of error (which is often insignificant). Figure 5.1 illustrates this point.

% Errors of Transient 'Frozen Flow' Periods for Material C1W1
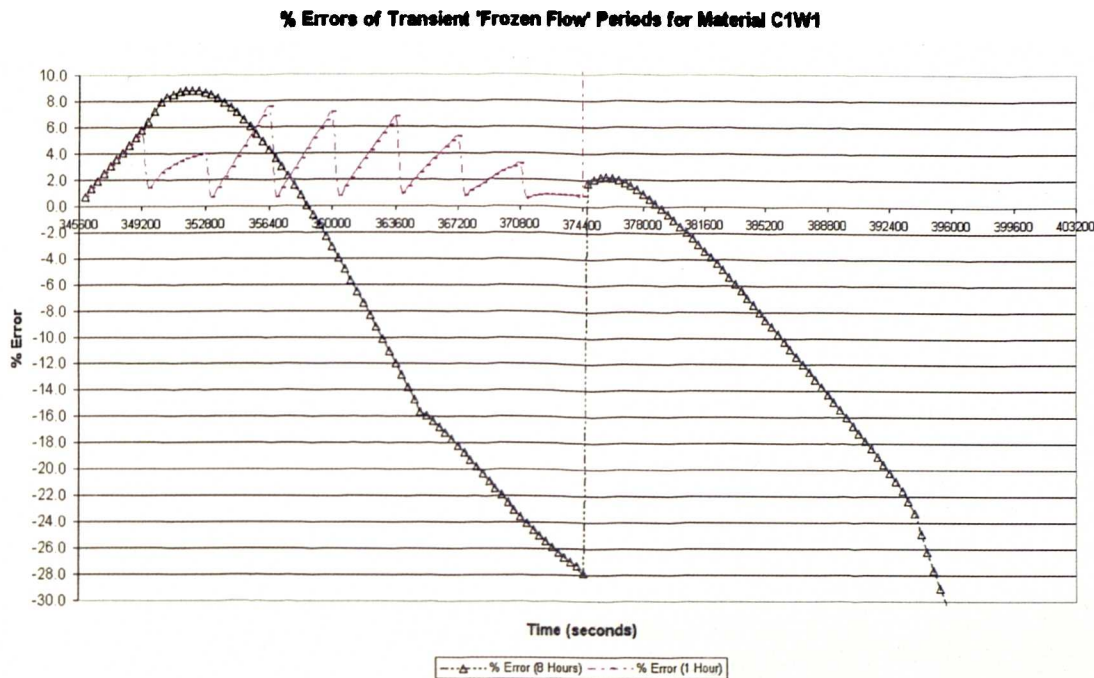
Figure 5.1: % Errors of Transient 'Frozen Flow' Periods for Material C1W1

A realistic representation of weather fluctuations in the UK was used on nine very diverse materials to test the performance of the DTM-CFD procedure. The outcome of these tests is positive, since the results over the comprehensive range of materials indicate that typical building materials respond well to the DTM-CFD procedure and that the errors incurred in using this procedure are not significant when dynamically modelling typical external ambient weather effects.

The materials have been exposed to typical diurnal external ambient conditions. As mentioned in Chapter 3, CIBSE Guide A approximates most external ambient conditions as varying sinusoidally. In reality weather patterns are highly unstable, but the results indicate that materials typically used in building construction will tend to dampen and delay the effect of sharp changes in external ambient conditions, and hence a wide range of transient frozen flow periods may be used.

5.2.4 Conclusions

One transient frozen flow period must be suitable for all materials because a building envelope is most likely to be composed of a combination of materials. The most suitable transient time periods range between less than 1 hour and 4 hours, for all materials. As a general rule, the choice of the length of transient period should be less than the length of thermal lag of the material. In composite building constructions, the material with the shortest thermal lag should be used as a guide. Perhaps a trigger could be installed which could calculate the shortest thermal lag and restrict the choice of transient periods to be less than the calculated thermal lag length. When using the DTM-CFD Procedure, the intervals at which data is to be obtained (a design choice), will also significantly affect the choice of transient frozen flow period used.

Low conductivity and high thermal mass materials respond well to the method of transient solving with frozen flow, the higher conductivity materials are most sensitive to the procedure. Longer transient periods may be used for materials with a low conductivity and high thermal mass. Generally, the results indicate that the DTM-CFD Procedure works well for a comprehensive variety of typical building materials, when exposed to typical diurnal external ambient conditions.

CFD is usually employed as a simulation tool that provides steady state analysis, but the research documented in this thesis aims to develop the scope of typical CFD simulations to account for the effect of a fluctuating external ambient. Initial tests using a highly sensitive test CFD model have shown that the effects of weather (although not accounting for solar radiation) through most building materials does not create a significant thermal effect within enclosures. Hence, using the developed Transient-Steady DTM-CFD solution procedure, weather effects can be efficiently incorporated into dynamic CFD modelling. To be able to include the effects of external ambient conditions is alone, a significant advancement in CFD modelling.

These initial tests have suggested that in a dynamic thermal model, the most significant effects on airflow within the enclosure are likely to arise from internal

variations (which has not, as yet been tested) rather than fluctuations of an external ambient. External variations tend to be damped by most building material thermal resistances. In Section 5.4, a much harsher ambient condition is applied to the most responsive and sensitive material, to further scrutinise the performance of the developed DTM Procedure.

5.3 Determining Optimum Transient Time Step Lengths over the Enclosure Fabric

5.3.1 Test Procedure for analysing the Effects of Time Steps Lengths

A suitable transient time period for frozen flow solutions for a wide range of typical building materials can be one hour. The tests conducted to determine this transient period, used 360s time steps. The next step towards refining the DTM-CFD Procedure, is to examine the effects of the time step length within the transient frozen period. Time step lengths of 180s, 360s, 720s, and 3600s were tested on each of the nine materials, specified in Table 5.1.

The physical geometry and grid configuration of the tests remain unchanged to those of the test conducted in Section 4.5. After an hour period of transient frozen flow, a steady state update follows. A second one-hour period of transient frozen flow is subsequently solved. Hence, during this total of two hours, the external sinusoidal ambient will increase from 20°C to 23.75°C.

5.3.2 Results and Discussion

For all nine materials, tests have indicated that the choice of time steps creates an insignificant discrepancy between the results provided by the DTM-CFD Procedure and fully transient simulations, hence permitting the use of a range of time steps. This is consistent with DTM codes, which use large time steps of between 360s to 3600s for coarse nodal network calculations. Hence, the DTM-CFD procedure provides improved accuracy because the geometrical grid used over the CFD model

is far more detailed than those of conventional DTM models. When examining the results of the most thermally sensitive material, C3W1, even using one time step within the 1 hour transient period of frozen flow, incurred a maximum error of 2% of the external change in ambient (the external change being 3.75°C over that period of frozen flow) (See Figure 5.2). This amounts to less than 0.1°C of error between the DTM-CFD solution and the fully transient case.
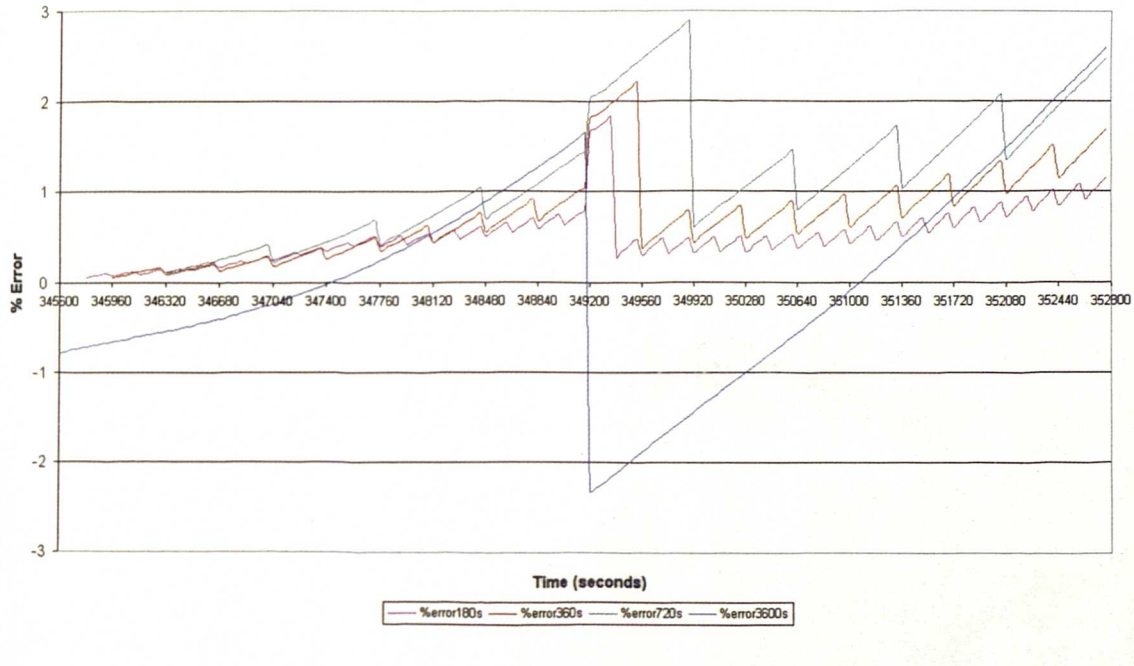
Figure 5.2:   % Error of Time Steps for Material C3W1 for an External Ambient Change of 3.75°C.

5.3.3   Conclusions

The effects of time steps lengths are so insignificant through solid materials, that a wide range of time steps lengths could be used during a transient frozen period. The choice of transient time step will be left to the engineering judgement of the users of the tool. The choice of transient time step affects the overall computational capacity required to solve the simulation since small transient time steps increase the overall density of the transient grid.

5.4 The Response of High Thermal Responsive Materials to Harsh Ambient Conditions - Parametric Studies

5.4.1 Introduction

The tests reported in Section 5.1, exposed that the most conductive material with the lightest thermal weight was most sensitive to the DTM-CFD Procedure. Using this most sensitive material, C3W1, additional tests have been conducted to further understand how and why the errors occur, by exposing the material to more harsh external ambient conditions. Three additional parametric studies were carried out in order to change the nature of external thermal change per time step imposed by the external ambient. The existing sinusoidal ambient conditions were therefore altered in the following ways:

1. doubling the amplitude of the original sinusoidal ambient;
2. increasing the frequency of the original sinusoidal ambient;
3. application of a linearly increasing thermal profile.

5.4.2 Doubling the Amplitude of the Original Sinusoidal Ambient

Test Configuration

The sinusoidal ambient profile that has been used in most of the research has had an amplitude of 15°C and a period of 1 day. The amplitude of sinusoidal ambient profile used in this test is 30°C, with a period of 1 day. The geometrical configuration will remain identical to those used in the tests documented in Section 5.1.

Results and Discussion

To obtain % error values, the results of the differences between the fully transient test solutions and the solution obtained from the DTM-CFD procedure were compared against the same ratio (15°C) as the tests conducted using the original sinusoid. As expected, when the external amplitude of the external sinusoid was doubled, the residual errors obtained after the steady state update were also doubled

compared to the residual errors obtained from using the original sinusoidal ambient (compare Figure 5.3 and 5.4 (Figure 5.4 also appears as Figure C9 in Appendix C9).
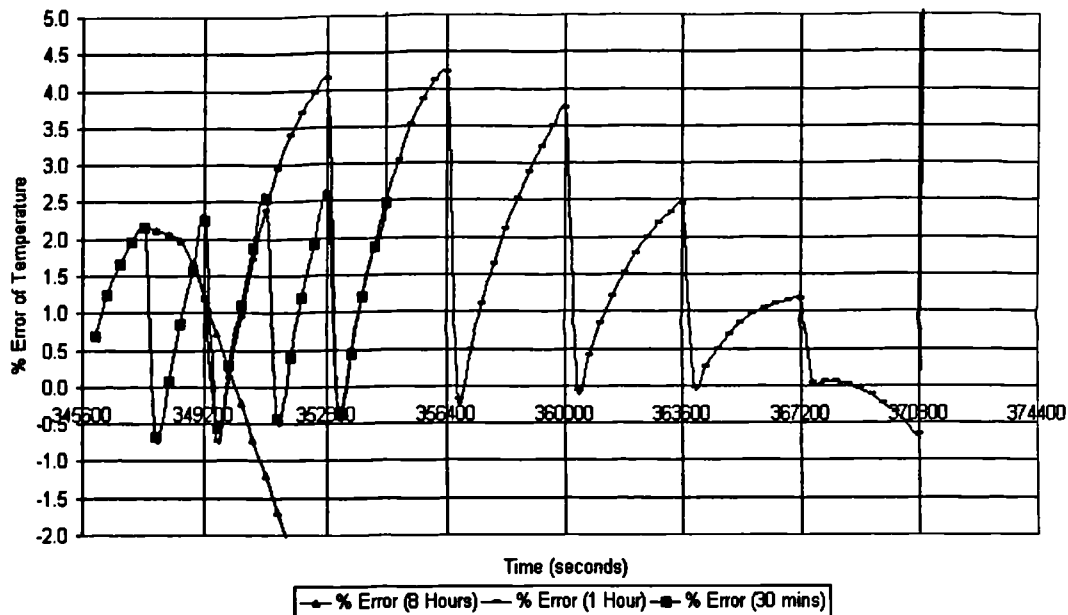
Figure 5.3: % Error of Transient 'Frozen Flow' Period for Material C3W1, using the Original Sinusoidal Ambient

A more unexpected result from the tests was that the errors generated along the transient period of frozen flow (i.e. before each update) were not doubled, when compared with the results of the original sinusoid. This result indicates that the errors generated by incorrect airflow patterns do not correlate with the rate of thermal change per time step. The results suggest that the overall quantity of energy within the enclosure affects the errors generated after a steady state update.
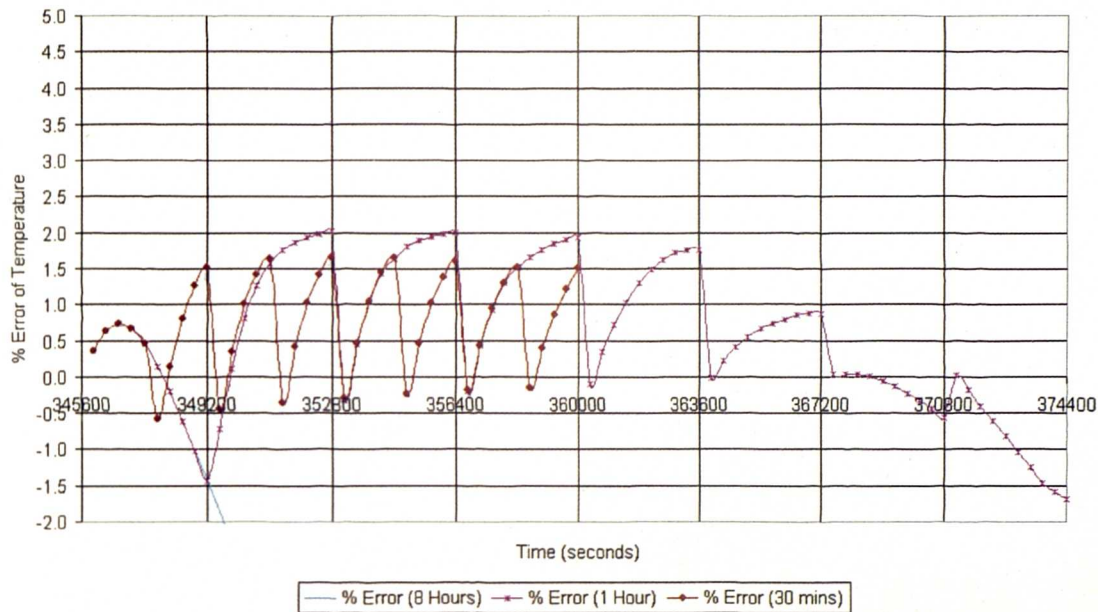
Figure 5.4:   % Error of Transient 'Frozen Flow' Period for Material C3W1, using a Double Amplitude Sinusoid

Also, defying original assumptions are the relationships between the lengths of transient periods and the residual errors remaining after a steady state update. It was initially assumed that the longer the transient period of frozen flow (i.e. the longer the exposure to the dynamic external ambients) using incorrect airflow patterns, the greater the residual error. The results, however, indicated that regardless of the transient period of unfrozen flow, the steady state update solution appeared to create proportional residual errors to the thermal input to the system.

For the two sets of tests, it is impossible to deduce exactly what the relationship between the overall thermal change and the residual errors may be. Evidence suggests that the residual errors are influenced by the thermal input to the enclosure. An exact correlation on a time-step by time-step basis is still, at this point in the research, indeterminate. The application of a sinusoidal external ambient contributes to this ambiguity, since the rate of change per time step is constantly changing.

The thermal lag of the material, although short, may be damping the effects of the external sinusoidal effects, and therefore reducing the errors generated along the transient frozen flow period. Alternatively, the steady state update could be causing

effects, which are at this point unclear. Certainly, the steady state update appears to respond to the doubled external sinusoidal amplitude. Nevertheless, in spite the exceptionally large amplitude of the overall sinusoid, the residual errors after a steady state update, were less than 0.1°C different from the fully transient cases.

Conclusions

The residual errors obtained after a steady state update have doubled, as a result of doubling the amplitude of the external sinusoidal ambient. The errors along the transient period of frozen flow have not doubled, suggesting that the update procedure is more responsive to the overall increase in thermal input to the enclosure. The exact relationship between the residual errors and the thermal input to the system on a time-step by time step basis is still obscure. Evidence suggests that the residual errors could be influenced by other factors besides the thermal input over a particular length of transient period, since residual errors reached similar values, despite using different lengths of transient frozen flow.

In the following set of tests, the amplitude of the external sinusoidal ambient remain the same as the original sinusoidal ambient condition, but the period of the sinusoidal variation is increased fivefold, in order to further ascertain how the residual errors remaining after a steady state update might be affected.

5.4.3 Increasing the frequency of the original sinusoidal ambient

<u>Test Configuration</u>

In the previous tests it was observed that the overall thermal input into the enclosure influenced the steady state updates and as a result, the residual errors remaining after a steady state update. The residual errors did not seem to be strongly influenced by the length of transient frozen flow, which would have preceded the update. Perhaps one of the reasons for the inconsequential effects of the transient frozen flow lengths may have been due to the relatively low rates of thermal change per time step. On a macroscopic level, perhaps exposure to the external ambients set thus far, over periods of 30 minutes and 1 hour was not particularly dissimilar. To challenge this abtruse effect, the external sinusoidal ambient was further altered by condensing the original period (1 day) by a factor of five. The amplitude of the sinusoid was kept the same at 15°C, (see Figure 5.5). The physical geometry and grid configuration remained the same as that documented in Section 5.1.
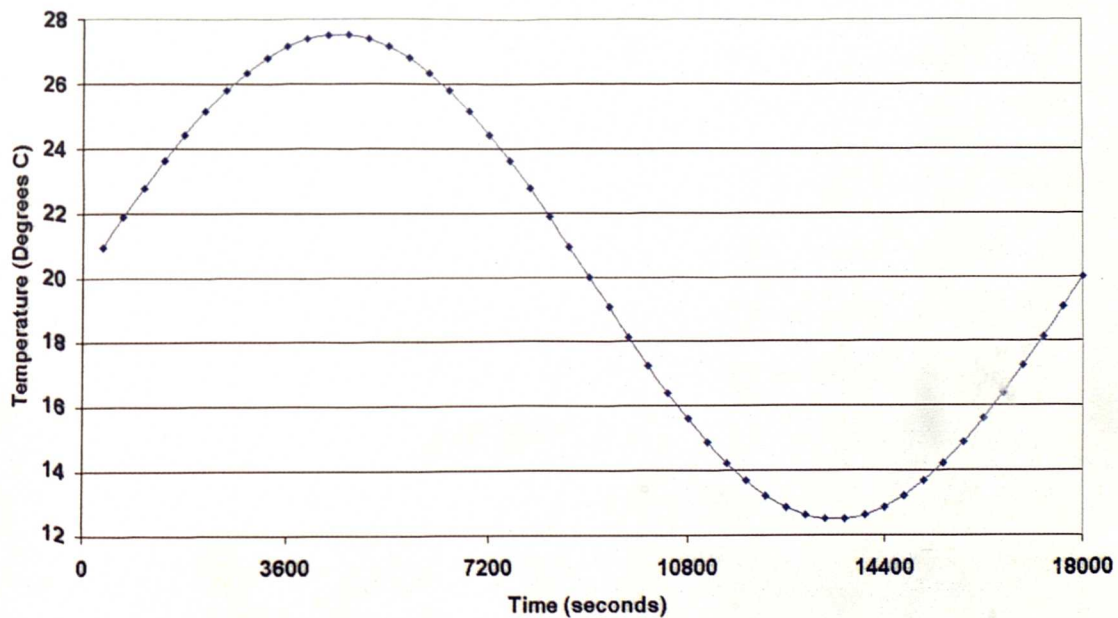
Figure 5.5:   Sinusoidal Ambient Profile (15°C Amplitude and 5 hour Period)

Results and Discussion
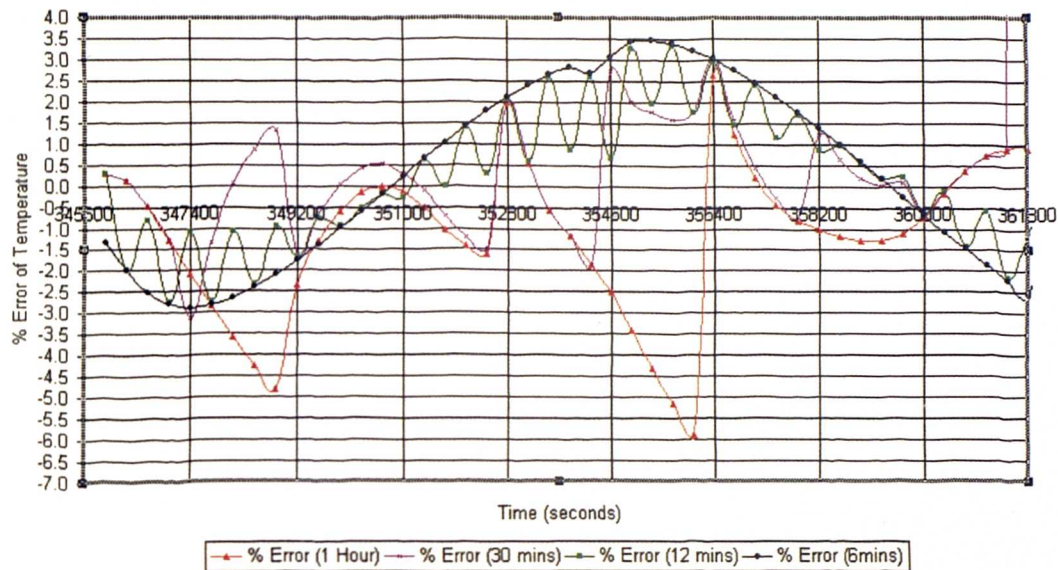
Figure 5.6:   % Error of Transient Frozen Flow for a High Frequency External Ambient Sinusoid tested on Material C3W1 (STEADY STATE VALUES)

Figure 5.6 above shows the % errors obtained at each time step along a total transient simulation. The % errors were calculated by dividing the difference between the fully transient results and the results collected from the DTM-CFD Procedure, by the amplitude of the external sinusoidal ambient variation (which in this case is 15°C). Figures 5.6 and 5.7 differ slightly. The % errors of Figure 5.6 are different at the start of each hour, because the results of temperatures after a steady state solution are inserted at this time, rather than the values of temperature at the end of a transient frozen flow period. Hence, at the start of each hour, Figure 5.6 contains % errors, which occur as a result of a steady state update.

The reason for presenting these two graphs is to show the effects on temperatures by performing a steady state update. Generally, the steady state updates incur more error into the solution process, but the % errors of the following transient time steps are reduced as a consequence of the steady state update. This is particularly evident when observing the % error profiles of the 6 minute transient frozen flow periods, see Figure 5.6 and 5.7.
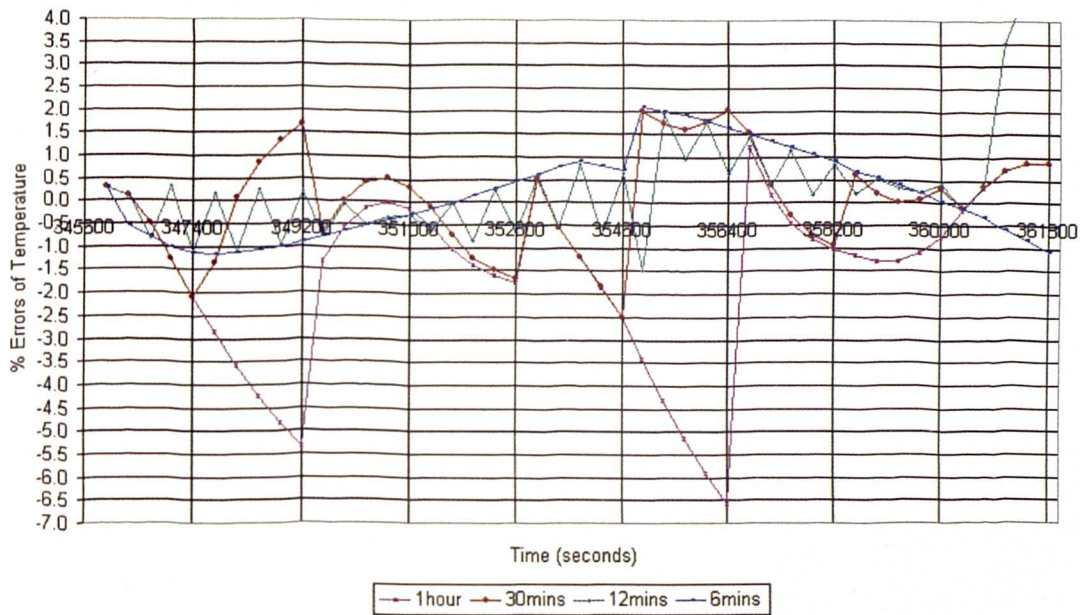
Figure 5.7:   % Error of Transient Frozen Flow for a High Frequency External Ambient Sinusoid tested on Material C3W1 (TRANSIENT VALUES)

For high rates of change of temperature, caused by condensing the frequency of the external sinusoidal variation, the error caused by using the DTM-CFD procedure of freeze flow are increased. Again, the results show that regardless of the length of transient time period used, the errors after each update are similar, see Figure 5.6. The results indicate that despite using smaller transient periods, the procedure causes similar inaccuracies for high rates of thermal change per time step compared to the longer transient periods. At some points in time, the longer transient periods actually achieve smaller errors (compare error profiles of transient periods of 6 minutes and 1 hour at time 356400s, Figure 5.6).

The results show that to avoid unnecessary additional error, a transient period must contain two or more time steps, since a time step following an update accommodates for the thermal adjustments, but the second time step within a transient period, actually calculates for the adjustments that have been made. Figure 5.6 shows the residual errors with steady state calculations for the temperature inserted. Generally the magnitudes of the errors are much higher than Figure 5.7, which only uses the

transient temperatures. For natural convection cases, steady state updates are necessary for correcting thermal conditions inside an enclosure, as the corrected transient data maintains low errors. The data produced during a steady state update, however, is only useful for the following time step in the next transient period of frozen flow. This observation dispels original assumptions that the most accurate data was to be collected immediately after a steady state update. It indicates that the most veritable data should be collected after the first few time steps in the following transient period.

For high rates of change of external ambient conditions, short time periods are more prone to inaccuracies than longer time periods. This is partly due to the inevitable time lag associated with using the transient-steady procedure. For short time periods, airflow patterns are being updated to outdated thermal conditions, i.e. to thermal conditions that occurred earlier in time. Longer transient time periods allow more thermal change to pass, thus increasing the chance that the frozen airflow patterns will be more representative after long frozen flow periods. This is because set frozen airflow patterns may be an average of the fluctuations of thermal conditions that occur over a larger transient period. Short time periods exaggerate the effect of the time lag associated with freeze flow and updating, so short time periods tend to generate a greater cumulative error.
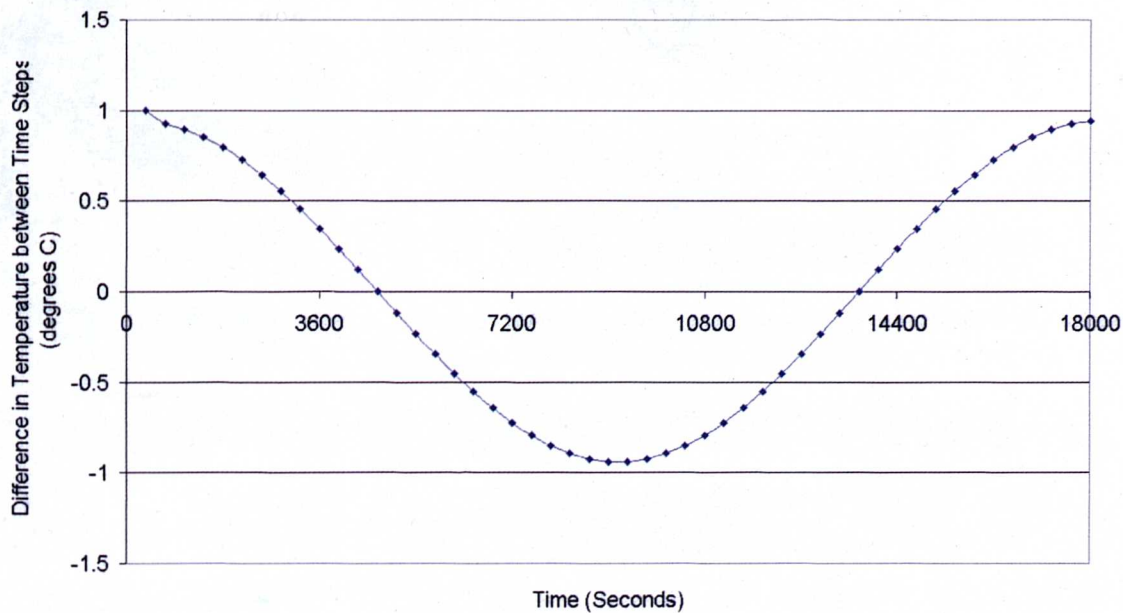
Figure 5.8: Rate of Change of Sinusoidal Ambient Profile (15°C Amplitude and 5 hour Period)

There will be points in time, when both the short and long transient steady state update will occur at the 'wrong' points in time, for example, just before the point in time when the conditions of the external thermal ambient drastically change. This effect is observed in this test after approximately 2 hours of solving, when the external boundary wall switches from being a heating to a cooling wall, i.e. the external ambient temperature falls below 20°C, whilst the internal partition remains constant at 20°C. During this period of time, the rate of change of temperature per time step is at a maximum of 1°C, see Figure 5.8. The airflow within the enclosure switches from circulating in a clockwise to an anti-clockwise direction.

When the external wall does switch from being a heating to a cooling wall, the errors generated by the transient-steady procedure are at a maximum for all lengths of transient frozen flow periods. The results suggest that for all periods of transient frozen flow, a steady state update must be performed for significant adjustments in airflow patterns, otherwise the lag in correct airflow patterns generates errors for many subsequent transient periods.

For natural convection cases, whereby the external conditions are likely to cause incremental thermal changes and not significantly change airflow patterns, steady state updates can be safely performed after periods of transient frozen flow. For mechanical internal thermal loads, however, significant airflow pattern changes are likely to occur i.e. at times when a ventilation system is switched on, or a heating system switched off. Judging by the error profiles generated by the external wall switching from a heating source to a cooling source, it is likely that mechanical thermal changes will cause even greater adjustments to airflow patterns. Hence, as a consequence, generate even more significant errors due to the procedure's inability to capture airflow patterns in time. For these types of scenarios, it is likely that a steady state update may have to be performed at times when significant thermal loads within an enclosure change airflow patterns within the room. This issue is investigated further in Chapter 6.

At four common points in time over the total simulation time, the results of the residual % errors after the steady state update have been tabulated (Table 5.2), from the 4 tests of transient period lengths (which are at 60 mins, 120 mins, 180 mins and 240 mins). Errors are calculated by dividing the difference between the fully transient case and the DTM-CFD solution by 15°C.

Table 5.2: *% Errors of the Differences between the DTM-CFD solutions and the Fully Transient solutions, for set times*

	Transient Frozen Flow Period			
Mins	**1 hour**	**30 mins**	**12 mins**	**6 mins**
240	**-0.74**	**-0.64**	**-0.63**	**-0.66**
180	**2.62**	**3.079**	**2.95**	**3.03**
120	**1.98**	**1.99**	**2.06**	**2.12**
60	**-2.36**	**-1.63**	**-1.70**	**-1.76**

Table 5.2 indicates that the length of transient time period does not correlate with the magnitude of residual error after a steady state update. .This is an unexpected observation since different lengths of transient periods of frozen flow will experience

different proportions of the external fluctuations of the ambient. Yet despite these different exposures, the errors after the steady state updates cannot be proportioned to the length of the transient period to which it preceded.

If Table 5.2 is consulted together with Figure 5.8, it is evident that when the boundary temperatures are decreasing, the solution method tends to under-predict and when the boundary conditions are increasing the DTM-CFD solution tends to over-predict. The errors caused by the 6 min time steps are initially negative, suggesting that the temperatures predicted using the 6 mins time steps were warmer than the fully transient case. The external ambient would have been increasing during this time, so the airflow pattern would have been too weak and would not have been convecting the heat away from the wall. After approximately 1 hour, the external ambient sinusoidal temperatures start to fall and the errors caused by using 6 min time steps start to increase. This is because the air flow patterns are too strong and too much heat is being convected away than what realistically occurs.

The high errors of approximately 3% cluster around the time zone where the highest rates of thermal change occur. The rate of change of temperature per time step can be approximately ±1°C at peak time (see figure 5.8), which causes error of approximately 2% during the following transient period. This can be compared to the maximum rates of change of ±0.2°C of the original sinusoidal ambient, which saw maximum errors of 0.3% at the first time step after a steady state update (see Figure 5.3). When the amplitude of the original external sinsusoidal ambient was doubled, the maximum errors incurred using 1 hour periods was 0.6% at the first time step after a steady state update (see Figure 5.4).

Figure 5.9 shows the temperature adjustment of air adjacent to the wall, which occurs during a steady state update, i.e. the temperature difference between the beginning and end of a steady state update solution (referred to as dT Air (w) (SS) in Figure 5.9). The original assumption (stated in Section 5.1) that the length of transient frozen flow influenced the accuracy of the DTM-CFD Procedure is partly true. However, the research of Section 5.4 has added to the assumption that the amount of change, which occurs over a transient frozen flow period and hence the

amount of adjustment required during a steady state update, has a greater influence on the overall accuracy of the solution. This is especially true for sinusoidal and other fluctuating ambients. The amount of temperature change in the air adjacent to one of the enclosure walls, during a steady state update (referred to as dT Air (w) (SS)) of the 6 min and 12 min profiles were compared with the % errors after each steady state update. The results are illustrated in Figures 5.9 and 5.10.

Figure 5.9: 6-minute transient period showing the Relationship between dT Air (w) (ss) and RE (cumulative) [Note: the number labels represent the time step numbers].

There is a distinct pattern emerging between the temperature adjustment within the air that occurs during a steady state update and the residual error that prevails after a steady state update has been performed. As the amount of adjustment during the steady state update tends towards zero (see Figure 5.9), the residual error also tends towards zero. This is evident, particularly at time steps, labelled on Figure 5.9 as points 12, 13, 14 and 15, where the errors between the DTM-CFD simulation are less than 0.1°C.

At times when there is zero error between the DTM-CFD results and the fully transient solution, the gradient of the rate of change of the external ambient is zero, (see Figure 5.9). Zero rates of change of the external ambient cause the airflow

patterns between steady state updates to change very little. This observation is apparent between the 3rd and 4th hours (between 10800s-14400s) and also slightly after the 4th hour (after 14400s), where the low rate of change of external ambient temperatures occurs, see Figure 5.8. It must be noted that there will be a slight lag between the rates of change of the external ambient and its effects upon the air within the enclosure.

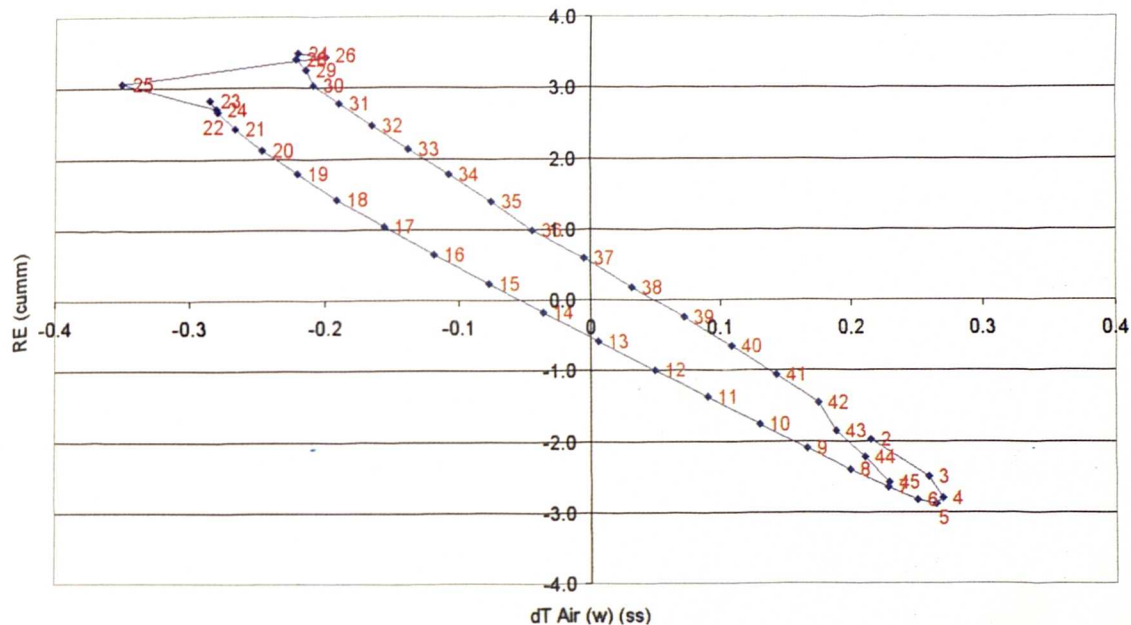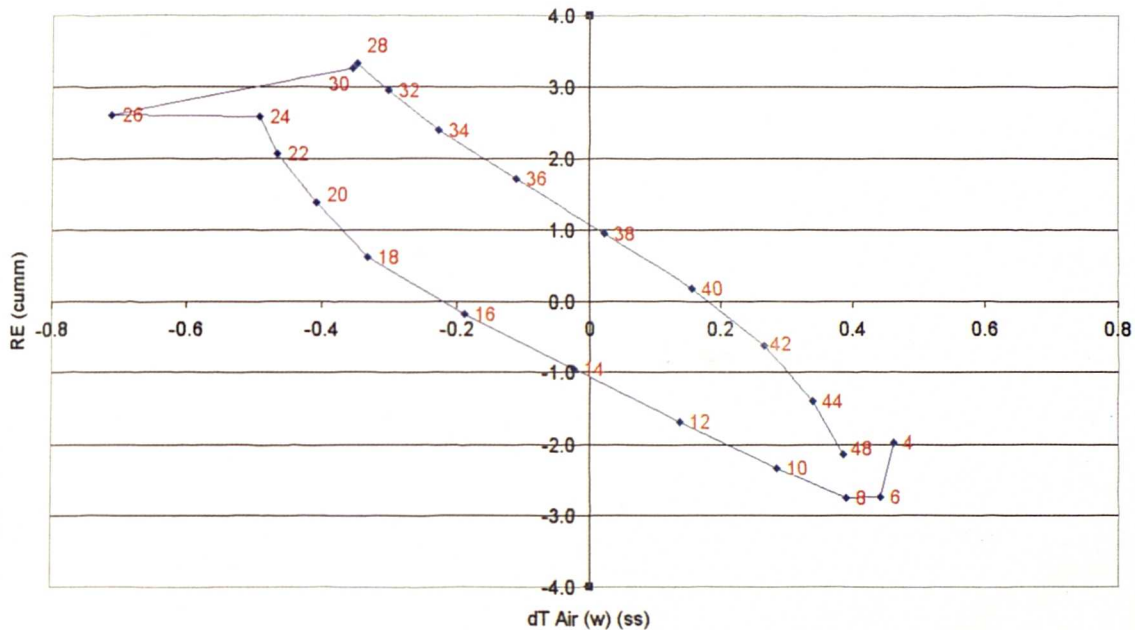Fig. 5.10:   12-minute transient period showing the Relationship between dT Air (w) (ss) and RE (cumulative). [Note: the number labels represent the time step numbers].

On the 12 min profile (Figure 5.10), the location of time step results along the RE axis and dT Air (w) (ss) are very similar to the 6 minute profiles. The time step numbers have been labelled on the data points on Figure 5.10. The maximum range of errors are very similar for both lengths of transient frozen periods of no more than approximately 3.5%, indicating that the length of transient time period does not have a significant impact of the overall magnitude of errors incurred by using the DTM-CFD procedure. The results also indicate that the errors may also be affected by an additional factor, since the errors before (time steps 1-24) and after (time steps 24-48) the maximum rate of change do not lie on a straight line. This additional error

could be caused by the thermal lag of the material, and/or the cumulative error generated by the procedure.

Similar error profiles are also observed from the profiles showing the relationship between the temperatures change within the solid during the transient frozen period (dT Solids (trans)) and the residual error at the end of a steady state update (see Figure 5.11). By comparing these two parameters, it was expected that the larger the change during the transient period within the solids, the higher the residual error inflicted. A large change in the solid temperatures will mean that the flow patterns would have been significantly non-representative of the true air flow patterns within the room.
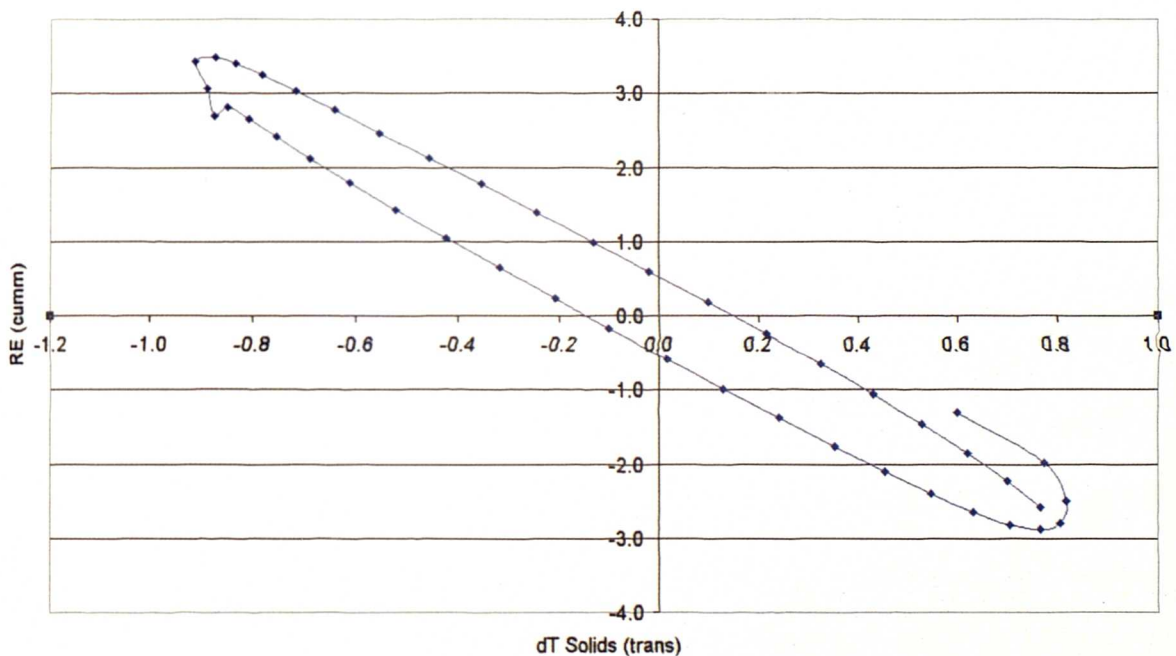
Figure 5.11:   6-minute transient period showing the Relationship between dT Solids (trans) and RE (cumulative)

In fact, the results show a direct correlation between the amount of thermal change that occurs within the solid boundaries and the magnitude of residual errors that prevail after a steady state update. The error profile is more distinctive because the temperature difference over the transient period has a more linear change. This is because the airflow patterns remain constant, whereas the temperature change over the steady state update within the air is subject to the effects of the adjustment of the

heat transfer coefficient (HTC). Hence, the error profiles of the thermal change within the air during a steady state update (Figure 5.9 and 5.10) are more erratic.

A trigger could be placed within the internal surface of the solid material to restrict the change in the temperatures in the last cell of the boundaries to not exceed ±0.5°C. The choice of the temperature trigger depends on the magnitudes of the errors that are chosen by the user to be acceptable. If the changes within the internal surfaces of the boundaries are restricted to ±0.5°C, then errors would be restricted to under 2% (or less than 0.3°C difference between the fully transient and DTM-CFD solutions).

The residual errors remaining after a steady state update were also examined against other flow characteristics, to examine whether a 'trigger' could be further designed based on the change of heat transfer coefficients for example. A comprehensive series of error matrices (see section C3, Appendix C) were developed to determine other flow characteristics, before and after a steady state update and during transient periods of frozen flow, which would possibly influence the residual errors. Unfortunately none of the flow characteristics tested, correlated to the residual errors remaining after a steady state update.

With regards to the relationship between thermal change across the boundaries and residual errors the overall thermal change within the solids during a 6-minute transient period is equivalent to a thermal change over a time step. The similarities between the error profiles against the thermal change of air over steady state update show that each time step records similar errors. The similarities of error profiles shown in Figures 5.9 and 5.10 are also comparable to the similarities between the equivalent error profiles of the 6 minutes and 12 minute profiles for the dT Solids (trans) values. These observations suggest that the residual errors may be created by the conditions set in the update itself. This is also supported by the observation that at some points in time, longer periods provide slightly more accurate results.

The entire 12 min profile, shown in Figures 5.7 and 5.8 suggests that there could be a flaw in the DTM-CFD steady state unfrozen updating procedure. The 6 min % error profile is slightly misleading because there are no time steps after a steady state

update, and hence the effects of the lag in the airflow updating just accumulates with time, until fluctuations in the thermal input to the system (the external sinusoid) cancel out errors.

The error profile of the 12-minute transient time periods, however, does have one transient frozen time step in between steady state updates. The profile shows that the steady state update actually pulls the solution results away from the results recorded by the fully transient solution. The transient frozen time step temperatures after a steady state update are closer to the fully transient values, with % errors closer to zero. The results of the 12 min profile confirm that an error is actually installed into the solution by completing a steady state update and reduced in the following transient frozen time step.

In the steady state update procedure, the temperatures in the solid boundaries are temporarily frozen, whilst the airflow patterns are updated. The errors generated by performing a steady state update indicate that additional bogus thermal loads are actually installed into the enclosure. Although this appears to be the case, from the error profiles, what is actually happening is that the thermal lag of air is being misrepresented during the steady state update. Hence, when the solid boundaries are frozen, the steady state update simulates the conditions within the room, as a result of the non-dynamic boundary conditions.

In reality, the thermal lag of air (even though short) would take time to transport the effects of the boundary conditions around the room. In the steady state update, there is no time taken for transportation of thermal conditions around the room. After an update, (which are the results used for the subsequent transient period) the thermal effects of the boundary conditions are immediately delivered to points around the room, i.e. the effects of air lag are completely dismissed. For increasingly high rates of thermal change, the effects of ignoring the thermal lag becomes of greater significance and consequence.

It should be noted that this flaw in the steady state update occurs for high rates of change within the boundaries. Typical rates of change caused by weather over more representative building materials are not likely to be affected by the error of the

procedure. However, in an attempt to completely eliminate the flaw, additional tests were conducted. These tests used a modified updating procedure. Instead of switching all equations on, the entire set of equations of fluid flow, except temperature were activated during the steady state update. The objective of this modification was to avoid the addition of 'bogus' energy into the enclosure.

The tests indicate that freezing the temperature equations during the steady state update does not reduce errors in the solution procedure. The results of the 12-min error profiles (See Figure C14, Appendix C) indicate that the steady state update does not eliminate errors (which was the initial objective of performing an 'update'). Effectively, in all cases, thermal loads are input into the enclosure but are inaccurately distributed around the room due to misrepresentative airflow patterns.

The latest alternative steady state update performs an over exaggerated simulation of the thermal conditions within the room, due to the frozen boundaries of the solids. Since the airflow patterns cannot interact with the solids boundaries, they can only respond to the thermal loads that were directly input into the enclosure during the transient period. By reactivating the temperatures in the following transient period, the airflow patterns that were established in the previous update are most concurrent with the thermal conditions within the room. Temperatures are able to interact with the temperatures of the solid boundaries after a steady state update.

Conclusions

A flaw in the steady state procedure has been identified for high rates of change of the external ambient. The flaw is not likely to cause a significant impact when used in realistic test cases, since typical weather patterns are not likely to reach such high rates of change as tested here. Nevertheless a flaw in the updating procedure has been found and an alternative methodology to the procedure has been tested and found not to improve the errors obtained. For fluctuating external ambients, the error generated by the flaw in the updating procedure obscures any potential correlation between the extent of the thermal change over a transient period of frozen flow and residual errors.

In the following section, a further attempt has been made to unearth a relationship between the thermal change over the transient period and the residual errors remaining after a steady state update. In order to expose the potential relationships more clearly, the external ambient has been modified to provide a constant thermal input. Hence a linearly increasing thermal profile has been applied to the external face of the wall.

5.4.4 Linearly increasing External Ambient

<u>Test Configuration</u>

The linear tests cases have been designed as a final attempt to observe the true effects of the steady state update under harsh ambient conditions. It was observed from previous tests that the procedure used to update airflow patterns during the steady state update, actually contributed to inputting errors into the enclosure. The steady state update, however, was proven to be necessary in correcting the errors generated during a transient period of frozen flow.

The geometry of the small enclosure used throughout Section 5 thus far, was again used in these linear tests. The preconditioning of the enclosure involved solving a steady state simulation, with all equations fully functioning, where the external wall was set to 0°C. Two linear tests were performed. The first involved exposing the enclosure to a linearly increasing ambient, which increased from 0°C by 0.125°C/min or 0.75°C/transient time step. The second linear test involved exposing the external wall to a linearly increasing ambient, which increased from 0°C, by 0.06°C/min or 0.36°C/transient time step, chosen to observe the effects of a less harsh rate of change of external ambient. These rates of change were chosen as they lie above and below the rates of change discussed in Section 5.3.

These particular rates of thermal change were chosen based on a point raised in Section 5.4.3. In section 5.4.3 it was discussed that perhaps a trigger could be placed within the DTM-CFD Procedure, which would automatically stimulate a steady state update if thermal changes in the boundaries of the enclosure exceeded ±0.5°C. Hence the following tests were designed to also tackle the effects of a thermal rate of change per transient time step of 360s (6 mins), of a thermal rate of change which would be above and below the 0.5°C threshold.

The aim of the two different linear patterns was to observe the effects of the different rates of change per time step. The different lengths of transient frozen flow periods of 6, 12 and 18 minutes were tested, to observe their effects upon residual errors remaining after a steady state update.

Results and Discussion

From the data collected, two graphs have been constructed shown in Figure 5.12 and 5.13. Figures 5.12 and 5.13 show the difference between the fully transient simulations and the DTM-CFD Procedure, expressed as a % error of the fully transient value. Figure 5.12 shows % errors generated at each time step and after a steady state update, when the enclosure was exposed to a linear ambient of 0.125°C/min. Figure 5.13 shows % errors generated at each time step and after a steady state update, when the enclosure was exposed to a linear ambient of 0.06°C/min.
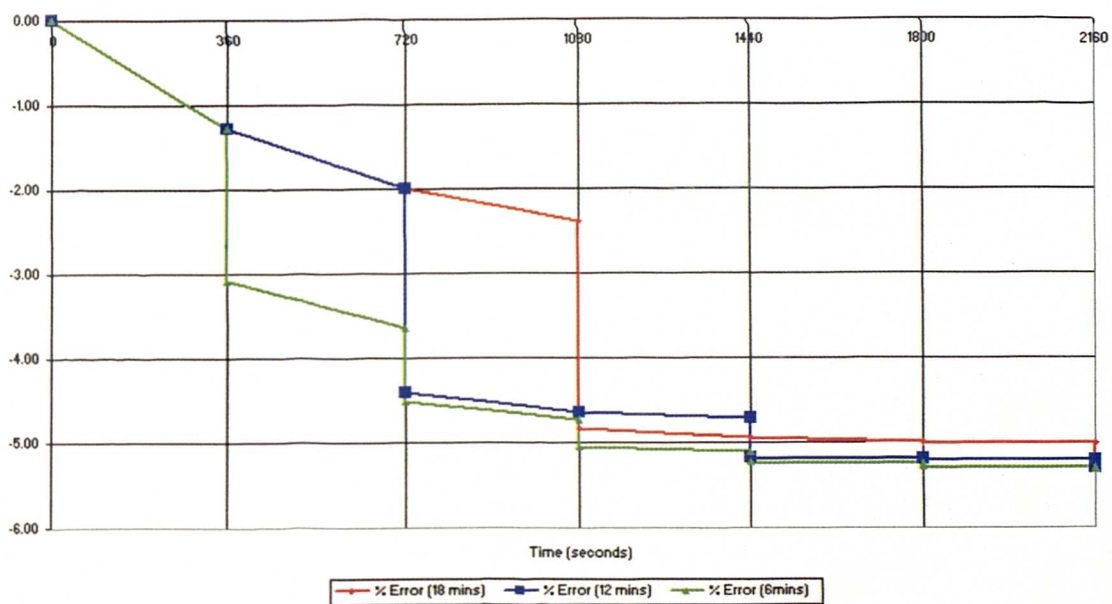
Figure 5.12: Error profiles generated by a linearly increasing ambient of 0.125°C/min.

With high rates of change per time step input into the enclosure by the ambient that varies by 0.125°/min, the DTM-CFD Procedure tended to immediately over-predict the temperatures (all errors were negative). Per time step, relatively large amounts of thermal load are input into the system. These tests indicated that the steady state update would have installed bogus energy into the enclosure because of the complete dismissal of the thermal lag of air. The amount of energy installed into the system, as a result of the update does not correlate with the thermal change during the preceding transient period of frozen flow. This is because the error installed is also

affected by the cumulative error generated by previous updates performed. Hence, the error profiles tend to be higher with more frequent updates, see Figure 5.12.

The first update generates the largest error (see Figure 5.12), regardless of the transient length of frozen flow (and consequently, the extent of thermal change). This is because significant adjustments have to be made to the airflow patterns, which generates large residual errors. After the first update, the error is relatively smaller, again independent of the length of transient frozen flow, and the errors do not correspond to the rates of change of the boundary condition. The most influential factor of the residual errors obtained during the update, is the extent by which the airflow patterns must be adjusted within the room. This adjustment will inevitably be affected by the thermal changes across the boundaries. The relationship between the steady state update thermal adjustments and the % errors appear to be highly complex and could be the main focus of further research.
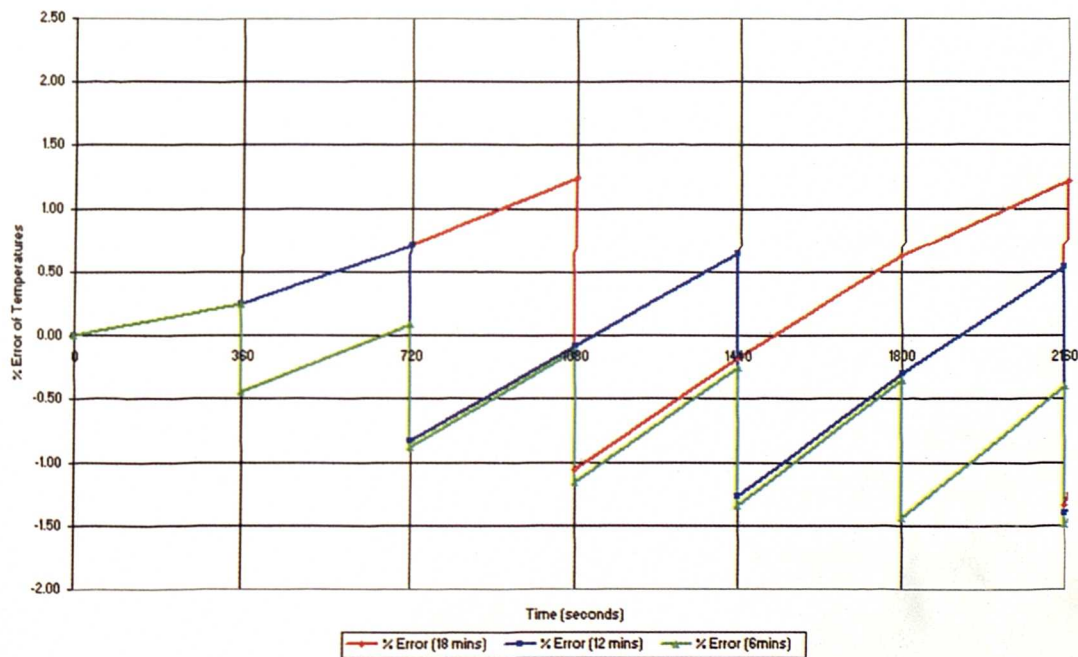
Figure 5.13: Error profiles generated by a linearly increasing ambient of 0.06°C/min.

Despite the complex relationship, the assumption that the overall thermal change affects the residual errors hold true for the error profiles for the linear external ambient tests of 0.06°C/min, where the overall range of errors was approximately halved. Errors are input into the system by the process of updating, but the steady

state update is necessary for correcting the transient procedures of frozen flow, and are not likely to cause significant errors for typical diurnal ranges.

Conclusions

A fundamental flaw in the DTM-CFD steady state update procedure has been identified. The cause of the flaw appears to be a highly complex relationship involving time factors and rates of thermal change, both in the air and the building fabric of the enclosure. The research has established that the steady state update is an effective method of aligning the solutions of the equations of fluid flow within the overall DTM-CFD transient solution process. The flaw of the steady state solution process is largely affected by the level of energy present within the system or enclosure, and the rate at which the level of energy changes.

The energy of the system of the enclosure has been supplied by external ambient conditions and as the research has progressed through this chapter, the external ambient conditions have become increasingly harsh. These harsh conditions are also unrealistic, firstly due to the fact that external ambient conditions are not likely to change as rapidly as some of the tests have simulated. Also, typical enclosures modelled in industry using the developed DTM-CFD Procedure are not likely to be so sensitive. The sensitivity of the enclosure used in the research contained in this chapter has been successful in identifying potential problems with the DTM-CFD Procedure, but also in confirming the probable success in applying the procedure to more realistic design cases.

5.5 Assessment of the Process of Refining the DTM-CFD Tool

In order to determine the success of the DTM-CFD procedure, much emphasis has been placed upon the comparison between the data produced by a fully transient solution and data produced by the DTM-CFD procedure. The differences have provided an opportunity to identify how the procedure operates and the circumstances under which the procedure falls short.

Interrelated to these differences are the errors caused by the geometrical configuration of the test case itself. This section presents additional literature on the subject, which reveals that the test case used throughout the majority of this research was highly sensitive such as heat transfer coefficients determined by natural convection. The fact that the errors arose from such harsh sensitive conditions is highly favourable towards the success of the procedure, when applied to realistic commercial applications.

Another source of error and a topic of extensive research has been turbulence modelling. The Revised k-ε Turbulence model that was used in the test cases is a good turbulence model for predicting general air flow and heat transfer within a single zonal room, Beasoliel-Morrison (2002).

Research conducted by Beasoliel-Morrison (2002) discovered that poor surface convection predictions are the result of the inability of the log-law functions to resolve the near-wall regions in the room air flows. The wall functions assume the form of the velocity and temperature profiles within the boundary layer and the k-ε Turbulence model tends to over-predict μ_t in low flow regions.

Recent literature proposes alternative turbulence models that can be used in natural convection cases. One which is particularly relevant to room airflow modelling is the zero-equation model proposed by Chen and Xu (1998). For the test cases used to develop the DTM-CFD Procedure, the wall functions developed by Yuan et al. ((1993), may have been more appropriate, since the functions are for buoyancy driven flow over vertical surfaces, i.e. wall functions appropriate for natural

convection flows. The disadvantages of using these wall-functions, however, is that they can not be universally used, unlike the Log-Law Wall Functions. New near-wall treatments for the k-ε Turbulence model, suitable for room air flow prediction are now available and more are under development.

Ideally, automatic selection of appropriate turbulence and wall-functions within the DTM-CFD Procedure should be developed to improve the accuracy of the simulations depending on the nature of the flow within the room, Beausoleil-Morison (2002). Beausoleil-Morrison assessed the performance of various turbulence models, since their DTM code, which included patches of CFD, was designed to be able to automatically select the best turbulence models to be used, depending on the airflow within the solution domain.

Similar test cases to the natural convection case used in this research have been used by Karajiannis et al (2000); they also identified that the study of turbulent natural convection in cavities is still at an early stage. In the two equation standard k-ε turbulence model numerical simulations, the wall functions, i.e., the logarithmic velocity profile near a solid wall, is helpful since it saves many grid cells. However, the logarithmic velocity profile does not exist in this low turbulence natural convection in a square cavity. The research on turbulence models has existed for decades, and continues to be an investigated academic field for time to come. The research into turbulence models for natural convection is further behind, but nevertheless exists.

The test case used to refine the DTM-CFD procedure was threatened by large potential sources of error due to the levels of sensitivity within the flow. Ultimately, regardless of the errors, flaws in the procedure were identifiable and in actuality proved to establish the success of the procedure, since realistic design cases are not likely to contain such thermally reactive conditions. Errors generated by turbulence models would have been consistent throughout the development of the research, since the choice of turbulence model did not change.

5.6 Conclusions

The procedure used in the DTM-CFD tool has been further refined. The transient frozen flow periods have been tested over a comprehensive spectrum of materials that vary in their thermal conductivities and thermal capacity. For further investigative purposes, the most thermally responsive material was then subjected to more harsh ambient conditions.

Overall, the DTM-CFD procedure is highly successful in modelling the thermal effects of typical dynamic weather patterns in buildings constructed from conventional materials. A wide choice of transient periods of frozen flow can be used, although it is recommended that the lengths of transient flow should be shorter than the thermal lag of the most thermally responsive materials, used in the building construction. It was proved that time steps within a transient period of frozen flow do not significantly affect the accuracy of the procedure. As with geometrical grid, the increase in transient grid density will increase the load on computational capacity.

Highly thermally responsive materials, particularly due to high thermal conductivities, are more sensitive to the DTM-CFD procedure. The results of the tests showed that transient periods should contain more than one time step in order to capture information from preceding steady state updates. Tests also concluded that the steady state update methodology is flawed. For high rates of change, the update procedure tended to input 'bogus' energy into the system, due to the neglecting of the thermal lag of air. Measures were taken to correct this flaw, but no better alternative to the original steady state update procedure was found.

As a result of the discovery of the flaw in the steady state update procedure, high rates of change must be restricted and if high rates of thermal change do occur, the frequency of steady state updates should be limited. Longer lengths of transient periods of frozen flow appeared to avoid the increase of residual and cumulative errors generated by numerous steady state updates.

The original hypothesis of building envelope thermal lag and the requirement of large temperature adjustments after long periods of frozen flow being the major source of residual error have been disproved. In actual fact, thermal lag and large temperature adjustments affect the errors input to the system by the steady state procedure. The overall error caused by the steady state procedure supersedes errors generated by any other effect. These other effects appear to relate to the steady state updates in a highly complex form and could be the focus for further research.

For very significant airflow adjustments, due to a major thermal change, a steady state update should be performed as soon as possible, so as to limit cumulative errors for subsequent transient periods of frozen flow. The results suggest that for adjustments to airflow patterns caused by internal thermal mechanical loads, such as the activation of ventilation systems, steady state airflow patterns should be performed beforehand or simultaneously with the thermal change. This effect will be investigated further in the following chapter.

The efficiency of the established DTM-CFD procedure is greater than expected, since a wide variety of transient periods of frozen flow may be used for a wide variety of typical building materials and the thermal sensitivity of realistic design cases is likely to be less. Users of the tool, are likely to find this characteristic of the tool particularly useful. It means that materials can be safely changed throughout the development of the geometrical DTM-CFD model, without too much alteration and repetition of the CFD simulation. Steady state updates need only be performed when desired, or when airflow patterns significantly change.

5.7 Chapter Summary

After establishing a DTM-CFD procedure (Chapter 4), this chapter discussed its refinement. The research reported in this chapter sought to establish the perimeter within which the procedure could function successfully. The effect of transient frozen flow lengths was tested over a comprehensive spectrum of building materials. The most sensitive material to the DTM-CFD procedure was then selected for further testing by exposing it to harsh ambient conditions. All the tests revealed the circumstances under which the procedure could function successfully and the context within which the procedure falls short.

Overall the research reported within this chapter promotes the capability of the DTM-CFD procedure as an efficient and effective dynamic thermal modelling tool within CFD. The following chapter applies the knowledge gained to a realistic design case study.

CHAPTER 6

APPLICATION OF THE DTM-CFD TOOL

CHAPTER 6 – Application of the DTM-CFD Tool

6.1 Introduction

A dynamic thermal modelling procedure using only CFD has been developed. This DTM-CFD Procedure can be applied as a simulation tool to model typical buildings, and is predicted to provide an efficient and effective method of accounting for the thermal effects of time-varying external ambient conditions. Through rigorous testing (Chapters 3-5), the fundamental performance of the DTM-CFD Procedure has been established and assessed.

The tool has been developed for use by building services designers. In order to assess the performance of the developed tool on a realistic test case, the tool has been used to dynamically model a representative office space. In this chapter, construction of a realistic test case through a number of stages is presented. At each stage the results using the DTM-CFD Procedure is compared and evaluated against a geometrically equivalent fully transient case. The realistic office space is based upon the work conducted for the PII Project conducted in collaboration with CIBSE, CIBSE (2002).

Intermodel comparisons have been selected as the best method of assessing the developed DTM-CFD Procedure, since efficiency and accuracy of the procedure compared to the standard method of fully transient modelling within CFD is of prime interest. The accuracy of fundamental CFD modelling is not being judged in this research, since the overall high performance of conventional CFD simulation has been accomplished through the undertaking of other research groups, largely through comparisons with experimental data, and their work currently continues, Oberkampf (2002).

6.2 Realistic DTM Design Case Study

The newly developed DTM-CFD Procedure was used to simulate the dynamic thermal conditions of an office enclosure located in the UK. An ambient weather pattern was simulated using a sinusoidal thermal profile, set within the CFD code. This weather pattern mimics the typical daily weather variation for the 23rd July, which occurred during a representative year of 1964, recorded at Kew, UK. On this day an extreme variation of weather occurred, where the temperatures fluctuated through 15°C over 24 hours, see Figure 6.1.

Detailed specifications of the ambient conditions are frequently used in other DTM codes, such as FACET, which are based on actual weather data recorded in Kew, UK in the year 1964. A further development of the DTM-CFD Procedure, established in this research, would also enable to the DTM-CFD Procedure to read from actual weather data files.
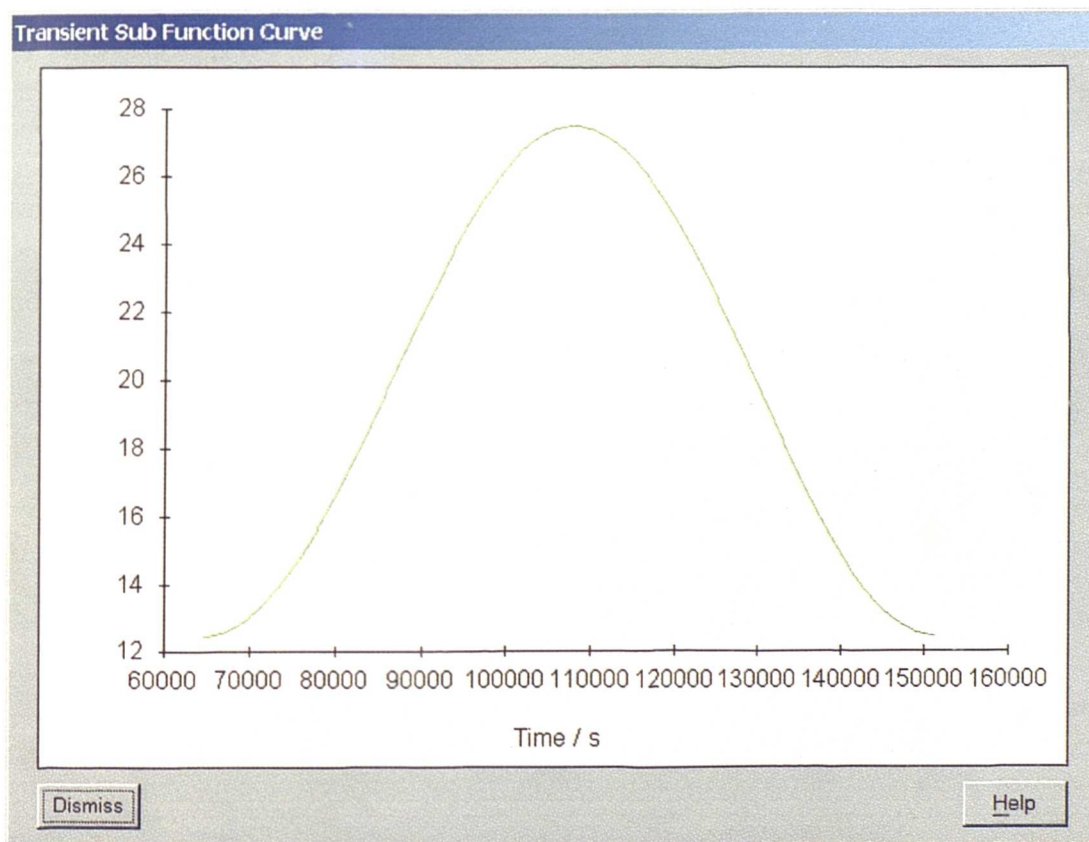

Figure 6.1: Temperature variation over a period of 1 day, used in Stages 4-6

Harsh external ambient conditions have been thus far tested (see Section 5.4, Chapter 5) as part of the development of the DTM-CFD tool. The results of which provide only a representational fragment of evidence as to how the DTM-CFD Procedure behaves under realistic conditions. Most current CFD models are able to effectively model dynamic internal thermal conditions, but not able to efficiently model dynamic heat transfer through building fabric. The objective of most of the research documented in this thesis was to find a method of incorporating the effects of dynamic external ambients.

The effects, however, upon a dynamic CFD simulation of time-varying internal thermal loads are quite different to external thermal loads in that they can appear very suddenly, such as the switching on of an air-conditioning unit, for example. The effects of such instantaneous thermal loads upon the accuracy of the DTM-CFD Procedure can only be inferred from the research conducted in Section 5.4. The research presented in Chapter 5 concluded that a steady state update might have to be performed at the moment a thermal load becomes activated. By applying this hypothesis to a realistic design case, it is hoped that a more complete understanding of the DTM-CFD Procedure can be gained. Hence, in order to absolve any outstanding predicaments in the performance of the tool, arising from a more complex geometry, the realistic test case has been developed in 6 stages. Each stage is described in the following sections:

Stage 0:

The geometry of this stage has been used throughout most of the development of the DTM-CFD Procedure. The $1m^3$ enclosure consists of one external wall (brickwork, outer leaf) 0.22m thick. The external wall is exposed to a sinusoidally varying ambient condition, which varies between 27.5°C and 12.5°C over a period of one day. For a more detailed description see Chapter 5, Section 5.2. The geometry of further stages will be developed from this base case model.

6.2.1   Stage 1

An additional layer of building fabric has been added to the inside surface of the existing brickwork (outer leaf) external wall of the $1m^3$ enclosure. This additional layer consists of a thin cavity-walled insulation of UF Foam (50mm thick), which forms part of a multi-layered external wall construction, to be developed in later stages. See Figure 6.2.

Additional   UF   Foam
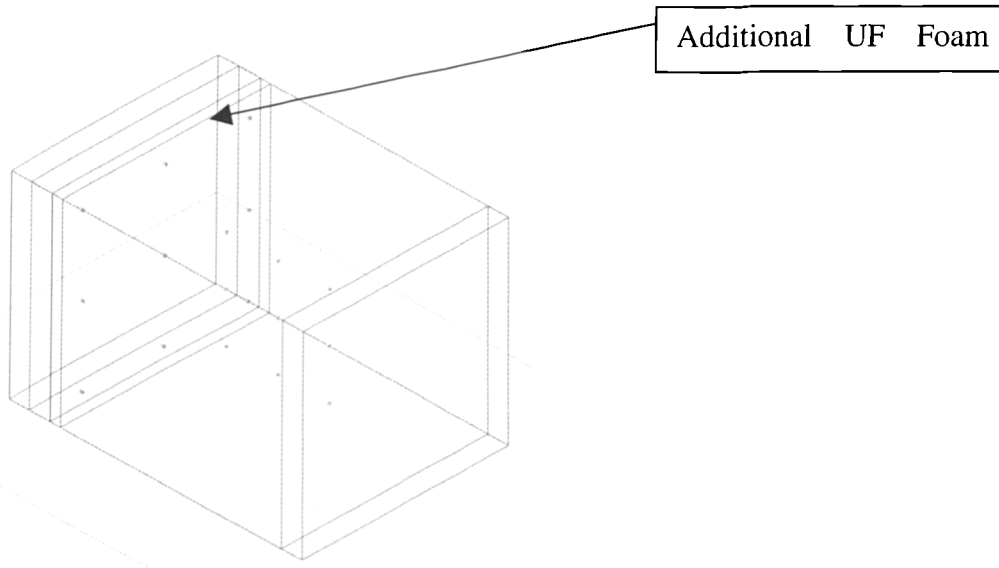
Figure 6.2: Geometry of stage 1

6.2.2   Stage 2:

A 2nd layer of building fabric (also 0.22m thick) was added to the internal surface of the existing 2-layer enclosure. This layer is constructed from brickwork (inner leaf). For additional thermal information on all the materials used in this case study, see Table 6.4. The outer dimensions of the enclosure remain identical to Stage 1, see Figure 6.3.

Additional layer of Brickwork (inner leaf)

Y

Z   X
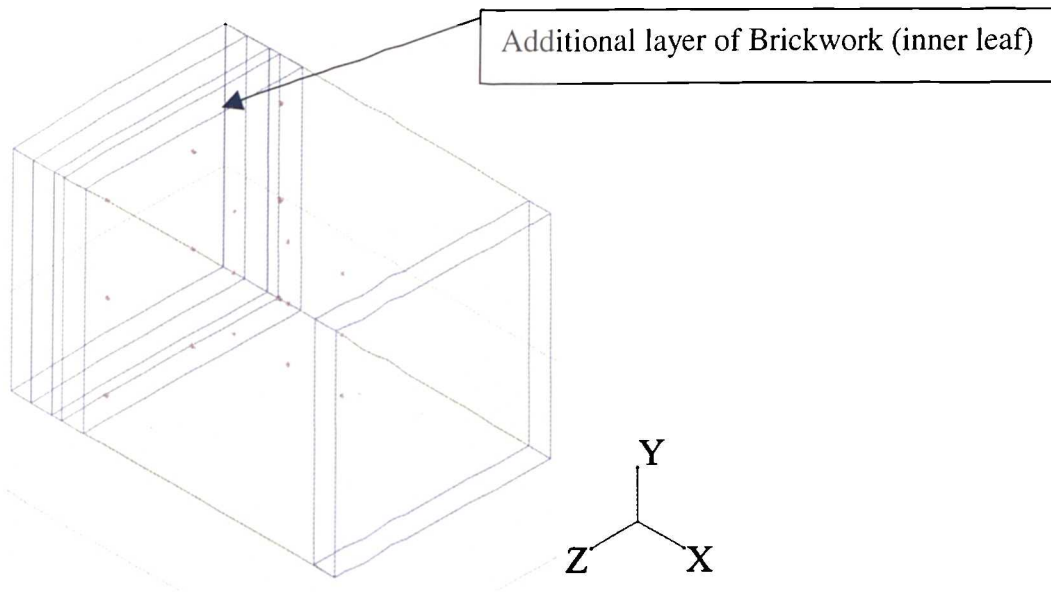
Figure 6.3: Geometry of Stage 2

6.2.3   Stage 3:

The dimensions of the enclosure, used in Stages 1 and 2 was increased to a more realistic office size. To observe the effects of increasing the room size, the small enclosure was enlarged to 6.5m x 3.2m x 2.8m (floor to ceiling height) (or 3.3m, floor to slab height). The room size has been based on the research conducted in conjunction with CIBSE (2002) (see Figure 6.4).

Materials have been added to the boundaries of the expanded geometry. The external wall remains as a multi-three-layered construction of brickwork (outer leaf), UF Foam, and Brickwork (inner leaf). The details of the material thermal characteristics used at this stage may be found in Table 6.4. The other vertical walls and computational ceiling of the enclosure are two-layered construction of brickwork

(inner leaf) and a thin internal layer (13mm) of plasterboard. All walls except the external wall are considered to be internal partitions, separating the modeled office zones from other similar office zones, which are not modeled in the CFD model. All walls except the external wall are modelled as symmetrical, hence, the thermal conditions on their internal surface are mirrored on their external faces. The floor consists of a three-layered construction. The top layer being a 25mm thick layer of wood flooring. The middle layer being 50mm of screed (floor insulation) and then 150mm of cast concrete.
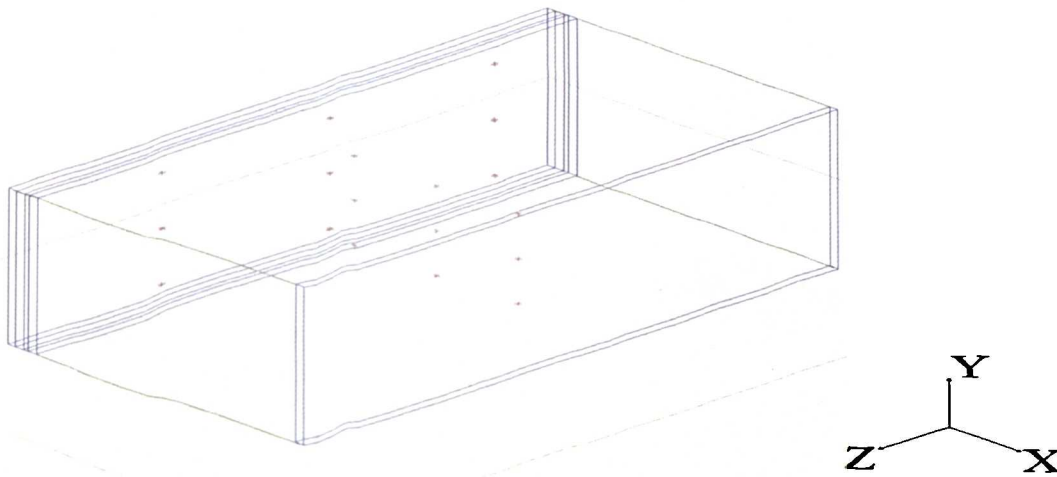
Figure 6.4: Geometry of Stage 3

6.2.4   Stage 4:

Doors and windows with their relevant materials were inserted into the CFD model, such as wood and glass respectively, see Table 6.4. A ventilation system was switched on for half a day, between the hours of 6am and 6pm. Air was supplied to the room via a floor mounted fixed flow device located underneath the window, supplying air at 20°C at a rate of 114.4l/s or 6ach^{-1}. A ceiling level extract duct located above the door was activated during the hours of 6am and 6pm, extracting air at a rate of 114.4l/s. The dimensions of the supply and extract grilles were 0.018m x 3.174m. Office furniture in the form of 3 desks has also been installed into the model. See Figure 6.5.

The conventional DTM-CFD procedure (transient/frozen – steady state/unfrozen) was used. This conventional procedure was compared to a fully transient solution. The DTM-CFD procedure is expected to be altered in order to more accurately capture the changes to the airflow patterns as a result of the activity of the ventilation system. The nature of this alteration was determined through trial and error. Table 6.1 provides a summary of the DTM-CFD procedure to be used in Stage 4 of the realistic design case study.
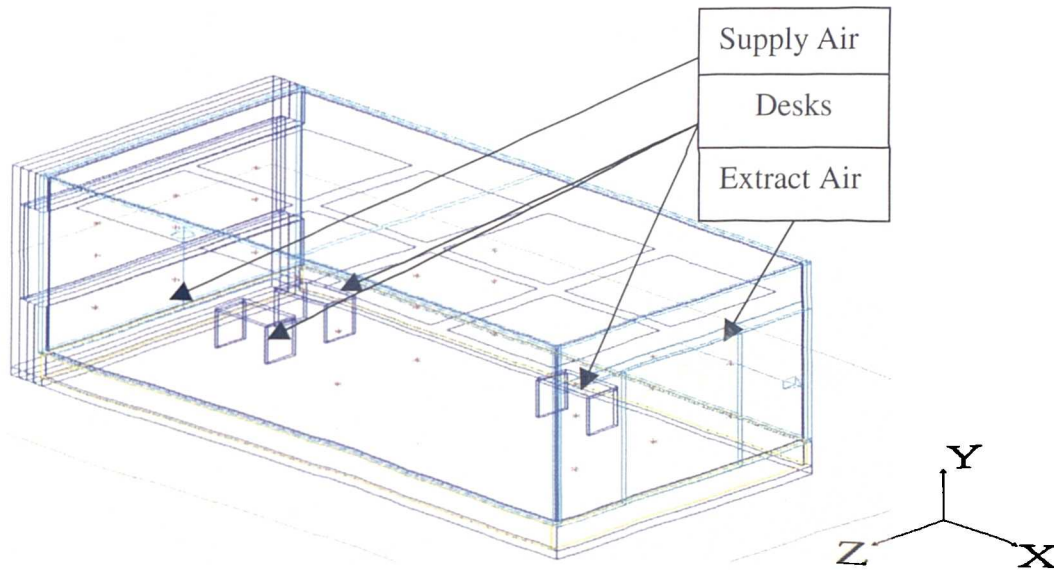
Figure 6.5: Geometry of Stage 4

Table 6.1: Summary of DTM-CFD Procedure of solving Stage 4:

Time	Details of CFD Model
Steady State Solution/Unfrozen Flow	Pre-conditioning of the office enclosure. Ventilation system is deactivated.
Transient Solution/Frozen Flow Midnight to 6am	Ventilation system is deactivated.
Steady State Solution/Unfrozen Flow	To update airflow patterns.
Transient Solution/Frozen Flow 6am – 6pm	The supply and extract ducts have been activated.
Steady State Solution/Unfrozen Flow	To update airflow patterns.
Transient Solution/Frozen Flow 6pm - Midnight	Supply and extract ductst have been deactivated.
Steady State Solution/Unfrozen Flow	To update airflow patterns.

6.2.5   Stage 5:

Stage 5 of the design case introduced additional internal thermal loads. Various thermal loads have been designed to take effect at various times during the day, based on typical office activities. The thermal loads include the introduction of occupants, machine gains and lights, see Figure 6.6.
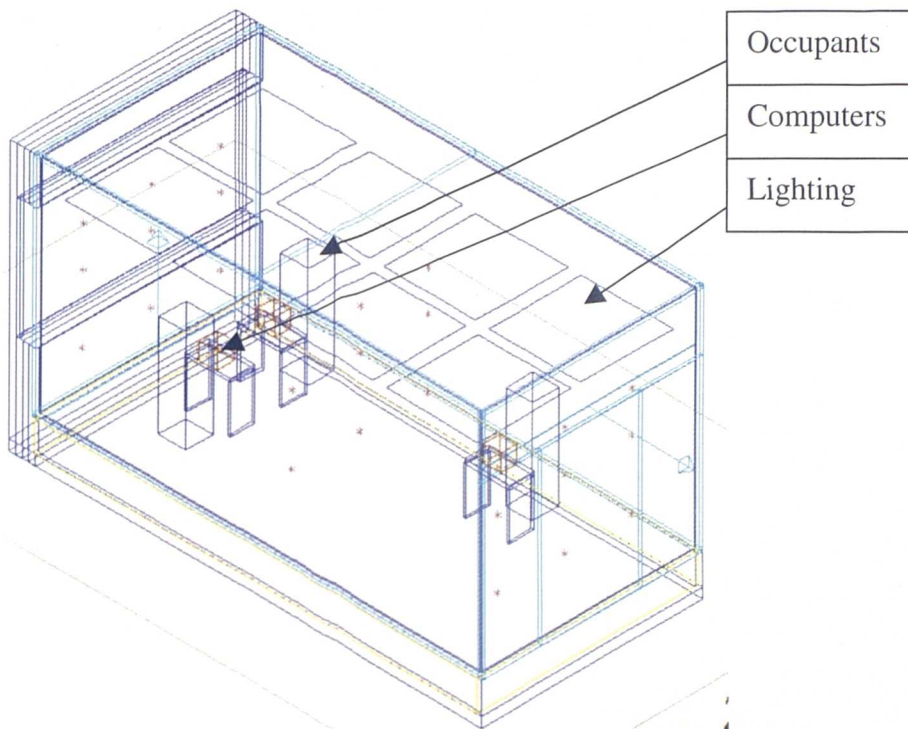
Figure 6.6: Geometry of Stage 5

Two members of staff and a visitor to the office space was simulated over the day of dynamic thermal modelling. The three occupants generate thermal changes in internal air flow patterns due to their presence within the office space. They also evoke other thermal loads within the room, due to activating other sources of thermal gains, such as their computers, or lights (see Table 6.5 for thermal loads). Table 6.2 summarises the activities of the three people who occupy the enclosure, while Table 6.3 provides a summary of the overall thermal events, which occur over the day of transient simulation, including details of the proposed DTM-CFD Procedure used. The DTM-CFD Procedure outlined in Table 6.3 is likely to be subject to change due to the necessity of updating airflow patterns to significant thermal events. The most suitable DTM-CFD Procedure is yet to be determined during the implementation stages.

Table 6.2:   *The movements of the people within the Office*

Person	Actions
1	Arrive into the office at 9am. Switches on their computer immediately. Switches off their computer before leaving the office at 5pm. Leaves the office for a 1-hour lunch break between 1pm-2pm.
2	This visitor arrives at 11am and spends 2 hours in the office. This person does not use a computer.
3	Arrives to the office at 9am. Switches on their computer immediately. Switches off their computer before leaving the office at 5pm. Takes a lunch break between 1pm-2pm. (Note the movements of Persons 1 and 3 are identical)

Table 6.3:   *Summary of the Events which occur over a typical 24-hour period of Stage 5*

Time	Details of CFD Model Thermal Settings
Steady State Solution/Unfrozen Flow	Pre-conditioning of the office enclosure. Ventilation system is deactivated.
Transient Solution/Frozen Flow Midnight – 6am	Supply and extract ducts have been deactivated.
Steady State Solution/Unfrozen Flow	To update airflow patterns.
Transient Solution/Frozen Flow 6am-9am	Supply and extract ducts have been activated.
Steady State Solution/Unfrozen Flow	To update airflow patterns.
Transient Solution/Frozen Flow 9am-11am	Persons 1 and 3 arrive to work.
Steady State Solution/Unfrozen Flow	To update airflow patterns.
Transient Solution/Frozen Flow 11am-1pm	Person 2 arrives
Steady State Solution/Unfrozen Flow	To update airflow patterns.

Transient Solution/Frozen Flow 1pm-2pm	Persons 1, 2 and 3 leave for lunch.
Steady State Solution/Unfrozen Flow	To update airflow patterns.
Transient Solution/Frozen Flow 2pm-3pm	Persons 1 and 2 return to the office.
Steady State Solution/Unfrozen Flow	To update airflow patterns.
Transient Solution/Frozen Flow 3pm-4pm	Lights are switched on
Steady State Solution/Unfrozen Flow	To update airflow patterns.
Transient Solution/Frozen Flow 5pm-6pm	Persons 1 and 2 leave, switching off their computer and the lights.
Steady State Solution/Unfrozen Flow	To update airflow patterns.
Transient Solution/Frozen Flow 6pm-Midnight	Supply and extract are switched off
Steady State Solution/Unfrozen Flow	To update airflow patterns.

6.2.6 Stage 6

Solar calculations are a relatively new function within the CFD code used in this research, and hence the use of solar analysis under transient conditions is not very well established. For the purpose of the research reported in this chapter, the successful representation of the solar radiation has had to be tested to ensure compatibility with the pseudo ambient representation within transient scenarios.

The main issue of concern is how solar radiation can penetrate through the solid 'ambient' cuboid. As previously explained in Chapter 3, the modelling of transient ambient profiles can not be readily specified within transient solutions. Ambient settings have had to be replicated with a series of cuboids. These cuboids have thermal specifications such as a thermal resistance to represent an external surface heat transfer coefficient and a temperature profile to represent external wet-bulb temperatures. An alternative solution to the simulation of time-varying ambient conditions has proved to be successful in allowing solar radiation to take effect.

'Ambient-acting' solids have thus far been specified as non-transparent, which will prove to be a problem when modelling direct solar radiation through windows. Following from the research conducted on transient ambient specifications (section A5, Appendix A), additional tests were conducted to find a methodology of applying a time-varying transient condition using a physically transparent thermal source. The tests conducted in Section A5.4.2 were developed further whereby the 'collapsed' thermal sources were then uncollapsed. Effectively, the solid ambient cuboids were replaced by invisible thermal sources. The tests have been documented in Section D1 of Appendix D and prove that solar radiation could successfully penetrate through thermal sources.

After having established a solution to modelling solar radiation through the series of pseudo ambient cuboids, the solar analysis available within the CFD code could be incorporated into the final stage of the realistic model of an office enclosure. The thermal events, occurring within the enclosure remain identical to those modelled in Stage 5, tabulated in Table 6.3. Solar times must be specified at the start of each hour. Other settings necessary for solar radiation calculations are illustrated in Figure 6.7, below. Note from Figure 6.7, that the orientation of the office enclosure must be specified, along with the solar position. The solar time will have to be altered manually each hour.

Figure 6.7: Solar Radiation settings within the CFD code

6.2.7 General Geometrical Details of the Realistic Case Study

The grid configuration has been constructed to follow the choices typically made by building services designers (i.e. typical users of the tool). A fine grid is therefore used in the last stage of the development of the realistic case study (approximately 650,000 cells). The grid is non-uniform, i.e. grid cells are smaller at the boundaries of the model (the smallest cells at the boundaries are 10mm wide) to accurately capture the thermal conditions and airflow patterns. The grid cell size decreases with increasing distance towards each of the six walls of the enclosure.

Each of the stages were analysed individually, by comparing temperatures and velocities at identical locations usually on an Y-Z plane in the first cell within the enclosed air adjacent to the solid boundary. Results are also analysed at various points within the space on an X-Y plane. The Revised k-ε Turbulence model was

143

chosen as being the most suitable turbulence model to be used in the application of the DTM-CFD tool to the office space.

All stages have been subjected to a fully transient pre-conditioning solution. Stages 1, 2 and 3 are subjected to 3 days of fabric preconditioning, whereby the CFD model is solved for the first 3 days under fully transient conditions and exposed to 3 cycles of the 24 hour sinusoidal external ambient. Stages 4-6 did not use a fully transient solution preconditioning solution. Due to the increasing complexity of the CFD models of stage 4-6, fully transient preconditioning required extortionate computational capacity over several weeks. Instead, stages 4-6 were subjected to a steady state preconditioning solution, whereby all equations were solved to the initial settings of the start of the 24-hour transient solution. Both techniques were effective in preconditioning the CFD models, but the steady state method was the least time-consuming.

Table 6.4: Thermal Characteristics of Materials to be used in the Case Study

Material	Thermal Conductivity (W/mK)	Density (Kg/m3)	Specific Heat Capacity (J/KgK)
Brickwork (outer leaf)	0.84	1700	800
UF Foam	0.04	10	1400
Brickwork (inner leaf)	0.62	1700	800
Perlite Plasterboard	0.18	800	837
Wood Flooring	0.14	650	1200
Screed (floor insulation)	0.41	1200	8400
Cast Concrete	1.13	2000	1000
Typical Glass [Solar Absorption Coefficient = 20 1/m Refractive Index = 1.3]	1.33	2300	836
Hardboard (Standard) Door	0.14	650	1200
Ceiling Panels (Mild Steel)	0.41	7900	490

Table 6.5:   Thermal Characteristics of Materials to be used in the Case Study
Thermal Loads

Thermal Load	Thermal Input
Office Worker (Light Work, as defined by CIBSE)	100W each
Computers	300W each
Lights (Area of Luminare = $0.3m^2$ each)	$10W/m^2$

6.3 Results and Discussion

6.3.1 Stage 1

<u>Test Geometry</u>

The grid construction used within the enclosure is non-uniform, where the smallest cells are located at the boundaries of the enclosure, and gradually become larger towards the centre of the enclosure. The first grid cell adjacent to the wall has dimensions of 4mm in all coordinate directions. The largest cell within the enclosure has dimensions of 30 mm in all coordinate dimensions. The temperatures at three specific locations were compared with the fully transient results, at a central location within the air adjacent to the wall in the Y-Z plane and the air within the enclosure within the X-Y.

In Section 2.4 of Chapter 2, literature concerning geometrical grid was discussed. Previous researchers had concluded that to accurately capture flow at the boundaries of a CFD model without wall functions at the wall, grid cell sizes had to be confined to less than $0.1mm^3$, Craft et al. (2002). The Revised k-ε Turbulence model was used in the development of this realistic case study, with a Log Law function at the wall. Hence, less fine grid could also accurately capture flow at the boundaries of the enclosure. $4mm^3$ of grid at the boundaries of the enclosure was the smallest grid cell size used, which could be installed in order to restrict the total number of grid cells within the entire model. It was necessary to limit the number of geometrical grid cells to 300, 000 cells, in order to confine the total computational load imposed by the combination of transient and geometrical grid.

<u>Results and Discussion</u>

The Temperatures of the Air adjacent to the Wall

During the first four hours, the external ambient temperatures are steadily increasing. [Note that the sinusoidal ambient conditions have an identical profile to the ambient conditions applied in section 4.5, Chapter 4. The sinusoidal profile shown in Figure 6.1 is used in Stages 3-6. Due to the nature of the materials (brickwork (outer leaf) and UF Foam), the thermal lag of the combined material (approximately 2.5 hours)

will have a significant effect. When using 1 hour transient periods of frozen flow, the errors are less than ± 0.1°C different from the fully transient solution.
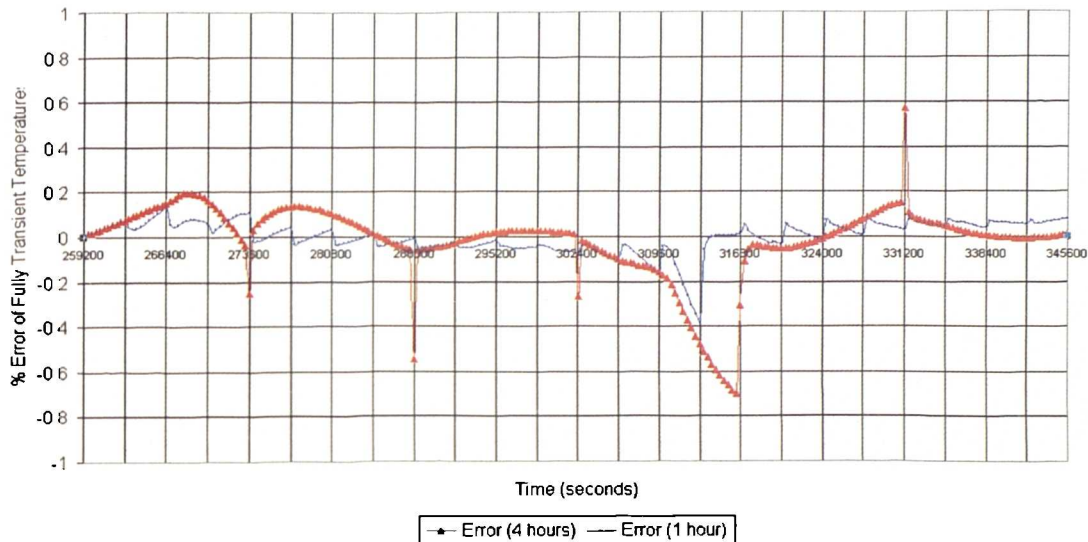
Figure 6.8: Stage 1 – Differences between Fully Transient and DTM-CFD Procedure Temperature Solutions generated at the first cell of air adjacent to the wall

The steady state solution does not reduce the errors to zero after an update has been completed. The following transient step after a steady state update, however, does reduce to zero because the airflow patterns have been corrected. This is certainly the case with the four-hour steps, where the errors become quite large during the transient frozen period and then quickly reduce to approximately zero in the following transient steps of the next period of frozen flow.

There is a slight cumulative effect of error in using the DTM-CFD procedure, but the effect is so minute, that it can almost be disregarded. Between the 4th and 12th hour (273600s – 306000s) (see Figure 6.8), the error profile of the 1-hour period of transient flow is relatively constant. The thermal lag of the material is evident in the solution process, since the materials respond to external temperatures that switch from causing the external wall to cool, rather than heat. This occurs at approximately the 12th hour (306000s) in the external ambient sinusoidal profile, but the solution

process shows evidence of this change in thermal boundary conditions approximately 2 hours later.

The switch of the external wall from heating to cooling obviously has a very high impact on the airflow patterns within the room, because it is only this wall that drives the airflow patterns within the space. For significant changes in airflow patterns that have not been captured by frequent updates, the cumulative error generated is likely to be greater.

The errors generated in at this stage of the realistic case study are more influenced by the lack of correct airflow patterns within the room. As a result, correct thermal loads are not being appropriately convected away from the boundaries of the enclosure. Using longer transient frozen flow periods of 4 hours worsens this negative effect.

The error profiles are behaving as expected, because during the first four hours of the total DTM-CFD simulation time, the external temperatures are steadily increasing since frozen airflow patterns would be too weak compared to the actual airflow patterns. The heat, therefore, is not being adequately convected away from the wall. Between the 8th and the 4th hour (288000s – 273600s) (see Figure 6.8), the DTM-CFD procedure over-predicts the temperatures because the external temperatures start to decrease at this time and the set airflow patterns are too strong.

Mid-point within the Enclosure

The velocities within the enclosure are purely driven by the thermal changes that occur across the external wall, therefore, their magnitudes are very low. The velocities within the room are of the order 0.06m/s. The airflow patterns are strongest at the boundaries of the room and weakest at the centre of the room. It is therefore most likely that the worst errors will occur at the centre of the room, where the airflow patterns have a higher chance of being misrepresented by the DTM-CFD Procedure, because it has to exactly match the result of the fully transient case.

Nevertheless, the maximum error of temperature after a steady state update is ±0.3°C difference between the DTM-CFD procedure and the fully transient case, both for 1 hour and 4 hours transient periods at a central location within the enclosure. The errors along the transient frozen period of flow do not exceed ±0.5° C differences, both for 1 hour and 4 hour transient periods of flow. There is a clear response to the increase in the thermal rate of change/transient period. See Figure 6.9.
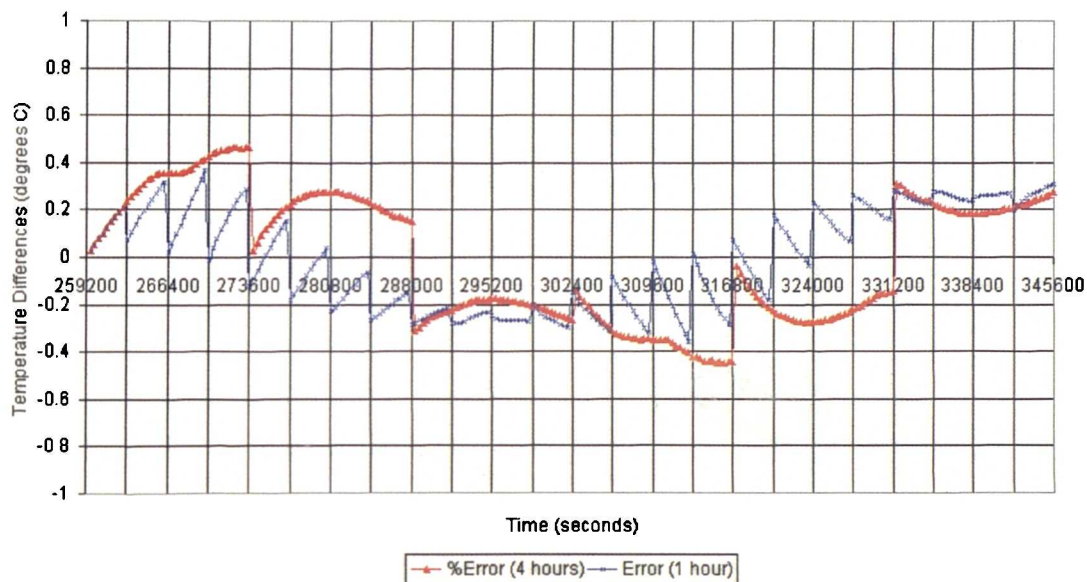
Figure 6.9:   Stage 1 – Difference between Errors of Fully Transient and DTM-CFD Procedure Temperature Solutions generated at the midpoint of the enclosure

6.3.2 Stage 2

Test Geometry

The grid configuration within the multi-layered wall construction is uniform in all three coordinate directions, consisting of 7, 3 and 6 grid cells within the thickness of the brickwork (outer leaf), UF Foam and Brickwork (inner leaf) layers, respectively. The grid cells along the x-direction of the wall materials thickness, will determine the conduction of the external ambient through the material. Research conducted in Section 4.4, Chapter 4, indicated that the number of grid cells embedded within the walls thickness, did not significantly affect the accuracy of the heat conducted

through the material. The grid configuration used over the air enclosed within the volume remains identical to that of Stage 1.

Results and Discussion
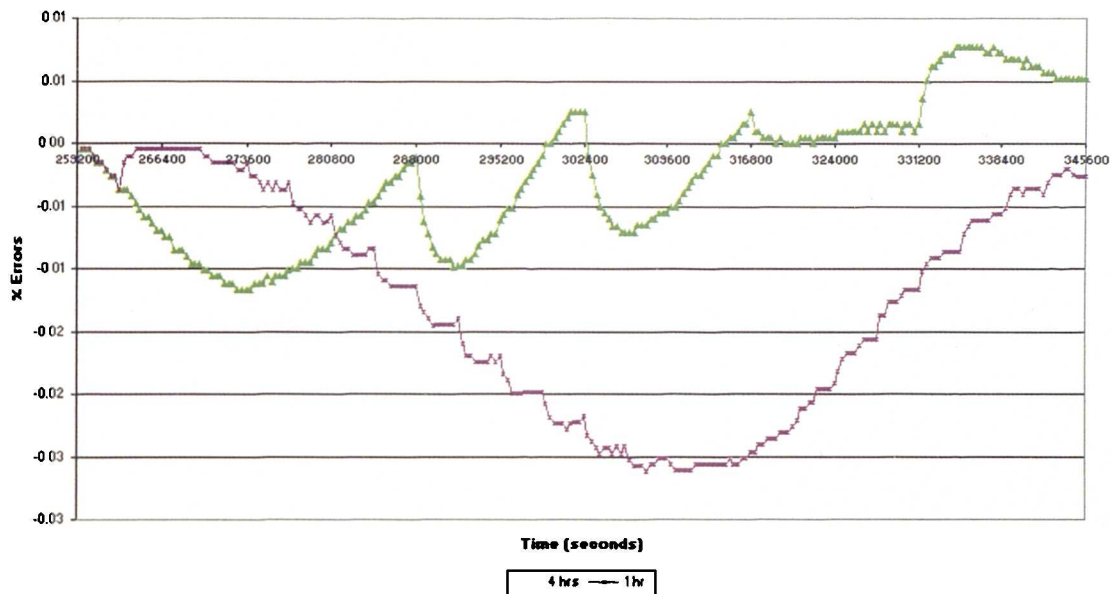
Figure 6.10: Stage 2 – Temperature Difference between Fully Transient Simulation and the DTM-CFD procedure for data collected adjacent to the wall.

The effect of adding another layer to the existing double-layered external wall construction of Stage 1 was to further dampen the thermal fluctuations of the external ambient. As a result, the changes to the internal airflow patterns were minimal, and hence in using 1-hour periods of frozen flow generated maximum errors of ±0.03% of the fully transient temperature solutions (whereby the % error was calculated as the difference between the fully transient and DTM-CFD solutions divided by the fully transient solution). The results of these tests confirmed that for typical building materials, exposed to external fluctuating thermal loads, the DTM-CFD procedure provides excellent accuracy within a fraction of the time it would otherwise take to solve a fully transient solution.

It is evident from the results that the steady state procedure was responsible for errors into the system. For highly resistant building fabric, it is better to use longer transient periods of frozen flow, since airflow patterns are not likely to alter within the enclosure, due to incremental external ambient changes. Choosing to use long

periods of transient flow, however, are not likely to be possible, since results may be required regularly, and the input and output of internal thermal loads are likely to necessitate steady state updates.

6.3.3 Stage 3

Test Geometry

The smallest grid cell occurs immediately adjacent to the boundaries of the enclosure. This cell is 10mm in all dimensions. The cell gradually increases in size with increased distance from the boundaries. The largest cell occurs within the centre of the room and is approximately 30mm^3, the entire enclosure contains approximately 300,000 grid cells. 3 XY Planes containing a 4 x 4 matrix of data recording points have been placed within the enclosure. The first matrix is embedded within the inner surface of the external solid wall. The second matrix lies immediately adjacent to the solid wall within the air, and the third matrix lies within the air, adjacent to the vertical wall which is located opposite the external wall.

The sinusoidal ambient used to simulate external ambient conditions has been redesigned for this stage in the series of tests. Instead of the ambient increasing from 20°C at the start of the transient solution, the starting temperature is 12.5°C. The external ambient used in the simulation is illustrated in Figure 6.1. The objective of altering the sinusoidal ambient setting is in preparation for the following stages, whereby, the pre-conditioning solution of the enclosure is solved as a steady state solution, rather than a transient solution spanning three days. Hence a different starting condition was chosen, so as to ensure defined airflow patterns (since the original sinusoid began at 20°C, while the other walls or internal partitions also had initial conditions of 20°C) are generated before the first transient frozen flow period is solved.

Results and Discussion

The results display similar trends to the error results generated in stage 2, but the magnitude of error generated in stage 3 at locations adjacent to the wall are higher by an approximate factor of 4. At significant points in time, the external ambient causes particular thermal events within the enclosure, such as the switching of the thermal effects of the external wall from being a cooling to a heating wall. In stage 2, this effect causes the largest error of approximately 0.03% after midday.

At this stage, the period of the sinusoid has been shifted, so that the minimum and maximum temperatures of the ambient conditions occur at 6am and 6pm. During the 1-day solution process, this thermal switch effect (from cooling to heating) is seen after the first 6 hours and before the last 6 hours (from heating to cooling). The errors generated by this effect generate similar errors of less than -0.002°C and 0.004°C, respectively, see Figure 6.11.
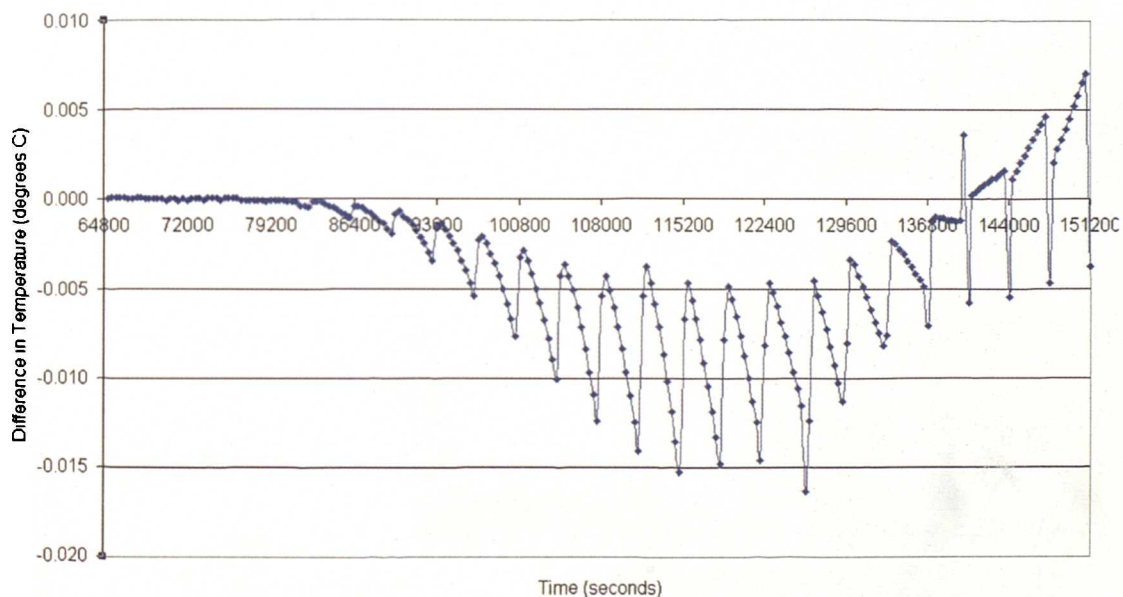
Figure 6.11: Stage 3 – Temperatures Differences between the Fully Transient and the DTM-CFD Procedure for data collected for the first air cell adjacent to the wall

In Section 4.4.2, Chapter 4, it was evident from the tests that an relatively insignificant effect was caused when expanding the geometry of the enclosure. The same conclusions can be drawn from the tests conducted at this stage. The effect of expanding the geometry does not significantly affect the errors generated against the wall, since the most prominent flow occurs close to the boundaries of the enclosure.

6.3.4 Stage 4

Test Geometry

The enclosure constructed in Stage 3, will now be further developed to include a ventilation system and 3 wooden desks. The desks have been installed to create obstructions for the airflow within the room during the transient simulation. The ventilation system is based on the system experimentally modelled at BRE (Garston, UK) as part of the PII Project, CIBSE (2002). Stage 4 contains a fixed flow device located in the floor, underneath the window, which is used to supply air at a rate of 114.4l/s at 20°C. An extract duct mounted above the door on the opposite wall to the window extracts at a rate of 114.4l/s.

The smallest grid cells are at the boundaries of the enclosure and are $10mm^3$. The largest cells are $10cm^3$ located centrally within the enclosure. The thickness of the UF foam was increased to 0.1m in order to increase the U-value of the building materials, so as to conform to the office modelled as part of the research conducted as part of the PII Project,

Results and Discussions
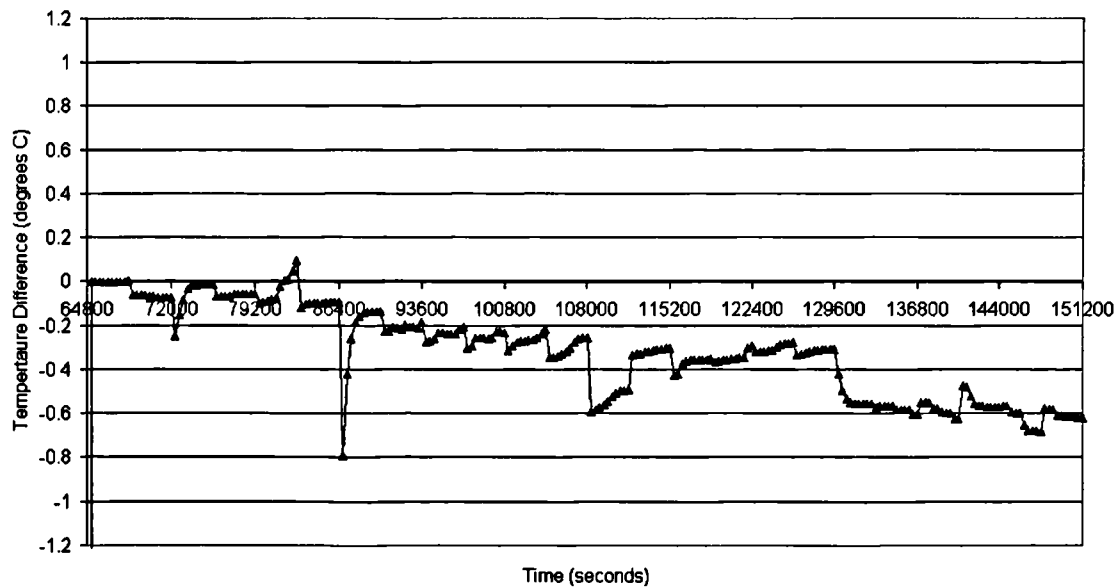
Figure 6.12:   Stage 4:   Temperature Difference between the Fully Transient and DTM-CFD Procedure Solution for Temperature generated within the air adjacent to the wall

In order to restrict cumulative errors over the complete transient simulation, it is vital that the preconditioning solution is as close to the initial conditions of the first time step as possible. A steady state solution was used as a preconditioning solution at this stage, since the 3 days of fully transient preconditioning was proving to be problematic, due to convergence difficulties, which required computational capacity and time. The settings of the steady state preconditioning model were exactly the same initial conditions of the first time step of the initial transient frozen flow period.

Through performing the steady state pre-conditioning solution the frozen airflow patterns were a good representation of the airflow patterns required over the first transient period of frozen flow. In fact, the first few transient periods of frozen flow achieved very small errors because the time-varying thermal conditions within the space were only generated by the external ambient. The resistance of the building materials also damped the effects of the external ambient.

At this stage in the realistic case study, there were two points along the total transient solution at which the DTM-CFD Procedure was likely to fail. The first being the effect of the external ambient switching the external wall from cooling to heating after the 6th hour (86400s on the simulation time axis), at this same point in time, the ventilation system was also activated. The second hotspot was the switching off of the ventilation system, occurring at hour 18 (129600s on the simulation time axis), which was also the same point in time when the external wall switched from heating to cooling.

At the 6th hour, the ventilation system was activated and as suggested in the conclusions of Chapter 5, it was necessary to perform an additional steady state update procedure. During the transient frozen flow period of Hour 5, the ventilation system was switched off, the usual steady state solution followed, whereby the equations of flow were unfrozen. An additional steady state update immediately followed, but the ventilation system was switched on during this update in preparation for the following transient.

As a result of the additional steady state update after transient frozen flow period 5, the following transient period of frozen flow (6th hour) then had more appropriate frozen airflow patterns. The sharp increase in error, shown in Figure 6.12, on the 6th hour (86400s) is an illustration of the effect of solving an additional steady state update. Despite this sharp increase, the error between the fully transient solution and the DTM-CFD Procedure is effectively reduced. See Figure 6.13.

An additional steady state case was highly effective in tackling the sudden thermal input of a ventilation system switching on. Unfortunately, this was not the case for the deactivation of the ventilation system, since an additional steady state update did not effectively reduce errors. The fundamental difference between the switching on and off of the ventilation system was the type of flow generated within the office. The activation of the ventilation system caused airflow patterns, which would have been dominated by forced flow. Conversely, the deactivation of the ventilation system would have caused airflow patterns to form as a result of natural convection.

The reason why an additional steady state update was not effective in correcting the airflow patterns after the ventilation system was turned off was because the airflow patterns would have relied heavily upon the interaction between the building fabric and the air adjacent to the building fabric. Airflow patterns dominated by natural convection form as a result of surface heat transfer coefficients and buoyancy effects present within the room. Hence, the effects of freezing and unfreezing the flow would have prevented these factors taking effect.

By freezing the boundaries, surface heat transfer coefficients could not effectively adjusted. By freezing the airflow patterns, the heat transfer coefficients were also unable to correct themselves in the following transient period of frozen flow. As a result, heat could not be effectively transferred away from the office space, resulting from higher temperatures within the zone. A comparison of the airflow and thermal solutions at each period before (hour 18) and after (hour 19) with the fully transient solutions can be observed from the visualisation plots located in Appendix D, Section D2. The visualisations plots indicate that despite slight differences in temperatures, the overall airflow patterns within the room are similar to the fully transient solutions.

Since erroneous solutions were generated using the freeze flow and steady state update procedure, different methods were tested to overcome the errors generated when the ventilation system switched off. One update method was based on the solution strategy of DTSP#1 see Section 4.3, Chapter 4, whereby instead of solving an additional steady state update, a partially unfrozen transient period was used instead. This partially unfrozen transient period contained 3 time steps of unfrozen flow and the remaining 7 time steps of frozen flow. This procedure was intended to allow both the boundaries and enclosed air to interact. The number of time steps of unfrozen flow was limited to the minimum and the length of time steps (s) were kept to a maximum to avoid additional computational load. Evidently the greater the number of unfrozen time steps the better the accuracy of the solution, but also the greater the computational time required to solve them.

However, even the unfrozen flow time steps did not significantly improve the accuracy of the DTM-CFD Procedure or the additional steady state update method.

Figures 6.12 and 6.13 both contain the results generated by the partially unfrozen transient periods of frozen flow. Despite being unsuccessful in completely reducing the errors generated at the point when the ventilation switched off, the solution was the best method compared to other steady state updating methods.
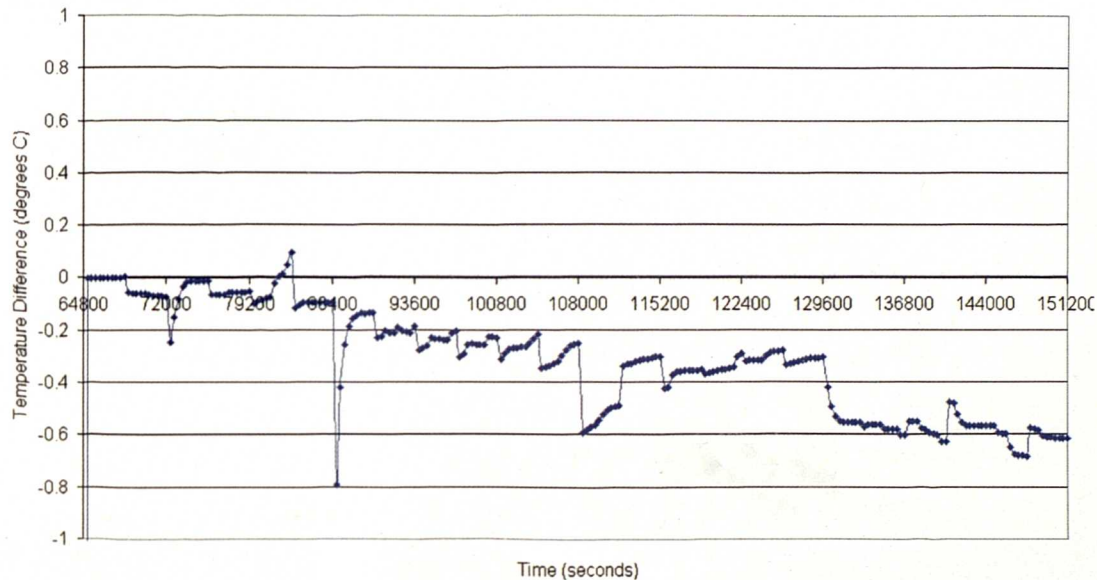
Figure 6.13:   Differences between the fully transient and DTM-CFD Procedure
temperature solutions generated within the centre of the enclosure

At time 129600s, as shown on Figures 6.12 and 6.13, the results appear to display a delayed reaction to the switching of the external wall from heating to cooling. A steady state update is performed at the point in time when the ventilation system switches off, but there is no definite point in time at which internal conditions are influenced by the external wall. What is required is a trigger within the boundaries of a model that can detect thermal differences that could stimulate significant airflow pattern changes.

By comparing Figures 6.12 and 6.13, it is evident that the error within the room is consistently distributed around the office space. The errors do appear to be cumulative, but do not exceed 1°C from the fully transient case. The visualisation plots, located in Appendix D also illustrate that airflow patterns and heat transfer

distribution are satisfactorily modelled by using the DTM-CFD Procedure. Error, however, is also influenced by several other factors, listed below:

1. geometrical grid;
2. turbulence models;
3. convergence.

Convergence is probably the most significant source of discrepancy between the fully transient and DTM-CFD Procedure, since reaching convergence after the ventilation system was either activated or deactivated gave rise to convergence problems, both for the fully transient and DTM-CFD Procedure simulations.

6.3.5 Stage 5

Test Geometry

Achieving convergence of the fully transient case became increasingly difficult as the stages progressed in complexity. This was particularly the case at this stage when modelling the movements of people within the office space. Several tests were conducted in order to establish the most suitable method of modelling people and eventually they were constructed as solid fixed thermal sources. Achieving convergence of the fully transient case was fundamental to the purpose of the real test case, which was to be able to provide a good comparison for the DTM-CFD Procedure.

Results and Discussion

Due to the introduction of people, the airflow within the room was highly turbulent and sensitive. By comparing the fully transient results with the DTM-CFD Procedure an assessment could be made as to the performance of the DTM-CFD Procedure in providing simulations results. At this point in the modelling of the realistic test case, the method of fully transient modelling is also unsatisfactory in modelling the movements of people. In the fully transient case, people appear or disappear on the hour, i.e. occupant gains/losses instantaneously take effect. In reality, the effect of people will occur gradually. Both the fully transient case and

the DTM-CFD Procedure perform equally in the modelling of various occupant and other thermal loads.

6.3.6 Stage 6

<u>Test Geometry</u>

Solar radiation was incorporated into the final stage of this realistic test model. Solar radiation modelling is a relatively new function within the CFD code used in this research. Hence additional testing was required in order to firmly establish how the solar function works under transient conditions, and the *adjustments that would have* to be made to the CFD geometry of Stage 5 in order to successfully include solar radiation into Stage 6 of the realistic case study. The results of the additional solar testing are documented in Appendix D. In summary, the adjustments that had to be made were largely at the boundaries of the CFD model, since the geometry of Stage 5 would not have permitted solar transmittance to take effect.

The combination of solids that formed the pseudo external ambient, had to be adjusted. The solid cuboid used to apply the sinusoidal thermal ambient had to be respecified as a thermal source, i.e. a physically non-existent object emitting a thermal load. The solid cuboid acting as an external surface heat transfer coefficient was then modeled as being transparent, in order to allow direct sunlight to penetrate through the window. The other boundaries of Stage 5 geometry, modelled as symmetrical thermal surfaces, i.e. the thermal conditions on their internal surfaces were mirrored on their external surfaces, had to be remodelled. Solar radiation does not function effectively for symmetrical boundaries, hence their external faces were reset to be exposed to ambient settings of 20°C, assuming that adjacent 'office spaces' would have been maintained at an average temperature of 20°C.

The floor of the geometry of Stage 5 was remodelled as a result of reviewing the overall suitability of the model. Instead of a multi layered floor construction, it was decided that a more efficient use of geometrical grid in this region would be to only model the top layer of the floor. The floor was then specified as a solid cast concrete

slab (thickness 150mm) and exposed to an external surface heat transfer coefficient of 1000W/mK, which would have arisen from earth.

Results and Discussion
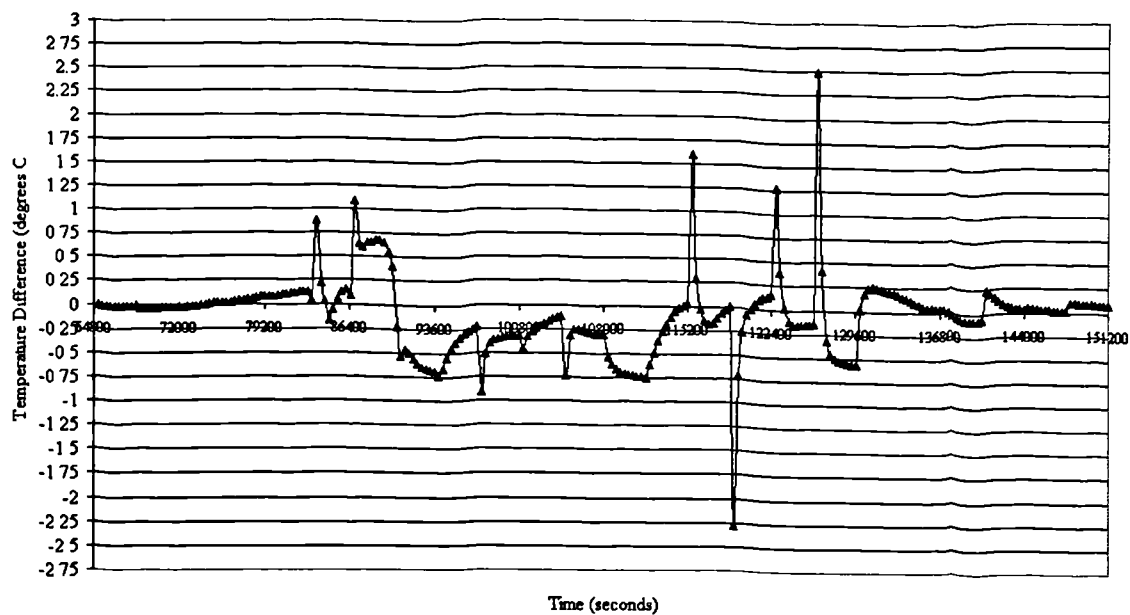
Figure 6.14:   Comparison of the Fully Transient and DTM-CFD Procedure
Temperature Results within the air adjacent to the wall

The overall results for the final stage of DTM-CFD Procedure modelling of a realistic office building are good.   On average, the difference between the fully Transient and DTM-CFD Procedure results for temperature for a location adjacent to the window wall are approximately 0.5°C on average.   The times at which the temperatures exceed a difference of 0.5°C occur mostly when a significant thermal event occurs, such as the entering of occupants to the space.   See Figure 6.14. Generally, the procedure is successful in providing an effective alternative to the fully transient solution procedure of dynamic thermal modelling.

An almost identical updating schedule to that of Stage 5 was used in this final stage. Additional measures, however, had to be taken in order to account for the effects of solar radiation.   Solar radiation first commenced on the 5th hour (hour beginning 82800s), with solar intensity of 275W/m^2.   The strength of the effect of solar intensity increased, reaching a peak at midday of 875W/m^2.   The effects of solar radiation gradually decreased after midday to 0W/m^2 after 5pm.   From 0 hours to 5am, the airflow within the room would have been extremely ineffectual.   The

airflow patterns within the room were solely domainated by external ambient variations. At 5am, the first effects of solar radiation would have been transmitted through the transparent window, and hence would have dominated the nature of the airflow patterns within the room.

The influence of the solar radiation upon airflow patterns had to be captured by an additional update solution, in order to correct the airflow patterns for the following transient frozen flow period (5th hour). The conventional steady state updating method at the start of the 5th hour proved to be unsuccessful in correcting airflow patterns. An alternative had to be found in correcting the airflow patterns within the room as a result of the initial solar radiation effects. This was in the form of a partially fully-transient period (i.e. solving 5 time steps out of ten using unfrozen flow and 5 time steps out of ten using frozen flow), replacing the 5th transient period of frozen flow, a solution loosely resorting back to the concepts behind DTSP#1, see Chapter 4.

The partially fully transient method of correcting the airflow patterns within the office space was successful, and a comparison between the fully transient and DTM-CFD Procedure, using both the partially unfrozen transient method and the additional steady state update method results can be viewed in the form of visualisations plots, located in section D2, Appendix D. The reason for this particular method of updating was similar to those experienced in Stage 4 of the realistic test case. The airflow patterns generated by the effects of solar radiation were dominated by an interaction between the boundaries of the test case and the air within the enclosure. Hence the method of updating had to allow for the exchange of heat transfer data between the air and the solid boundaries. .

Surprisingly, the departure of the effects of solar radiation at 5pm did not require an additional update, since the airflow patterns were more dominated by the presence of other thermal loads within the room, such as the occupants. The instigation of the other thermal events did require additional steady state updating methods. The scheduling of these additional steady state updates followed that of Stage 5. Only larger thermal loads required an additional steady state update. For example, it was not necessary to perform a steady state update when the visitor to the office joined

163

the room on the 12th hour (108000s), see Figure 6.14. This was because the thermal load caused by the visitor was not significant enough to change the existing airflow patterns within the room.

For the introduction of each thermal load into the CFD model, a trial and error method was used to determine the most suitable updating method of update. Hence substantial further work must be conducted to establish what constitutes the requirement of a steady state update, and the correlation between the type of thermal load introduced and the nature of the most appropriate update procedure.

The DTM-CFD Procedure used to model stage 6 would have been typical of the methodology used in industry. One of the main objectives in developing the procedure was to increase the efficiency of modelling dynamic thermal models within CFD. In order to establish whether this objective had been met, every step of the DTM-CFD Procedure of stage 6 was timed and compared to the total time taken to solve the fully transient case. A full itemization of the times is documented in Table D2, Appendix D, but in total a reduction of 16.4% of the fully transient case was achieved by using the DTM-CFD Procedure.

The most time consuming solutions were often the steady state solutions, especially when performing two in succession. Measures can be taken to speed up the process of conducting the procedure, by eliminating the double steady state updating method. Such a measure could reduce the computational capacity drastically. This could be an option for the user of the tool, who may not require the updated conditions of the previous transient conditions. This would not affect the overall accuracy of the simulation, but would alter the presentation of the output results, since pieces of information of airflow patterns would be missing. It would be left to the judgment of the user of the tool as to whether these pieces of information are necessary.

Further work conducted to develop an automatic steady state update trigger could also be developed, which could reduce the overall time taken to complete the whole solution process, since long steady state updates were often due to significant alterations within the flow.

Research has to be conducted on the output of the results. The results should be put into some form of movie format.

6.4 Conclusions

A realistic office enclosure has been designed and modelled using the DTM-CFD Procedure. The case study was developed through a number of stages beginning with a base case model similar to the geometry used to develop the DTM-CFD Procedure, through to the final stage which included solar radiation. The dimensions and thermal activities within the office enclosure were based upon research conducted in association with CIBSE on the PII Project, CIBSE (2002). In order to establish the success of the DTM-CFD Procedure, the results were compared to a fully transient solution.

Applying the DTM-CFD Procedure to a realistic case study through six progressive stages highlighted other aspects in the functionality of the tool that were undetected through research presented in earlier chapters. The nature of updating unfrozen flow depended on the nature of the change of airflow patterns. For significant instantaneous changes in the airflow patterns such as the activation of a ventilation system, an additional steady state update was required. For thermal activities that required the interaction of airflow patterns and boundary conditions, such as the effects of solar radiation, the partially unfrozen transient period was required to allow correct airflow patterns to be generated.

The development of the realistic case study through six stages was an extremely arduous task, since the early stages often contained convergence problems due to significantly weak airflow patterns within the room. The final stage in the construction of the model was the easiest to complete since the schedule of transient and steady state solutions had been determined in Stage 5. The additional effect of solar radiation in Stage 6 caused the enclosed airflow patterns to be even more strongly influenced, and hence, the procedure was able to capture most of the heat transfer and airflow patterns within the room without significant convergence problems. The results indicate that the more dynamic the airflow patterns within the room, usually caused by the presence of high thermal activity, the more effective and useful the DTM-CFD Procedure is likely to be.

In accuracy the DTM-CFD Procedure performed well, when compared to the results of the fully transient case. The time required to complete the DTM-CFD Procedure at the final stage was compared with the fully transient case indicated that the DTM-CFD Procedure was not as efficient as had been initially predicted. By using the DTM-CFD Procedure, the solution time in completing the overall transient solution was reduced by approximately 1/5 of solving the fully transient case.

Using the DTM-CFD Procedure is an effective method of dynamically modelling enclosures. The solution procedure is also more efficient than solving a fully transient case. However, further research must be conducted to develop the method into a fully automated tool, which contains various automatic triggers that can detect whether a steady state updating solution is required. Further work on the development of the tool, will contribute to increasing the effectiveness and efficiency of the existing developed DTM-CFD Procedure.

6.5 Chapter Summary

In this chapter the performance of the developed DTM-CFD Procedure was assessed. The DTM-CFD Procedure was applied to a realistic office case, which was developed through a number of stages. The office case study was based on research conducted within CIBSE (2002), a project which would have significantly benefited from the use of an efficient dynamic thermal modelling tool, had it existed.

At each stage the performance of the DTM-CFD Procedure was assessed and reviewed and the office case model was constantly reviewed until the final stage. The application of the DTM-CFD Procedure at the final stage was successful in modelling the final stage which also included the effects of solar radiation. The efficiency of using the tool, however, was not as significant as had initially been hoped. It has been suggested that there may be possible methods to increase the efficiency of the developed DTM-CFD Procedure. These methods have been discussed in the following chapter, which draws conclusions from the research conducted, and suggestions for future work.

CHAPTER 7

CONCLUSIONS AND FUTURE WORK

CHAPTER 7 – Conclusions and Future Work

7.1 Summary of Conclusions

The research contained within this thesis was conducted to develop a single dynamic thermal modeling (DTM) tool within CFD. It was proposed that this single tool should provide the facility to simulate time dependant airflow and heat transfer within buildings, including their envelopes. An existing CFD code (typically used for steady state simulations) was developed from first principles to incorporate some of the functionalities of typical independent DTM codes available within industry. The second main objective of the research was then to apply the developed tool to model a typical 24-hour period of a realistic office space.

The emphasis of the development of the single DTM-CFD Procedure was more towards incorporating the thermal effects through solid building envelopes. Vast differences in thermal response between solids and air appeared to be one of the main obstacles in combining DTM and CFD codes in the past. Simulating for the thermal effects of solids and air simultaneously was successfully achieved within this research.

When applying the developed DTM-CFD Procedure to model a realistic office space, it was evident that internal thermal activities were far more influential than the thermal effects transferred through the building envelopes. Nevertheless, the DTM-CFD Procedure, developed within this research, was able to provide useful simulations of a variety of internal thermal events as well as simultaneously incorporating the effects of the external ambient conditions through the building materials. Further work, however, is required to fully establish an optimum simulation procedure for modeling dynamic internal conditions.

Overall, the procedure is highly successful in providing a simulation tool capable of dynamically modeling buildings and their envelopes to an accuracy comparable to that typically provided by CFD and superceding the level of detail provided by

typical DTM codes. The tool meets its overall objective of placing itself as a design solution existing between those provided by individual DTM and CFD codes currently available within industry today.

It is widely acknowledged that reducing energy consumption in buildings can significantly reduce adverse environmental impact due to use of fossil fuels. The dynamic interactions between internal and external conditions are key to improving the efficiency of building design, indicated by many studies including the PII Project, CIBSE (2002) with which the research engineer participated.

The PII Project, CIBSE (2002) specifically aimed to capitalise on the use of thermal energy stored within building materials in order to reduce building energy costs and improve space ultilsation. The method of investigation involved combining the analysis of two computer simulations (DTM and CFD codes) and experimental testing. The present engineer contributed CFD analysis to this largely commercial project. It became obvious that a single dynamic CFD tool would have been extremely advantageous towards improving the efficiency and accuracy of the research conducted for the project.

The experience and knowledge gained from contributing to the PII Project significantly influenced the course of the research reported in this thesis. It seemed essential to develop a single dynamic CFD tool, from which commercial applications would benefit. The emphasis of the research reported in this thesis was based upon improving the performance of simulation tools that existed within industry at that time. This had the full backing of the sponsoring company who would benefit from such a development. For at least a decade, researchers had been trying to combine the technologies of DTM and CFD coding. A variety of methods were used, but none managed to develop a single tool that could be easily applied to commercial applications.

For the research reported in this thesis, the largest obstacle of incorporating the dynamic thermal effects of building materials into CFD, was the problem of time constants. Building materials respond at a far slower rate than air. To account for

both time constants of air and building fabric would have required extortionate computational capacity, and hence, a route around this problem was the first objective of the research.

A technique was developed to overcome the problem of incompatible time constants, which used functions already available within the CFD software. A 'Freeze Flow' function enabling the iterative solution process of all equations except temperature to be temporarily paused was combined with a time-varying grid schedule. Long periods of time were allocated for the 'Freeze Flow' function to be activated. This time period was followed by a relatively short period of time, where the 'Freeze Flow' function was deactivated. This transient time schedule effectively allowed for the solution process over both building materials, followed by a period of time whereby the air enclosed by the fabric could update to any changes in boundary conditions, which would have occurred over the previous transient period. The whole solution process was referred to as a transient/frozen – transient/unfrozen dynamic thermal modelling procedure or DTSP#1.

DTSP#1 proved to be successful and so further research was conducted to refine the technique further. The thermal conditions during the transient/unfrozen solution were solved to steady state. Initial research was conducted to determine the length of time required for all temperatures and velocities during an update to stablise/converge for a variety of temperature step changes. Research was also conducted to examine the effects of time steps within a transient period. The conclusions of this research were twofold. Firstly, the optimum overall transient time period required for updating the airflow patterns for a variety of temperature step changes was one hour and secondly, that the number of time steps contained within a transient period did not affect the accuracy of the solution, but did affect the CPU time. A denser transient grid, i.e. using smaller time steps increased computational load. The second conclusion was consistent with existing performance of DTM codes, suggesting that the DTSP#1 still provided enhanced accuracy (compared to a DTM) through the use of a geometrical grid, rather than a transient grid.

In the process of reviewing, the latter part of the dynamic thermal modelling procedure, i.e. the transient/unfrozen part, was subject to reconsideration. Since the temperatures and velocities in the transient/unfrozen solution were allowed to reach convergence, it seemed questionable why the whole process could not be solved as a steady state solution, hence eliminating the time factor of the updating process and hence increasing the accuracy of the converged solution. This question was subject to analysis, which led to the discovery of one significant limitation.

Since both building fabric and air were combined within the overall dynamic thermal analysis, the proposed steady state solution part of the DTM Procedure would have solved both the building fabric and the air to steady state, i.e. both mediums would have reached a thermal equilibrium. For the purpose of updating airflows to changes in boundary conditions, a conventional steady state solution would have been completely unacceptable. To overcome the limitation posed by steady state solution, a 'Boundary Freeze Function' was developed, whereby temperatures within the boundaries of the CFD model could be temporarily paused during a steady state update. The function appeared to be highly effective and eliminated the problem of both boundaries and air reaching thermal equilibrium during a steady state update solution.

With the introduction of the steady state updating procedure, there then became two different methods of dynamic modelling within CFD. Firstly, the transient/frozen – transient/unfrozen method (DTSP#1) and secondly, the transient/frozen – steady state/unfrozen method (DTSP#2). In order to choose the better method, a series of sensitivity tests were conducted in order to establish a suitable geometrical grid over the boundaries of the CFD model and the air it enclosed. Due to the significant computational load imposed by the transient solution process of the two dynamic thermal modelling procedures, the geometrical grid over a simple test enclosure was carefully constructed and selected so as not to impose additional computational load, whilst achieving good accuracy. The two methods were compared against each other and their performance was assessed against a fully transient solution process.

Both methods provided very good accuracy when compared against a fully transient procedure. DTSP#2, the transient/frozen – steady state/unfrozen method, however,

was far more efficient in completing the whole dynamic simulation, when compared to the fully transient solution since solving the double transient solution of DTSP#1 was more time consuming and cumbersome. DTSP#2, was therefore selected for further development, while the studies conducted on DTSP#1 were set aside. Further research was conducted to establish optimal criteria for both the transient and steady state solution processes of DTSP#2, now referred to at this stage in the research as the DTM-CFD Procedure. The research on the transient solution was largely dominated by examining the thermal response of a variety of building materials to transient ambient fluctuating conditions, i.e. the transient/frozen part of the solution process. Nine representative materials were fabricated, so as to span a comprehensive array of typical building material characteristics.

A variety of transient time periods were tested over the nine materials to find a correlation between the length of the transient period and the accuracy of the solution for a selection of thermal material characteristics. The conclusions of the tests suggested that a variety of transient periods could be used over the spectrum of building materials, because the steady state update was effective in correcting the thermal conditions of the solution. The choice of transient period, therefore, would depend largely on the thermal lag of the material and the rate at which the design engineer required simulation results.

Generally, the results of the fabric tests concluded that typical building materials were likely to respond well to the dynamic thermal modelling procedure. Tests were also conducted over the nine materials to determine the effects of time step lengths within a transient period. The results of these tests indicated that the number of time steps within a transient/frozen flow period, did not significantly affect the accuracy of the results, although more than one time step was recommended.

The most thermally lightweight material was selected to aid further research of the steady state updating procedure, since fabric tests indicated that this material was most sensitive to the DTM-CFD Procedure. This lightweight material was subjected to a series of harsh tests, whereby ambient conditions were altered in three ways so as to increase the rate of thermal change per time step and the extent of thermal change per time step. The initial objective of these harsh tests was to discover a

correlation between the rate of thermal change of the external ambient and the residual error remaining after a steady state update.

The tests did not reveal any such relationship, but did highlight a flaw in the steady state updating procedure. The flaw took effect for high rates of thermal change and was caused by the inability for the dynamic thermal modelling procedure to account for the thermal lag of air. Hence, for high rates of change, performing a steady state update effectively ignored the thermal lag of air, which should have delayed the transportation of thermal energy around the enclosed space. In reality, air would have taken a certain amount of time to distribute thermal energy around the enclosure, but by performing the steady state update, the thermal energy would have been 'dumped' at its end location, and the time taken for its delivery would have been disregarded.

Attempts were made to find an alternative solution to the steady state update procedure, by freezing the temperature equation during the steady state solution, but this only reduced the overall effectiveness of the steady state update procedure. The flaw in the procedure only took effect for exceedingly high rates of thermal change, i.e. at rates higher than the thermal lag of air, and would not have had a significant effect for realistic rates of change of ambient conditions.

The discovery of a flaw in the steady state solution process did alter initial assumptions that the length of time between updates was likely to correlate with the residual error remaining after a steady state update. Instead, the research revealed that errors were generated within the steady state updating procedure itself, which under realistic ambient conditions were unapparent. For high rates of change, however, the flaw in the system became more significant due to the incapacity to account for the effects of thermal lag.

After extensive scrutiny of the DTM-CFD Procedure, and the overall objective of efficiently incorporating building fabric into the CFD simulation had been achieved, the procedure was then applied to a realistic design case. The design case was based upon one used in a PII Project, CIBSE (2002) and was constructed through six stages. The final case contained a multi-layered building fabric construction of a

174

simple office space. During the transient simulation three office workers occupied the office space at various points of the day. The model also contained the effects of a ventilation system and solar radiation.

By applying the DTM-CFD Procedure to the realistic office design case, other non-researched factors surfaced; such as the necessity to perform additional updates to capture significant airflow patterns changes, before they happened. For example, additional updates were required when the ventilation system switched on. By applying the DTM-CFD Procedure to the realistic case, a trial and error method was used to determine the most appropriate method of updating internal thermal events. For specific internal thermal loads, the original transient/unfrozen method of updating was the only option for correcting the airflow patterns within the room. The choice of method of updating depended upon the factors dominating the airflow patterns at the time.

If natural convection effects dominated airflow patterns, such as the deactivation of a ventilation system, then the original transient/unfrozen updating method was required, since the interaction between the boundaries and the air they enclosed was vital. If the airflow patterns were dominated by forced convection, such as the arrival of occupants, then an additional steady state update, before the thermal event was necessary. It was concluded that the nature of updating airflow patterns in the DTM-CFD Procedure could be the subject of extensive future work.

Overall, the procedure worked very well in modelling the realistic design office space. In performing a thorough survey of previous research, it was evident that no single tool has been developed that could provide dynamic thermal simulations to a level of accuracy comparable to the accuracy provided by CFD. The tool developed in this research, fulfilled the objective of placing itself in between the simulations provided separately by a DTM and CFD code. The research conducted for the PII Project would have significantly benefited from the use of the tool developed in this thesis.

In terms of efficiency, the DTM-CFD tool provided a transient simulation in 16.4% less of the time taken to run a fully transient case. The reduction in computational

time was not as high as had initially been expected. However, recommendations for future work have been made, which are expected to further improve the efficiency of the developed tool.

7.2 Future Work

The DTM-CFD Procedure performed well in providing dynamic thermal simulations of the realistic office design case, but many functions of the procedure had to be set manually. There is vast scope for the further development of the tool, which will require additional research in order to improve upon the foundations, which have been laid in this thesis for an effective and efficient *DTM-CFD Procedure*. There are three main aspects of future work that are recommended.

- The first aspect requires the development of the way in which external ambient conditions are simulated within the software.

- The second aspect calls for a far more in-depth investigation into the relationship between the types of updating procedure and the thermal conditions within a CFD model.

- The third aspect suggests that 'triggers' are developed within the software to detect if and when a steady state update is required.

In order to improve the way in which external ambient conditions are specified within the software, additional facilities could be installed into the software code. These facilities should store, supply and process data concerning ambient conditions based upon actual weather data. For the purpose of the research reported in this thesis, ambient conditions were represented as sinusoidally varying. With increasing sophistication of the specification of weather, other effects such as wind, could be eventually incorporated into the tool. At present, the limitation in the software for modelling ambient conditions in transient scenarios must be overcome. A temporary solution was developed within this research that simulated transient ambient conditions by applying thermal profiles to a series of cuboids.

Solar radiation modelling must be further developed to function as a fully automated function. In doing so, the user of the DTM-CFD Procedure will have more choice as to the length of the transient periods to be used. For the purpose of this research, solar radiation calculations were set every hour, and hence the transient periods had to be confined to one hour. Automating the specification of solar radiation would allow the user of the DTM-CFD Procedure, greater choice of transient frozen flow periods.

Extensive research must be conducted on the steady state updating procedure. Various methods were experimented with, which used a combination of conventional steady state solutions and/or a transient/unfrozen update allowed to converge to steady state. What is required is a specially designed steady state update procedure, which solves under transient settings, i.e. allows the boundaries of CFD model to maintain their thermal conditions. Effectively, an ideal steady state update would be similar to the solution process of the first time step of a transient/unfrozen update period. Achieving this would allow the boundaries and air of an enclosure to interact, which was not possible in the steady state updates used in this research. By improving the steady state update procedure, as recommended above, it may not be necessary to have a variety of methods of updating the airflow patterns. The present study, however, highlighted that different thermal scenarios required distinct methods of updating.

If one method of updating cannot be developed, then a trigger should be developed which can detect the type of update, which may be required by the solution process. This study highlighted that natural convection thermal scenarios required an update procedure, which had to allow for the interaction between boundaries and the air it enclosed, while forced convection cases required an additional steady state update to reset airflow patterns.

If one steady state update procedure could be developed, which could allow for the interaction between boundaries and air (i.e. as a time step in a transient period is able to do), then general update triggers could be placed at various locations within the CFD model, such as the boundaries, internal space and also within thermal loads,

such as occupants. These various triggers would communicate with each other and detect when their relationships have changed, which could stimulate an update. Other mechanical systems should also call for an automatic update when switched off or on, as manually modelled in this research. The development of triggers within the software is already underway, since mechanical systems contain thermostatic control, which could also be linked to a steady state update trigger.

Improvement in the steady state procedure and the ability to automatically detect when a steady state procedure is required will enhance the overall performance of the DTM-CFD Procedure. For the research reported in this thesis, most of the DTM-CFD Procedure was implemented using the necessary functions manually. Transient periods had to be stopped, steady state solution had to be re-specified and 'freeze' functions and 'Boundary Freeze' Functions had to be activated and deactivated manually.

As a result of this largely manual dynamic thermal simulation procedure, errors along the transient period were allowed to increase. Often these errors were quickly eliminated by the steady state update procedure. In the future, it would be ideal to provide the users of the tool with a facility, which would allow them to choose the level of accuracy required. If highly accurate simulations were desired, then triggers in the code would not allow errors to increase above a certain limit which in turn would require longer computational time, since more steady state updates would be solved.

Conversely, if a general picture was required by the user of the tool of the dynamic thermal conditions of a CFD model, a less fine simulation could be conducted. This more coarse simulation would allow errors to increase and steady state simulations would probably not be performed so frequently. Having a choice in the level of detail provided by the DTM-CFD Procedure would allow the engineer more control over the time in which a solution would be obtained. This would be useful throughout a design project, since the tool could be used from the concept stage of a project, through to the final stages, where high-level accuracy would be required.

Post-processing of the results therefore is the last aspect and probably the most important recommendation for future work. Due to the vast quantities of data generated in the research conducted for this thesis, it was impossible to show the complete set of results of the dynamic simulations over a 24 hour simulation period. To convey all of the data generated by the DTM-CFD Procedure, the results could be displayed in the form of a movie. At present, steady state CFD simulations can be displayed as an animation, through the interpolation of results, so the adaptation of the present facility to accommodate for time varying data, should be developed.

Generally, there is vast scope for the improvement of the overall efficiency of the DTM-CFD Procedure developed and reported within this thesis. The functions introduced in this research need extensive additional research, which will inevitably increase the overall performance of the tool. For now, the research conducted has been successful in creating a commercial tool, which stands comfortably between the existing DTM codes and CFD, to provide useful and accurate dynamic thermal simulations of buildings.

List of References:

Agonafer D, Liao G-Li, Spalding DB (1996) "The LVEL turbulence model for

   conjugate heat transfer at low Reynolds numbers" EEP6, ASME International

   Mechanical Congress and Exposition, Atlanta

ASHRAE, (1975), Task Group on Energy Requirements 'Procedure for

   computerising Calculations'. ASHRAE, New York, USA.

Bartak, M. Beasoleil-Morrison, I. Clarke, J.A. Denev, J. Drkal, F. Lain, M

   Macdonanld, I.A. Melicov, A. Popiolek, Z. Stankov, P. (2002) Integrating

   CFD and Building Simulation, Building and Environment, 37 865-871.

Beausoleil-Morrison, I. (2002) The adaptive conflation of computational fluid

   dynamics with whole-building thermal simulation, Energy and Buildings, 34

   857-871

Beausoleil-Morrison I. (2000) The adaptive coupling of heat and air flow modelling

   within dynamic whole-building simulation. Ph.D. thesis, University of

   Strathclyde, Glasgow.

Boyer, H., Chabriat, J. P., Grondin-Perez, B., Tourrand, C., and Brau, J., (1996),

   Thermal Building Simulation and Computer Generation of Nodal Models,

   Building and Environment, vol. 31, No. 3, pp. 207-214.

Boyer, H., Garde, F., Gatina, J.C., Brau, J., (1998), A multimodel approach to

   building thermal simulation for design and research purposes, Energy and

   Buildings 28 (1998) 71-78.

Cebeci, T., Smith, A. M. O. (1974) Analysis of Turbulent Boundary Layers,

   Academic Press.

Chen, T. Y. (2001) Real-time predictive supervisory operation of building thermal

   systems with thermal mass, Energy and Buildings 33 141-150.

Chen, Q., and Jiang, Z., (1992) Significant questions in Predicting Room Air Motion,

   ASHRAE *Transactions*, Vol. 98, Pt. 1, pp. 929-939.

Chen, Q. Xu, W. (1998) A zero-equation turbulence model for indoor air flow

   simulation, Energy and Buildings, 28 137-144.

Chien, Y. P., Ecer, A., Akay, H. U., Secer, S., Blech, R. (2002) Communication cost

   estimation for parallel CFD using variable time-stepping algorithms,

   Comput. Methods Appl. Mech Engrg. 190 1379-1389.

CIBSE Guide, (1986) Volume A: Design Data, Section A5: Thermal Responses of

Buildings, CIBSE, London. ·

CIBSE TM29: (2002) HVAC Strategies for Well-Insulated Airtight Buildings

Clarke, J. (2001) Domain Integration in Building Simulation, Energy and Buildings 33 303-308

Clarke, J., Irving, A. D., (1988), Building Energy Simulation: An Introduction, Energy and Buildings 10, 157-159

Clarke, J. A., (1989), Building Energy Simulation: The State-of-the-Art, Solar and Wind Technology Vol. 6, No. 4, pp. 345-355.

Craft, T. J., Gerasimnov, A. V., Iacovides, H., and Launder, B. E. (2002) Progress in the generalization of wall function treatments, International Journal of Heat and Fluid Flow 23 148-160.

Daly B. J., Harlow, F. H., (1970) The generalized gradient diffusion hypothesis, Physics of Fluids 13, 2634.

Davies, M. G. (2001) Hourly Estimation of Temperature using Wall Transfer Coefficiencts, Building and Environment, Vol. 36, 199-217.

Donn, M. (2001) Tools for Quality Control in Simulation, Building and Environment 36, 673-680.

DTI, (2002), Publication on Energy Consumption in the UK

Hazim, A. B. (1998) Calculation of Convection Heat Transfer Coefficients of Room Surfaces for Natural Convection, Energy and Buildings 28, 219-227.

Hekes, R. A. W. M., Hoogendoorn, C. J., (1989) Comparison of Turbulence models for the natural convection boundary layer along a heated vertical plate, International Journal of Heat and Mass Transfer 32, 157-169.

Hinze, J. (1975). Turbulence. McGraw-Hill, New York, second edition.

Holmes, M. J., Lan, J. K-W., Ruddick K. G., and Whittle G. E., (1990), Computation of Conduction, Convection and Radiation in the Perimeter Zone of an Office Space. Proceedings ROOMVENT '90, Oslo, Norway.

Hong, T., Zhang, J., and Jiang, Y., (1997), IISABRE: An Integrated Building Simulation Environment, Building and Environment, Vol., 32, No. 3, pp. 219-224.

IEA (1995), Building Energy Simulation Test (BESTEST) and Diagnostic Method, National Renewable Energy Laboratory, Golden Colorado.

ISO 10303 (1992) Industrial Automation Systems -- Product Data Representation and

Exchange – Part 11: Description Methods: The EXPRESS Language Reference Manual

Karajiannis, T.G., and Tian, Y.S., (2000) Low turbulence natural convection in an air filled square cavity Part I: the thermal and fluid flow fields, International Journal of Heat and Mass Transfer 43, 849-866.

Kato, S., Murakami, S., Shoya, S., Hanyu, F., and Zeng, J., (1995), CFD Analysis of Flow and Temperature Fields in Atrium with Ceiling Height of 130m, ASHRAE Transactions, Vol. 101, Part 2, pp. 1144-1157.

Kitagawa, K., Hayano, H., Saito T., and Onishi J., (1996), Numerical Simulation for Radiant Air-Conditioning System, Proc. 5th Int. Conference ROOMVENT '96, Yokohama, Japan, Vol. 1, pp. 205-212.

Lam, K. P., Mahdavi, A., Gupta, S., Wong, N. H., Brahme, R., Kang, Z., (2002), Integrated and Distributed Support for Building Performance Evaluation, Advances in Engineering Software, Vol 33, pp. 199-206.

Launder, B. E. and Sharma, B. I., 1974, Application of the Energy-Dissipation Model of Turbulence to the Calcualtion of Flow Near a Spinning Disc, Letters in Hear and Mass Transfer, Vol. 1, pp. 131--138

Moser, A., Schalin, A., Off, F., Yuan X., (1995), Numerical Modelling of Heat Transfer by Radiation and Convection in an Atrium with Thermal Inertia, ASHRAE Transactions, Vol. 101, Part 2, pp. 1136-1143.D.

Musy, M., Winklemann, F., Wurtz, E., Sergent, (2002) Automatically generated zonal models for building air flow simulation: principles and applications, Building and Environment 37, 873-881.

Negrao, O. R., (1998) Integration of Computational fluid dynamics with building thermal and mass flow simulation, Energy and Buildings 27, 155-165.

Neilson P. V., and Tryggvason, T., (1998), Computational Fluid Dynamics and Building Energy Performances Simulation, Aalborg University, Aalborg, Denmark. International Conference on Air Distribution in Rooms, Stockholm.

Oberkampf, W. L., Trucano, T. G., (2002) Verification and Validation in Computational Fluid Dynamics, Progress in Aerospace Sciences, Vol 38, pp. 209-272.

Onishi, J., Kurimura M., and Tanaka, M., (1990), Applicability and Limitations of a Numerical Method in Thermal Environmental Analysis for air-conditioned Rooms. Proc. 2nd Int. Conference ROOMVENT '90, Oslo, Norway.

Schibuola, L., (1997), An analysis of next generation building energy simulation tools, International Journal of Ambient Energy, Volume 18, Number 4.

Schild, P., (1997) Accurate Prediction of Indoor Climate in Glazed Enclosures, PhD Dissertation, Norwegian University of Science and Technology, Trondheim, Norway.

Schild, P., (1997), Accurate Prediction of Indoor Climate in Glazed Enclosures. Ph.D. Thesis, Dep. Of Refrigeration and Air-Conditioning, Norwegian University of Science and Technology (NTNU), Norway.

Seigel R. Howell J. R. (1992), Thermal Radiation Heat Transfer pp. 1030-1031

STEP, (1992) Standard for the exchange of product model data, proposed as ISO 10303, TC184/SC4,

Takeya, N., Onishi, J., Koga, S. M., Izuno, M., Kitagawa, K., (1998), Computer Effort Saving methods in Unsteady Calculations of Room Airflows and Thermal Environments, Department of Environmental Engineering, Osaka University, International Conference on Air Distribution in Rooms, Stockholm.

Tang, D., (1998), Virtual Environment for the Prediction of Air Movement in Buildings, Integrated Environmental Solutions Limited, Glasgow, UK, International Conference on Air Distribution in Rooms, Stockholm 1998.

Tuomaala P., and Rahola, J., (1994), Combined Air Flow and Thermal Simulation of Buildings, Building and Environment, Vol. 30, No. 2, pp. 255-265.

Yuan, X., Moser, A., Suter, P. (1993) Wall functions for numerical simulation of turbulent natural convection along vertical plates, International Journal of Heat and Mass Transfer 36, (18) 4477-4485.

Yuan, X., Huber, A., Schaelin, A., Hachmann, P., Moser, A., (1992) New wall functions for the numerical simulation of airflow pattern in rooms, Proc. of Roomvent '92. Vol. 1, Aalborg, Denmark, pp. 75-91.

Zhang, Y., (1990), Implementation of Combined Building Energy and Air Flow Simulation, MSc Thesis, University of Strathclyde.

APPENDICES

APPENDIX A

APPENDIX A - ·

VERIFICATION TESTS OF BASIC THERMAL PROCESSES THROUGH A MATERIAL USING CFD

A.1 Introduction

The main overall objective of the research documented in this thesis is to develop CFD to efficiently and effectively model dynamic thermal conditions. The current method in achieving this objective is to use DTM and CFD in tandem. In order to develop CFD to dynamically simulate zones of a building, the techniques conventionally used by a DTM must be adopted into a CFD code.

The solution processes of both DTM and CFD are similar. Both function on the basis of the conservation of energy and provide heat transfer within a building zone. CFD contains the equations of conservation of momentum, in addition to all the governing equations used within DTM (see Chapter 1, section 1.2). Hence, theoretically CFD should be capable of dynamically modelling heat transfer through materials.

CFD is typically used to simulate steady state conditions of fluid flow. In order to begin dynamically modelling solid materials within CFD, however, three basic thermal processes of heat transfer through solids usually undertaken by a DTM, must be verified. The physical processes involved in modelling a building dynamically are:

1. **Heat Conduction**
2. **Convective Heat Transfer**
3. **Radiant Heat Exchange**

Each one of these modes of heat transfer will be tested using very simplistic geometrical cases in FLOVENT. A further hindrance towards dynamically modelling within FLOVENT is the representation of ambient conditions within a transient solution. A solution to this obstacle is has been developed and documented in Part A5.

Table A1: Summary of Basic Thermal Processes Tests Conducted

Test Name	Test Description
Conduction	Examining whether the heat through a building fabric is successfully transferred by conduction.
Convection	Air blown over a wall surface to demonstrate the effects of forced convection. The surface has a set Surface Heat Transfer Coefficient (SHTC).
Radiation Exchange	Direct heat exchange between a cold and hot surface at opposite ends of an airspace by radiation (no significant interaction with the air).
Simulating Transient Ambient Conditions	1. Examining the effects of a sinusoidal profile through the application of a series of cuboids in steady state; and the development of this model into transient scenarios. 2. Observing the failure of applying a transient thermal profile to a collapsed cuboid (i.e. a cuboid that contains no grid cells). 3. Observing the failure of applying a transient profile to a collapsed thermal heat source. A source does not have a physical presence.

A.2 Heat Transfer By Conduction

A2.1 Introduction to the Theory of Conduction

Conduction in a solid takes place due to the molecular interactions between molecules of different energy levels. A molecule with a higher temperature has a higher energy level than a molecule with a cooler temperature (lower energy level). A constant transfer of energy occurs, when neighbouring molecules collide. The transfer of energy is from the more energetic to the less energetic, hence, heat is transferred in the direction from hot to cold.

The equation for the rate of heat conduction is called Fourier's Law, shown below:

$$q = -\lambda \frac{dT}{dx}$$
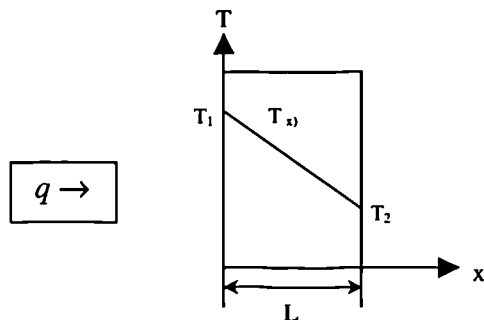
Fig.A1: One-dimensional Heat Transfer by Conduction

The heat flux, q (W/m^2), is the heat transfer rate in the direction x per unit area perpendicular to the direction of transfer, and it is proportional to the temperature gradient, dT/dx, in this direction. The proportionality constant, λ, is a transport property known as thermal conductivity (W/mK) and is a thermal property of the wall. The minus sign is due to the heat travelling in the direction of decreasing temperature. A test has been designed in order to verify the whether the process of conduction can be successfully modelled within CFD.

A2.2 Conduction Test - Steady State Case using a Standard Ambient Setting

A2.2.1 Model Description

This test starts from first principles by displaying the effect of heat transfer through solid materials exposed to an ambient setting at steady state. Ambient conditions are prescribed adjacent to a solid using the standard procedure (including a prescribed external surface heat transfer coefficient), available within the CFD code. A simple wall is modelled in FLOVENT. The wall (1m x 1m x 1m) is made from brickwork (outer leaf). The Y-Z face of the wall, at X=0m is exposed to a constant ambient temperature of 0°C. The Y-Z face of the wall at X=1m is exposed to a constant ambient temperature of 10°C. The wall has a thickness of 1m. All other faces of the wall are set to be adiabatic, i.e. no heat transfer occurs on any of the faces apart from those faces on the Y-Z planes. The case is run as a steady state case.

X-Low and X-High Open Faces Ambient Attached of 0°C and 10°C, respectively.
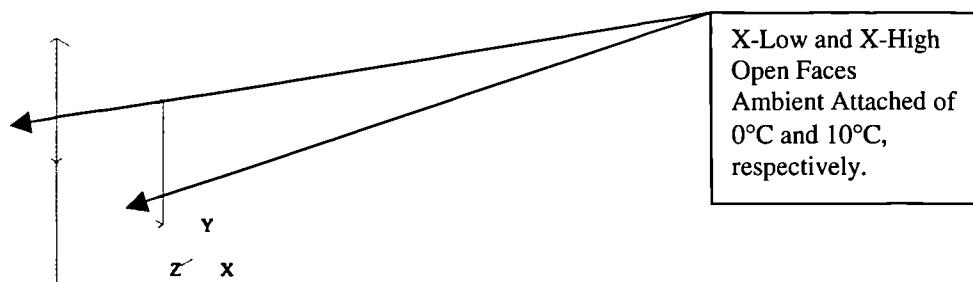
Fig. A2: Geometry of Conduction Test

The physical grid of the CFD model contains cells with maximum dimensions of 0.1m in the X, Y and Z co-ordinate directions.

A2.2.2 Comparisons of the CFD Results and Analytical Solution

The result for the heat transfer within the wall is recorded within the CFD model as being 37.5W. For comparative purposes, the rate of heat transfer through the wall can be solved analytically, using the equation for conduction.

The Rate of Heat Transfer Q = UAΔT through the fabric is calculated as follows:

Where Q = Rate of Heat Transfer (W)

U = U-Value (W/m^2K)

A = Surface Area of Material (m^2)

ΔT = Temperature Difference between external and internal surfaces (°C)

R = Total Resistance (m^2K/W)

He = External surface Heat Transfer Coefficient (W/m^2K)

Hi = Internal surface Heat Transfer Coefficient (W/m^2K)

Rm = Resistance of Material (m^2K/W)

$$U = \frac{1}{R} = \frac{1}{\frac{1}{H_e} + R_m + \frac{1}{H_i}}$$

$$= \frac{1}{\frac{1}{12} + \frac{1}{10} + \frac{1}{12}} \tag{A6}$$

$$U = 3.75 \frac{W}{m^2 K}$$

Q = UAΔT

= 3.75 x (1 x 1) x 10

= 37.5W

Note: Thermal conductivity (W/mK) = U (W/m^2K) x A (m^2)

A2.2.3 Conclusions

The rate of heat transfer obtained in the CFD model, is identical to the analytical solutions.

A.3 Surface Heat Transfer By Convection

A3.1 Introduction to the Theory of Convection

Convective heat transfer may be classified according to the nature of the fluid flow involved. Forced convection is when the flow of fluid arises by external means, such as by a fan or a pump. Free (or natural) convection, occurs when the fluid flow is induced by buoyancy forces. Buoyancy forces arise due to differences in density within the flow in a single fluid; density differences are caused by temperature variations. Significant convective effects occur between solid and air interfaces of different temperatures. The equation that describes the rate of heat transfer due to convection is:

$$q_{conv} = h_c A(t_2 - t_1) \qquad\qquad (A2)$$

where:

q_{conv}= Convective heat transfer (W)

h_c= Surface Convective heat transfer coefficient (W/m^{2}K)

A= Surface Area (m^2)

t_1 and t_2 are temperatures (°C and K)

A3.2 Test Description

A cuboid (1 x 1 x 1m) with a fixed temperature of 10°C is maintained. Air is blown through a fixed flow device, across one of the cuboids surfaces, at a rate of 1m^3/s. The air leaves the fixed flow device at a temperature of 20°C, in the direction of an exhaust. A planar region has been installed at the top of the wall, opposite the opening of the fixed flow device. The purpose of the planar region is to be able to measure the average heat flux through its volume, and hence gauge the average temperature of the air after having been cooled by the wall.

The cooling effect of the wall purely by surface heat transfer, cools the forced supplied air. The surface over which the air is blown, has a constant heat transfer coefficient 10 W/m²K. This test case is modelled in steady state.

All faces of the entire CFD solution domain are adiabatic except the top surface of the cuboid, which enables the air to flow towards the sink, see Figure A4, below.
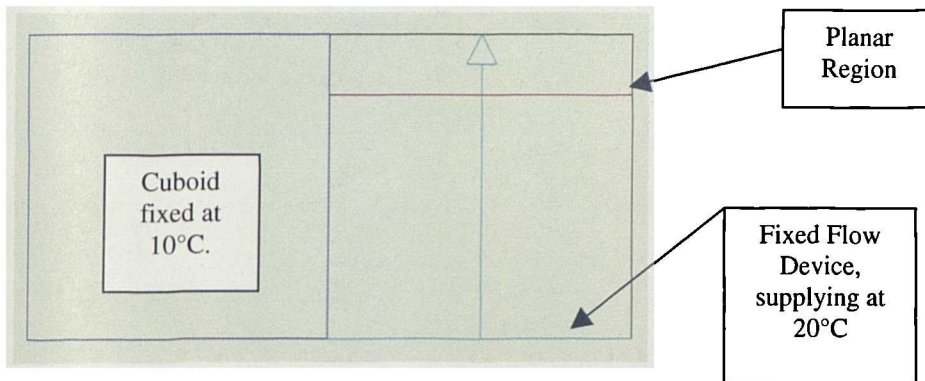
Fig. A3: Geometry of Convection Test Case, as constructed within FLOVENT

A3.3 Test Objectives

To test whether surface heat transfer coefficents and forced convection are accurately represented within FLOVENT (the CFD code, used in this research).

A3.4 Analytic Calculations

The predicted temperature in the planar region, is as calculated:

Heat Loss due to surface heat transfer by convection from the cuboid:

Applying Equation A2: $Q_{Conv} = h \, A \, (T_A - T_s)$

Where h = Surface Heat Transfer Coefficient (W/m²K)

A = Area of Cuboid Surface over which the fluid flows (m²)

T_A = Bulk Temperature of Air flowing over the surface of the cuboid (K)

T_s = Surface temperature of cuboid (K)

Heat Transfer due to the fixed flow device:

$$Q_{FFI} = mC_p\Delta T$$

Where m = mass flow rate of the supply air (kg/s)

C_p = Specific Heat Capacity of Air (J/kgK)

ΔT = Temperature Difference between inlet and outlet (K)

$$Q_{FFI} = 1.19 \times 1005 \times 20 = 23919W$$

$$Q_{Conv} = 10 \times (1 \times 1) \times (T_A - 10)$$
$$= 100W$$

$Q_{FFO\ is}$ reported as being 23823W in FlOVENT.

$$Q_{FFO} = Q_{FFI} - Q_{Conv}$$
$$= 23919W - 100W$$
$$= 23819W$$

A3.5 Conclusions

A region, set up in the CFD model records a heat flow of 23823W. The theoretical calculation of the heat transfer through this same region was calculated at 23819W. Comparing the theoretical and CFD results of the solution indicates a 4W difference between the amount of heat convected from the wall surface. The error between the theoretical and CFD solution is approximately 4% . [(% of 4W / 100W), 100 W being the heat transferred by convection].

These results prove that CFD can successfully predict the effects of convection, to a high degree of accuracy. The % error obtained from the results may have been caused by the over-simplification of the theoretical calculations. The analytic calculations use a bulk temperature for the wall and supply air. In reality, the fixed flow of air will

be cooling down as it passes over the cool wall, and the wall will also be increasing in temperature, hence influencing the rate of convective heat transfer across the wall.

A-10

A4 Heat Transfer By Radiant Exchange

A4.1 Introduction to Theory of Radiation

Heat transfer by radiation is different to conduction and convection, in that it does not require a medium, through which to transfer energy. Radiation is the transfer of energy through space by electromagnetic waves, and hence, radiation occurs most efficiently in a vacuum. The maximum flux (W/m^2) at which radiation may be emitted from a surface is given by the Stefan-Boltzmann law.

$$q = \sigma T_s^{\,4} \tag{A3}$$

Where Ts is the absolute temperature (K) of the surface and σ is the Stefan-Boltzmann constant (σ=5.67e-8 W/m^2/K^4). This equation applies to ideal radiators, which are perfectly black bodies. The heat flux (q) emitted by a real surface, i.e. less than that of a perfectly black body is given by:

$$q = \varepsilon \sigma T_s^{\,4} \tag{A4}$$

where, ε is a radiative property of the surface called the emmisivity. The value of ε ranges between 0 and 1.

View Factor: Seigel et al., (1992)
For a square plate the View Factor, VF reduces to:

$$VF = \frac{1}{\pi}\left[\frac{1}{B^2}\ln\left(\frac{(1+B^2)^2}{(1+2B^2)} \right) - \frac{4}{B}\tan^{-1} B + \frac{4}{B}\sqrt{1+b^2}\,\tan^{-1}\frac{B}{\sqrt{1+B^2}} \right] \text{ rads}$$

B = b/a = 1/1 = 1
C = c/a = 1/1 = 1

$$VF = \frac{1}{\pi}\left[\ln\left(\frac{(2)^2}{1+2^2}\right) + \frac{4}{1}\sqrt{2}\tan^{-1}\frac{1}{\sqrt{2}}\right]$$

=0.1998 rads

A4.2 Test Description

A thin-walled enclosure (1m x 1m x 1m) has six adiabatic faces. A perfectly black cuboid (with an Emissivity, $\varepsilon = 1.0$) will be embedded within the base of the enclosure (with the dimensions of the enclosure, but a thickness of 0.1m). This cuboid has a fixed temperature of 200°C (T_1). A second cuboid (with identical physical dimensions) will be embedded at the top of the enclosure, i.e. at a distance of 1m from the bottom slab. This cuboid has a fixed temperature of 0°C (T_2). A plane of thermal symmetry is placed above the top cuboid to prevent any radiative loss through the top of the cuboid.

To ensure that only radiation heat transfer occurs within the solution domain, the CFD modelling solution is specified as being a conduction only solution, this eliminates convection effects. The default value of the conductivity of air at 20°C and 50% relative humidity is low enough, where conduction is negligible. This test case is modelled in steady state.
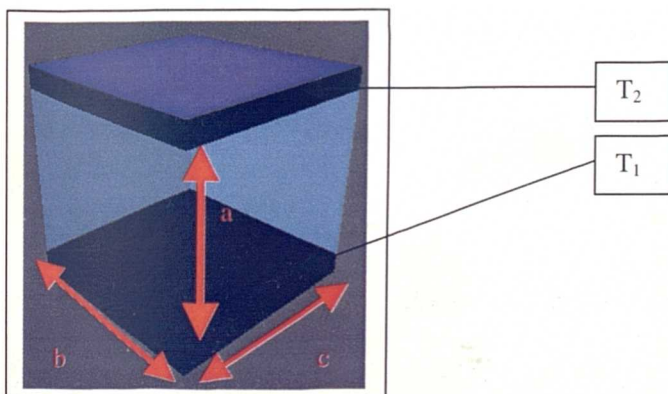

Fig. A4: Geometry of Radiation test as constructed within FLOVENT

A4.3 Analytic Calculations

Radiation for Cuboids at T_1 and T_2 both with an Emissivity of 1.0

Applying Equation A3: $Q = VF\varepsilon\sigma A(T_1^4 - T_2^4)$

$A = 1\text{m}^2$

$\sigma = 5.67 \times 10^{-8} \text{ W/m}^2\text{K}^4$

$VF = 0.1998$ rads

Let $T_1 = 200°C = 473.15\text{K}$

        $T_2 = 0°C = 273.15\text{K}$

$Q = 504.7\text{W}$

The software confirms that the temperature of the top cuboid is zero ($10^{-28}°C$). The radiation received by the top cuboid is 534.08W.

A4.4 Test Objective

To compare the theoretical calculations of heat transfer by radiation exchange, with the results obtained from the simple CFD model.

A4.5 Results and Conclusions

Radiation between solid objects can be modelled within FLOVENT. Discrepancies between the analytical and software calculations are caused by the method of calculating view factors. The software calculates the view factors using the Ray Tracing Method, which considers all geometries at various angles to one another. The analytical calculation is exact in calculating the view factor between two parallel plates.

A4.6 Conclusions

FLOVENT is predominantly used to simulate fluid flow. In order to model the dynamic thermal changes through a building envelope, heat transfer must be calculated through solid fabrics. The 'Basic Physical Processes' tests, Sections A1-A4, verified that conduction, convection and radiation can be successfully modelled through the fabric using CFD alone.

A5 Transient Ambient Conditions

A5.1 Introduction

One further hindrance towards dynamically modelling with CFD is the representation of ambients within transient solutions. The particular code used for this research contains an omission, whereby, an ambient setting can be directly specified within a steady state solution, but the same method setting can not be used to provide a time-varying setting within a transient scenario. Various methods have been tested in order to establish a solution that overcomes this particular obstacle and have been summarised in the table below.

Table A2: Summary of the tests carried out to develop a transient ambient solution

Section of Appendix A	Test Description
A5.2	Steady state case using standard ambient settings.
A5.3	Steady state case replacing the standard steady state ambient with fixed temperature cuboids
A5.4	Fixed temperature cuboids in a transient scenario
A5.5	Fixed temperature collapsed cuboids (i.e. containing no grid cells) in a transient scenario
A5.6	Fixed temperature collapsed cuboidal sources of thermal load in a transient scenario

Test A5.2 is identical to The Heat Conduction test reported in Section A2

A5.3 Replacement of Steady State Ambient Condition with Fixed Temperature Cuboids

A5.3.1 Introduction to Test Geometry

The model used in Section A5.2 (or the Heat conduction Test of Section A2) will be modified by replacing the ambient temperature setting on the X-Low face of the wall, with physical cuboids with fixed temperature settings and thermal resistances at steady state. Fixed temperature settings override all thermal characteristics of cuboids. The dimensions of the wall remain as $1m^3$ as in the test of Section A5.2. The results of this test will be compared to the results of Section A5.2.

In order to mimic the complete effect of a real external ambient condition, a resistance must be imposed onto the external surface of the wall. This resistance represents an external surface heat transfer coefficient of 12 W/m^2K. This resistance is also represented as a cuboid, with a fixed conductivity and notional thickness, and hence resistance, is placed in between the cuboid representing the ambient, and the wall slab. This sandwiched cuboid has no thickness, i.e. it contains no grid cells. Cuboids with no physical thickness (i.e. a cuboid containing no grid cells) will be regularly used in the development of future tests, and will be often referred to as a 'collapsed' cuboid. The CFD model of the wall (made from Brickwork (outer leaf)) contains grid cells with a maximum size of 0.1m in the X, Y and Z directions.

Summary of Ambient Construction using Cuboids:

1. The first cuboid has a fixed set temperature (at 0°C), and hence the material of the collapsed cuboid is irrelevant.
2. The second cuboid has been collapsed (contains no grid cells within its width) and is used to represent the heat transfer coefficient of the wall that is 12 W/m^2K.
3. The third cuboid is used to represent the actual wall of a typical building. Its X-High face is still exposed to an ambient condition of 10°C.

The model has been maintained as a 3-Dimensional model, but equivalent results can be achieved if the model is 2 or even 1-dimensional.

A5.3.2 Comparison of Results and Conclusions

The result of the heat transfer recorded through the wall on the CFD Model is 37.5W. This result is identical to the analytic solutions (Section A5.2.2) and also the results of the test conducted in Section A5.2. These results indicate that standard ambient settings can be simulated using a series of cuboids to mimic effects of temperature and surface heat transfer coefficients, at steady state.

A5.4 Parametric Tests of Transient Ambient Representation

A5.4.1 Collapsed Ambient Cuboids

This section contains parametric tests to try to find alternative solutions to attaching a transient ambient, without imposing additional grid cells onto the CFD model. The outermost cuboid of the series of cuboids, used to simulate a complete ambient condition requires grid cells within its thickness, which could prove to be computationally expensive during complex transient solutions. Various methods have been tested to observe the effects of collapsing this outermost cuboid.

The steady state tests which replaced standard ambient conditions with a series of cuboids conducted in Sections A5.2 and A5.3, was assumed to also be a successful ambient solution in a transient scenario. The following parametric tests, however, carried out in this section have highlighted a few 'bugs' in the software.

Firstly, a parametric test was conducted, whereby the outermost cuboid was also collapsed whilst still modelled as a fixed temperature block. Results of the tests indicated that within a transient scenario, collapsed cuboids, could not appropriately mimic fixed temperatures. The tests suggest that due to the non-existence of grid cells within the collapsed outermost cuboid (which should have provided a sinusoidal temperature variation), the transient temperature profile could not be applied or detected. This is because the collapsed cuboids are defined in the same place and the second cuboid overwrites the first.

This test demonstrated that a transient temperature profile can not be attached to a collapsed cuboid. The cuboid used to represent the external temperature must be uncollapsed within transient solutions.

A5.4.2 Replacing the Ambient Cuboid with a Collapsed thermal Source

The collapsed cuboid has been further replaced by a collapsed thermal source. A source within the CFD code is an 'invisible' thermal load, which can be placed within CFD models, or attached to objects. All other geometry remains identical to the two previous tests of Section A5.3 and A5.4.

The results of the tests should have been identical to transient tests conducted using cuboids with their own thickness'. This however, is not the case indicating that attaching a thermal source to the collapsed cuboidal thermal resistance, does not effectively simulate an ambient condition. From these tests, it would seem that the *most effective method of imposing a transient thermal sinusoidal* profile would be to apply a fixed temperature to an uncollapsed cuboid.

A6 Conclusions

The fundamental processes of thermal heat transfer, required to model dynamic thermal transfer through solids within Flovent have been verified. One further obstacle towards dynamically modelling ambient conditions within a transient scenario has also been firmly overcome. Replacing the standard ambient setting of a steady state case with a series of cuboids in a transient case, is an effective method of mimicking the effects of thermal fluctuations and surface heat transfer coefficients, to which an external wall would be typically exposed.

A7 Heat Capacity Test

A7.1 Model Description

A solid copper block (1m x 2m x 1m) is set to emit 10kW. The six faces of the solid cuboid are adiabatic, hence no heat fluxes occur across the cuboid faces. The cuboids initial conditions begin at 0kW and the time taken for the cuboid to heat up to its setting of 10kW is timed during this transient solution.
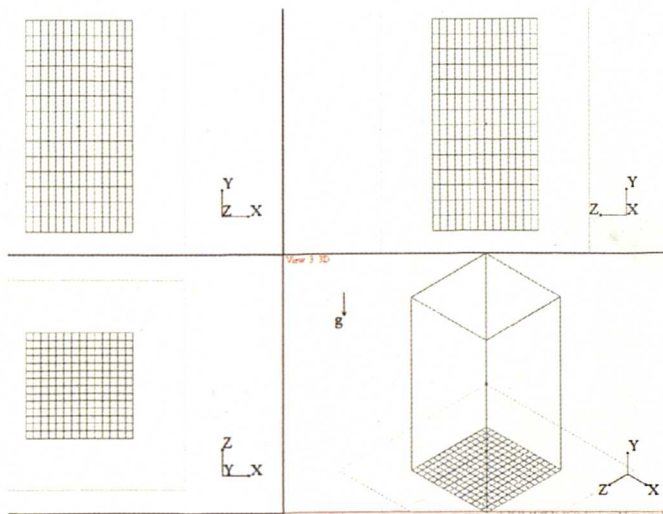
Fig A5: Cuboid including the configuration of the 3-Dimensional Grid

A7.2 Analytic Calculations of Conduction through a Solid Block

Thermal Properties of the Material:

Density of Copper ρ = 8900 Kg/m^3

Specific Heat Capacity of Copper, C_p = 418 J / Kg K

Volume of Copper Block, V = 2m^3

$$Q = \frac{C_p \rho V}{\Delta t} \text{ per 1°C in temperature rise.} \qquad \text{(A1)}$$

Q = Heat Input of Volume source = 10KW

$$100000 = \frac{418 \times 8900 \times 2}{\Delta t}$$

$\Delta t = 744$ seconds

A7.3 Test Objectives

The objectives of the test are to confirm that the analytic solutions of the rate at which the block heats up is identical to the rate of temperature increase recorded at center of gravity of the cuboidal block. Hence verifying that conduction can be accurately modelled using CFD.

A7.4 Results

The graph below, shows the increase in temperature of the cuboid, over time. As recorded at the centre of the solid block. It is evident that the block heats up by 1°C in 745 secs.
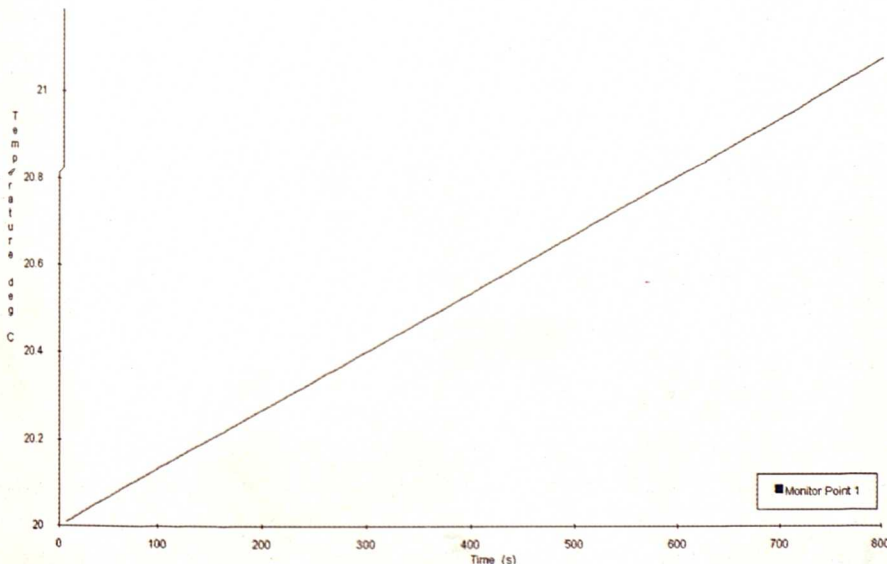
Fig. A6:   A graph to show Temperature (°C) over Time (s) as recorded at the single monitor point located within the solution domain).

A7.5 Conclusion

The theoretical calculation of the rate of temperature increase of the solid block is identical to the gradient of the graph of Temperature vs Time Profile produced in FLOVENT for the solid copper block (See Figure 4.3). Hence, conduction is accurately represented within FLOVENT.

APPENDIX B

Appendix B: Simulating a Transient Ambient Condition using Cuboids

B0 Introduction

Preliminary tests have established a new method for simulating time-varying ambient conditions. The new technique involves the use of a series of cuboids, to which the thermal characteristics of a typical ambient, such as thermal resistance due to surface heat transfer effects and temperature, are assigned.

Tests documented in this appendix develop further, the concept of modelling ambients using cuboids within a transient scenario. In order to provide a form of comparison for the results obtained in this test, the results will be compared to Admittance procedure calculations, outlined by CIBSE Guide A Section A3-21 (1986). Section A3-21 of CIBSE Guide A (1986) describes the procedure for calculating non-steady state thermal indexes, which are used to evaluate dynamic thermal heat transfer characteristics through building envelopes, as a result of the materials thermal properties. Definitions of the factors calculated and used in the Admittance Procedure are described in Section 3.2, Chapter 3.

Firstly, CIBSE Guide A (1986), approximates external ambient conditions as varying sinusoidally. As the external conditions (which vary sinusoidally) pass through the thermal resistance of the solid building material, the heat transferred will be thermally lagged and deflected. The amount by which the external ambient sinusoidal profile is deflected and delayed as it passes through the material can be mathematically determined. It is these analytic solutions, which will provide some form of comparison to the effects illustrated by the CFD simulations.

Table B1: Summary of the Tests conducted and documented in this Appendix

Test No.	Description
TRANSIENT THERMAL MODELLING THROUGH A SOLID INTERFACE	
B1	Transient Modelling of Conduction through a Solid – 1st Ambient cuboid is given a transient sinusoidal profile. 5 Tests are conducted, each using wall materials with different thermal characteristics. Qualitative comparisons made between CFD results and analytical solutions as advised from CIBSE Guide A (1986).
TRANSIENT THERMAL MODELLING THROUGH A SOLID-AIR INTERFACE	
B2	The solution domain of Test B1 is extended to include a thin slice of air containing a fixed flow device. This is a forced transient convection test.
TRANSIENT MODELLING WITHIN AN ENCLOSURE – PRELIMINARY TEST	
B3	Air space is extended, to resemble an enclosure. Temperatures and speeds of the air are collected at specific points within the room. The case is run as a steady state case.

Tests B1 - Transient Thermal Modelling Through a Solid Interface

B1.1 Introduction

Test B1 contains 5 transient tests, which examine the effect of heat transfer through 5 different materials with different thermal characteristics (see Table B2). The thermal characteristics of each of the five materials have been derived by the manipulation of the thermal characteristics of the base case materials of Brickwork (outer leaf). The external ambient has been represented as a combination of two cuboids. This sinusoidal ambient temperature profile will penetrate through each of the 5 materials tested, but will inevitably be deflected by a phase lag and deflection, due to the resistance of the material and the effect of surface heat transfer coefficients. The phase lag and deflection is specific for each material and these values have been analytically calculated using the admittance procedure, the full calculations are located in Section B7.

B1.2 Test Description

A base case test (Test B1(i)) is constructed first. The geometry of Test B1(i), consists of a simple brickwork (outer layer) wall slab, the thermal characteristics of the material have been listed in Table B2. The dimensions of the wall slab are 220mm wide (x-direction) and 1m in the both the y and Z dimensions.

The cuboid, acting as an external ambient, is superimposed onto the outermost face of the external wall slab. The outermost face of the external cuboid (X-Low face) is adiabatic, hence any heat transfer is directly into the adjacent wall slab. This cuboid representing an ambient, has a fixed transient thermal profile, the thickness of the cuboid is therefore irrelevant. The temperature of the cuboid representing the ambient, varies between -10°C and 10°C, over a period of 24 hours.

A third cuboid is sandwiched between the 'external ambient' cuboid and the wall slab. This third cuboid represents the surface heat transfer coefficient ($10W/m^2K$) and has no thickness, i.e. it is 'collapsed' and therefore contains no grid cells.

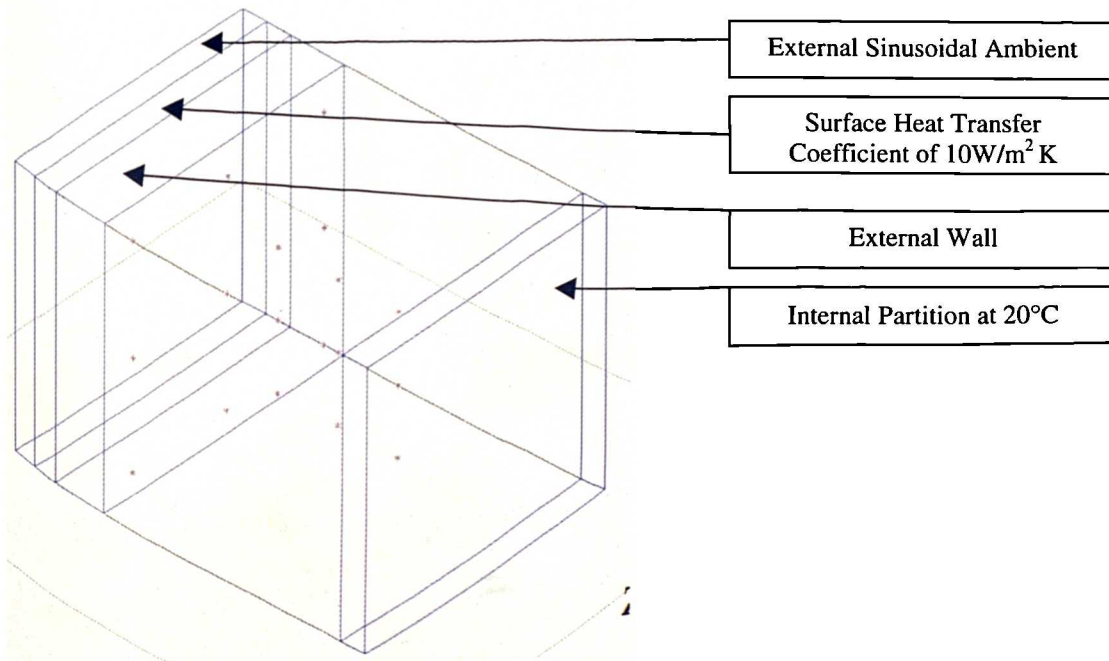|	
External Sinusoidal Ambient	
Surface Heat Transfer Coefficient of $10W/m^2 K$	
External Wall	
Internal Partition at 20°C	

Fig B1: Geometry of Test B1

Every free surface in the CFD model has been specifically modelled so that heat can not be transferred across them. The wall opposite the external wall slab, acts as an internal partition, and has a fixed temperature of 30°C. This represents a typical constant internal room temperature.

Table B2: Thermal characteristics of the materials to be tested in Test B1

Test No.	Thickness (mm)	Thermal Conductivity (W/mK)	Density (kg/m³)	Specific Heat Capacity (J/kgK)	Phase Lag (h)
B1(i)	220	0.84	1700	800	5.64
B1(ii)	220	1.68	1700	800	5.33
B1(iii)	220	0.84	850	800	3.81
B1(iv)	220	0.84	1700	400	3.81
B1(v)	110	0.84	1700	800	2.96

22 Grid cells are embedded into the wall slab, whose wall thicknesses are 220mm. Hence, the temperature at 22 grid cell centres across the wall's surface area are calculated and recorded. The maximum grid cell size in the X, Y and Z directions is 0.1m. In the case of Test No. B1(v), the maximum grid cell size is also 0.1m in the X, Y, and Z directions, but due to the thickness of the materials, only contains 11 grid cells.

The sinusoidal external temperature profile has a period of 1 day (86400 seconds), but the total solution period is five days, hence the sinusoidal profile will repeat itself five times. The transient grid is very detailed, where each transient grid cell to 6 minutes long. The start and finish times of the transient thermal profile are tabulated in Table B3.

Table B3:   *Start Time and Finish Times of the Transient Thermal Profile*
             over 5 days solving

Transient Profile Name	Start Time	Finish Time
Sinusoid Day 1	0	86400
Sinusoid Day 2	86400	172800
Sinusoid Day 3	172800	259200
Sinusoid Day 4	259200	345600
Sinusoid Day 5	345600	432000

B1.3 Test Objective

To establish qualitatively and quantitatively whether the phase lag of the external sinusoidal temperature profile in the CFD model corresponds to the phase lag determined using the Admittance Procedure, specified by CIBSE (1986).

B1.4 Results

The results from the CFD calculations and admittance method calculations are shown in Table B4. Table B4 shows the phase lags of the external sinusoidal transient thermal profile obtained from both the CFD solutions and admittance method calculations, for the series of 5 tests of Test B1.

From the results, it would appear that a combination of two cuboids, each with assigned thermal characteristics can act as an ambient setting. The transient external sinusoidal thermal profile has been deflected and lagged, as a result of the thermal resistance of the wall. The magnitudes of the phase lags of the CFD results are of the correct magnitude compared to the CIBSE Guide A Admittance Method (1986).

The CFD results of phase lags of the external sinusoidal thermal profiles for the different tests have been determined as the length of time in between the peak in external ambient temperature and the corresponding peak in temperature located at the 22nd grid cell, i.e. the grid cell within the wall, near to it's inside surface, see

Figure B2. Four peaks were identified both in the external ambient temperatures and the temperatures within the wall, and the time differences four the four peaks were averaged, see Table B4.

Table B4:   Comparison of phase lags provided by the CFD results as compared with the Admittance Procedure calculations.

Test No.	Av. Phase Lag from CFD Sol^n	Phase Lag from Admittance Procedure	% Error
B1(i)	6.8	5.67	19.9
B1(ii)	5.5	5.33	3.2
B1(iii)	4.5	3.81	18.1
B1(iv)	4.5	3.81	18.1
B1(v)	3.8	2.96	28.4

B1.4 Discussion

The CIBSE (1986) Admittance Procedure is a heavily simplified procedure, which is pragmatically satisfactory for the application for which it was designed, Davies (2001). The Admittance Procedure does, however, contain serious flaws, Davies (2001) and is likely to be a source of the discrepancy between the CFD results and the analytical solution. The crude method used to determine the phase lag of the CFD models is also an additional source of error, especially since an average value was taken, despite not all materials reaching stability during the transient solution.

Some of the materials used in these tests were still unaccustomed to the fluctuating thermal conditions. Some materials would not have reached steady state within the five days of transient solving. Figure B2 illustrates the time taken for the data recording points to record temperatures that have become stable, since at the beginning of the transient period, the temperatures are adjusting to the initial conditions of the sinusoidal external ambient.

-

Another major cause of error may also be due to the location within the CFD model, from which the results for temperature are taken. The CFD results for temperature are taken at the centre of the last grid cell within the wall. These CFD results are being compared to the analytical solutions, but the analytical solutions provide analysis for the air immediately adjacent to the wall. Hence the CFD results do not account for the additional resistance due to the half grid cell of thermal mass of the wall, and the surface heat transfer coefficient on the inside surface of the internal wall.

Test 3.2_air_1.68
TEMPERATURES RECORDED AT MONITORING POINTS Vs TIME
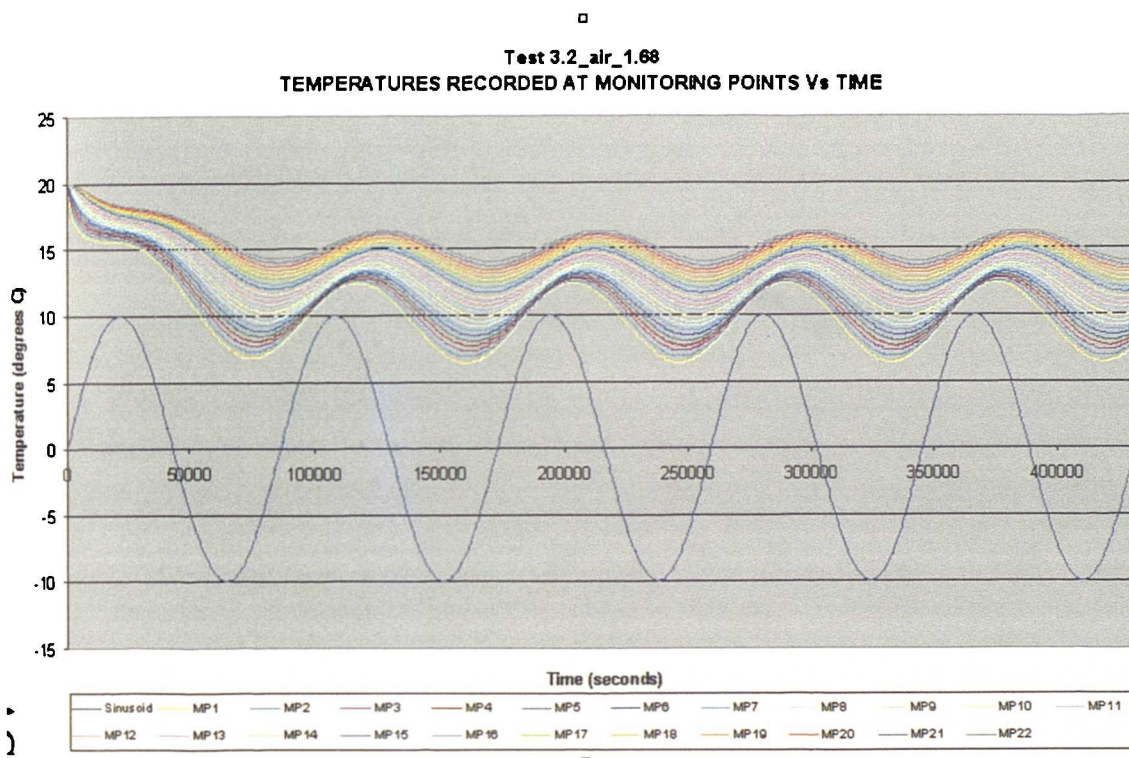
Fig B2:   Temperatures recorded at the 2 MPs using Brickwork (outer leaf) as the wall slab

The thermal characteristics of the base case material (brickwork) of Test B1(i), were changed by various factors in subsequent tests. So, in Test B1(ii), for example, the thermal conductivity of the base case material was doubled. The % errors for the phase lags also decreased as a result. The most significant cause of this effect was likely to be due to the way in which the CFD phase lag results were collected. For the high conductivity materials, the thermal response to the external sinusoidal ambient

was likely to stablise much more quickly than the materials with a higher thermal mass.

In Test B1(iii) and B1(iv), heat is not lagged within the material, because the materials' heat capacities are lower in both cases. Hence, any heat transferred from the external sinusoidal ambient is not trapped within the material i.e. will be transferred to the air adjacent to the internal surface of the wall. This air is not represented in the CFD model, which may account for the higher % errors between the admittance procedure and CFD results.

A profile of the development of the phase lag within the brickwork (Test No. B1(i)) was effectively compared with detailed manual calculations of phase lags in every grid cell centre of the materials thickness, accordance to CIBSE Guide A (1986). This study showed that the phase lags through the material increased fairly linearly, but tended towards the internal surface, to approximately the value provided by CIBSE Guide A (1986), of 5.7 hours. (See Fig B3).
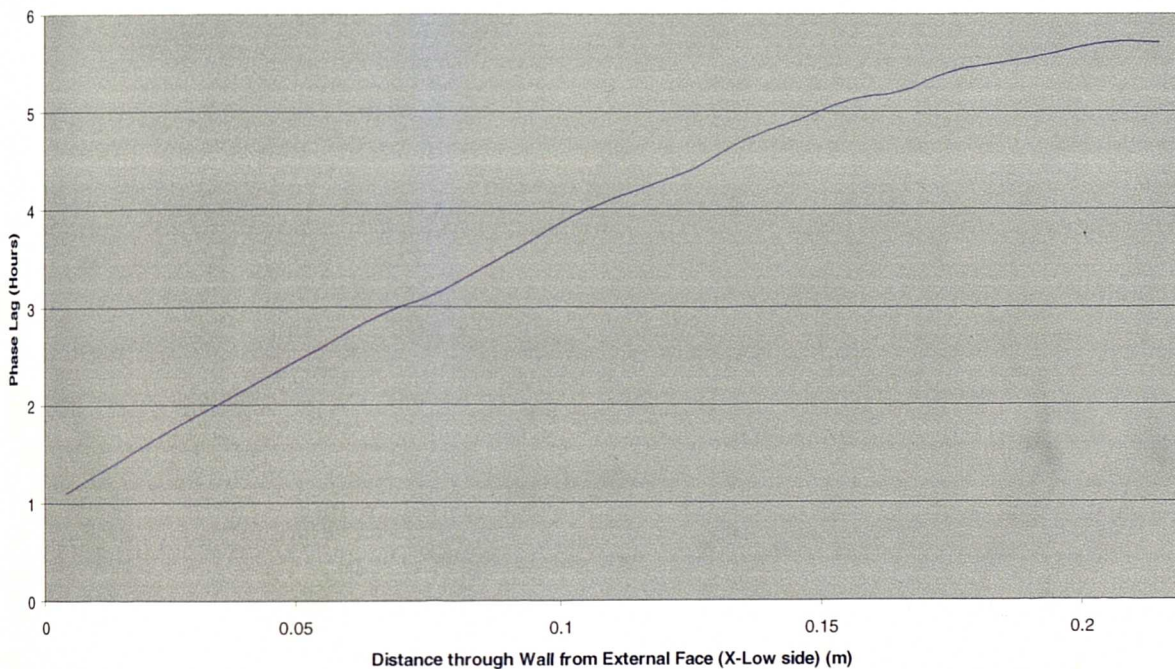

Fig B3: Phase Lag through the wall as recorded at each monitoring point within the wall, recorded at time 367200s

B1.5 Conclusions

The Admittance Procedure was chosen as an appropriate comparison to steady cyclic representation of external ambient within a CFD model. A brick wall was exposed to ambient conditions, which was successfully represented by a series of cuboids.

Despite the identification of a number of sources of error in the comparisons made, the order of magnitude of the phase lag of the external ambient sinusoidal thermal profile were close to their equivalent analytical solutions as outlined by CIBSE Guide A for the Admittance Procedure (1986).

The % errors obtained are largely caused by dissimilarity between the geometry of the analytical solutions and CFD results. The CFD results are obtained from data recorded at the centre of a grid cell, located just on the inside surface of the wall while the analytical solution is calculated for the air adjacent to the inside surface of the wall. This dissimilarity will be rectified in the following section.

B2 TRANSIENT THERMAL MODELLING THROUGH A SOLID-AIR INTERFACE

Test B2 - Comparison of deflection of Sinusoidal Ambient Thermal Profile with CIBSE Guide A Admittance Procedure (1986)

B3.1 Introduction

Tests B1 concluded that FLOVENT is able to account for the dynamic thermal changes across the building fabric. Phase lags of the external sinusoid, caused by through the thermal resistance of the wall correlate with the analytical solutions, as specified by CIBSE Guide A Admittance Procedure (1986).

Another parameter calculated by the Admittance Procedure is the ratio of deflection of the amplitude of the external sinusoid as it passes through the material. The CFD model of Test B1 modelled solid materials only, under transient conditions. The results of the tests gave good similarities between the CFD and Admittance Procedure calculations of the phase lag of the external ambient. Deflections of the external ambient could not, however, be well represented, without the effects of air on the internal face of the wall. Hence, the comparison of the deflection of the external ambient were reserved to Test B2, in which air was added to the CFD model of Test B1.

This test will examine the heat transfer through a solid and introduce an adjoining air interface onto the inside surface of the wall. The tests have been developed from the Second 'Basic Processes' Test (located in Appendix A, section A3), that proved that FLOVENT can accurately simulate forced convection. The 2nd Basic Processes Test has been developed (in this test, Test B2) to include a transient external ambient profile, instead of a case in steady state, with a constant ambient setting.

B2.2 Test Model Geometry

The geometry consists of 3 cuboids sandwiched together, every cuboid has a Y-dimension of 1m and a Z-dimension of 1m. The first cuboid in the series has a X-dimension of 0.1m (the thickness of 1 grid cell, in the X-direction). This cuboid has no material attached but has a transient external sinusoidal profile, which varies between 10°C and -10°C, over a period of 24 hours. Over the 24 hours, the wall fabric will create a cooling effect, for the air passing over it from the fixed flow device. The second cuboid in the series has no X-dimension, i.e. it contains no grid cells. The purpose of this cuboid is to provide a resistance, equivalent to a surface heat transfer coefficient of $10W/m^2K$. The third cuboid in the series has an X-dimension of 0.22m. This cuboid represents a wall made from Brickwork (outerleaf) (0.22m x 1m x 1m). This wall contains 22 grid cells, in the X-direction, with a width of 0.1m. The grid cell sizes in the Y and Z dimensions are also 0.1m.

Adjacent to the inside surface of the wall, (X-high side) is an air space, 0.1m wide. At the base of the airspace (at Y=0) is a fixed flow device (with dimensions X=0.1m and Z=1m), which is blowing air in a vertical direction, i.e. Y-direction at a rate of 0.1 l/s. This supply air from the fixed flow, enters the airspace at 20°C and is travelling towards an ambient temperature sink of 0°C at Y=1m. (See Fig. B4 below).
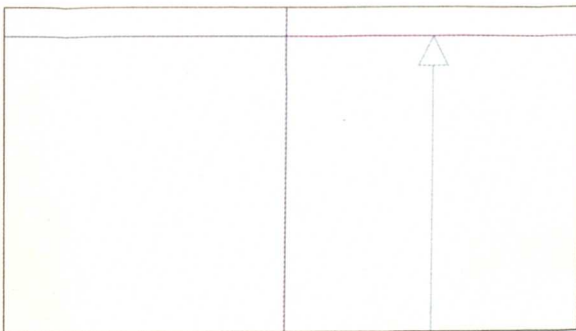

Fig. B4: Geometry of Test B3

To ignore the effects of buoyancy, gravity has been switched off. There is only 1 grid cell within the airspace (along the X-Axis), with dimensions of 0.1m.

B2.3 Test Objectives

To confirm the estimate of deflection, provided by CIBSE Guide A Admittance Procedure (1986), of the transient external sinusoidal thermal profile, by obtaining the temperature profile of an air gap immediately adjacent to a wall.

B2.4 Results and Discussions

The temperature of the air was recorded at the centre of the airspace. These temperatures were plotted against the external ambient sine wave. The deflection of the external sinusoidal ambient thermal profile was obtained from the CFD results (See Fig B5). The comparisons show that the deflection of the external sinusoid is approximately 0.43, and the admittance procedure from CIBSE is 0.5, indicating a good correlation with analytical solutions.
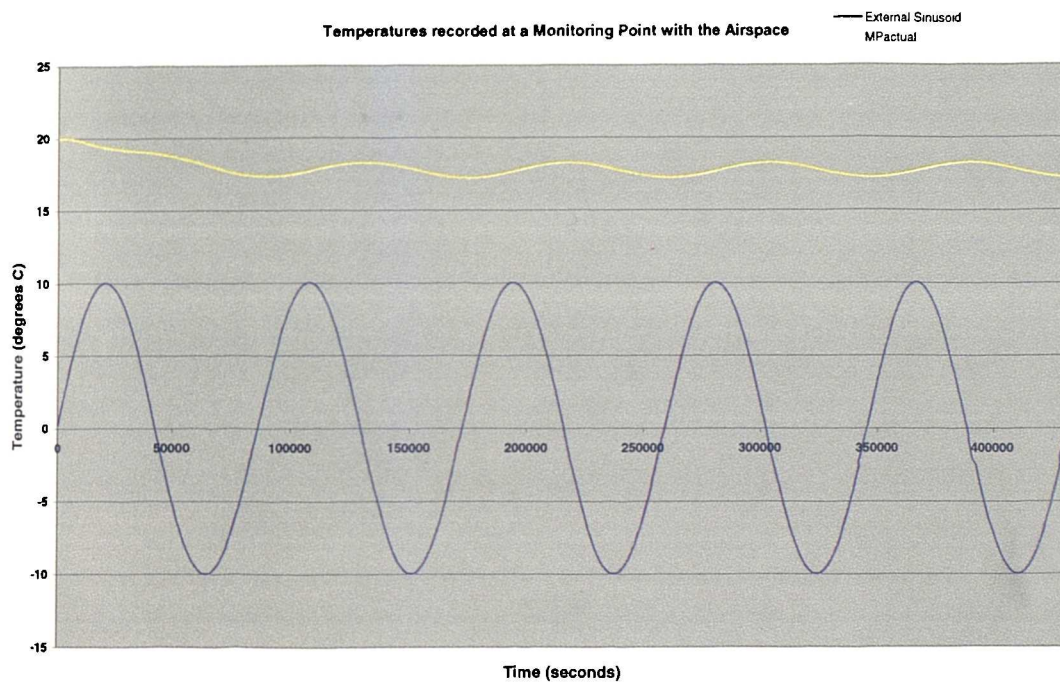

Figure B5: Graph of Temperatures recorded at a Monitoring Point located within the airspace

The visualisation plane shown in Fig B6, indicates that there is some temperature variation within the airspace, despite measures to avoid this, by switching buoyancy

off and only placing one grid cell within the airspace. The monitor point location is subject to significant temperature variation, due to the cold surface ambient of 0°C at the Y-high surface of the geometry.
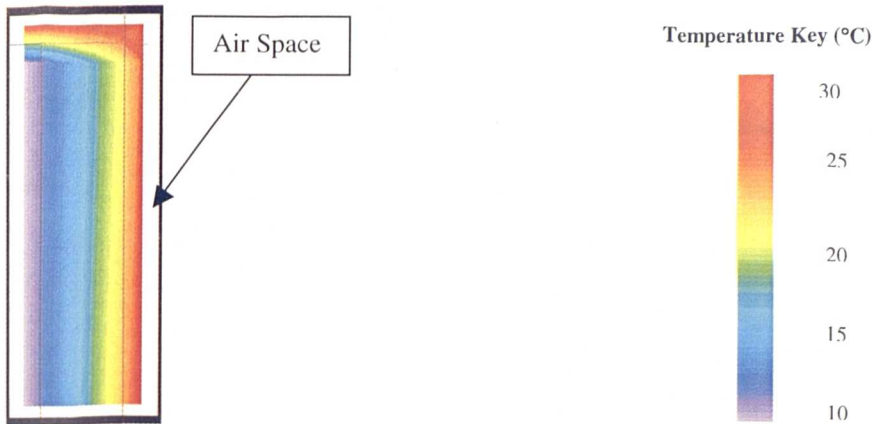

Fig: B6 Z-Plane Visualisation of the Temperature Results

B2.5 Conclusions

This test has successfully demonstrated that a solid-air interface can be modelled in FLOVENT. This result was reached through comparing the temperatures recorded at the centre of an airspace *adjacent to the inside surface of a wall. The wall was* subjected to external sinusoidal temperature variations. Analytical solutions for the deflection of the external sinusoidal temperature profiles through the building fabric (following the admittance procedure of CIBSE Guide A (1986)) was compared to the CFD results of temperature within the air adjacent to the wall. The comparisons are satisfactory.

B3 DEVELOPMENT OF SOLID-AIR MODELLING OF AN ENCLOSURE

Test B3 – Transient Modelling of an Enclosure with a Sinusoidal External Ambient

B3.1 Introduction

The results of Tests B1-B2 have shown that the phase lag and deflection correspond to the admittance procedure calculations from CIBSE Guide A (1986). The geometry of Test B2 is further developed in this test, Test B4, to include a larger air space with dimensions of 1m x 1m x 1m.

B3.2 Test Description

This test case will initially be run as a steady state case to observe the effects of the combination of a cooling wall (Y-Z Plane, at X=0m) and a heated wall (Y-Z Plane, at X=1m) within the enclosure. The series of two cuboids, representing an ambient temperature and surface heat transfer coefficient, respectively, remains exactly the same as in Test B1. The transient external sinusoidal profile of the first cuboid, will be replaced by a constant temperature of 0°C, since this test runs at steady state.

To encase the enclosure air, additional cuboids have been placed on all 5 remaining sides of the cuboid shaped geometry, see Figure B7. The cuboids located at the X-Z planes at Y=0m and Y=1m and the Y-X Plane at Z=0m and Z=1m have no thickness, i.e. they contain no grid cells. They also, do not have any thermal profiles and material characteristics. The cuboids make no contribution to the thermal effect within the room, and their surfaces are adiabatic.

The cuboid in the Y-Z plane at X=1m, acts as a heated wall and has a fixed temperature of 30°C, this cuboid has a thickness of 0.1m. The thickness and material specification of the cuboid is insignificant, since it has a fixed temperature (which represents an internal ambient).

The effects of gravity are considered in this test. Grid has been assigned to the air space, where the maximum grid cell size is 0.1 x 0.1m. The model is in 2-Dimensions.
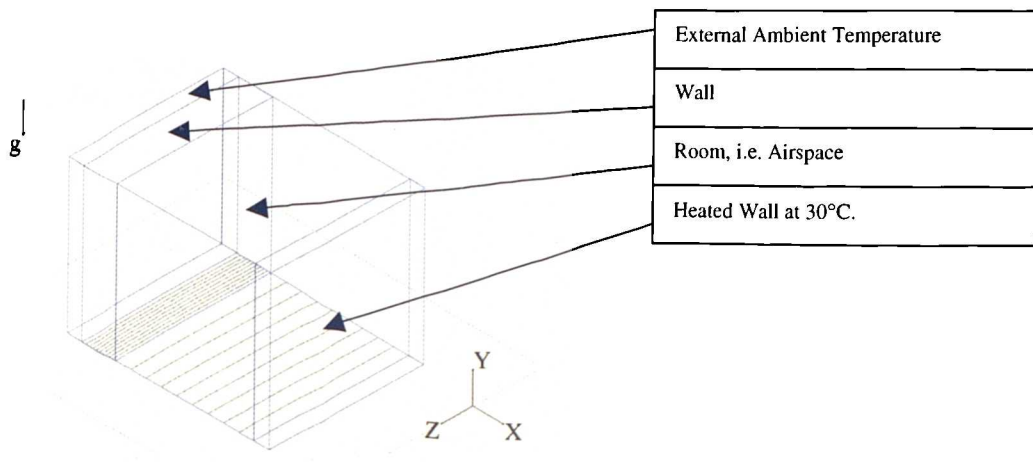

Fig B7: Geometry of Test B4

B3.3 Test Objective

To observe the heat transfer effects within a small enclosure, which contains a heated wall and cooling wall.

B3.4 Results and Discussion

With one wall acting as a heater, and the external wall acting as a cooler, a circulation pattern within the room was anti-clockwise. The results showed the effect of the cool external air from outside providing a temperature difference to the heated wall of the room, as shown in Fig. B8. The vector plot shows the circulation of the air, as illustrated in Fig. B9.

Temperature (°C)

30

25

20

15

10

Velocity (m/s)

0.04

0.03

0.02

0.01

0
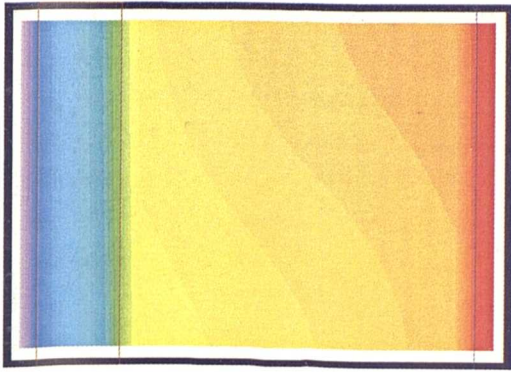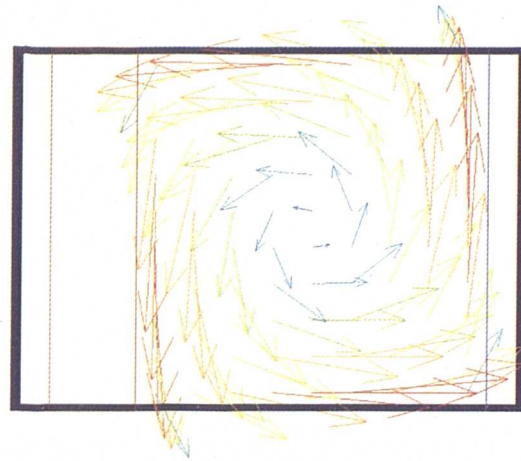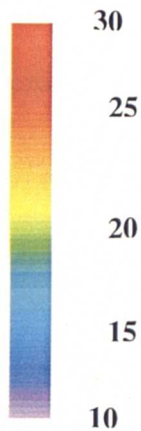
Fig. B9: Steady state temperature profile of Test B3

Fig. B9: Steady state velocity profile of Test B3

B3.5 Conclusions

The results of air flow patterns obtained within the enclosure in the steady state case were as expected, and hence the model of Test B3 can be developed into a transient scenario, where the external temperature has a sinusoidal temperature variation.

B4 DEVELOPMENT OF SOLID-AIR TRANSIENT MODELLING OF AN ENCLOSURE

Test B4 - Modelling an Enclosure under transient conditions

B4.1 Introduction

Test B3 was run under steady state conditions, but to dynamically model within CFD, a transient scenario must be constructed. Transient modelling is most fundamental to dynamically modelling buildings within a CFD package, to be able to simulate changing thermal conditions over time. Hence Test B3 will be further developed to simulate under transient conditions. The results of this transient case will eventually be used as referenced data, for comparison with results from dynamic thermal modelling procedures (to be developed in Chapter 3).

B4.2 Test Geometry

The physical geometry of the test case will remain identical to Test B3 (see section B3), this test case, however, is now set to simulate under transient conditions, and hence has a transient ambient temperature profile. An external wall in the Y-Z Plane where X=0m, is exposed to this ambient thermal setting. The ambient profile varies sinusoidally over 24 hours, varying between 10°C and -10°C. This wall will still cool the room, but by varying degrees over the 24 hours.

The entire transient solving time of this test will last for 5 days. The first four days provides ample time for the enclosure to become accustomed to the sinusoidal variation. The four days can be regarded as some form of pre-heat time for the enclosure.

On the fifth day of solving, the transient solution period will be manually interrupted every four hours. The air flow pattern (temperature and speeds) within the room will be recorded at a series of points, located in the airspace, as shown in Table B5.

Table B5: Monitor Point locations within the enclosure of Test B4.

Monitor Point	X-Coordinate	Y-Coordinate	Z-Coordinate
1	0.47	0.1	0.5
2	0.77	0.1	0.5
3	1.07	0.1	0.5
4	0.47	0.3	0.5
5	0.77	0.3	0.5
6	1.07	0.3	0.5
7	0.47	0.5	0.5
8	0.77	0.5	0.5
9	1.07	0.5	0.5
10	0.47	0.7	0.5
11	0.77	0.7	0.5
12	1.07	0.7	0.5
13	0.47	0.9	0.5
14	0.77	0.9	0.5
15	1.07	0.9	0.5

Six frames (due to stopping the solution every four hours) of the thermal conditions of temperature and velocity will be captured during the fifth day in the solution period. The times at which the data is recorded are shown in Table B6.

Table B6: Transient Grid Solution Periods (Finish Times), Day 1

Transient Solution Period	End Time of Solution Period (s)
To 4 Days (pre-conditioning)	345600
Frame 1	360000
Frame 2	374400
Frame 3	388800
Frame 4	403200
Frame 5	417600
Frame 6	432000

Table B7: Transient Grid Solution Periods for Test 3A (Finish Times), Day 2

Transient Solution Period	End Time of Solution Period (s)
End of Fifth Day	432000
Frame 1	446400
Frame 2	460800
Frame 3	475200
Frame 4	489600
Frame 5	504000
Frame 6	518400

B4.3 Results and Discussion

As expected, the velocity plots display similar anticlockwise circular patterns of airflow with the room, as observed in Test B3, see Figure B9 and B10. The magnitudes of the vectors do not seem to be significantly changing, despite the varying degrees of cooling at the external wall, as a result of the sinusoidal variation.

B4.4 Conclusions

A record has now been kept of the temperature and velocities every 4th hour of the fifth day. These results will act as reference data for the following tests. The

following tests in the next chapter will be conducted to establish a provisional dynamic thermal modelling procedure.

B5 Summary of Conclusions

Research has been carried out in this chapter in order to firmly establish how enclosures (including solids and air) may be modelled within CFD under transient conditions. Simple steady state CFD models of solid materials have been successfully tested for their ability to conduct and then have been further developed into larger enclosures, which include air in a transient scenario.

The results of most transient tests have been largely compared to the analytic procedures outlined by CIBSE Guide A, which provide an indication of the extent to which transient ambient conditions are deflected and lagged by the thermal resistance of building materials. CFD results of phase lags and deflections of the ambient sinusoidal thermal profile compare well with the analytic solutions provided by CIBSE Guide A.

The test conducted in this Appendix, formed part of the preparatory work in order to collect data with which to compare the results of a preliminary dynamic thermal modelling procedure. The initial results of the procedure contained in Chapter 3, section 3.4, will be compared to the results obtained in Test B5 of this appendix.

B6 CIBSE CALCULATIONS - DECREMENT FACTORS AND SINUSOIDAL TIME LAG

The temperature distribution in a homogenous slab subject to one-dimensional heat flow is given by the diffusion equation:

$$\frac{\partial^2 t}{\partial x^2} = \frac{\rho c \partial t}{\lambda \partial \theta}$$

where:

t = temperature	°C
x = x-direction (perpendicular to surface of slab)	m
ρ = density	Kg/m³
c = specific heat capacity	J/KgK
λ = thermal conductivity	W/mK
θ = time	s

For finite slabs and for sinusoidal temperature variations the temperature variations, the temperature and energy cycles can be linked by the use of matrix algebra:

$$\begin{bmatrix} t_1 \\ q_1 \end{bmatrix} = \begin{bmatrix} m_1 & m_2 \\ m_3 & m_1 \end{bmatrix} \begin{bmatrix} t_2 \\ q_2 \end{bmatrix}$$

where

q = heat flow   W

For a slab of homogeneous material, the coefficients of the matrix are given by:

$$m_1 = \cosh(p + ip)$$

$$m_2 = \frac{l \sinh(p + ip)}{\lambda(p + ip)}$$

$$m_3 = \frac{\lambda(P + ip)\sinh(p + ip)}{l}$$

and for a 24 hour cycle:

$$p = \left(\frac{\pi l^2 \rho c}{86400\lambda} \right)^{0.5}$$

For an air gap, or a surface resistance between a layer and the air, where the diffusivity ($=\lambda/\rho c$) is high, the coefficients of the matrix are given by:

$m_1 = 1$
$m_2 = R_a$ or R_s

$m_3 = 0$

Clearly, for a composite wall, the matrices of each of the layers can be multiplied together to give the relation between inside and outside as:

$$\begin{bmatrix} t_i \\ q_i \end{bmatrix} = \begin{bmatrix} 1 & R_{si} \\ 0 & 1 \end{bmatrix} \begin{bmatrix} m_1 & m_2 \\ m_3 & m_1 \end{bmatrix} \begin{bmatrix} n_1 & n_2 \\ n_3 & n_1 \end{bmatrix} \cdots \begin{bmatrix} 1 & R_{so} \\ 0 & 1 \end{bmatrix} \begin{bmatrix} t_0 \\ q_0 \end{bmatrix}$$

which can be written as:

$$\begin{bmatrix} t_i \\ q_i \end{bmatrix} = \begin{bmatrix} M_1 & M_2 \\ M_3 & M_4 \end{bmatrix} \begin{bmatrix} t_o \\ q_o \end{bmatrix}$$

The non-steady-state parameters are defined as:

Admittance:

$$Y_c = \frac{M_4}{M_2}$$

$$Y = |Y_c|$$

$$\omega = \frac{12}{\pi} \arctan\left(\frac{\text{Im}(Y_c)}{\text{Re}(Y_c)} \right)$$

The arctangent should be evaluated in the range 0 to π radians, thus ω is a time lead.

Decrement Factor

$$f_c = \frac{1}{UM_2}$$

$$f = |f_c|$$

$$\phi = \frac{12}{\pi} \arctan\left(\frac{\text{Im}(f_c)}{\text{Re}(f_c)} \right)$$

The arctangent should be evaluated in the range $-\pi$ to 0 radians. Thus ϕ is a time lag:

To find the surface Factor:

$$F_C = 1 - R_{si}Y_C$$

$$F = |F_C|$$

$$\psi = \frac{12}{\pi}\arctan\left(\frac{\text{Im}(F_C)}{\text{Re}(F_C)}\right)$$

DECREMENT FACTORS FOR THE INDIVIDUAL MATERIALS:

Material B1(i) – Base Case Material: - Brickwork (Outerleaf)

The properties of the brick are:

$\rho = 1700$ Kg/m^3
$\lambda = 0.84$ W/m K
$c = 800$ J/Kg K

Thickness of the material = 220mm

Internal Surface Heat Transfer Coefficient = 0.1 W/m^{2}K
External Surface Heat Transfer Coefficient = 0.1 W/m^{2}K

The U-Value is:

$$U = \frac{1}{0.1 + \dfrac{0.22}{0.84} + 0.1}$$

$$= 2.16 W / m^2 K$$

p = 1.688

For manual calculations, it is convenient to express cosh(p+ip) and sinh (p+ip) in terms of functions sin p, cos p and e^p which are available on most slide rules, pocket calculators and books of tables:

$$\cosh(p + ip) = \frac{1}{2}\left[(e^p + e^{-p})\cos p + i(e^p - e^{-p})\sin p\right]$$

$$\sinh(p + ip) = \frac{1}{2}\left[(e^p - e^{-p})\cos p + i(e^p + e^{-p})\sin p\right]$$

In the Matrix, the coefficient m_1, is given by the equation shown above, while m_2 and m_3 are given by:

$$m_2 = \frac{l\left[\left(e^p - e^{-p}\right)\cos p + \left(e^p + e^{-p}\right)\sin p - i\left(e^p - e^{-p}\right)\cos p + i\left(e^p - e^{-p}\right)\sin p\right]}{4\lambda p}$$

$$m_3 = \frac{\lambda p\left[\left(e^p - e^{-p}\right)\cos p - \left(e^p + e^{-p}\right)\sin p + i\left(e^p - e^{-p}\right)\cos p + i\left(e^p + e^{-p}\right)\sin p\right]}{2l}$$

which gives the matrix as:

$$\begin{bmatrix} -0.33 + i2.59 & 0.19 + i0.239 \\ -19.9 + i15.9 & -0.33 + i2.59 \end{bmatrix}$$

Performing the matrix multiplication from left to right (which corresponds to inside to outside):

$$\begin{bmatrix} 1 & 0.1 \\ 0 & 1 \end{bmatrix} \times \begin{bmatrix} -0.33 + i2.59 & 0.19 + i0.239 \\ -19.9 + i15.9 & -0.33 + i2.59 \end{bmatrix}$$

$$= \begin{bmatrix} (-0.33 + i2.59) + (-1.99 + i1.59) & (0.19 + i0.239) + (-0.033 + i0.259) \\ -19.9 + i15.9 & -0.33 + i2.59 \end{bmatrix}$$

$$= \begin{bmatrix} -2.32 + i4.18 & 0.157 + i0.498 \\ -19.9 + i15.9 & -0.33 + 2.59 \end{bmatrix}$$

The second stage only requires the evaluation of the right-hand column of the product matrix as only M_2 and M_4 are required:

$$\begin{bmatrix} -2.32 + i4.18 & 0.157 + i0.498 \\ -19.9 + i15.9 & -0.33 + i2.59 \end{bmatrix}\begin{bmatrix} 1 & 0.1 \\ 0 & 1 \end{bmatrix} = \begin{bmatrix} * & (-0.232 + i0.418) + (0.157 + i0.498) \\ * & (-1.99 + i1.59) + (-0.33 + i2.59) \end{bmatrix}$$

$$= \begin{bmatrix} * & -0.075 + i0.916 \\ * & -2.32 + i4.18 \end{bmatrix}$$

From the equation to calculate the Admittance Factor:

$$Y_c = \frac{-2.32 + i4.18}{-0.075 + i0.916} = \frac{(-2.32 + i4.18)(-0.075 - i0.916)}{0.075^2 + 0.916^2}$$

$$= [0.174 + 3.833 + i(2.127 - 0.3135)] / 0.8465$$

$$= 4.734 + i2.142$$

$$Y = \sqrt{4.734^2 + 2.142^2} = 5.20$$

$$\omega = \frac{12}{\pi} \arctan\left(\frac{Im(2.142)}{Re(4.734)}\right)$$

$$= 1.623h$$

Using the equation to calculate the Decrement Factor:

$$f_c = \frac{1}{2.16(-0.075 + i0.917))} = \frac{(-0.075 - i0.917)}{2.16(0.075^2 + 0.917^2)} = -0.041 - i0.502$$

$$f = 0.503$$

$$\phi = \frac{12}{\pi} \arctan\left(\frac{Im(0.502)}{Re(0.041)}\right)$$

$$= 5.69h$$

To find the surface factor:

$$F_C = 1 - 0.1(4.734 + 2.142i)$$
$$= 1 - (0.4734 + 0.214i)$$
$$= 0.5266 - 0.214i$$

$$F = |0.599 - 0.214i|$$
$$= 0.568 \, jj$$

$$\psi = \frac{12}{\pi} \arctan\left(\frac{0.214}{0.599}\right)$$
$$= 1.311$$

Material B1(ii) – Thermal conductivity is increased by a factor of 2

The properties of the brick are:

ρ = 1700 Kg/m^3
λ = 1.68 W/m K
c = 800 J/Kg K

Thickness of the material is 220mm.

Internal Surface Heat Transfer Coefficient = 0.1 W/m^{2}K
External Surface Heat Transfer Coefficient = 0.1 W/m^{2}K

The U-Value is:

$$U = \frac{1}{0.1 + \dfrac{0.22}{0.84} + 0.1}$$
$$= 1.68 W / m^2 K$$

p = 1.194

For manual calculations, it is convenient to express cosh (p+ip) and sinh (p+ip) in terms of functions sin p, cos p and e^p which are available on most slide rules, pocket calculators and books of tables:

$$\cosh(p + ip) = \frac{1}{2}\left[(e^p + e^{-p})\cos p + i(e^p - e^{-p})\sin p\right]$$

$$\sinh(p + ip) = \frac{1}{2}\left[(e^p - e^{-p})\cos p + i(e^p + e^{-p})\sin p\right]$$

In the Matrix, the coefficient m_1, is given by the equation shown above, while m_2 and m_3 are given by:

$$m_2 = \frac{l\left[\left(e^p - e^{-p}\right)\cos p + \left(e^p + e^{-p}\right)\sin p - i\left(e^p - e^{-p}\right)\cos p + i\left(e^p - e^{-p}\right)\sin p\right]}{4\lambda p}$$

$$m_3 = \frac{\lambda p\left[\left(e^p - e^{-p}\right)\cos p - \left(e^p + e^{-p}\right)\sin p + i\left(e^p - e^{-p}\right)\cos p + i\left(e^p + e^{-p}\right)\sin p\right]}{2l}$$

which gives the matrix as:

$$\begin{bmatrix} 0.66 + i1.39 & 0.122 + i0.061 \\ -10.23 + i20.29 & 0.66 + i1.39 \end{bmatrix}$$

Performing the matrix multiplication from left to right (which corresponds to inside to outside):

$$\begin{bmatrix} 1 & 0.1 \\ 0 & 1 \end{bmatrix} \times \begin{bmatrix} 0.66 + i1.39 & 0.122 + i0.061 \\ -10.23 + i20.29 & 0.66 + i1.39 \end{bmatrix}$$

$$= \begin{bmatrix} (0.66 + i1.39) + (-1.023 + i2.020) & (0.122 + i0.061) + (0.066 + i0.139) \\ (-10.23 + i20.29) & (0.66 + i1.39) \end{bmatrix}$$

$$= \begin{bmatrix} -0.363 + i3.41 & 0.188 + i0.2 \\ -10.23 + i20.29 & 0.66 + i1.39 \end{bmatrix}$$

The second stage only requires the evaluation of the right-hand column of the product matrix as only M_2 and M_4 are required:

$$\begin{bmatrix} -0.363 + i3.41 & 0.188 + i0.2 \\ -10.23 + i20.29 & 0.66 + 1.39 \end{bmatrix}\begin{bmatrix} 1 & 0.1 \\ 0 & 1 \end{bmatrix} = \begin{bmatrix} * & (-0.0363 + i0.341) + (0.188 + i0.2) \\ * & (-1.023 + i2.029) + (0.66 + i1.39) \end{bmatrix}$$

$$= \begin{bmatrix} * & 0.152 + i0.541 \\ * & -0.363 + i3.419 \end{bmatrix}$$

From the equation to calculate the Admittance Factor:

$$Y_c = \frac{-0.363 + i3.419}{0.152 + 0.541} = \frac{(-0.363 + i3.419)(0.152 - i0.541)}{0.152^2 + 0.541^2}$$

$$= [-0.0552 + 1.85 + i(0.196 + 0.520)]/0.316$$

$$= 5.679 + i2.266$$

Y=6.114

$\omega = 1.632h$

Using the equation to calculate the Decrement Factor:

$$f_c = \frac{1}{3.02(0.287 + i0.28)} = \frac{(0.287 - i0.28)}{3.02(0.287^2 + 0.28^2)} = 0.591 - i0.577$$

$$f = 0.826$$

$$\phi = -5.33h$$

To find the surface factor:

$$F_C = 1 - 0.1(4.236 + 1.9282i)$$

$$= 1 - (0.4235 + 0.19282i)$$

$$= 0.5765 - i0.19282$$

$$F = |0.5765 - 0.19282i| \qquad \text{The properties of the brick are:}$$

$$= 0.61$$

$$\psi = \frac{12}{\pi}\arctan\left(\frac{0.19282}{0.5765}\right)$$

$$= 1.233h$$

Material B1(iii) – The Density is reduced by a factor of 0.5

The properties of the brick are:

$\rho = 850 \text{ Kg/m}^3$
$\lambda = 0.84 \text{ W/m K}$
$c = 800 \text{ J/Kg K}$

Thickness of the material is 220mm.

Internal Surface Heat Transfer Coefficient $= 0.1 \text{ W/m}^2\text{K}$
External Surface Heat Transfer Coefficient $= 0.1 \text{ W/m}^2\text{K}$

The U-Value is:

$$U = \frac{1}{0.1 + \dfrac{0.22}{0.84} + 0.1}$$

$$= 2.16 W/m^2 K$$

p = 1.194

For manual calculations, it is convenient to express cosh (p+ip) and sinh (p+ip) in terms of functions sin p, cos p and e^p which are available on most slide rules, pocket calculators and books of tables:

$$\cosh(p+ip) = \frac{1}{2}\left[\left(e^p + e^{-p}\right)\cos p + i\left(e^p - e^{-p}\right)\sin p\right]$$

$$\sinh(p+ip) = \frac{1}{2}\left[\left(e^p - e^{-p}\right)\cos p + i\left(e^p + e^{-p}\right)\sin p\right]$$

In the Matrix, the coefficient m_1, is given by the equation shown above, while m_2 and m_3 are given by:

$$m_2 = \frac{l\left[\left(e^p - e^{-p}\right)\cos p + \left(e^p + e^{-p}\right)\sin p - i\left(e^p - e^{-p}\right)\cos p + i\left(e^p - e^{-p}\right)\sin p\right]}{4\lambda p}$$

$$m_3 = \frac{\lambda p\left[\left(e^p - e^{-p}\right)\cos p - \left(e^p + e^{-p}\right)\sin p + i\left(e^p - e^{-p}\right)\cos p + i\left(e^p + e^{-p}\right)\sin p\right]}{2l}$$

which gives the matrix as:

$$\begin{bmatrix} 0.663 + i1.393 & 0.244 + i0.123 \\ -5.117 + i10.145 & 0.663 + i1.393 \end{bmatrix}$$

Performing the matrix multiplication from left to right (which corresponds to inside to outside):

$$\begin{bmatrix} 1 & 0.1 \\ 0 & 1 \end{bmatrix} \times \begin{bmatrix} 0.663 + i1.393 & 0.244 + i0.123 \\ -5.117 + i10.145 & 0.663 + i1.393 \end{bmatrix}$$

$$= \begin{bmatrix} (0.663 + i1.393) + (-0.512 + i1.015) & (0.244 + i0.123) + (0.066 + i0.139) \\ (-5.117 + i10.145) & (0.663 + i1.393) \end{bmatrix}$$

$$= \begin{bmatrix} 0.151 + i2.408 & 0.31 + i0.262 \\ -5.117 + i10.145 & 0.663 + 1.393 \end{bmatrix}$$

The second stage only requires the evaluation of the right-hand column of the product matrix as only M_2 and M_4 are required:

$$\begin{bmatrix} 0.153 + i2.408 & 0.31 + i0.262 \\ -5.117 + i10.145 & 0.663 + 1.393 \end{bmatrix}\begin{bmatrix} 1 & 0.1 \\ 0 & 1 \end{bmatrix} = \begin{bmatrix} * & (0.0153 + i0.2408) + (0.31 + i0.262) \\ * & (-0.512 + i1.015) + (0.663 + i1.393) \end{bmatrix}$$

$$= \begin{bmatrix} * & 0.3253 + i0.528 \\ * & 0.151 + i2.408 \end{bmatrix}$$

From the equation to calculate the Admittance Factor:

$$Y_c = \frac{0.151 + i2.408}{0.3253 + i0.5028} = \frac{(0.151 + i2.408)(0.3253 - i0.5028)}{0.3253^2 + 0.5028^2}$$

$$= [0.04912 + 1.211 + i(-0.0759 + 0.783)]/0.3586$$

$$= 3.514 + i1.972$$

Y=4.03

$\omega = 1.95h$

Using the equation to calculate the Decrement Factor:

$$f_c = \frac{1}{2.16(0.3253 + i0.2237)} = \frac{(0.3253 - i0.5028)}{2.16(0.3253^2 + 0.5028^2)} = 0.420 - i0.6491$$

$$f = 0.773$$

$$\phi = 3.81h$$

To find the surface factor:

$$F_C = 1 - 0.1(3.514 + i1.972)$$

$$= 1 + (-0.3514 - 0.1972i)$$

$$= 0.6486 + 0.1972i$$

$$F = |0.6486 + 0.1972i|$$

$$= 0.678$$

$$\psi = \frac{12}{\pi} \arctan\left(\frac{0.1972}{0.6486}\right)$$

$$= 1.127h$$

Material B1(iv) – The Specific Heat Capacity is reduced by a factor of 0.5

The properties of the brick are:

$\rho = 850$ Kg/m^3
$\lambda = 0.084$ W/m K
$c = 800$ J/Kg K

Thickness of the material is 220mm.

Internal Surface Heat Transfer Coefficient $= 0.1$ W/m^{2}K
External Surface Heat Transfer Coefficient $= 0.1$ W/m^{2}K

The U-Value is:

$$U = \frac{1}{0.1 + \dfrac{0.22}{0.84} + 0.1}$$

$$= 2.16 W/m^2 K$$

p = 1.194

For manual calculations, it is convenient to express cosh (p+ip) and sinh (p+ip) in terms of functions sin p, cos p and e^p which are available on most slide rules, pocket calculators and books of tables:

$$\cosh(p+ip) = \frac{1}{2}\left[\left(e^p + e^{-p}\right)\cos p + i\left(e^p - e^{-p}\right)\sin p\right]$$

$$\sinh(p+ip) = \frac{1}{2}\left[\left(e^p - e^{-p}\right)\cos p + i\left(e^p + e^{-p}\right)\sin p\right]$$

In the Matrix, the coefficient m_1, is given by the equation shown above, while m_2 and m_3 are given by:

$$m_2 = \frac{i\left[\left(e^p - e^{-p}\right)\cos p + \left(e^p + e^{-p}\right)\sin p - i\left(e^p - e^{-p}\right)\cos p + i\left(e^p - e^{-p}\right)\sin p\right]}{4\lambda p}$$

$$m_3 = \frac{\lambda p\left[\left(e^p - e^{-p}\right)\cos p - \left(e^p + e^{-p}\right)\sin p + i\left(e^p - e^{-p}\right)\cos p + i\left(e^p + e^{-p}\right)\sin p\right]}{2l}$$

which gives the matrix as:

$$\begin{bmatrix} 0.663 + i1.393 & 0.244 + i0.123 \\ -5.117 + i10.145 & 0.663 + i1.393 \end{bmatrix}$$

Performing the matrix multiplication from left to right (which corresponds to inside to outside):

$$\begin{bmatrix} 1 & 0.1 \\ 0 & 1 \end{bmatrix} \times \begin{bmatrix} 0.663 + i1.393 & 0.244 + i0.123 \\ -5.117 + i10.145 & 0.663 + i1.393 \end{bmatrix}$$

$$= \begin{bmatrix} (0.663 + i1.393) + (-0.512 + i1.015) & (0.244 + i0.123) + (0.066 + i0.139) \\ (-5.117 + i10.145) & (0.663 + i1.393) \end{bmatrix}$$

$$= \begin{bmatrix} 0.151 + i2.408 & 0.31 + i0.262 \\ -5.117 + i10.145 & 0.663 + 1.393 \end{bmatrix}$$

The second stage only requires the evaluation of the right-hand column of the product matrix as only M_2 and M_4 are required:

$$\begin{bmatrix} 0.153 + i2.408 & 0.31 + i0.262 \\ -5.117 + i10.145 & 0.663 + 1.393 \end{bmatrix}\begin{bmatrix} 1 & 0.1 \\ 0 & 1 \end{bmatrix} = \begin{bmatrix} * & (0.0153 + i0.2408) + (0.31 + i0.262) \\ * & (-0.512 + i1.015) + (0.663 + i1.393) \end{bmatrix}$$

$$= \begin{bmatrix} * & 0.3253 + i0.528 \\ * & 0.151 + i2.408 \end{bmatrix}$$

From the equation to calculate the Admittance Factor:

$$Y_c = \frac{0.151 + i2.408}{0.3253 + i0.5028} = \frac{(0.151 + i2.408)(0.3253 - i0.5028)}{0.3253^2 + 0.5028^2}$$

$$= [0.04912 + 1.211 + i(-0.0759 + 0.783)]/0.3586$$

$$= 3.514 + i1.972$$

Y=4.03

$\omega = 1.95h$

Using the equation to calculate the Decrement Factor:

$$f_c = \frac{1}{2.16(0.3253 + i0.2237)} = \frac{(0.3253 - i0.5028)}{2.16(0.3253^2 + 0.5028^2)} = 0.420 - i0.6491$$

$f = 0.773$

$\phi = 3.81h$

To find the surface factor:

$$F_C = 1 - 0.1(3.514 + i1.972)$$
$$= 1 + (-0.3514 - 0.1972i)$$
$$= 0.6486 + 0.1972i$$

$$F = |0.6486 + 0.1972i|$$
$$= 0.678$$

$$\psi = \frac{12}{\pi} \arctan\left(\frac{0.1972}{0.6486}\right)$$
$$= 1.127h$$

Material B1(v) – The thickness of the material is reduced by a factor of 0.5.

The properties of the brick are:

$\rho = 1700$ Kg/m^3
$\lambda = 0.84$ W/m K
$c = 800$ J/Kg K

Thickness of the material is 110mm.

Internal Surface Heat Transfer Coefficient $= 0.1$ W/m^{2}K
External Surface Heat Transfer Coefficient $= 0.1$ W/m^{2}K

The U-Value is:

$$U = \frac{1}{0.1 + \dfrac{0.11}{0.84} + 0.1}$$

$$= 3.02 W / m^2 K$$

p = 0.844

For manual calculations, it is convenient to express cosh (p+ip) and sinh (p+ip) in terms of functions sin p, cos p and e^p which are available on most slide rules, pocket calculators and books of tables:

$$\cosh(p + ip) = \frac{1}{2}\left[\left(e^p + e^{-p}\right)\cos p + i\left(e^p - e^{-p}\right)\sin p\right]$$

$$\sinh(p + ip) = \frac{1}{2}\left[\left(e^p - e^{-p}\right)\cos p + i\left(e^p + e^{-p}\right)\sin p\right]$$

In the Matrix, the coefficient m_1, is given by the equation shown above, while m_2 and m_3 are given by:

$$m_2 = \frac{l\left[\left(e^p - e^{-p}\right)\cos p + \left(e^p + e^{-p}\right)\sin p - i\left(e^p - e^{-p}\right)\cos p + i\left(e^p - e^{-p}\right)\sin p\right]}{4\lambda p}$$

$$m_3 = \frac{\lambda p\left[\left(e^p - e^{-p}\right)\cos p - \left(e^p + e^{-p}\right)\sin p + i\left(e^p - e^{-p}\right)\cos p + i\left(e^p + e^{-p}\right)\sin p\right]}{2l}$$

which gives the matrix as:

$$\begin{bmatrix} 0.916 + i0.708 & 0.129 + i0.031 \\ -2.577 + i10.695 & 0.916 + i0.708 \end{bmatrix}$$

Performing the matrix multiplication from left to right (which corresponds to inside to outside):

$$\begin{bmatrix} 1 & 0.1 \\ 0 & 1 \end{bmatrix} \times \begin{bmatrix} 0.916 + 0.708 & 0.129 + i0.031 \\ -2.577 + i10.695 & 0.916 + i0.708 \end{bmatrix}$$

$$= \begin{bmatrix} (0.916 + i0.708) + (-0.258 + i1.07) & (0.129 + i0.031) + (0.092 + i0.071) \\ (-2.577 + i10.695) & (0.916 + i0.708) \end{bmatrix}$$

$$= \begin{bmatrix} 0.658 + i1.778 & 0.221 + i0.102 \\ -2.577 + i10.695 & 0.916 + i0.708 \end{bmatrix}$$

The second stage only requires the evaluation of the right-hand column of the product matrix as only M_2 and M_4 are required:

$$\begin{bmatrix} 0.658 + i1.778 & 0.221 + i0.102 \\ -2.577 + i10.695 & 0.916 + 0.708 \end{bmatrix} \begin{bmatrix} 1 & 0.1 \\ 0 & 1 \end{bmatrix} = \begin{bmatrix} * & (0.066 + i0.178) + (0.221 + i0.102) \\ * & (-0.258 + i1.07) + (0.916 + i0.708) \end{bmatrix}$$

$$= \begin{bmatrix} * & 0.287 + i0.28 \\ * & 0.658 + i1.778 \end{bmatrix}$$

From the equation to calculate the Admittance Factor:

$$Y_c = \frac{0.658 + i1.148}{0.287 + 0.28} = \frac{(0.658 + i1.778)(0.278 - i0.28)}{0.287^2 + 0.28^2}$$
$$= [0.183 + 0.498 + i(-0.184 + 0.494)] / 0.161$$
$$= 4.236 + i1.9282$$

Y=4.65

$\omega = 1.632h$

Using the equation to calculate the Decrement Factor:

$$f_c = \frac{1}{3.02(0.287 + i0.28)} = \frac{(0.287 - i0.28)}{3.02(0.287^2 + 0.28^2)} = 0.591 - i0.577$$
$$f = 0.826$$
$$\phi = -2.96h$$

To find the surface factor:

$$F_C = 1 - 0.1(4.236 + 1.9282i)$$
$$= 1 - (0.4235 + 0.19282i)$$
$$= 0.5765 - i0.19282$$

$$F = |0.5765 - 0.19282i|$$
$$= 0.61$$

$$\psi = \frac{12}{\pi}\arctan\left(\frac{0.19282}{0.5765}\right)$$
$$= 1.233h$$

C-1

APPENDIX C

Appendix C

C1 Testing the 'Boundary Freeze Fabric' (BFF) Function

In order to test whether the 'Freeze' Fabric Function operates as designed, the same CFD test model used to develop the DTM-CFD procedure has been used, see Figure 4.1, Chapter 4. All of the tests conducted were implemented using the steady state solution process.
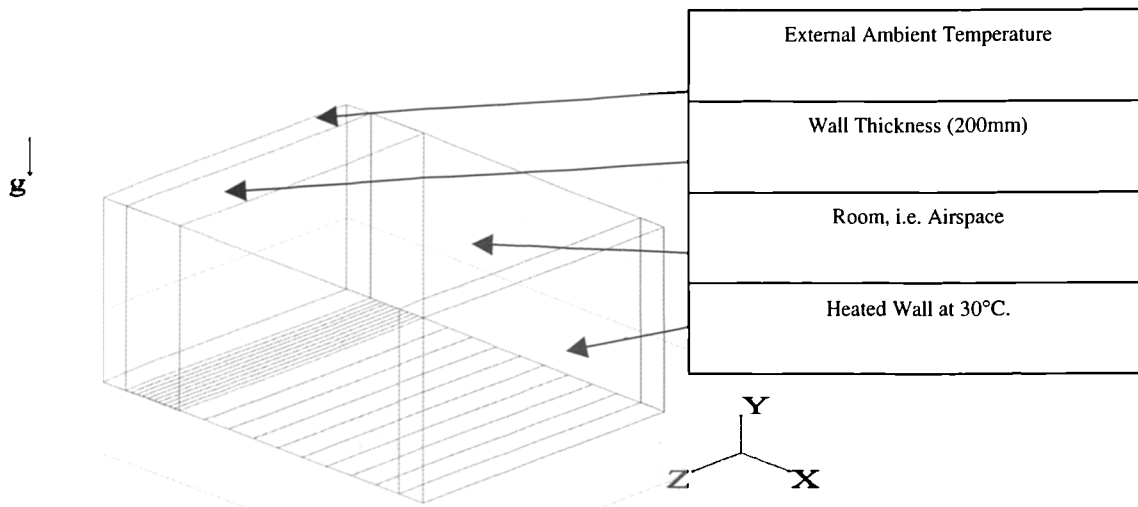

Fig C1: Test Geometry used to assess the performance of the 'Freeze Flow' Function

A temperature was applied to the outermost cuboid. The external cuboid acts as an external ambient setting, as developed in Appendix A, section A5. The second cuboid in the series was made from Brickwork (outer leaf). A third wall situated opposite the external wall, was given a fixed temperature of 30°C. This steady state case was then solved, requiring approximately 300 iterations to reach convergence.

After this steady state case was solved, the external brickwork wall was the replaced with the 'Freeze' Fabric function. To prove that the 'Boundary Freeze Fabric' function worked, the external ambient cuboid was given an excessively different temperature to see whether the external brickwork (outer leaf) wall would respond to this thermal change.

Temperature recording points were embedded within the solid external wall and at points within the air, adjacent to the internal surface of the wall and the data recorded is illustrated in Fig C2.

Despite changing the external ambient settings, via the outermost cuboid, the temperatures within the solid wall remained constant as a result of activating the 'Freeze' Fabric function, proving that the function does work successfully. From Fig. C2, it is evident that at Monitor Point 1 (a data collection point located within the wall thickness, which maintained a temperature of less than 13.5°C did not respond to the changes in the external ambient temperatures.
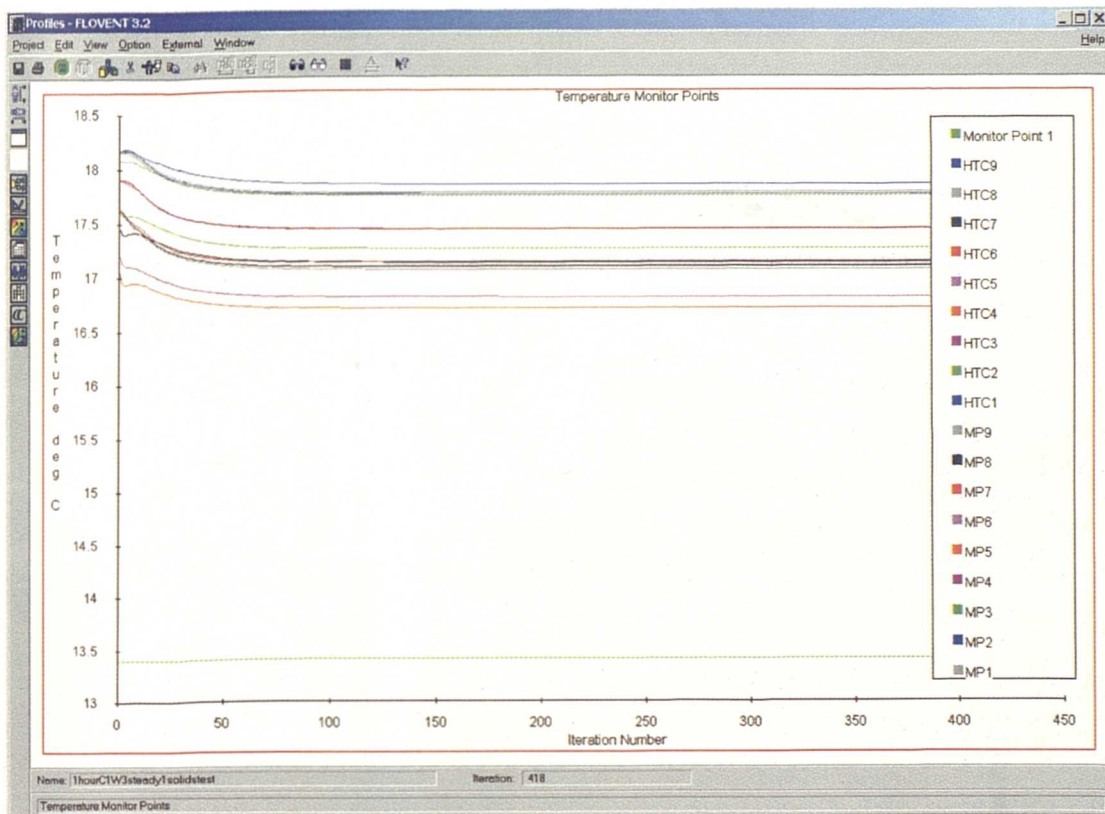

Fig C2:   Temperature profiles of the Temperature data collection points within the Enclosure

C2 Materials Testing

C2.1 Introduction

Nine materials have been fabricated by combining a range of thermal characteristics. The nine materials form a comprehensive spectrum of typical building fabrics used in common constructions. The errors incurred by using the established DTM-CFD procedure (transient-steady) are analysed for evidence of a correlation between the magnitudes of error and the thermal characteristics of the materials. The following parameters have been tested on each of the nine materials:

1. length of the transient frozen flow period;
2. length of the time steps lengths within the frozen flow period;
3. The amount of temperature change within the boundaries between steady state updates;

The main findings of these tests have been documented in Chapter 5.

C2.2 Results and Discussion

C1W1

C1W1 has the lightest thermal weight and the lowest conductivity of all the materials tested. The material therefore, responds relatively quickly to any thermal changes that occur, but heat is not easily transferred through the material.

Using 1 hour of transient flow followed by a steady state update causes 1% error difference of the maximum temperature range over the 16 hours of the fully transient case (maximum range is 1.1°C, in this case). The errors of the steady state are not cumulative, but never fully reduce to zero, because of the delay of true airflow patterns caused by using the transient-steady procedure, see Figure C3.

Errors when using 1 hour of transient solving are so insignificant that greater transient solution periods could even be increased to as much as 8 hours. By using longer

lengths of transient periods, the errors incurred increase with time. There is less concern, however, about the extent of the errors during the transient period. The important data is collected after a steady state update, therefore, the frequency of retrieving accurate data depends on the frequency of steady state updates.

Since errors do reduce to less than 2% for transient time periods of less than 8 hours, a wide choice of transient lengths can be made, depending on how frequently, accurate data is selected from steady state updates. With longer lengths of transient period, the % errors are negative because the DTM-CFD tool under predicts the temperatures within the room. This is because the frozen airflow patterns are too out-of-date to be able to correctly transfer heat away from the wall.
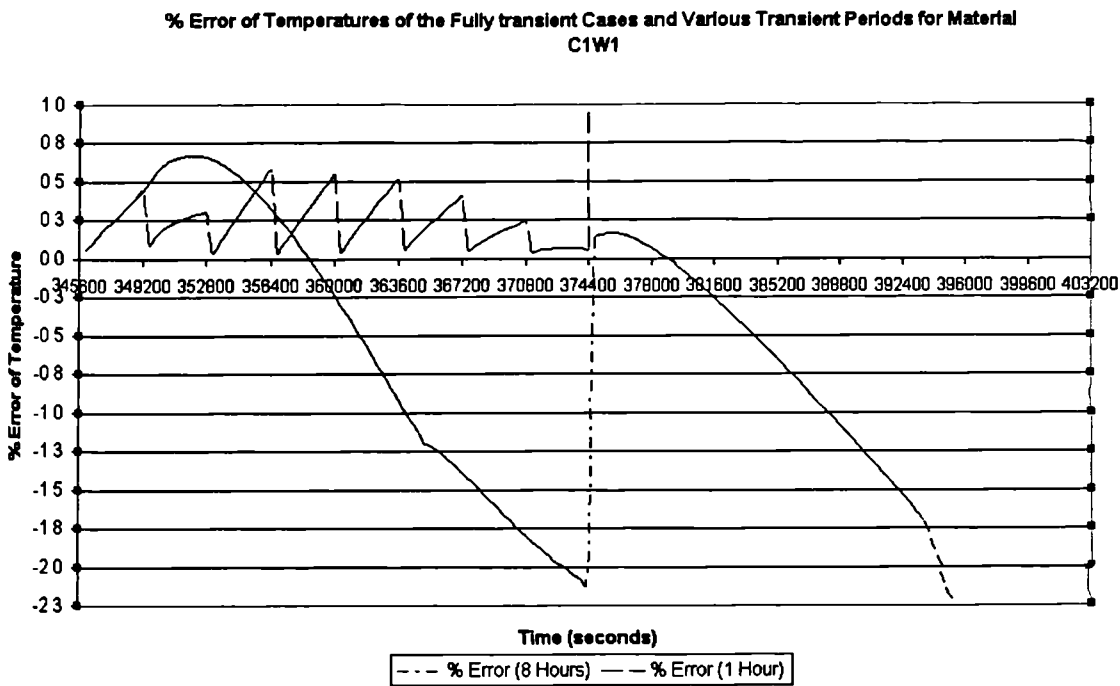

Figure C3: % Errors of Transient 'Frozen Flow' Periods for Material C1W1

C1W2

The material used in this test has a low thermal conductivity and a relatively average thermal mass. These thermal characteristics indicate that thermal heat transfer is passed slowly through the material, and heat can also be trapped within the material.

The procedure used in the DTM-CFD tool is very effective in dynamically modelling the heat transfer through C1W2. The increased thermal mass of this material reduces the rate of heat transfer across it, so the changes in the thermal conditions of this material are relatively small over time. This is turn means that the airflow patterns do not change significantly with each steady state update. The results of the test show that the errors at the end of a steady state update (occurring after an 8 hour transient period) are less than 2% of the maximum temperature range of the external ambient. Hence, any transient period of frozen flow may be used because in increasing the thermal weight, the errors incurred by freezing the flow have been reduced, see Figure C4.

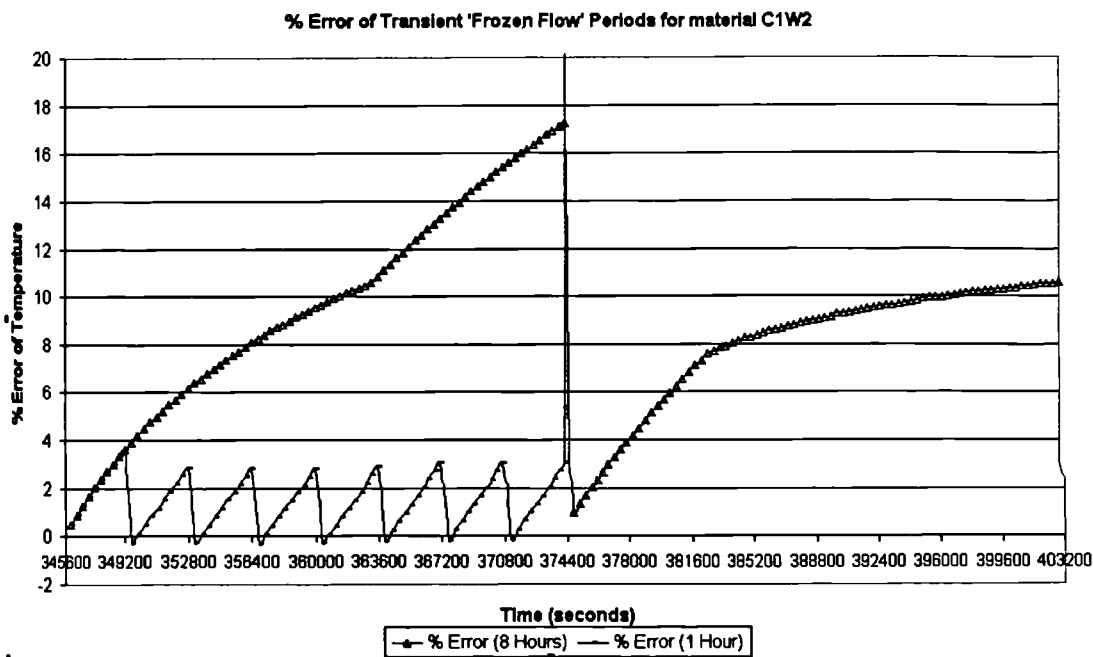**% Error of Transient 'Frozen Flow' Periods for material C1W2**

Figure C4: % Error of Transient 'Frozen Flow' Periods for Material C1W2

C1W3

The thermal conductivity of this material is low and the thermal weight is exceptionally high; therefore heat transfer is extremely difficult through this material. Due to the lack of change of the airflow patterns within the enclosure over time, the errors caused by using long transient periods of frozen flow are minimal. The steady state updates reduce the errors incurred over the transient period to zero.

A wide variety of transient times may be used because the material is so slow in responding to fluctuations in the external environment, see Figure C5.
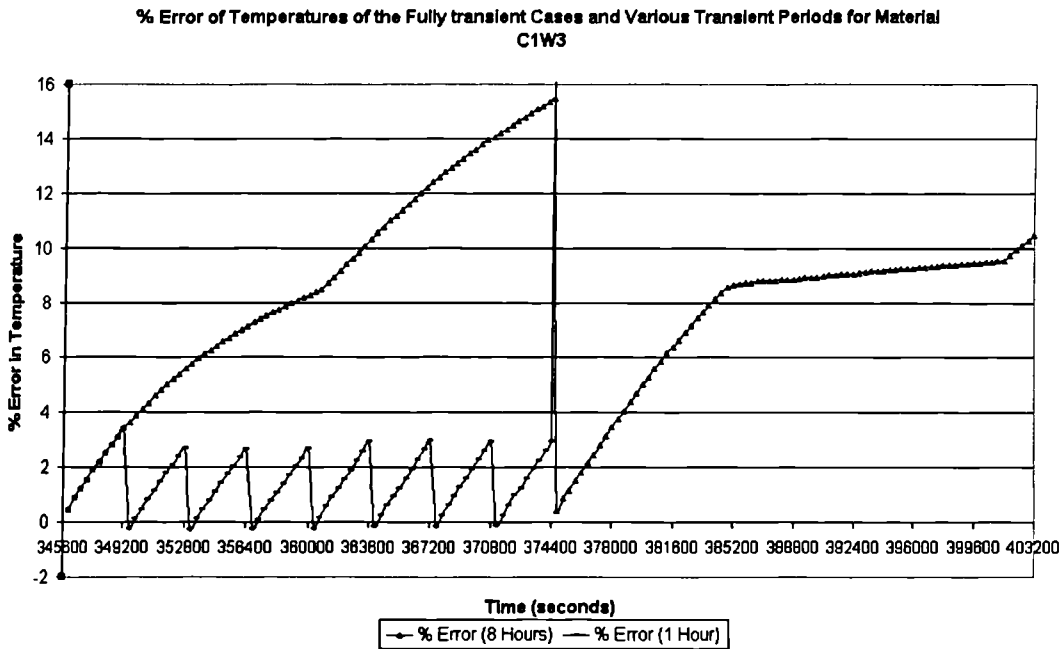
% Error of Temperatures of the Fully transient Cases and Various Transient Periods for Material C1W3

Figure C5:   % Error of Temperatures of the Fully Transient Cases and Various Transient Periods for Material C1W3

C2W1

This material has a higher conductivity than the materials using C1. Heat passes through the material quite easily. The material will respond to thermal changes at a much faster rate compared to the materials which have a thermal conductivity of C1, so larger errors are expected to occur over longer transient periods.

The results of the transient tests confirms that larger errors are incurred by using longer transient times for this materials, since approximately 30% error difference between the fully transient case and the DTSP#2 solution occurred when using 8 hours, see Figure C6.

Errors during a transient period, however, are of no real importance, the crucial and more accurate information must be collected after a steady state update. After a

steady state update (which would have followed a transient frozen flow period of 8 hours), accuracy is regained to approximately 3% of 6°C of maximum temperature range over the 16 of the fully transient solution.

For error less than 1%, 2 hours or less of transient frozen flow should be used before a steady state update because of this more conductive materials sensitivity to transient periods. More frequent steady state updates are therefore also required, otherwise the errors in representative frozen airflow patterns accumulate. For acceptable accuracy, transient times should be limited to under 4 hours, to capture the thermal response of the fabric (and to avoid the influence of thermal lag) to the changing ambient.
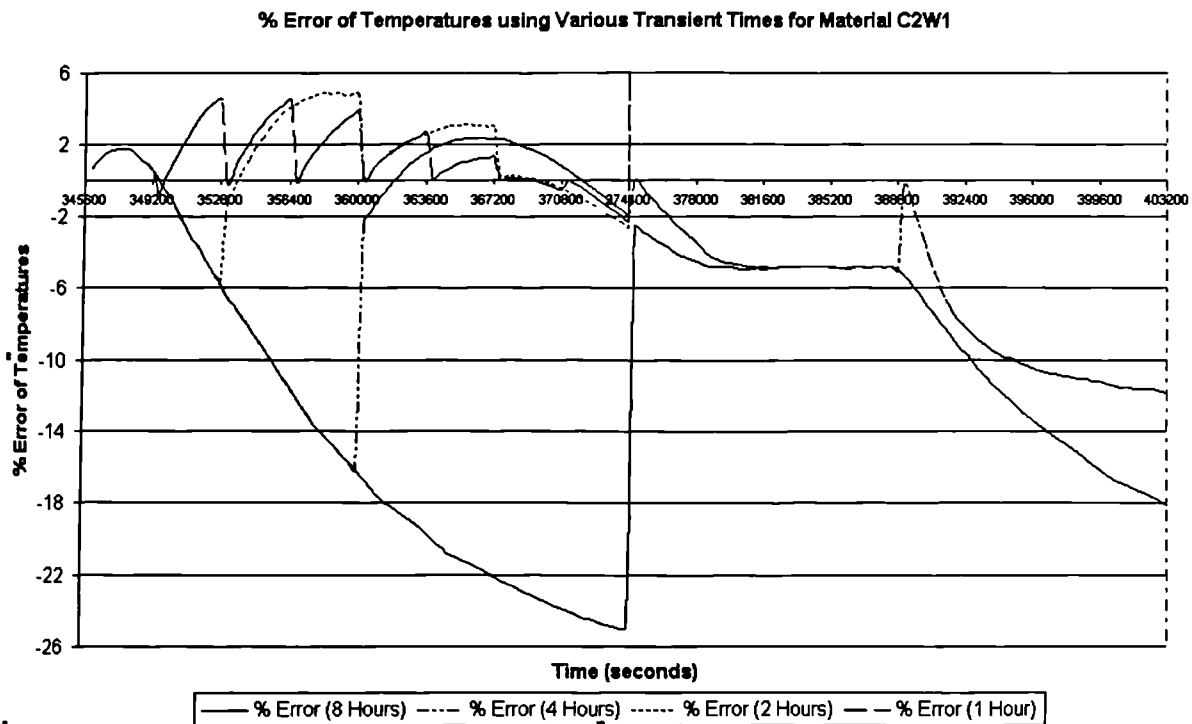

% Error of Temperatures using Various Transient Times for Material C2W1

Figure C6: % Error of Transient 'Frozen Flow' Periods for Material C2W1

C2W2

The main source of error is due to the thermal lag of the fabric, which was calculated as being 5/6 hours (see Appendix B, Section B1), from previous tests. During the 8 hours of solving, the brickwork would have responded to changes in the external ambient, since the effects of thermal lag would have taken effect during the 8-hour

period. During the 8-hour period the % errors in the solutions (compared to the fully transient cases) reached maximum values of 2.2%. This error was reached towards the latter end of the period of frozen flow. After a steady state unfrozen update solution period, the errors in temperature returned to 0%. The longer the time allocated for frozen flow, the greater the errors due to the misrepresentation of heat transfer coefficients at the wall, see Figure C7.
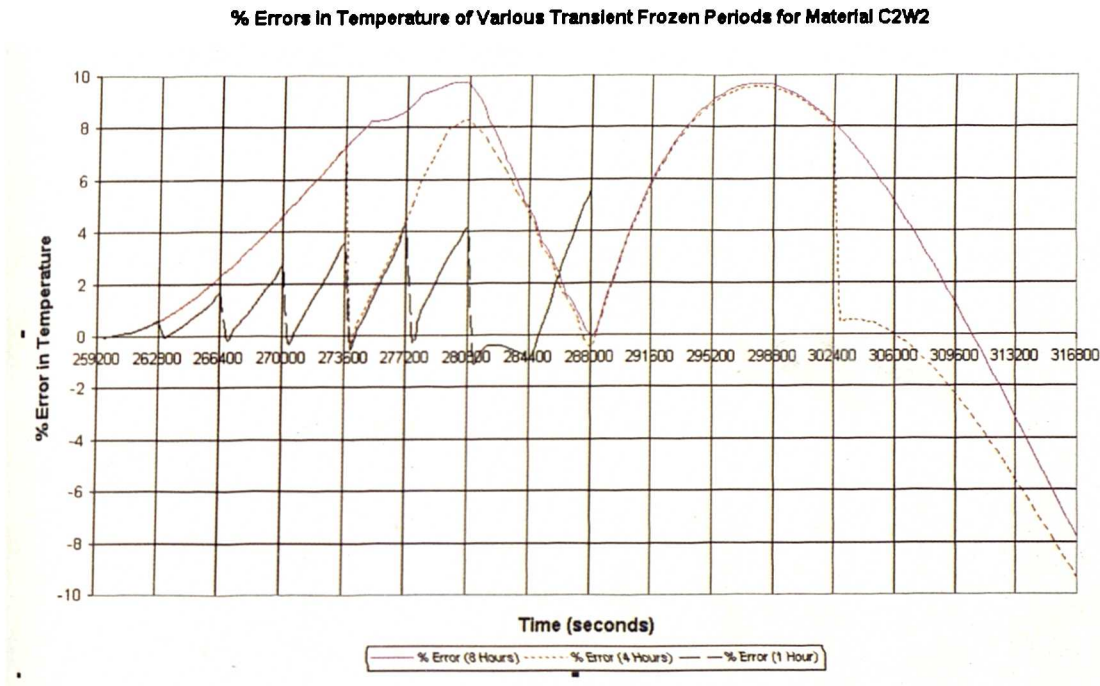

Figure C7: % Error of Transient 'Frozen Flow' Periods for Material C2W2

The most suitable length of transient frozen flow is 1 hour, where maximum errors appear to be less than ±1%, occurring during the 5th or 6th hour of frozen flow. During the 1-hour transient periods, the effects of thermal lag are well represented. Using a transient period that is smaller than 1 hour is not necessary and wasteful of computer resources.

The results indicate that maximum errors will occur at a point in time that corresponds with the thermal lag of the fabric, if airflows are non-representative. The aim of the length of the transient period of frozen should be to capture the correct temperatures during the time when the effects of thermal lag are felt.

The effects of errors in the airflow patterns, set during the steady state update are:

1. Outdated heat transfer coefficients during a period of frozen flow

2. A misrepresentation of the response of the internal air as a result of external ambient conditions.

3. Inaccurate simulations of the thermal interactions between internal and external thermal conditions.

The results indicate that the conductivity of the material influences the magnitude of error caused by using increasing lengths of frozen flow periods. The maximum errors of using 1 hour of transient flow compared to using the fully transient case (using 360s time steps) were approximately ±0.5% after a steady state update. The errors do appear to be cumulative, but increase if larger changes are required during a steady state period. The lengths of transient times do not appear to increase the errors incurred, as the 8 hour transient time incurs errors of 0.2% after its steady state period. Nevertheless, the results do indicate that more frequent transient frozen periods are required, in order to limit errors throughout the overall transient simulation.

C2W3

This material has a quite a high conductivity and a very high thermal weight. Therefore, heat is easily transferred through the material but gets trapped in the volume of the material. Using 1 hour of transient flow incurs error differences between the results provided by the DTM-CFD tool and the fully transient solution of less than 0.5% after a steady state update. During a transient period of frozen flow, errors are much larger along a transient period of 8 hours, but again errors reduce to approximately 0% after a steady state update period because of the thermal weight of the material, See Figure C8.
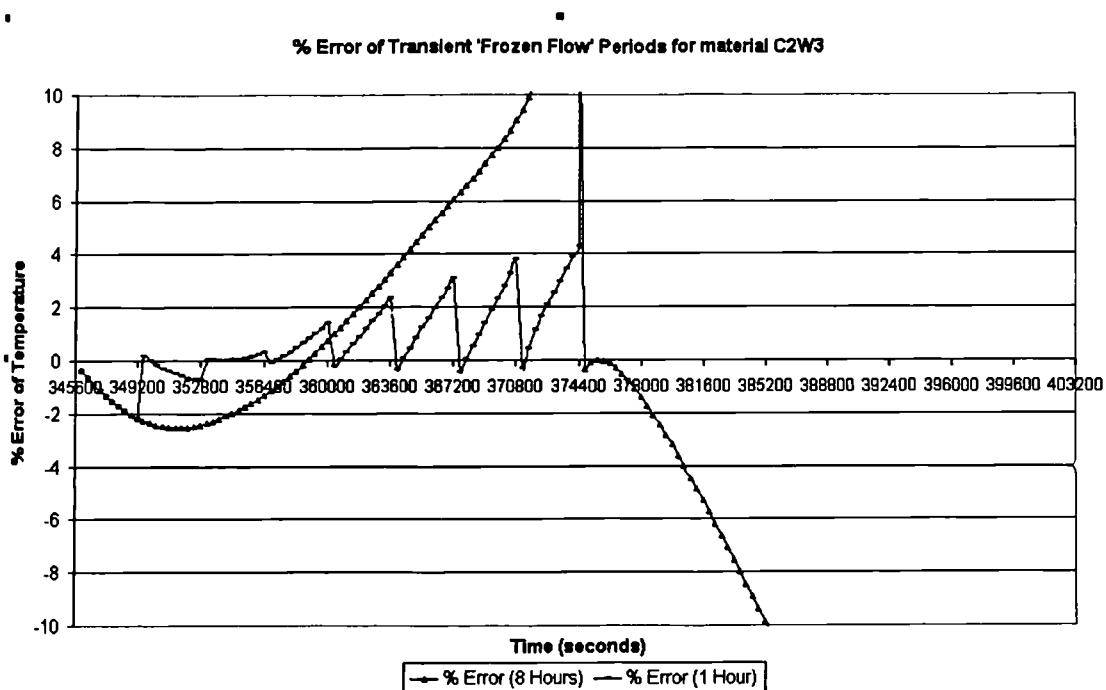
% Error of Transient 'Frozen Flow' Periods for material C2W3

Figure C8: % Error of Transient 'Frozen Flow' Periods for Material C2W3

C3W1

With high conductivity and low thermal weight, this material is the most sensitive to thermal change, since there will be a high rate of heat flux through the material and very little thermal energy will be absorbed within the resistance of the material. This material does respond quite well to the modelling procedure used by the DTM-CFD tool, but transient frozen flow times must be chosen with more care due to the

material's high thermal sensitivity. This is because heat transfer coefficients tend to change relatively quickly over time, so steady state updates need to occur more frequently to be able to transfer heat away from the wall properly and accurately. Transient frozen flow periods of one hour incur errors during a transient period of approximately 4% at worst. After a steady state update, the errors regress to less than approximately 0.1%.

By using transient periods of 30 minutes, the transient periods incur fewer errors during the solution time, but the errors after a steady state solution are only marginally improved compared to using 1 hour. 8 hours may also be used, but after a steady state update, the flow only recovers to approximately 1.5% of the actual values of the fully transient case, See Figure C9.
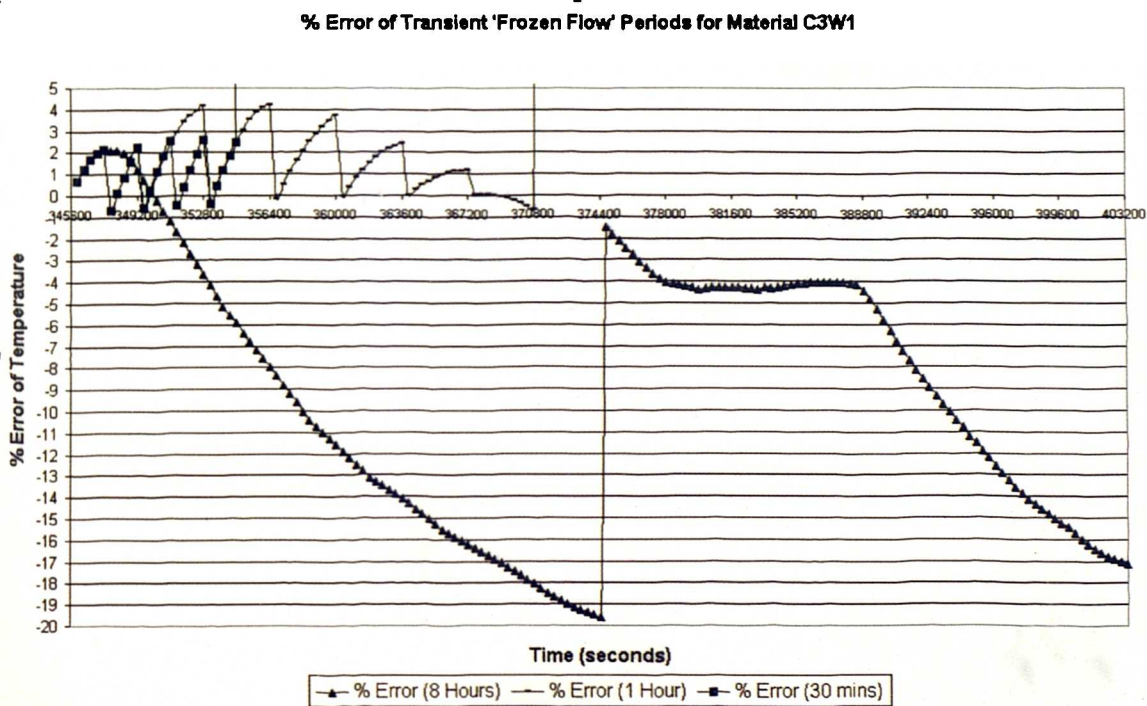
% Error of Transient 'Frozen Flow' Periods for Material C3W1

Figure C9: % Error of Transient 'Frozen Flow' Periods for Material C3W1

C3W2

This material has a very high conductivity and quite a high thermal mass. Heat is easily transferred through the material, but the heat gets trapped within the volume of the material. Essentially, heat does not easily pass through the material, so the airflow patterns do not change very significantly over time. At each steady state update, the airflow patterns do not significantly change, therefore the extent of the errors during the transient period are relatively small, even using a period of 8 hours. % Errors after the steady state updates were not significantly reduced by using shorter transient periods of 30 minutes, although the error was reduced along the transient period, see Figure C10.
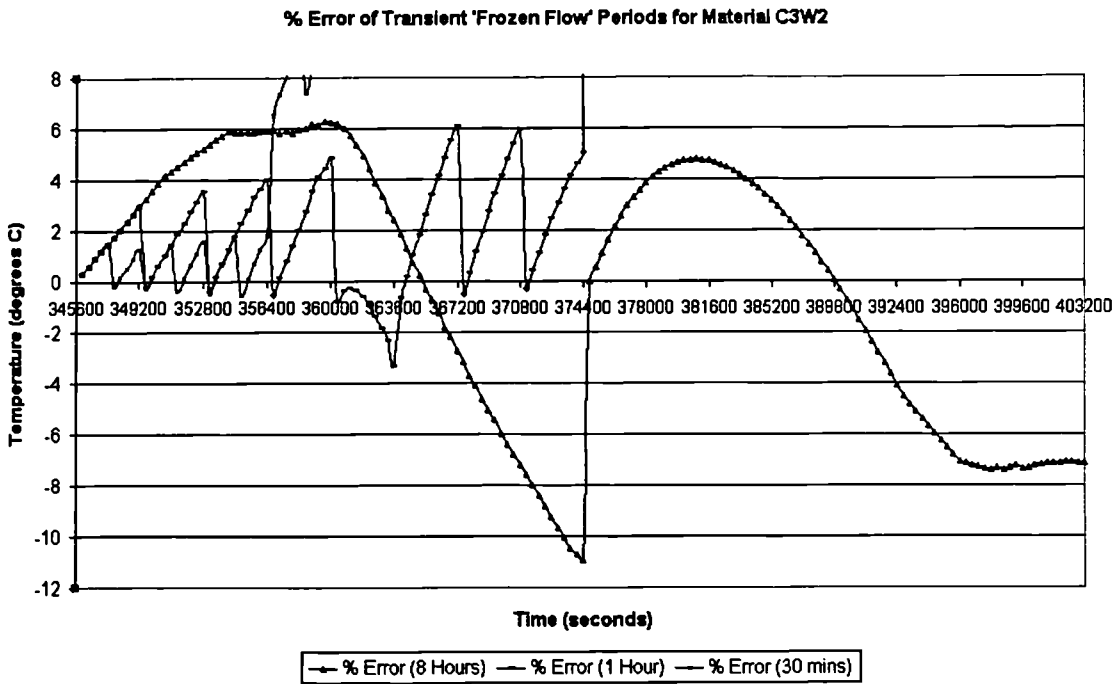
% Error of Transient 'Frozen Flow' Periods for Material C3W2

Figure C10: % Error of Transient 'Frozen Flow' Periods for Material C3W2

C3W3

Due to the high thermal conductivity of the material, but its large thermal mass, this material responds quickly to thermal changes and will retain heat within the material. During every update, not much would have occurred across the material because the changes in the external ambient would have slowly penetrated through the material.

Airflow patterns would not change significantly between updates, and so it is expected that the errors after a steady state update should be kept to a minimum. The error graph confirms this expectation, as after every steady state update period, the errors reduce to approximately zero. During the transient periods, the errors do not exceed 10%. A wide variety of transient times may be used for this high thermal weight material, See Figure C11, below.
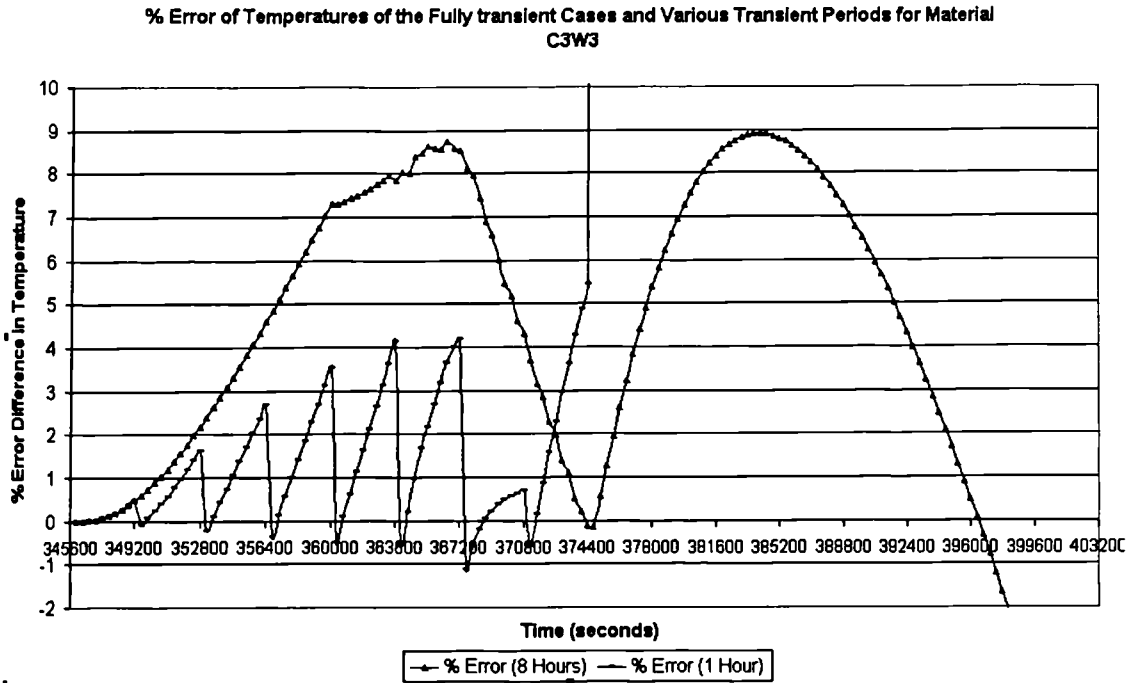

Figure C11: % Error of Temperatures of the Fully Transient Cases and Various Transient Periods for Material C3W3

C2.3 Conclusions

% errors for between the fully transient results and the various transient period results were compared against the amplitude of the external ambient temperature differential, which was 15°C. By using this common % error ratio over all the transient periods for all materials, patterns of errors began to emerge. The most conductive materials experienced larger errors along the transient period, but errors did reduce to approximately zero after a steady state update. Thermal conductivity of a material is more influential than thermal mass. Materials with a high thermal mass responded with more accuracy to the procedure used in the DTM-CFD tool.

In most cases, the longer the transient period of frozen flow, the more difficult (especially with highly conductive materials) it was to regain accurate airflow patterns after a steady state update. The results indicate that 1 hour is an ideal transient flow period to use for any materials, but the shorter the transient period, the less error generated over a transient period, and after a steady state update.

C3 Residual Errors and Flow Characteristics

C3.1 Introduction

At the end of a steady state update there is almost always a residual error caused by using the DTM-CFD Procedure, when compared to the fully transient solution process. In order to develop the DTM-CFD tool into a fully automated process, a link must be found between the errors induced after a steady state update and the thermal changes that occur over a transient period of frozen flow.

Freezing the flow within an enclosure introduces errors into the dynamic thermal simulation. [Residual error is defined as being the difference in temperature between the solution obtained by using the DTM-CFD and the fully transient solution, after a steady state update]. It is therefore fundamental to establish restrictions in the use of the freeze flow function to limit the errors introduced. Residual errors introduced into the solution are caused by the factors described in the flow chart below. All the factors are inter-linked and co-dependent:

| How much thermal change has occurred within a solid boundary of an enclosure over a transient period of frozen flow? | The extent to which the heat transfer coefficient on the inside surface of the enclosure becomes non-representative; | The extent to which the frozen airflow patterns are non-representative. |

Nature of the Change in Weather Patterns

Temperature difference between the solid temperature and the immediately adjacent air
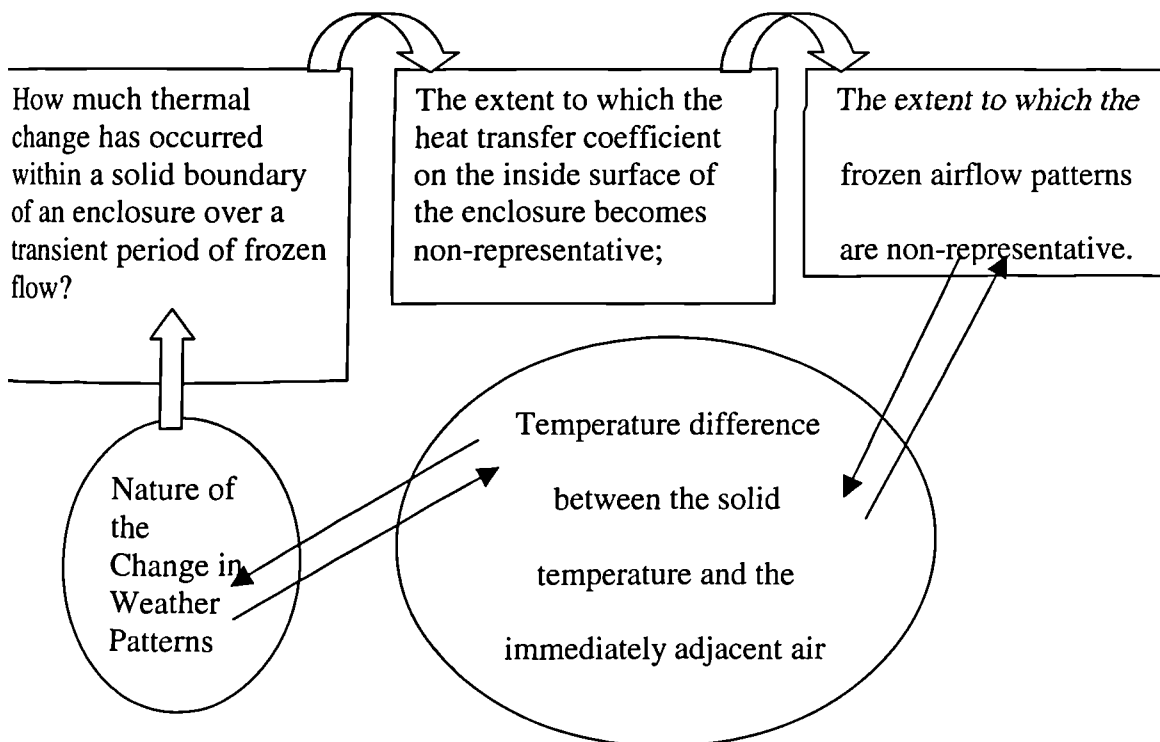
Fig C12:   Flow Chart indicating the influences upon error incurred by using the DTM-CFD tool

In summary, the factors that must be analysed are (also see Figure C13):

1. The change in the solid temperature (Tw) (on the inside surface of the wall) over the transient period of frozen flow; and the corresponding errors induced.

2. What temperature changes are occurring on the external surface of the solid (Te) due to the ambient; and the corresponding errors induced.

3. How much the air temperature within the enclosure (Ti) changes during a transient period of frozen flow; and the corresponding errors induced.
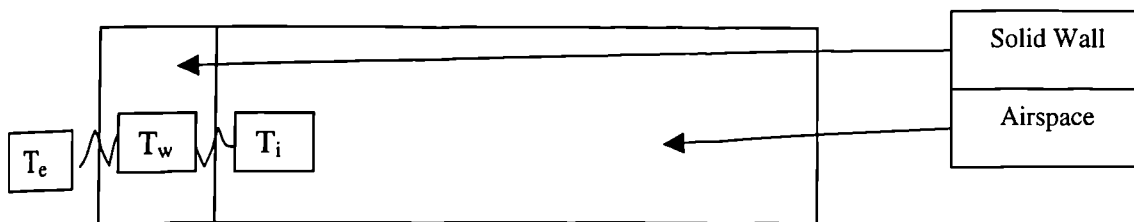

Fig C13: Cross-section of an Enclosure

C3.2 Error Analysis

In order to make sure that every possible cause of error is identified, a comprehensive list has been constructed. These sources of errors will be compared with each other to observe their relationships.

Factors, which are deemed to cause residual error after a steady state update, are:

1. By how much did the solid temperatures increase during the transient? Note that the solid temperatures do not change during the steady state update due to the Freeze-Fabric Function.

2. What is the temperature difference in the solid of the fully transient case and the DTM-CFD solution after a steady state update. This cannot be answered with the first sets of data, but additional tests have been conducted and this factor will be examined in a later section.

3. What was the difference between the temperatures in the air adjacent to the wall and the fully transient cases?

4. Is the adjustment to velocity proportional to residual error?

5. What is the velocity at MP5 (i.e. a data collection point central to the enclosure) at the end of the transient, and after the steady state update? Is it proportional to the temperature difference between the HTC5 in the air (a data collection point adjacent to the wall) within the room and the MP within the wall?

6. Is the adjustment to velocity proportional to the adjustment of the temperatures of the solids during the transient period?

7. Is the adjustment to the velocity proportional to the adjustment to the air adjacent to the wall during a steady state update?

8. How much did the air change over the transient frozen flow period? Is this proportional to the residual error?

9. How much did the air change over the steady state update? Is this proportional to the residual error?

10. How does the HTC change over the transient frozen flow period?

11. How does the HTC change over the steady state update?

All of the factors listed above have been summarised into a series of 3 matrices and tabulated below:

Error Matrix 1:   *Values are obtained After a Steady State Update (or beginning of Transient Update):*

	T Solid	ΔT Solid (RE)	ΔT Air(W) (RE)	V	T Air (W)	HTC
T Solid	X	Data Not Available	✓	✓	✓	✓
ΔT Solid (RE)	Data Not Available	X	Data Not Available	Data Not Available	Data Not Available	Data Not Available
ΔT Air(W) (RE)	✓	Data Not Available	X	✓	✓	✓

V	✓	Data Not Available	✓	X	✓	✓
T Air (W)	✓	Data Not Available	✓	✓	X	✓
HTC	✓	Data Not Available	✓	✓	✓	X

Error Matrix 2:   *Values After a Transient Frozen Flow Period (or Beginning of Steady State)*

	T Solid	**ΔT Solid (RE)**	**ΔT Air(W) (RE)**	**V**	**T Air (W)**	**HTC**
T Solid	X	Unavailable Data	✓	✓	✓	✓
ΔT Solid (RE)	Unavailable Data	X	Unavailable Data	Unavailable Data	Unavailable Data	Unavailable Data
ΔT Air(W) (RE)	✓	Unavailable Data	X	✓	✓	✓
V	✓	Unavailable Data	✓	X	✓	✓
T Air (W)	✓	Unavailable Data	✓	✓	X	✓
HTC	✓	Unavailable Data	✓	✓	✓	X

Error Matrix 3:   *Values After a Transient Frozen Flow Period (During the Transient Solution Process)*

	ΔT Solid (dTrans)	ΔT Solid (RE)	ΔT Air(W) (RE)	ΔV (dSS)	ΔT Air (W) (dSS)	ΔT Air (W) (dTrans)	ΔHTC (dTrans)	ΔHTC (dSS)
ΔT Solid (dTrans)	X	Data Not Available	✓	✓	✓	✓	✓	✓
ΔT Solid (RE)	Data Not Available	X	Data Not Available	Data Not Available	Data Not Available	Data Not Available	Data Not Available	Data Not Available
ΔT Air(W) (RE)	✓	Data Not Available	X	✓	✓	✓	✓	✓
ΔV (dSS)	✓	Data Not Available	✓	X	✓	✓	✓	✓
ΔT Air (W) (dSS)	✓	Data Not Available	✓	✓	X	✓	✓	✓
ΔT Air (W) (dTrans)	✓	Data Not Available	✓	✓	✓	X	✓	✓
ΔHTC (dTrans	✓	Data Not	✓	✓	✓	✓	X	✓

)		Avail able						
ΔHTC (dSS)	✓	Data Not Avail able	✓	✓	✓	✓	✓	X

C4 Testing the Performance of a Revised DTM-CFD Procedure

C4.1 Introduction

In order to observe the effects of the most thermally responsive material, a harsh ambient was attached to the ambient cuboid. The results of the various transient periods indicated that the error did not directly correlate to the length of the transient period. In fact, a transient period of 6 mins, contained more errors than larger transient periods.

The results of this tests documented in Chapter 4 suggested that errors were input into the solution procedure by performing a steady state update, since the error in the solution procedure could not be eliminated, despite increasing the frequency of steady state updates.

Further tests were carried out in order to establish whether there was a problem with the updating procedure within the DTM-CFD tool. One possible explanation for the error could have been due to, the method of 'unfreezing' the flow, thereby possibly causing additional thermal input into the space due to solving the steady state update case, with all the equations fully functioning – i.e. effectively solving the temperature equation twice during a transient-unfrozen and steady state unfrozen solution series.

C4.2 Test Geometry

The test geometry remains exactly identical to the geometry of the test conducted in section 5.4.3, Chapter 5. The difference between that test and this test is the procedure used in the DTM-CFD Procedure. During the steady state update, the temperature equation is technically frozen. I.e. the temperature equation was solved during the transient period of frozen flow, but not during the steady state update. The procedure was performed to observe whether repetition of the temperature equations was causing the residual errors. Transient frozen flow of 12 minutes will be used in this test, to limit the computational capacity of this test, but also accommodate one 2 time steps within each transient period.
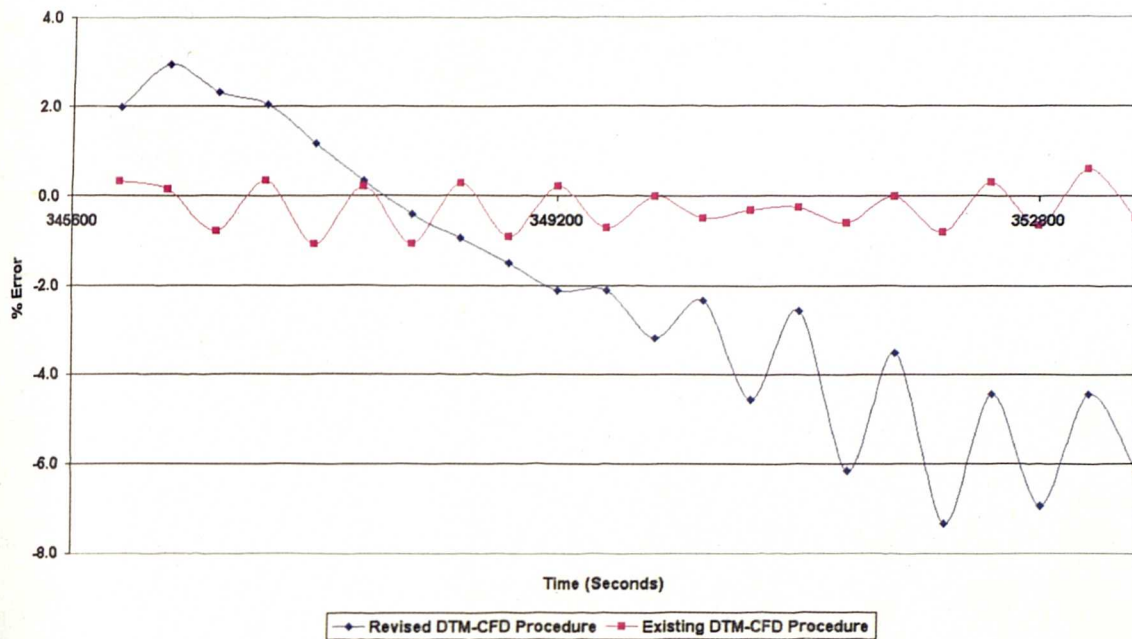
C4.3 Results and Discussion

Fig C14:   Comparison between Simulation Results Collected for the Existing and
Revised DTM-CFD Procedure using 12 min transient periods of
Frozen Flow

Research implemented and documented in Chapter 5 suggested that there may have
been a possible flaw in the steady state update solution process of the established
DTM-CFD Procedure. This possible explanation for this flaw was the nature of the
steady state update, whereby all equations were unfrozen, after a transient period of
frozen flow. Since, the temperature equations in the DTM-CFD Procedure is
consistently solved, through both the transient solution and steady state solution, there
may have been some form of repetition causing an additional thermal input into the
enclosure.

In order to test this theory, the steady state procedure was altered. Rather than solving
the temperature equation for the second time during the update solution process, the
temperature equation was then frozen.

Figure C14 show the comparison of the % Error difference between the DTM-CFD Procedure and the fully transient solution and the % Error difference between the revised steady state solution method and the fully transient case. Figure C14 indicates that after a few time steps, the revised steady state solution is not effective in reducing the errors imposed by freezing the flow during a transient solution period. Hence, the revision made to the DTM-CFD Procedure did not improve the performance of the tool.

C4.4 Conclusions

An alternative method to the original method of the steady state update solution procedure was devised in order to reduce the errors imposed into the DTM-CFD procedure, when simulating high rates of thermal change. This alternative solution method was unsuccessful in improving the steady state solution procedure. It must be stressed that the flaw in the original steady state update solution procedure only takes effect for unrealistically high rates of change of external ambient conditions, on exceptionally highly conductive materials, and hence is not likely to impose errors when simulating realistic buildings.

APPENDIX D

Appendix D

D1 Solar Representation

D1.1 Introduction to Solar Calculations within Flovent

Solar representation within Flovent is a relatively new functionality. Hence the performance of this function, especially within a transient solution, is not well-established or understood. The representation of thermal loads caused by direct solar radiation has to be tested, especially since the transient ambient, represented as a series of solid opaque cuboids for the purpose of this research, are likely to block the penetration of direct solar radiation through materials such as glass. In order to find a solution around this potential problem, a series of simple tests have been devised.

D1.2 Test Configurations

An enclosure with dimensions of 1m x 1m x 1m was constructed, containing a concrete floor slab (thickness 100mm), one external wall and one internal partition maintained at 20°C (the specification of the material for the internal partition is not important since the fixed temperature overrides any material thermal characteristics). The external wall was given a material of typical transparent glass, with the following thermal characteristics:

Table D1: Material Characteristics of Typical Glass

Thermal Characteristics	Typical Glass	Cuboid Representing Surface Heat Transfer Coefficient	Concrete Slab
Thermal Conductivity (W/mK)	1.05	0.008	1.4

Density (Kg/m3)	2300	1	2100
Specific Heat Capacity (J/KgK)	836	1	840
Solar Absorption Coefficient (1/m)	20	0	
Refractive Index	1.3	0	/
Thickness (m)	0.01	0	0.1

A solar calculations was performed for the following conditions:

Latitude - 51° to the North

Day - 23rd July

Time – 12 noon

All surfaces were exposed to an ambient setting of 20°C, except the concrete slab, which was exposed to a ground ambient setting of 15°C and an external surface heat transfer coefficient of 1000W/mK.

As established from the research conducted in Section A5.4.2, Appendix A, collapsed thermal sources are ineffective. In order to develop the research conducted in section A5.4.2 for the purpose of solar radiation modelling, the collapsed cuboid will be expanded. In this test, a conventional ambient setting will be simulated first. These results will be compared to an ambient setting constructed from a series of a transparent thermal source and a transparent solid representing an external surface heat transfer coefficient. All tests will be conducted at steady state and then expanded to a transient solution.
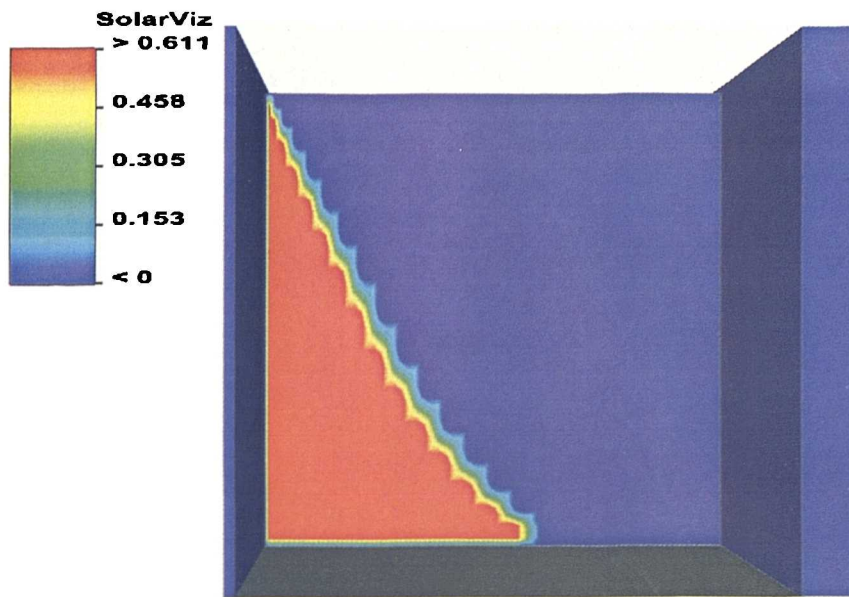
D1.3 Results and Discussion

Figure D1:   Solar Visualisation of solar radiation penetrating through the
transparent glass window

As can be observed from Figure D1, solar radiation successfully penetrated through
the transparent glass window. The following adjustments had to be made to the
model, in order for the solar representation to be successful:

1. Symmetrical walls could not be used and were replaced with constant
    temperatures. They could have also been replaced with transient thermal
    sources.
2. A solid cuboid had to be replaced by a transparent thermal source of identical
    geometry to the cuboid.
3. An additional transparent cuboid was used to apply an external surface heat
    transfer coefficient.
4. Radiant exchange had to be switched on.

D1.4 Conclusions

Solar radiation can successfully penetrate through transparent materials, but the ambient conditions must be specified as a series of two cuboids, both of which must be transparent. The first cuboid must have a thermal resistance to represent an external surface heat transfer coefficient. The second cuboid must be a thermal source with a transient profile, to represent external ambient conditions.
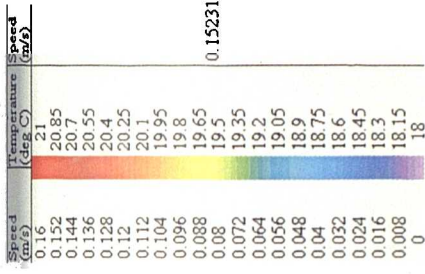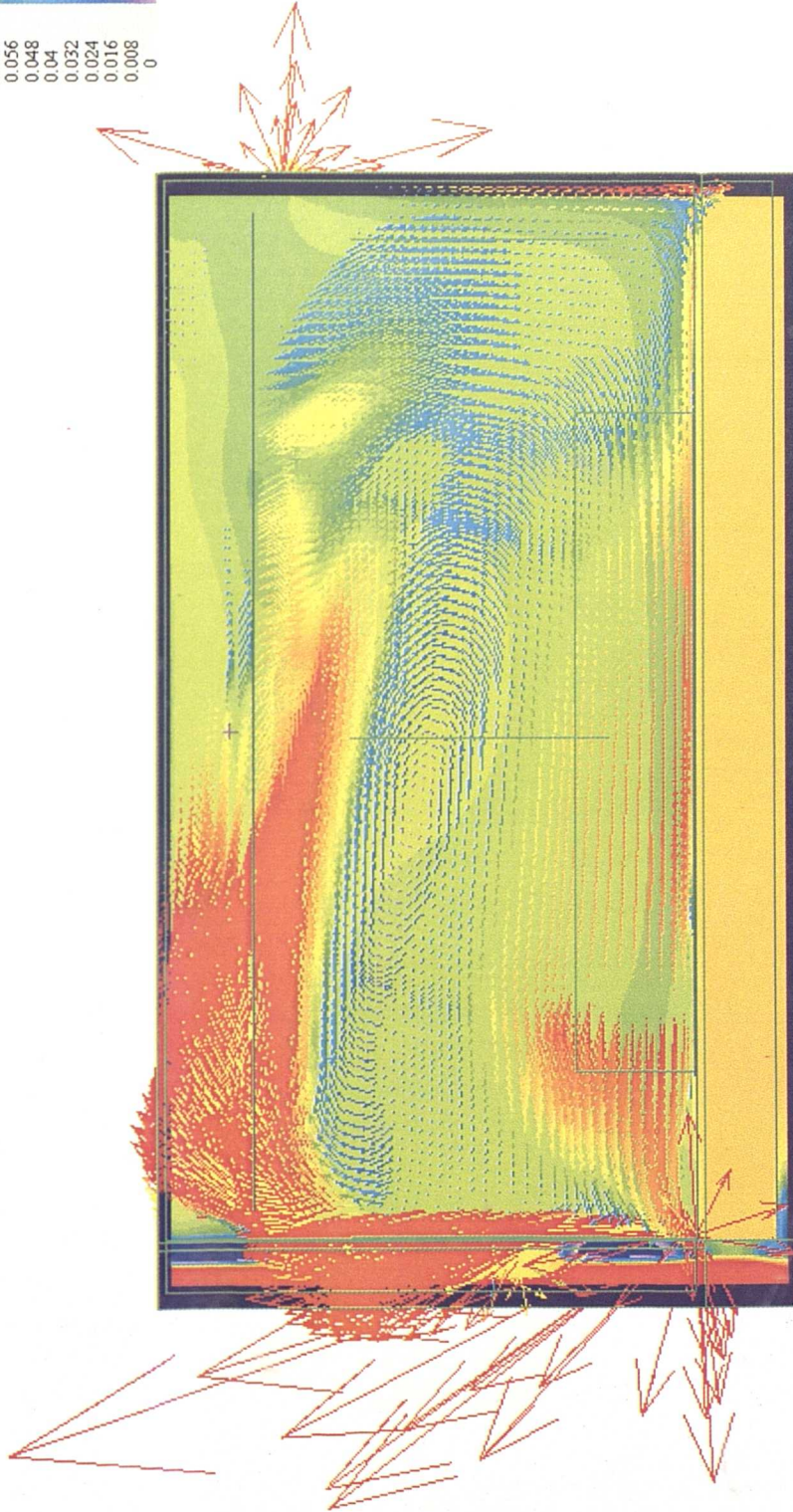
Section D2

Visualisation Plots

Powerpoint Presentation File: Stage4VENTOFF.ppt
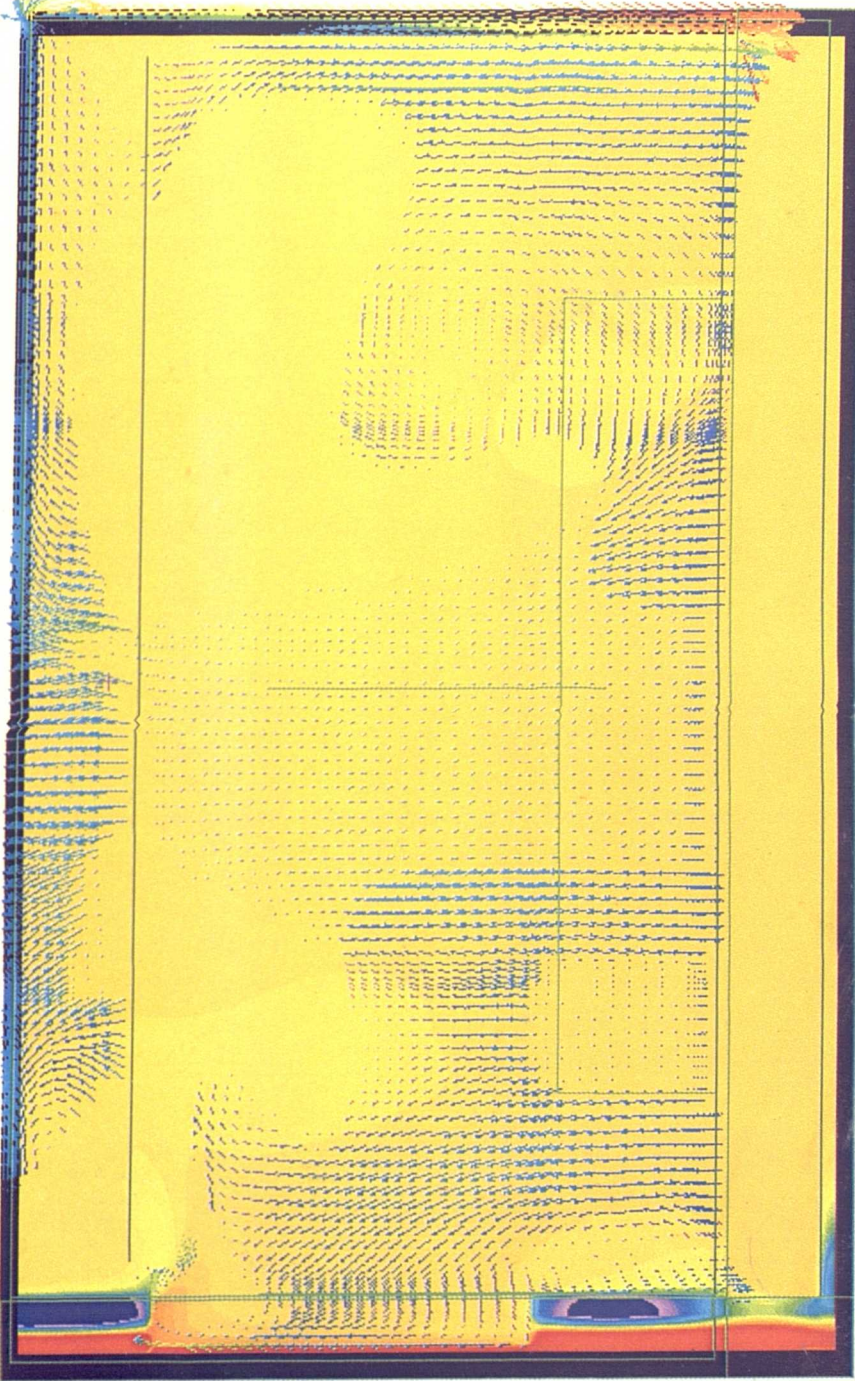Powerpoint Presentation File: Stage6SOLARON.ppt
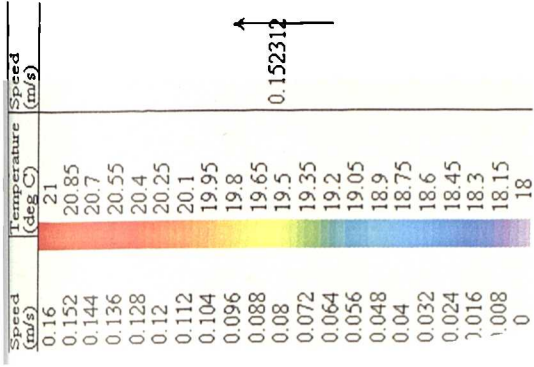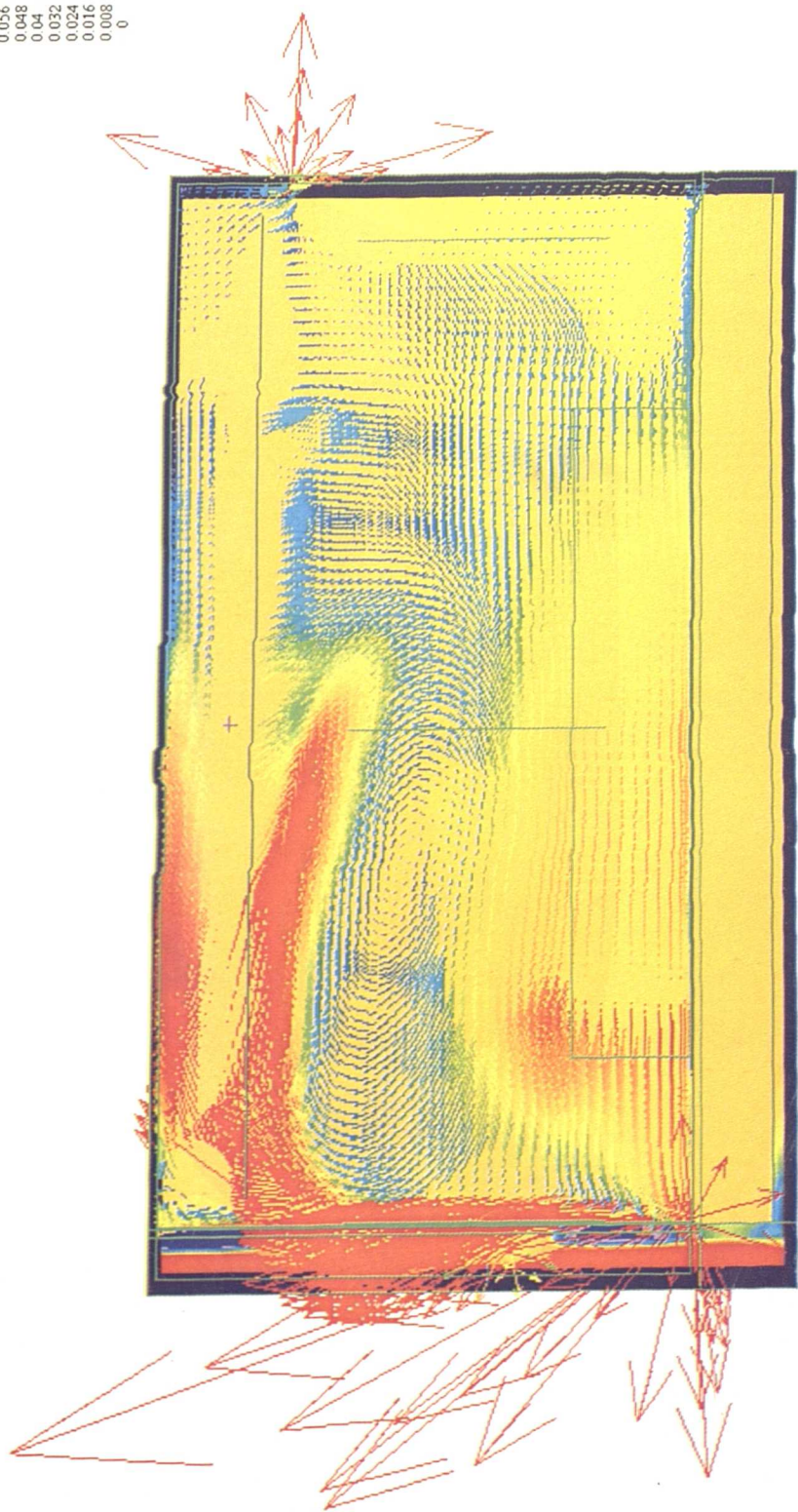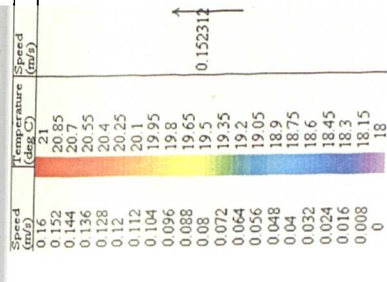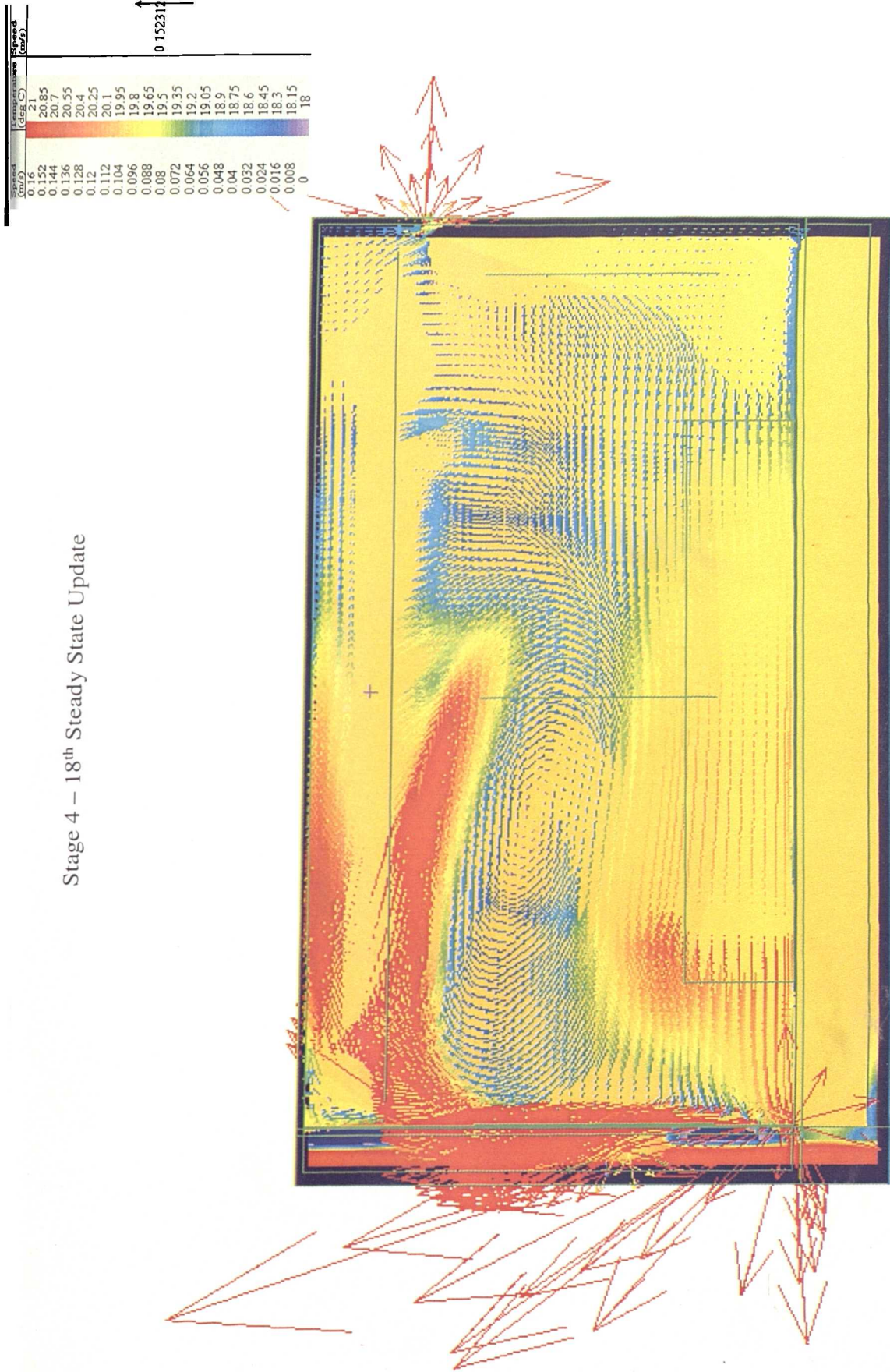
Stage 4 – Hour 18 – Fully Transient Solution

Stage 4 – Hour 19 – Fully Transient

Stage 4 ~ 18th Hour Transient Frozen Flow Period

Speed (m/s)	Temperature (deg C)	Speed (m/s)
0.16	21	
0.152	20.85	
0.144	20.7	
0.136	20.55	
0.128	20.4	
0.12	20.25	
0.112	20.1	0.152312
0.104	19.95	
0.096	19.8	
0.088	19.65	
0.08	19.5	
0.072	19.35	
0.064	19.2	
0.056	19.05	
0.048	18.9	
0.04	18.75	
0.032	18.6	
0.024	18.45	
0.016	18.3	
0.008	18.15	
0	18	

Stage 4 – 18th Steady State Update

Stage 4 – Additional Steady State Update – Ventilation System Off

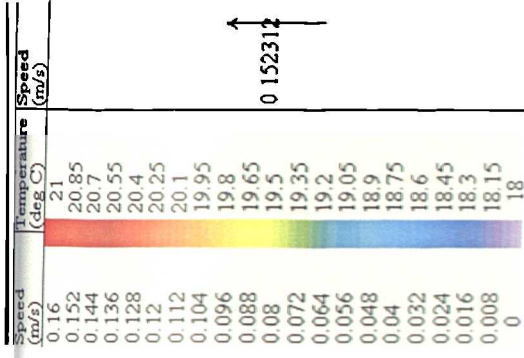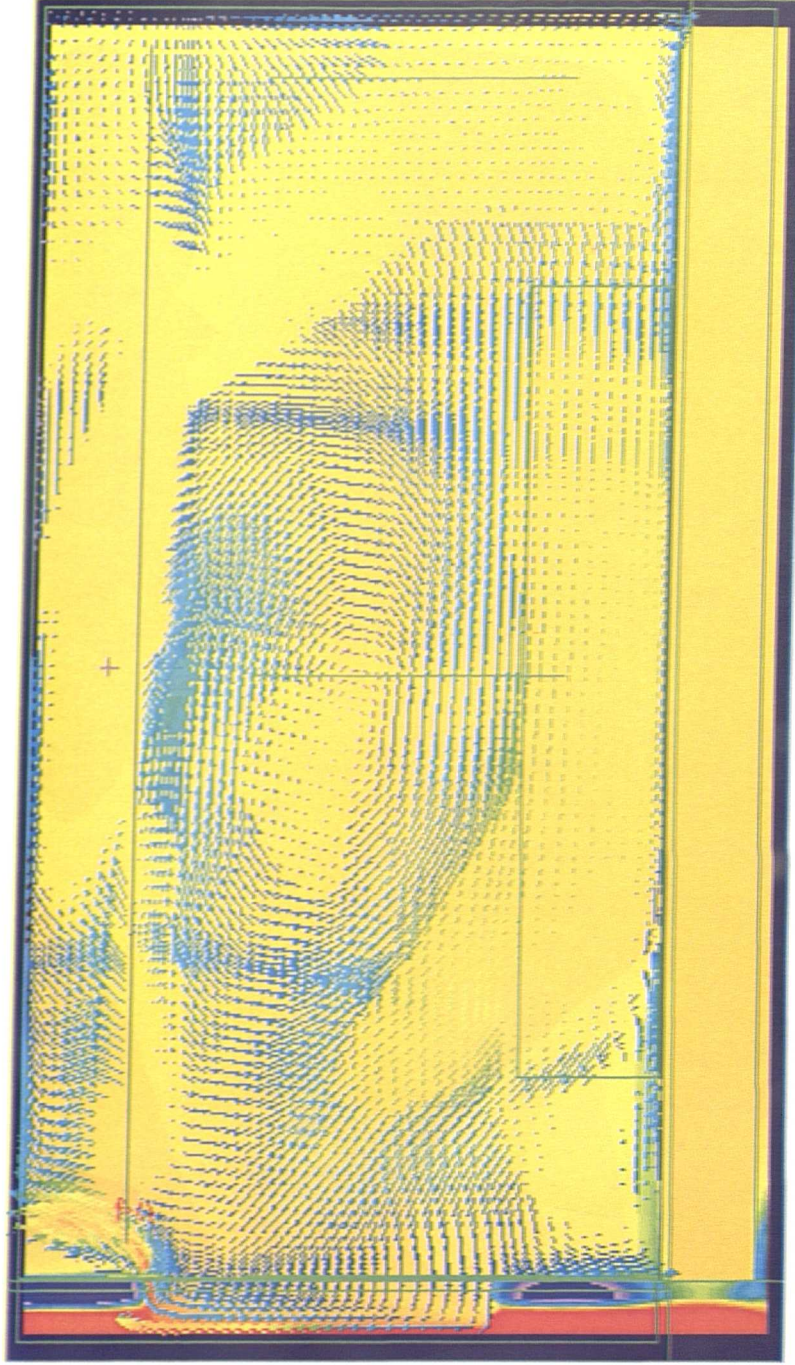| Speed (m/s)		Temperature (deg C)	Speed (m/s)
0.16		21	
0.152		20.85	
0.144		20.7	
0.136		20.55	
0.128		20.4	
0.12		20.25	
0.112		20.1	
0.104		19.95	
0.096		19.8	
0.088		19.65	
0.08		19.5	
0.072		19.35	
0.064		19.2	
0.056		19.05	
0.048		18.9	
0.04		18.75	
0.032		18.6	
0.024		18.45	
0.016		18.3	
0.008		18.15	
0		18	

0 152312

Stage 4 = 19th Hour Transient Frozen Flow Period
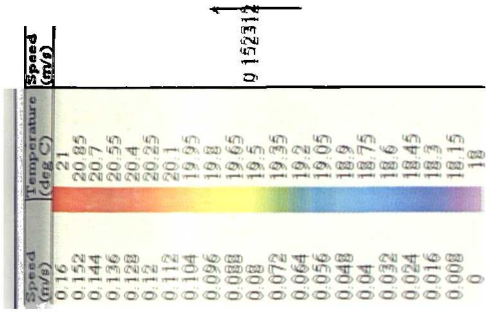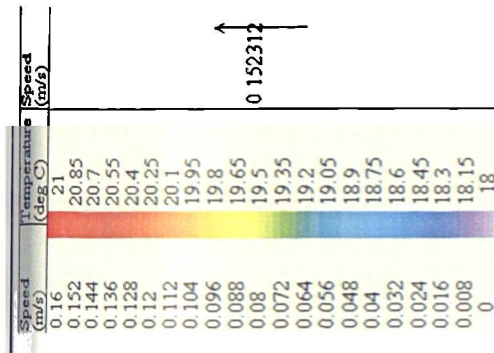
Stage 4 – 19th Hour Steady State Update

Stage 6   Hour 5 – Fully Transient Solution

Speed (m/s)		Temperature (deg C)	Speed (m/s)
0.4		23	1.89871
0.3		21.5	
0.2		20	
0.1		18.5	
0		17	
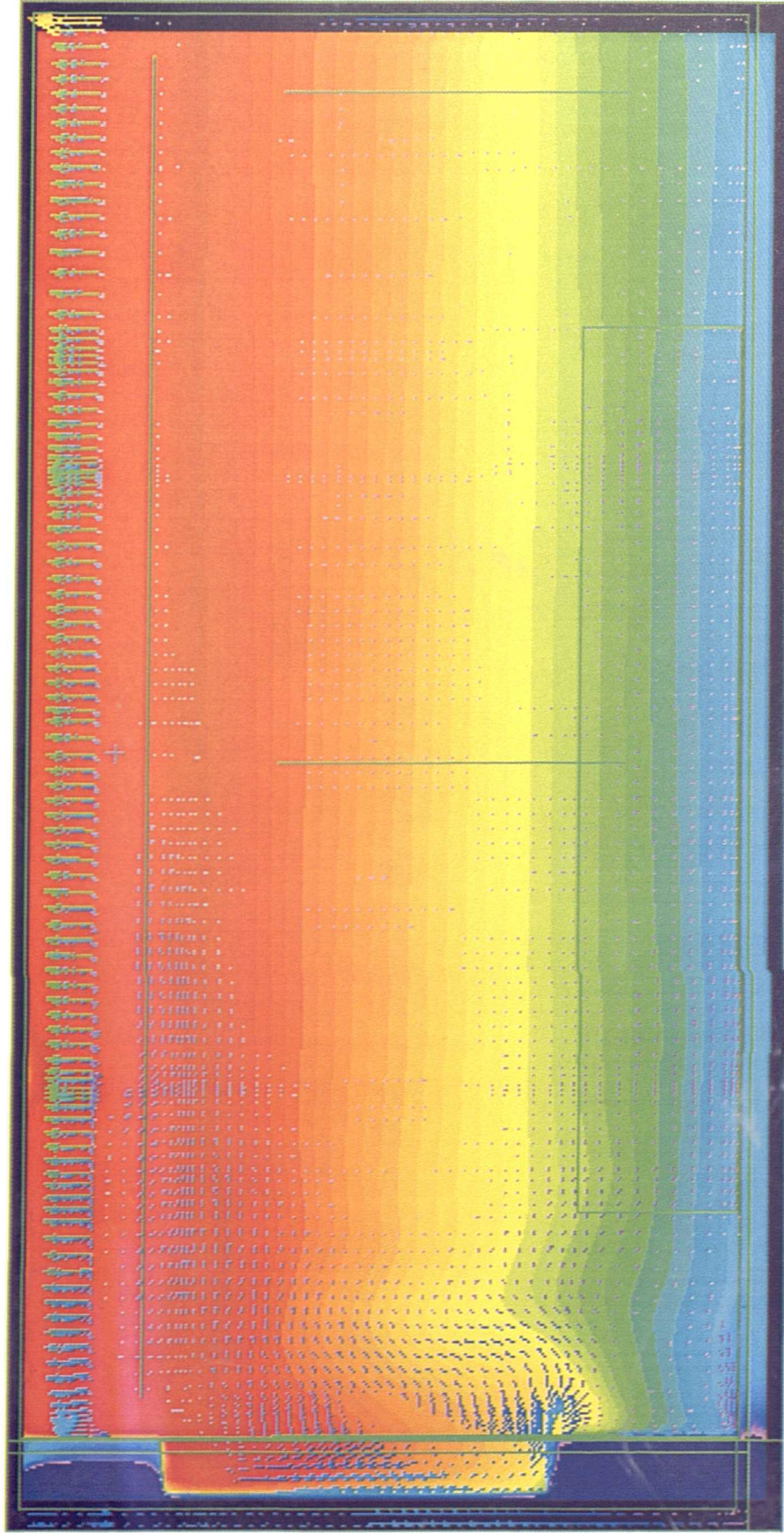
Stage 5 – Hour 5 – Partially Unfrozen Transient

Speed (m/s)	Temperature (deg C)	Speed (m/s)
0.4	23	1.89871
0.3	21.5	
0.2	20	
0.1	18.5	
0	17	
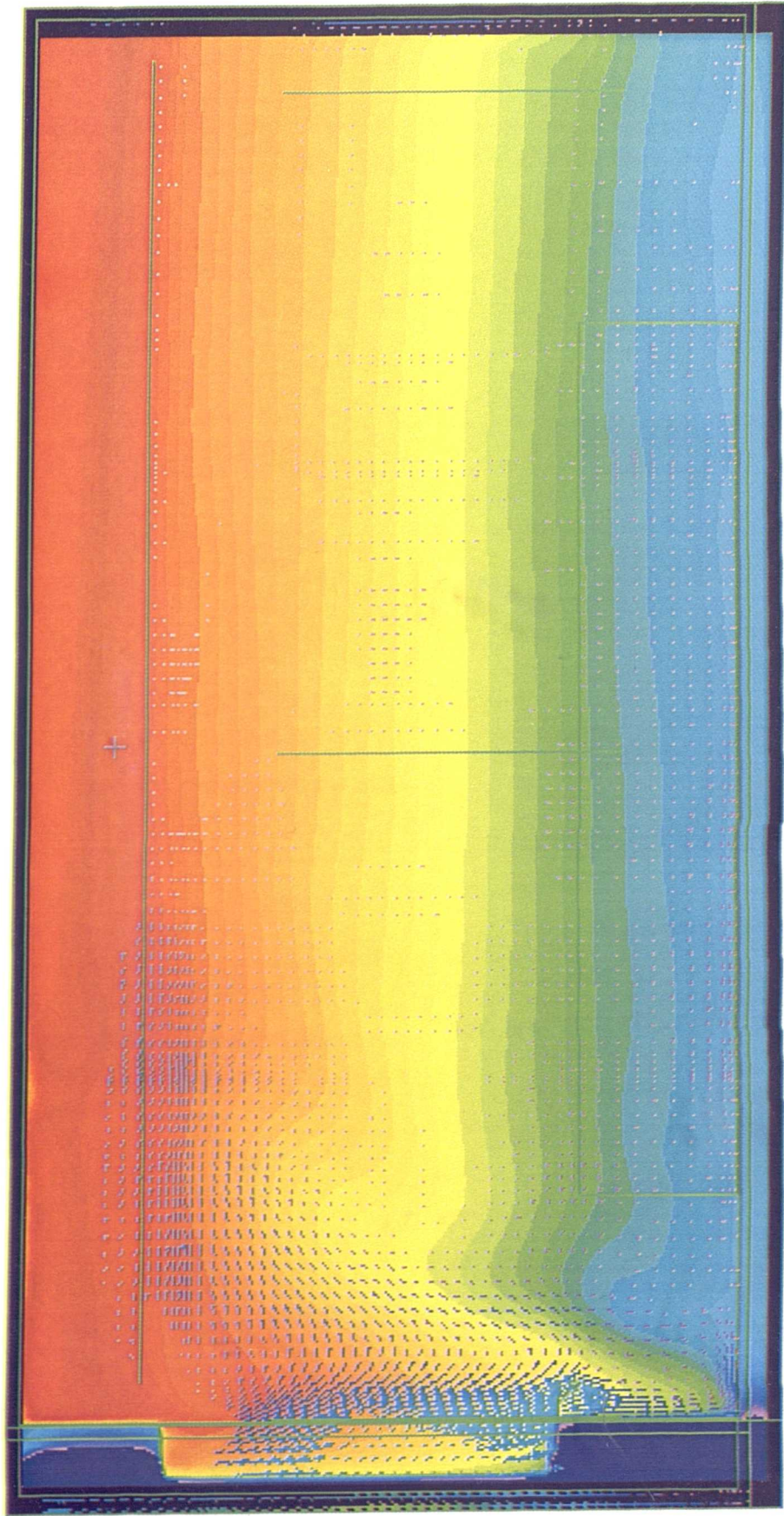
Stage 6 – Hour 4 Additional steady state Update

Speed (m/s)		Temperature (deg C)	Speed (m/s)
0.4		23	1.89871
0.3		21.5	
0.2		20	
0.1		18.5	
0		17	
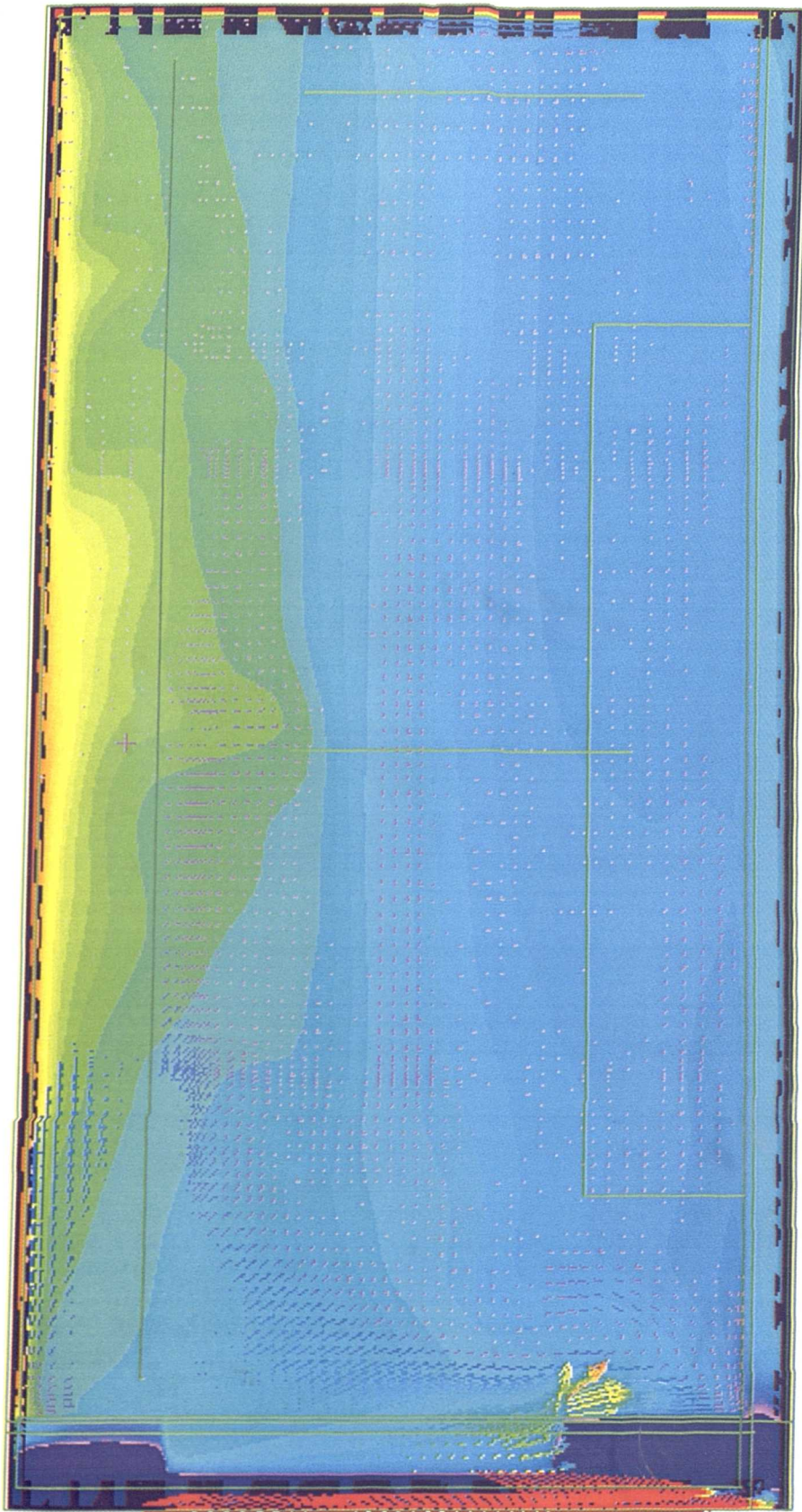
D3   Comparison of CPU Times

A fully transient procedure and DTM-CFD Procedure were both used to simulate a dynamic thermal model of Stage 6 of the realistic case study. The time taken to solve each period along the total 24-hour simulation, using the two simulation procedures was timed. The results have been tabulated and compared below.

Table D2:   *Comparison of CPU times for the fully transient case and the DTM-CFD case*

Fully Transient		DTM-CFD Procedure	
Solution	Time	Solution	Time
Hour 0	15m 8s	Trans 0	58s
		Steady 0	14m 37s
Hour 1	3m 40s	Trans1	1m 3s
		Steady 1	1m 33s
Hour 2	5m 13s	Trans 2	1m 3s
		Steady 2	1m 13s
Hour 3	6m 28s	Trans3	1m 3s
		Steady 3	56s
Hour 4	6m 43s	Trans 4	1m 3s
		Steady 4	56s
Hour 5	41m 23s	Trans 5FT (incl. 5 Fully Transient Time Steps)	37m 8s
		Steady 5	4h 2m 12s
Hour 6	8h 51m 25s	Trans 6	21m 3s
		Steady 6	2h 24m 28s
Hour 7	2h 22m	Trans 7	12m 43s
		Steady 7	1h 44m 27s
Hour 8	2h 59m 28s	Trans 8	6m 45s
		Steady 8	2h 10m 28s
		Steady 8 +1	2h 43m 28s
Hour 9	7h 22m 24s	Trans 9	21m 37s

		Steady 9	2h 6m 8s
Hour 10	3h 42m 11s	Trans 10	35m 41s
		Steady 10	3h 50m 49s
Hour 11 (interrupted)	11h 32m 34s	Trans 11	36m 47s
		Steady 11 (interrupted)	2h 42m
Hour 12	16h 25m	Trans 12	4h 2m 30s
		Steady 12	8h 33m 46s
Hour 13	16h 38m 34s	Trans 13	4h 2m 10s
		Steady 13	10h 29m 40s
		Steady 13 +1	3h 59m 36s
Hour 14	6h 4m 48s	Trans 14	59m 14s
		Steady 14	1h 10m 49s
		Steady 14 +1	9h 23m 23s
Hour 15	20h 53m 59s	Trans 15	4h 1m 57s
		Steady 15	6h 51m 48s
		Steady 15 +1	38m 33s
Hour 16	10h 18m 31s	Trans 16	2h 47m 32s
		Steady 16	5h 45m 40s
		Steady 16 + 1	2h 11m 31s
Hour 17	3h 38m 40s	Trans 17	1h 14m 44s
		Steady 17	14m 9s
		Steady 17 +1	3h 15m 15s
Hour 18	8h 9m 57s	Trans 18	6m 32s
		Steady 18	7h 21m 35s
Hour 19	4h 56m 54s	Trans 19	4m 8s
		Steady 19	3h 19m 26s
Hour 20	2h 43m 18s	Trans 20	2m 41s
		Steady 20	1h 36m 28s
Hour 21	53m 14s	Trans 21	1m 38s
		Steady 21	42m 38s
Hour 22	19m 57s	Trans 22	59s

		Steady 22	15m 13s
Hour 23	19m 57s	Trans 23	1m 0s
Total Time Taken	**5 days 9h 31m 26s**	D-8	**4 days 12h 14m 44s**

Appendix E

Appendix E - Publications

Somarathne, S., Seymour, M., Kolokotroni, M., (2003), Efficient Dynamic Thermal Modelling using CFD, Healthy Buildings Conference, Singapore

Somarathne, S., Seymour, M., Kolokotroni, M., (2002), Transient Solution Methods for Dynamic Thermal Modelling within CFD, International Journal of Ventilation Vol. 1, No. 2, pp141-156.

Somarathne, S., Seymour, M., Kolokotroni, M., (2002), A Single Tool To Assess The Heat And Airflows Within An Enclosure: Preliminary Test, ROOMVENT 2002 Eight International Conference, Air Distribution in Rooms, Copenhagen, Denmark 8-11 September, CD-ROM.

Somarathne, S., Seymour, M., Kolokotroni, M., (2001), A Single Tool To Assess the Thermal And Environmental Performance Of Office Buildings, Proc. Clima2000 Conference, Napoli, Italy, 15-18 September, CD-ROM.

The following pages have been removed from this thesis due to publisher copyright restrictions.

Thus far society has required the individual to specialize; there has been little time to read, to think, to ponder life's meaning without interruption. This is not resented; the game has carried its own satisfactions. But must the human spirit be indentured to society forever? The time has come to begin one's true adult education, to discover who one is and what life is about. What is the secret of the "I" with which one has been on such intimate terms all these years, yet which remains a stranger, full of inexplicable quirks, baffling surds, and irrational impulses? Why are we born to work and struggle, each with a portion of happiness and sorrow, only to die too soon? Generation after generation swells briefly like a wave, then breaks on the shore, subsiding into the anonymous fellowship of death. To find meaning in the mystery of existence is life's final and fascinating challenge...

(H. Smith, 1991)